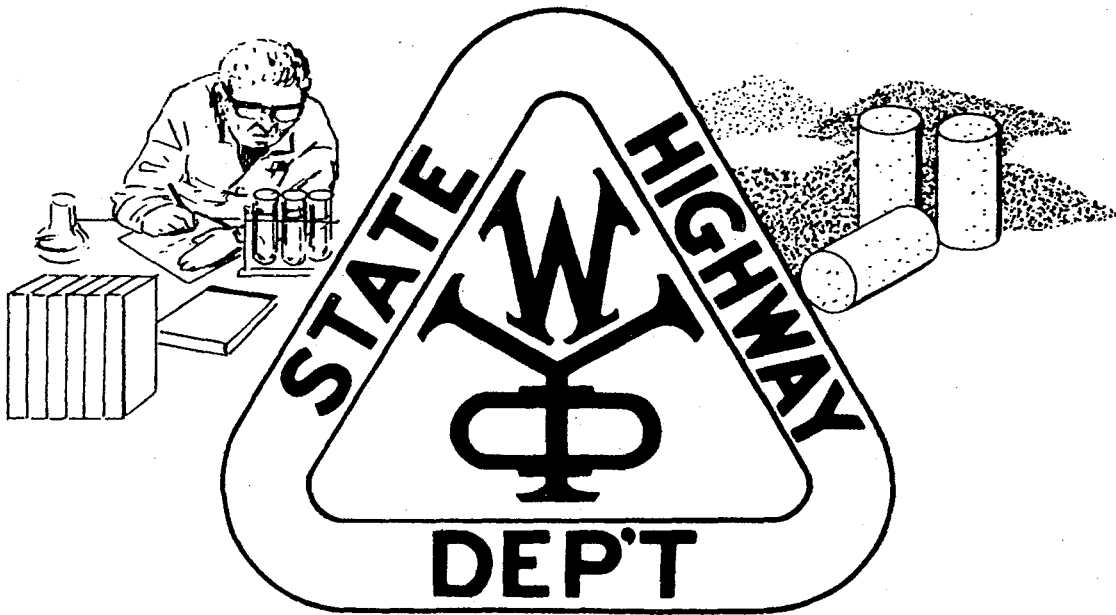


EVALUATION OF AN EARTH HEATED BRIDGE DECK



WYOMING HIGHWAY DEPARTMENT

RESEARCH

BRIDGE BRANCH

JUNE 84

TF  
24  
6 A22  
6/11/84



Federal Highway Administration  
Research Library  
Turner-Fairbank Highway Research Ctr.  
6000 Georgetown Pike  
McLean, VA 22101

EVALUATION OF AN EARTH HEATED BRIDGE DECK

Prepared by

John Nydahl

Kynric Pell

Ron Lee

John Sackos

University of Wyoming

April, 1984

Contract Number: DTFH 61-80-C-00053

Indonesian National Police  
KORPRI  
10122 Av. P. 10122

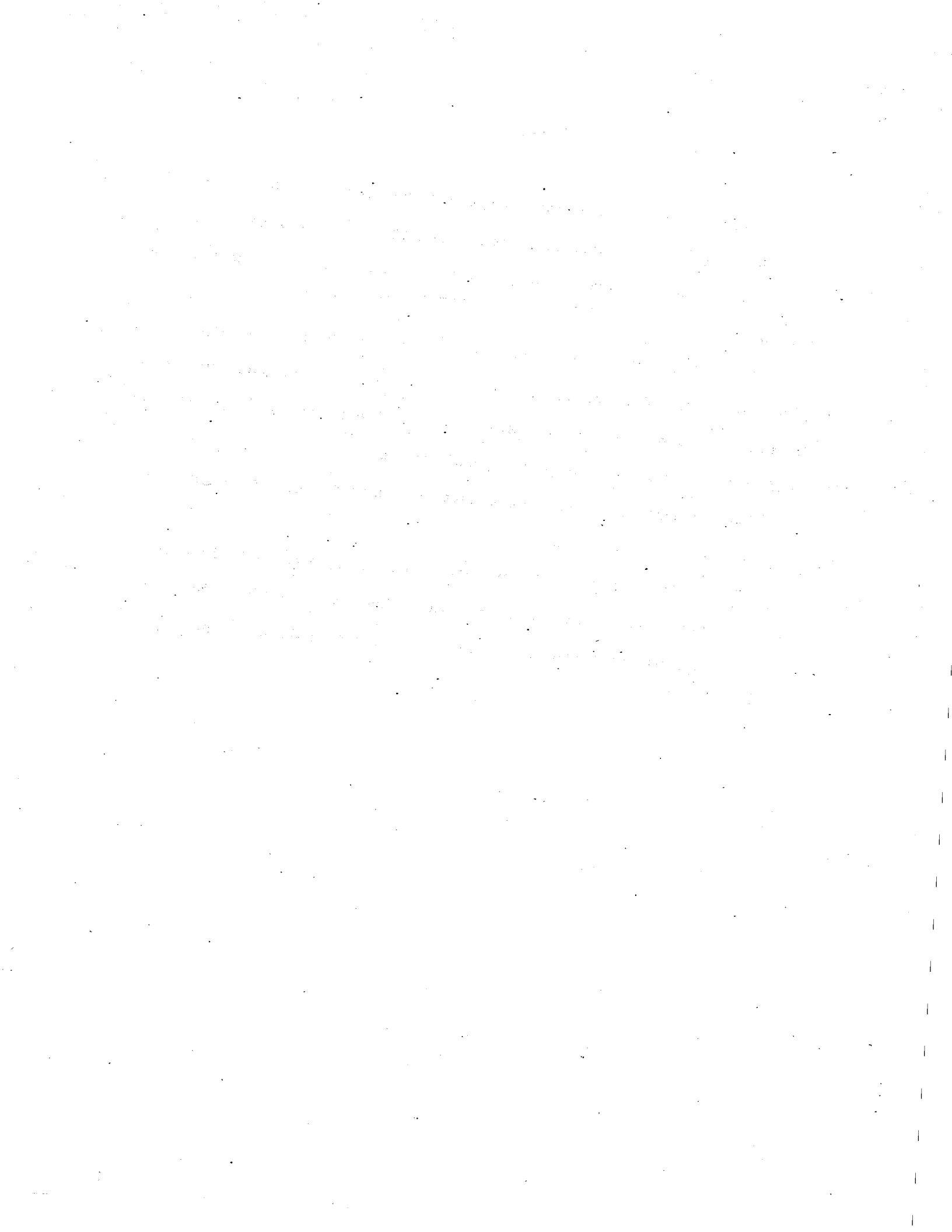
## NOTICE

This document is disseminated under the sponsorship of the U.S. Department of Transportation in the interest of information exchange. The United States Government assumes no liability for its contents or use thereof.

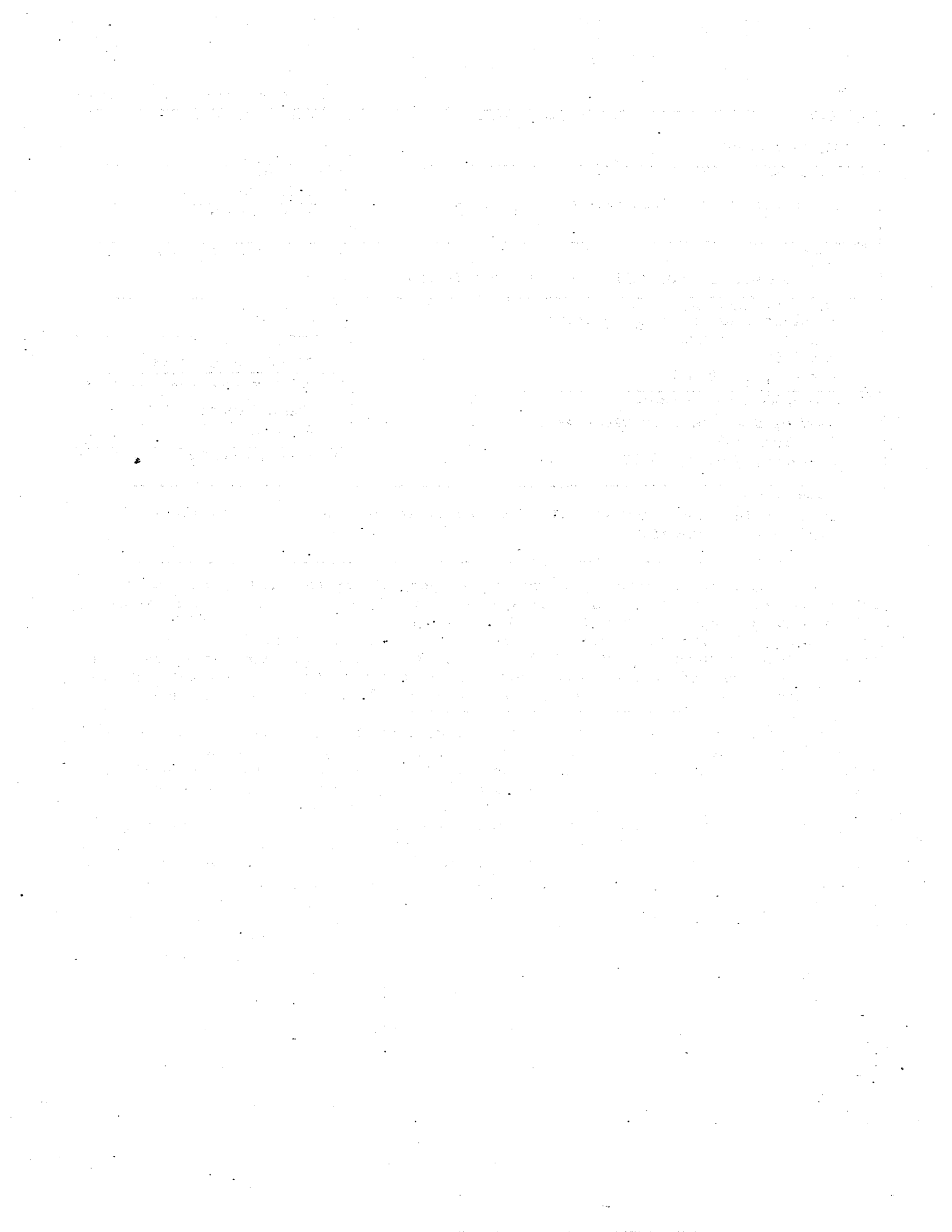
The contents of this report reflect the views of the authors who are responsible for the facts and the accuracy of the data presented herein. The contents do not necessarily reflect the official view or policies of the Federal Highway Administration.

This report does not constitute a standard, specification, or a regulation.

The United States Government does not endorse products or manufacturers. Trade or manufacturers' names may appear only because they are considered essential to the objective of this document.



1. Report No. FHWA-WY-84-001	2. Government Accession No.	3. Recipient's Catalog No.	
4. Title and Subtitle Evaluation of an Earth Heated Bridge Deck		5. Report Date April 1984	
		6. Performing Organization Code	
7. Author(s) John Nydahl, Kynric Pell, Ron Lee, John Sackos		8. Performing Organization Report No.	
9. Performing Organization Name and Address Mechanical Engineering Department University of Wyoming Box 3295 Laramie, WY 82071		10. Work Unit No.	
		11. Contract or Grant No. DTFH61-80-C-00053	
		13. Type of Report and Period Covered Final Report 4/79 to 6/84	
12. Sponsoring Agency Name and Address Wyoming State Highway Department P.O. Box 1708 Cheyenne, Wyoming 82001		14. Sponsoring Agency Code	
15. Supplementary Notes Prepared in cooperation with the U.S. Department of Transportation, Federal Highway Administration			
16. Abstract The design, construction, performance and analysis of the first ground heat pipe system to heat an entire bridge deck are detailed. Each of the sixty heat pipes in this system is comprised of a 6 cm (2.4") diameter, 31 m (100') long vertical ground evaporator, and a condenser that was formed by manifolding 2.5 cm (1") pipe on 15 cm (6") centers to heat 7.6 m <sup>2</sup> (82 ft <sup>2</sup> ) of deck surface. Ammonia vaporizes in an evaporator anytime the encompassing ground is warmer than the bridge deck, and this vapor ascends into the condenser section where it releases its heat of vaporization to the deck. The integration of the heat pipes into the bridge deck did not have a significant impact on the bridge construction. The heat pipes increased the deck's weekly averaged surface temperature up to 10°C (18°F), preventing preferential freezing of the deck relative to the adjacent road. Snow cover duration was decreased by 50% despite a ground temperature of only 8°C (46°F). The minimum dynamic conductance of this system during major heating events appears to be between 8 and 11 watts per m <sup>2</sup> of deck per °C temperature difference between the far-field ground and the deck surface. A thermal model was developed to accurately handle the complex dynamic interactions between the heat pipes, the deck, and the ground. Parametric studies based on this model were used to formulate a heat pipe system thermal design procedure which is presented in the design manual. The heat pipes accounted for 59% of the total bridge cost with the evaporators generating 69% of the system's expense; but it would be economically viable to utilize a few ground source heat pipes to heat only the tire tracks and gutters.			
17. Key Words bridge deck icing, preferential icing, ground source heat pipes		18. Distribution Statement No restriction. This document is available through the National Technical Information Service, Springfield, Virginia 22161.	
19. Security Classif. (of this report)	20. Security Classif. (of this page)	21. No. of Pages 229	22. Price



### Acknowledgements

A number of University of Wyoming personnel contributed to the success of this project besides the authors. The Mechanical Engineering Department's staff electronics engineer, George Twitchell, was responsible for much of the instrumentation and maintenance of the data acquisition system. Steve Ownbey, Mechanical Engineering computer systems engineer, programmed the computer that was utilized at the field site and assisted in the subsequent data reduction. Many of the research results obtained by former graduate students Dwight Senser and Vic Cundy were also incorporated into parts of the report. Several undergraduates also worked on this project but we wish to especially acknowledge the efforts of Mike Miller. Patty Winkel and Renee Kosmicki typed the manuscript and Dottie Bock handled the project's bookkeeping.

We wish to also acknowledge the long standing support and cooperation we have received from the Wyoming Highway Department--especially the contributions of Dave Pope and Charles Wilson of the Bridge Division who worked very closely with us. The Federal Highway Administration sponsorship is also greatly appreciated.

1. The first part of the document discusses the importance of maintaining accurate records of all transactions and activities. It emphasizes that proper record-keeping is essential for ensuring transparency and accountability in the organization's operations. This section also outlines the various methods and tools used to collect and store data, highlighting the need for consistency and reliability in the information gathered.

2. The second part of the document focuses on the analysis and interpretation of the collected data. It describes the various techniques and models used to identify trends, patterns, and anomalies in the data. This section also discusses the importance of contextualizing the data and understanding the underlying factors that may be influencing the results. The goal is to provide a clear and concise summary of the findings and their implications for the organization.

3. The third part of the document discusses the application of the findings to the organization's strategic goals and objectives. It outlines the various ways in which the data can be used to inform decision-making and improve performance. This section also discusses the importance of communication and collaboration in ensuring that the findings are effectively shared and acted upon by all relevant stakeholders. The goal is to ensure that the organization is able to leverage its data to achieve its long-term vision and mission.

## TABLE OF CONTENTS

Section	Page
Acknowledgements . . . . .	ii
List of Figures . . . . .	v
List of Tables . . . . .	ix
List of Symbols . . . . .	xi
I. INTRODUCTION . . . . .	1
II. SPRING CREEK HEAT PIPE FACILITY . . . . .	13
A. Heat Pipe System . . . . .	13
B. Data Acquisition System . . . . .	20
C. Instrumentation . . . . .	23
III. SPRING CREEK EXPERIMENTAL RESULTS . . . . .	31
IV. SYBILLE CANYON HEAT PIPE FACILITY . . . . .	53
V. HEAT TRANSFER MODEL. . . . .	66
A. General Description. . . . .	66
B. Deck Response Factors. . . . .	69
C. Isolated Evaporator Model. . . . .	73
D. Evaporator Pipe Interaction. . . . .	80
E. Far-Field Ground Temperature . . . . .	83
F. Numerical Model. . . . .	89
G. Model Validation . . . . .	91
H. Parametric Studies . . . . .	107

VI. DESIGN MANUAL . . . . .	118
A. Thermal Design Procedure . . . . .	118
B. System Performance . . . . .	132
C. Worked Example . . . . .	135
D. Mechanical Design. . . . .	145
VII. CONCLUSIONS AND RECOMMENDATIONS . . . . .	149
REFERENCES . . . . .	154
APPENDIX A - Construction Plans for Spring Creek Bridge, Laramie, Wyoming. . . . .	157
APPENDIX B - Example Special Provisions . . . . .	183
1. Excavation for Pavement Heating System. . . . .	184
2. Evaporator Holes. . . . .	186
3. Epoxy Coating Heat Pipes. . . . .	188
4. Fabrication and Installation of Heat Pipes. . . . .	194
5. Insulation for Pavement Heating System. . . . .	203
APPENDIX C - Construction Record and Costs . . . . .	205

## LIST OF FIGURES

Figure	Page
1.1 Oak Hill, West Virginia Ground Heat Pipe Installation . . .	7
1.2 Schematic of Sybille and Spring Creek Heat Pipes . . . . .	11
2.1 Photograph of the Spring Creek Heat Pipe Test Facility . .	14
2.2 Plan View of the Spring Creek Heat Pipe Test Facility . .	15
2.3 Schematic of the Spring Creek Heat Pipe System . . . . .	16
2.4 Evaporator Pipes under Construction and Two Evaporator Holes . . . . .	18
2.5 Evacuation of Evaporator Pipes at Construction Site . . .	18
2.6 Connector Pipes Before and After Insulation . . . . .	19
2.7 Photograph of Condenser Manifolds Prior to Insulation . .	21
2.8 Interconnecting Pipes Inside Service Vault . . . . .	21
2.9 Photographs of the Data Acquisition System during its Assembly and in the Instrumentation Vault . . . . .	22
2.10 Photograph of the Meteorological Instrumentation . . . . .	25
2.11 Temperature Instrumentation PVC Pipes in Bridge Deck . .	25
2.12 Placement of Thermistors in Bridge Deck . . . . .	27
2.13 Thermistor Locations within the Bridge Deck . . . . .	27
2.14 Ground Evaporator Pipe with Temperature Instrumentation .	29
2.15 Electrically Heated Evaporator . . . . .	29
3.1 Daily Averaged Remote Ground Temperature Distributions Versus Time . . . . .	34
3.2 Weekly Averaged Evaporator and Ground Temperatures . . .	36

3.3	Working and Failed Heat Pipes . . . . .	38
3.4	Liquid Lock . . . . .	38
3.5	Spring Creek Weekly Averaged Heated and Unheated Deck Surface Temperatures During Heating Events . . . . .	40
3.6	Spring Creek Snow Melting Sequence . . . . .	44
3.7	Clear Heated Deck and Iced Covered Road and Control . . .	46
3.8	Observation Sections Used in Photographic Record . . . .	47
4.1	Sybillle Creek Experimental Facility . . . . .	54
4.2	Sybillle Creek Heat Pipe Facility . . . . .	56
4.3	Sybillle Creek Weekly Averaged Heated and Unheated Deck Temperatures During Heating Events . . . . .	56
4.4	Sybillle Creek Snow Melting Sequence . . . . .	60
4.5	Weekly Averaged Experimental Ground and Evaporator Temperatures at Sybillle (12 m) . . . . .	65
5.1	Heat Transfer Schematic . . . . .	67
5.2	Deck Surface Designation and Temperature History Representation. . . . .	70
5.3	Line Source Representation of the Evaporator Pipe . . . .	77
5.4	Evaporator Pipe - Backfill Geometry . . . . .	79
5.5	Evaporator Pipe Interaction Geometry . . . . .	81
5.6	Discrete Representation of the Ground Surface Temperature History . . . . .	84
5.7	Temperature Pulses Used to Evaluate Z Response Factors. .	86
5.8	Sybillle and Spring Creek Evaporator Fields . . . . .	94
5.9	Predicted/Experimental Heated and Unheated Sybillle Top Surface Temperatures . . . . .	95

5.10	Predicted/Experimental Weekly Averaged Evaporator Temperatures at Sybille. Interactive Model . . . . .	97
5.11	Predicted/Experimental Weekly Averaged Evaporator Temperatures at Sybille. Isolated Model . . . . .	99
5.12	Predicted/Experimental Heated and Unheated Spring Creek Top Surface Temperatures. . . . .	101
5.13	Predicted/Experimental Weekly Averaged Evaporator Temperatures at Spring Creek. Interactive Model . . . . .	102
5.14	Predicted/Experimental Weekly Averaged Evaporator Temperatures at Spring Creek. Isolated Model. . . . .	104
5.15	Comparison of Measured and Predicted Heat Pipe Powers at Spring Creek. . . . .	106
5.16	Percent Change of Base Energy Extraction at Spring Creek as a Function of Various System Parameters. . . . .	108
5.17	Monthly Averaged Ground to Surface Conductance for Spring Creek. . . . .	111
5.18	Monthly Averaged Ground to Surface Conductance for Sybille . . . . .	111
5.19	Dynamic Ground to Surface Conductance Correlation Compared to Simulation Results. . . . .	116
6.1	Schematic Illustration of Required Geometric Design Parameters. . . . .	120
6.2	Schematic Illustration of Steady-State Thermal Resistances . . . . .	125
6.3	Non-Dimensional Interaction Resistance for Various Evaporator Field Geometries . . . . .	126
6.4	Dynamic Ground to Surface Conductance . . . . .	128

6.5	Shape Factor for a 1/2" Standard Embedded Pipe. . . . .	129
6.6	Shape Factor for a 3/4" Standard Embedded Pipe . . . . .	130
6.7	Shape Factor for a 1" Standard Embedded Pipe . . . . .	131
6.8	Minimum Power Required to Maintain a Wet Surface at 1°C with a Clear Sky . . . . .	133
6.9	Minimum Power Required to Maintain a Wet Surface at 1°C with a Heavy Overcast . . . . .	134
6.10	Power Required to Typically Melt Snow as Rapidly as It Falls in Eastern States Between Latitudes 38° and 42° . . .	136
B.1	System for Evacuation and Changing of Heat Pipes . . . . .	197

LIST OF TABLES.

Table	Page
2.1 Meteorological Instrumentation . . . . .	24
3.1 Monthly Meteorological Parameters at the Spring Creek Facility . . . . .	32
3.2 Spring Creek Top Surface Experimental and Predicted Freeze-Thaw Characteristics. . . . .	42
3.3 Spring Creek Non-Traffic Lane Surface Conditions . . . . .	48
3.4 Spring Creek Surface Conditions on Traffic Lanes . . . . .	50
4.1 Monthly Meteorological Record at the Sybille Creek Facility . . . . .	58
4.2 Sybille Top Surface Experimental and Predicted Surface Freeze-Thaw Characteristics. . . . .	61
4.3 Monthly Precipitation and Snow Cover Duration. . . . .	63
5.1 Environmental Heat Transfer Correlations . . . . .	74
5.2 Surface Energy Balances. . . . .	90
5.3 Sybille and Spring Creek System Parameters . . . . .	92
5.4 Monthly Energy Extracted Per Spring Creek Evaporator . . .	105
5.5 Parametric Studies of Dynamic Conductance . . . . .	113
6.1 Required Geometric Design Parameters . . . . .	119
6.2 Required Thermal Design Parameters . . . . .	122
6.3 Thermophysical Properties of Various Soils . . . . .	123

6.4	Steady-State Component Thermal Resistances ( $^{\circ}\text{C}/\text{W}$ ) . . . . .	124
6.5	Steady-State Subsystem Resistances and Steady-State and Dynamic System Conductances. . . . .	127
6.1A	Required Geometric Design Parameters for Spring Creek. . .	137
6.2A	Required Thermal Design Parameters for Spring Creek. . . .	138
6.4A	Steady-State Component Thermal Resistances for Spring Creek . . . . .	140
6.5A	Steady-State Subsystem Resistances, and Steady-State and Dynamic System Conductances for Spring Creek . . . . .	142
C.1	Cost Summary of Spring Creek Bridge. . . . .	210
C.2	Chronological Listing of Major Construction Activities . .	212

## LIST OF SYMBOLS

### English symbols

- $A_{\text{cond}}$  ..... Condenser surface area per evaporator
- $A_{\text{deck}}$  ..... Deck surface area per evaporator
- $A_i$  ..... Area of surface  $i$
- $B$  ..... Magnitude of surface temperature step
- $b$  ..... Condenser spacing
- $C$  ..... Slope of triangular ground temperature pulse
- $c$  ..... Specific heat capacity
- $CR$  ..... Common ratio of  $X_{ijk}$  response factors
- $d_b$  ..... Semi-minor axis of ellipsoidal representation of the back-fill hole
- $d_{ci}$  ..... Inside diameter of the condenser pipe
- $d_{co}$  ..... Outside diameter of the condenser pipe
- $d_e$  ..... Semi-minor axis of ellipsoidal representation of the evaporator pipe
- $d_{ei}$  ..... Inside diameter of the evaporator pipe
- $d_{eo}$  ..... Outside diameter of the evaporator pipe
- $d_h$  ..... Diameter of the backfilled evaporator hole
- $D$  ..... Ground depth below the reference plane
- $D_o$  ..... Ground depth below the reference plane to the top of the evaporator pipe
- $D_\lambda$  ..... Ground depth below the reference plane to the bottom of the evaporator pipe
- $e_o$  ..... Partial pressure of air
- $f_1$  ..... Temperature response at depth  $D$  due to a ramp temperature change

## LIST OF SYMBOLS (Cont'd)

$f_2$ .....	Temperature response at depth D due to a step temperature change
$h$ .....	Distance from the top deck surface to the center of the embedded condenser pipe
$h_c$ .....	Condensing film coefficient of the heat pipe
$h_e$ .....	Evaporative film coefficient of the heat pipe
$h_l$ .....	Bottom surface convective film coefficient
$h_u$ .....	Top surface convective film coefficient
$H$ .....	Deck thickness
$K$ .....	Thermal conductivity
$K_b$ .....	Thermal conductivity of the backfill
$K_c$ .....	Thermal conductivity of the condenser pipe
$K_{conc}$ .....	Thermal conductivity of the deck concrete
$K_e$ .....	Thermal conductivity of the evaporator pipe
$K_g$ .....	Thermal conductivity of the ground
$l_c$ .....	Length of the condenser pipe per evaporator
$l_e$ .....	Length of the ellipsoidal evaporator pipe
$l_h$ .....	Length of the backfill hole
$l_p$ .....	Length of the evaporator pipe
$M$ .....	$D^2/2\alpha$
$N$ .....	Number of $X_{ijk}$ response factors prior to the occurrence of the common ratio (CR)
$N_e$ .....	Number of interacting evaporator pipes in a field
$NS$ .....	Number of deck surfaces (2 or 3)
$N_s$ .....	Number of surrounding evaporator pipes
$\dot{Q}_i$ .....	Power through deck surface i (see Figure 5.2)
$Q_{jk}$ .....	Power extracted by evaporator pipe j over time interval k

## LIST OF SYMBOLS (Cont'd)

$\dot{Q}_{pk}$ .....	Rectangular power pulse from primary line source over time interval k
$q_{atm}$ .....	Net long-wave atmospheric radiation to the top deck surface
$q_{conv}$ .....	Convective heat transfer at the top or bottom deck surface
$q_{i,0}$ .....	Current heat flux through deck surface i
$q_{i,1}$ .....	Heat flux through deck surface i, $\delta$ units of time previously
$q_{lw}$ .....	Long-wave radiation omitted by the top deck surface
$q_{melt}$ .....	Specific power supplied during snow melting
$q_{min}$ .....	Specific heat flux required to maintain a wet surface at 1°C
$q_s$ .....	Heat flux through top surface of the deck
$q_{solar}$ .....	Incoming solar radiation to the top deck surface
$r_e$ .....	Dimensionless effective radius ( $R_e/\ell_p$ )
$r_{ij}$ .....	Dimensionless evaporator spacing ( $R_{ij}/\ell_p$ )
$R$ .....	Radial distance from a point source
$R_c$ .....	Condensing resistance
$R_{conc}$ .....	Concrete deck resistance
$R_{cp}$ .....	Condenser pipe resistance
$R_e$ .....	Equivalent radius of the evaporator pipe-backfill combination
$R_{eg}$ .....	Steady-state thermal resistance between an isolated evaporator and the ground
$R_{ep}$ .....	Evaporator pipe resistance
$R_{es}$ .....	Thermal resistance between the evaporator pipe and the bridge top surface
$R_{evap}$ .....	Evaporation resistance
$R_{field}$ .....	Steady-state resistance between the far field ground and an evaporator in a field of evaporators
$R_I$ .....	Resistance due to evaporator pipe interactions

## LIST OF SYMBOLS (Cont'd)

$R_{ij}$ .....	Radial distance between evaporators i and j
$R_{insul}$ .....	Insulation thermal resistance on the deck's bottom surface
$R_{pipe}$ .....	Thermal resistance of the heat pipe
$R_s$ .....	Characteristic radial spacing of evaporator pipes
$S$ .....	Shape factor for embedded pipes
$t$ .....	Time
$T$ .....	Temperature
$T_{air}$ .....	Air temperature
$T_c$ .....	Control deck top surface temperature
$T_D$ .....	Far-field ground temperature at depth D.
$T_e$ .....	Temperature on adiabatic ground plane at a distance $R_e$ from line source, evaporator temperature
$T_g$ .....	Average far-field ground temperature along the length of the evaporator pipe
$T_h$ .....	Heated deck top surface temperature
$T_{jk}$ .....	Temperature of deck surface j at time $t_k$
$T_m$ .....	Mean temperature of the top or bottom surface and the air
$T_{sk}$ .....	Far-field ground temperature at time $t_k$ on the surface or at a specified depth
$T_{surf}$ .....	Deck top surface temperature
$\tilde{u}$ .....	Specific dynamic conductance between the far field ground and the deck surface
$U_{eg}$ .....	Steady-state conductance between an isolated evaporator and the ground
$U_{es}$ .....	Steady-state conductance between the evaporator pipe and the bridge top surface
$U_{field}$ .....	Steady-state conductance between the evaporator pipe and the far-field ground

## LIST OF SYMBOLS (Cont'd)

- $u_{dyn}$  ..... Dynamic specific conductance between the far-field ground and the deck surface  
 $U_{insul}$  ..... Specific thermal conductance of insulation on deck's bottom surface  
 $U_s$  ..... Line source steady-state conductance  
 $U_{ss}$  ..... Steady-state conductance between the ground and the deck top surface  
 $u_{ss}$  ..... Specific steady-state conductance between the ground and the deck top surface  
 $U_{system}$  ... See equation 5.31  
 $V$  ..... Wind speed  
 $W_{ak}$  ..... Primary evaporator temperature rise at time  $t_k$  due to a unit power pulse by the primary evaporator  
 $W_{jk}$  ..... Temperature rise of primary evaporator at  $t_k$  due to a unit power pulse by an adjacent evaporator  $j$   
 $W_k$  ..... Combined evaporator pipe response factor  
 $x$  ..... Coordinate along the line source  
 $X_{ijk}$  ..... Deck response factor of surface  $i$  due to a triangular pulse on surface  $j$  at time  $k$   
 $X'_{ijk}$  ..... Modified deck response factor  $\left\{ \begin{array}{l} X'_{ij0} = X_{ij0} \\ X'_{ijk} = X_{ijk} - CR \cdot X_{ij(k-1)}, k > 0 \end{array} \right.$   
 $z$  ..... Coordinate along primary evaporator pipe  
 $Z_k$  ..... Far-field ground response factor  
 $Z'_k$  ..... Average far-field ground response factor

Greek Symbols

- $\alpha$  ..... Thermal diffusivity  
 $\alpha_g$  ..... Thermal diffusivity of the ground  
 $\alpha_{lw}$  ..... Long-wave absorbtivity of the deck  
 $\alpha_{sw}$  ..... Short-wave absorbtivity of the deck

## LIST OF SYMBOLS (Cont'd)

$\delta$ .....	Constant time step used for deck response factors
$\delta_k$ .....	Variable time step used for evaporator response factors
$\epsilon_{\text{air}}$ .....	Long-wave emissivity of the atmosphere
$\epsilon_{\ell w}$ .....	Long-wave emissivity of the deck
$\zeta$ .....	Dimensionless coordinate along the line source ( $x/\ell_p$ )
$\theta$ .....	Dimensionless temperature $[(T-T_g)/(T_e-T_g)]$
$\mu$ .....	Dimensionless coordinate along primary evaporator pipe ( $z/\ell_p$ )
$\xi$ .....	Confocal ellipses in prolate spheroidal coordinates
$\xi_0$ .....	Ellipse representing the evaporator pipe
$\xi_1$ .....	Ellipse representing the backfill hole
$\rho$ .....	Mass density
$\sigma$ .....	Stefan-Boltzman constant
$\tau$ .....	Fourier modulus ( $\alpha t/\ell_p^2$ or $\alpha t/R_e^2$ )

Mathematical symbols

erfc .....	Complementary error function
exp .....	Exponential function
$\nabla^2$ .....	Laplacian operator

## I. INTRODUCTION

Our principle weapons in the perpetual struggle with winter for control of the highways have been the snowplow and the spreading of mountainous quantities of deicing chemicals and abrasives. The application of chloride salts has proved to be an effective and relatively inexpensive deicing agent in the milder climates; but one is forced to question salt's real cost-benefit because of its corrosion of vehicles, reinforcing steel and bridge structures, scaling of portland cement concrete, and pollution of water. One study estimates that the national cost of salt related damage is approximately 15 times its cost to purchase and apply (1). There is therefore an enormous incentive to develop deicing alternatives to chloride salts - especially on and around bridge decks.

Conventional snow and ice control procedures can also be disruptive to traffic and often prove to be inadequate if there is a significant delay in their commencement after snow accumulation occurs. For this reason, various thermal snow melting systems have been proposed for particularly critical or hazardous sections of highway. The more orthodox techniques employ either embedded electric resistive heating elements (2) or pipes that circulate a fossil fuel heated fluid, but the expense of both the hardware and these high-grade, non-renewable energy sources restrict their application to small installations.

Waste heat from power plants or industrial processes, and geothermal water (3) are viable inexpensive energy sources, but these

high-grade resources rarely exist in close proximity to a structure that requires heating. The utilization of geothermal water can also be difficult because of its corrosive and fouling nature (4,5), and the possibility of freezing generally precludes direct circulation of any water based source within the structure itself. An intermediate heat exchanger is usually employed in these cases to transfer the energy between the heated water and the structure.

Some recent efforts have been directed toward the development of systems that utilize the renewable thermal energy below the earth's frost level because of its accessibility and dependability. Conversely, this segment of ground is obviously too low-grade an energy source to be able to immediately handle severe snow storms and drifting, or to even prevent the pavement from freezing during frigid weather. In spite of this, the few field tests that have been conducted with these systems have been surprisingly successful in reducing the duration of icy surface conditions. In situations where snow accumulates, either melting or a decrease in the ice bonding strength occurs at the pavement-ice interface, which strongly augments the clearing action by traffic and plowing. Any snow melting system can aggravate an icy condition if partial melting and then refreezing occurs, but this does not appear to be a serious problem with these low power systems.

The first experimental facility to successfully demonstrate the snow melting capability of this form of geothermal energy was constructed in Trenton, New Jersey in 1969 (6). This system circulated an ethylene glycol-water mixture between pipes embedded 5 cm (2") below the pavement surface and a horizontal grid buried 0.9 to 4.0 m (3' to 13') below the pavement on 0.6 m (2') levels. The total length of the

ground pipes was twice as long as the pipes in the pavement. The measured undisturbed ground temperature at a 2.1 m (7') depth varied between 9° and 14°C (48 & 57°F) during the winter and the antifreeze temperature ranged between 4° and 11°C (40 & 52°F) during most of the snow storms. Typical measured snow melting rates were 0.6 to 1.3 cm/hr when the corresponding air temperature ranged between -7° and 2°C (20° & 35°F). The performance of this ground system proved to be superior to that of a companion 215 W/m<sup>2</sup> (68 BTUH/ft<sup>2</sup>) electric pavement heating system while requiring only 1/45 the electrical power to operate the circulation pump. Despite its impressive performance and very low operating cost, the New Jersey system is not practical because of its prohibitive expense--mainly due to the excavation required for placement of the ground pipes.

More recent research has concentrated on vertical ground heat exchangers since some cost savings can be obtained by replacing excavation with conventional drilling. This configuration also permits the utilization of long, gravity operated heat pipes to efficiently transport the low grade thermal energy from the ground to the road surface. J. R. Tippmann (7) was the first person to propose the use of this type of heat pipe in 1965, but it was not until the 1970's before any serious development efforts were initiated (8-23).

The gravity-operated heat pipe consists of a sealed tube which contains a fluid in the liquid-vapor state. The lower end of the pipe is the evaporator while the upper portion serves as the condenser. When the evaporator is warmer than the condenser, a portion of the liquid vaporizes and travels to the condenser where its latent heat of vaporization is released upon condensing. The evaporation and condensation processes

create the driving pressure potential that is required to transport the vapor upward, while gravity returns the condensate from the slightly slanted condenser to the vertical evaporator. This makes the gravity-operated heat pipe a very attractive heat exchanger since it is a completely passive system which does not require any mechanical or electrical parts. Because the thermal energy is transported in the form of latent heat of vaporization, the heat pipe can transport large amounts of energy over long distances [ $\sim 55\text{m}$  (180') at two installations] with a relatively small temperature difference. Ammonia and Freon have been utilized as the working fluid partly because they are not susceptible to the freezing problem that plagues water based systems, and they are chemically inert with respect to most steels.

The preliminary engineering concept studies that were performed in the early 1970's indicated that a viable ground heat pipe snow melting system could be developed. The key attributes of this system can be summarized as follows:

1. The availability of its renewable energy source. The ground temperature several meters below the surface is typically  $2^{\circ}$  or  $3^{\circ}\text{C}$  above the local yearly average air temperature. This implies that a very large media with temperatures at or above ten degrees celsius would be available throughout most of the continental United States right at the site of a proposed heating system (24). Source temperatures of this magnitude are capable of handling a majority of the snow storms in a moderate climate.

2. No operating or maintenance cost. The heat pipe self activates anytime the ground encasing the evaporator is warmer than the pavement in which the condenser is embedded. No external mechanical or electrical

power is therefore required.

3. Mechanically simple. The gravity operated heat pipe is a closed container that is formed by welding pipes together and charging it with a refrigerant. Since there are no moving or electrical parts, the system is very durable and will continue to operate as long as it remains sealed, properly orientated, and no noncondensable gases are internally generated.

The principal difficulties that were anticipated in its implementation were drilling costs, the integration of this system into standard construction procedures, and corrosion. The development of a design procedure was also required since a system's transient performance is a complex function of the local environment, heat pipe geometry, thermal properties of the ground and deck, and the thermal interactions between ground evaporators.

The experimental development of heat pipe snow melting systems was initiated in 1972 at the Turner-Fairbank Highway Research Station (8) when a field test slab was heated by 44 ground-coupled heat pipes. The pipes were spaced on 15.2 cm (6") to 20.3 cm (8") centers in the slab and extended from 9.1 m (30') to 12.2 m (40') into the ground where the average ground temperature below 9.1 m (30') was approximately 14°C. This test, which was proposed and conducted by the Dynatherm Corporation, successfully demonstrated the concept. It also pointed out the necessary construction precaution that proper internal cleaning of the heat pipe was essential to prevent the generation of noncondensable gases which subsequently reside in and, therefore, block the condenser.

The above experimental results were sufficiently promising to justify a full scale demonstration on a highway ramp in Oak Hill, West

Virginia (16). This system was constructed in 1975 and utilized 1213 ground heat pipes to heat  $1800 \text{ m}^2$  ( $19,200 \text{ ft}^2$ ) of pavement. Each heat pipe was 22.9 m (75') long and extended 18.3 m (60') into the ground. Several bundles of these heat pipes are pictured in the foreground of Figure 1.1A while the drilling operation is shown in the background. These ground heat pipes were generally successful in preventing snow and ice accumulation (Figure 1.1B) except when drifting occurred. The far field ground temperature at this site averaged around  $13^\circ\text{C}$ . Unfortunately, very little quantitative information has been published on the performance of this system that would assist an engineer in designing another system.

This facility cost essentially twice as much as an electrical system would have but it was felt that the price for this initial installation was inflated by approximately 40%. Mass production and efficient installation techniques were anticipated to make the installed cost of this type of heat pipe system competitive with an electrical system but it would be more durable and not require any maintenance or operating costs.

Another earth heated ramp went into service in Cheyenne, Wyoming in 1982 and its companion ramp is under construction. These 7% grade ramps interface overpasses and terminate at stop lights. Each ramp utilizes 177 field constructed heat pipes to warm 990 square meters ( $10,600 \text{ ft}^2$ ) of pavement. The design of these very large heat pipes (18) is similar to the Spring Creek design which is evaluated in this report. Each heat pipe has a 30.5 m (100') long evaporator attached to a manifolded condenser section with a total length of 37 m (120'). Due to the severity of the weather in Cheyenne, the ground temperature is only



Drilling  
Rig

Heat Pipe  
Bundle

A. Construction Site



Snow  
Covered  
Highway

Heated  
Ramp

B. Completed System

Figure 1.1. Oak Hill, West Virginia Ground Heat Pipe Installation.

12°C (54°F). The system was therefore designed to prevent preferential freezing of the ramp relative to the road and bridge surfaces, and to provide a moderate amount of snow melting. The performance of this system has not been quantified to date, but visual observations indicate that it has more than met the above objectives.

The use of heat pipes to transfer energy from the earth to roads is also under development in Europe and Japan. Small field tests were initiated in 1977 in Japan and, as of February 1982, twenty experimental installations were reported to have been completed or under construction in that nation (17,22).

A recent offshoot of the ground heat pipe research has been systems that utilize water energy sources. The Japanese (17,22) and the Colorado Department of Highways (4,5) have tested geothermal water powered heat pipe systems, and their use in some bridges on I-70 near Glenwood Springs, Colorado is under review. A similar heat pipe system that utilizes well water as the low grade energy source is currently being evaluated by the University of Wyoming under sponsorship of the Wyoming Highway Department and FHWA. Water powered heat pipes appear to be a promising snow melting alternative when an available water source that has both a reasonable temperature and a sufficient flow rate is in close proximity to the structure. These heat pipe systems can be integrated into highway structures without a lot of extra effort and expense, and the operational overhead is limited to the water pumping and disposal costs. The ratio of the renewable thermal energy that is delivered to the structure to the nonrenewable energy required to pump the water increases with the water temperature and decreases with the water transport distance. This ratio should be well over ten for ground water

systems that draw from a high and abundant water table, and well over 100 for adjacent hot water sources.

To develop ground heat pipe technology further, the University of Wyoming, under the sponsorship of the Wyoming Highway Department and FHWA, has designed and operated two experimental facilities in southeastern Wyoming. The goals of these projects have been to investigate the performance of ground heat pipe systems for bridge decks as well as to develop the analytical framework that is required to extend these experimental results into a general design procedure. A schematic of the two different types of ground heat pipes that were installed at these facilities is presented in Figure 1.2.

The Sybille Canyon facility (13-15) was constructed in 1976. A small section of this bridge was heated by twelve 24.4 m (80') long heat pipes with ground evaporator lengths that averaged around 12.2 m (40'). This experimental site was extensively instrumented to monitor both the environmental conditions and the resulting thermal response at various locations in the deck, roadway, and ground. At the conclusion of the study, 22 months of essentially continuous data had been collected.

The Sybille system proved to be capable of eliminating preferential freezing of the heated bridge relative to the adjacent road. The measured reductions in some of the other freezing parameters that were used to characterize its performance are as follows:

<u>Heated Surface Parameters</u>	<u>Percent Reduction</u>	
	<u>1977/78</u>	<u>1978/79</u>
Snow Cover Time	48	37
Time Frozen	72	57
Integrated Temperature below Freezing (°C Days)	90	79

The integrated temperature below freezing is the area under the freeze line ( $0^{\circ}\text{C}$ ) on a plot of surface temperature as a function of time. This parameter provides a measure of the severity of a freeze period. The performance of the Sybille system was reasonably impressive when one considers that it was heating a bridge exposed to the severe Wyoming climate (the second winter being unusually severe) whereas the West Virginia test was performed in a milder climate on a ramp in thermal contact with the ground. The far field ground temperature at Sybille Canyon averaged  $10^{\circ}\text{C}$  ( $50^{\circ}\text{F}$ ) as compared to  $13^{\circ}\text{C}$  ( $55^{\circ}\text{F}$ ) at the West Virginia installation.

The details of this experimental facility along with much of the experimental data obtained through December of 1978 are presented in a dissertation by Dr. Vic Cundy (15). Since these results are used to help verify the ground heat pipe model presented in this report, additional characteristics of this system will be presented in subsequent chapters.

The success of the small scale Sybille Canyon bridge heat pipe system encouraged the Wyoming Highway Department to pursue the development and testing of a system that would be capable of heating an entire bridge deck. This entailed major changes from previous ground heat pipe designs since the energy cannot be drawn from the ground that is directly below or alongside the heated pavement. The energy must instead be extracted from the ground adjoining the bridge-road interface which requires very long heat pipes as demonstrated by the Spring Creek bridge system in Figure 1.2. This complicates their utilization in bridges since these systems must be field assembled and charged. The Wyoming Highway Department was also interested in these large heat pipes.

SYBILLE HEAT EXCHANGER

SPRING CREEK HEAT EXCHANGER

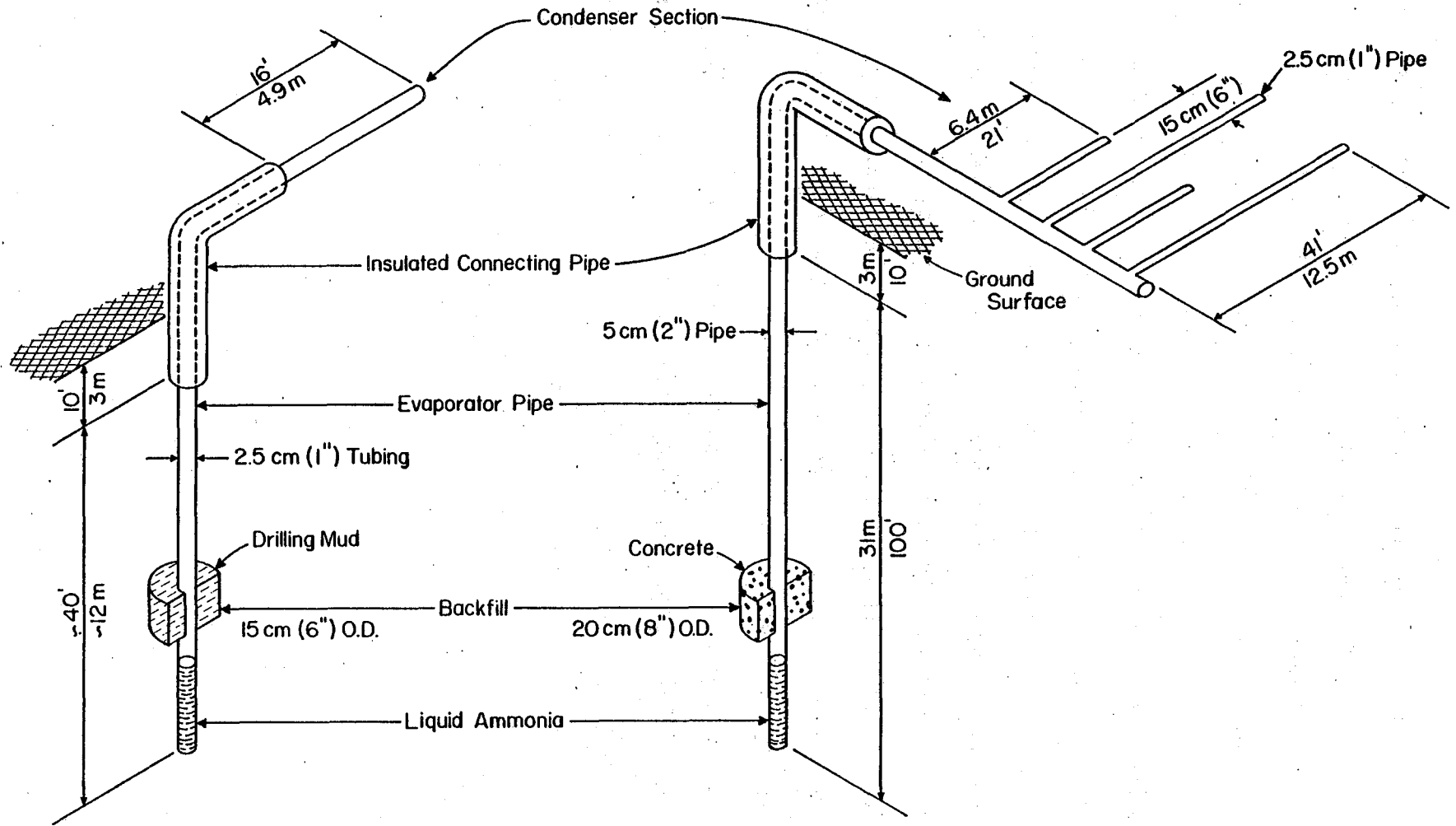


Figure 1.2. Schematic of Sybille and Spring Creek Heat Pipes.

for use in the previously mentioned ramps in Cheyenne and wished to obtain both performance data and some construction experience with them.

The thermal design procedures that were utilized in the earlier heat pipe systems were somewhat simplistic and empirical in nature. The development of a comprehensive analytical model which could accurately predict the dynamic thermal performance of these systems in a given environment was therefore needed. In July, 1980, the Wyoming Highway Department and the Federal Highway Administration contracted with the University of Wyoming to document, evaluate and report on the design, construction and subsequent operation of the Spring Creek bridge heat pipe system; and to prepare a bridge heat pipe design manual for State, County and City design and construction engineers. This document reports on the above scope of work.

Construction of the bridge was completed in the Spring of 1981 in Laramie, Wyoming. The instrumentation and the subsequent performance of this facility from January 1982 to February 1983 are described in a thesis by Mr. John Sackos (20). The refinement of the analytical model and its verification against experimental data from the two Wyoming bridge test facilities were addressed in a thesis by Mr. Ron Lee (21). These two theses should be consulted for details but this report is intended to be a self-sufficient documentation of the Spring Creek heat pipe project.

## II. SPRING CREEK HEAT PIPE FACILITY

Figure 2.1 is a picture of the completed Spring Creek Bridge heat pipe experimental facility in Laramie, Wyoming and Figure 2.2 is its corresponding plan view. The bridge deck is 24.4 meters (80') wide and 18.3 meters (60') long. The unique features of this facility include the sixty large heat pipes, two header pipe vaults, four service vaults, 7.6 cm (3") thick layer of polyurethane insulation on the under side of the heated portion of the deck, an array of thermal and environmental instrumentation, an instrumentation bunker, and a computer controlled data acquisition system.

### A. Heat Pipe System

As depicted in Figure 1.2, four condenser pipes were manifolded to each evaporator pipe which eliminated the need for placing one evaporator in the ground for each condenser pipe in the deck, and introduced some economies of scale that did not exist in the previous single pipe systems. In an effort to further reduce costs and simplify installation, the Spring Creek heating system was modularized as much as possible. The evaporator pipes, interconnecting pipes, and manifolded condenser sections that characterized this modular design (Figure 2.3) are detailed in Appendix A.

The evaporator pipes were constructed from 2" (5cm) schedule 80 steel pipe with a spiral groove machined on the internal surface to enhance the wetting of the wall by the returning condensate. Previous

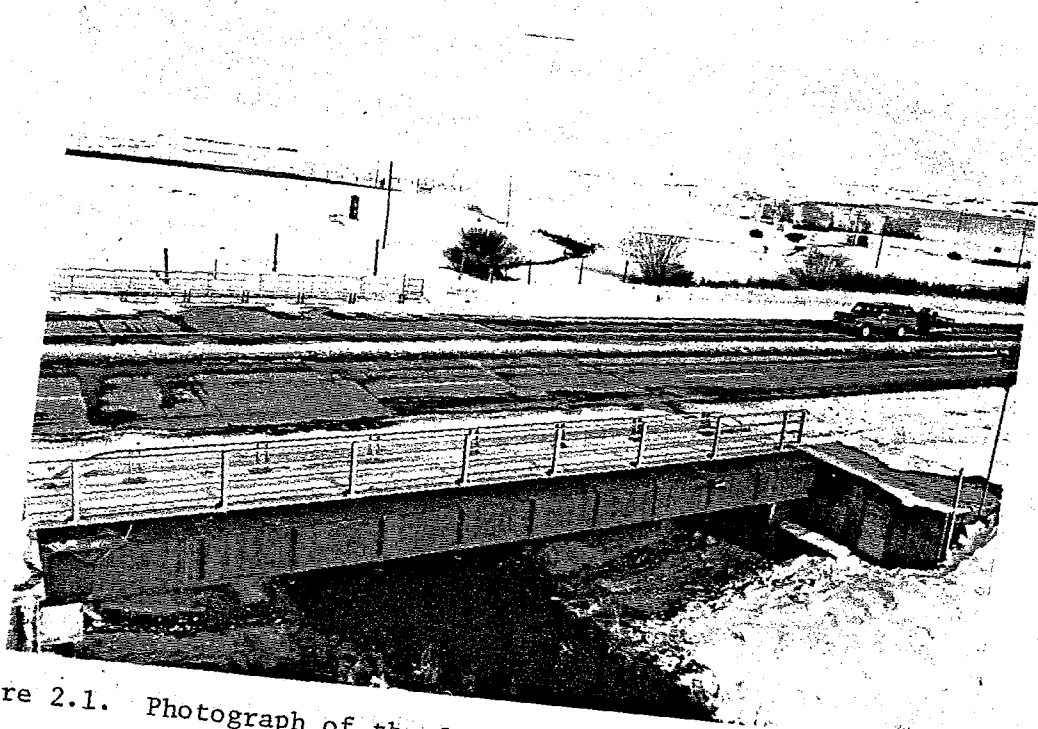


Figure 2.1. Photograph of the Spring Creek Heat Pipe Test Facility.

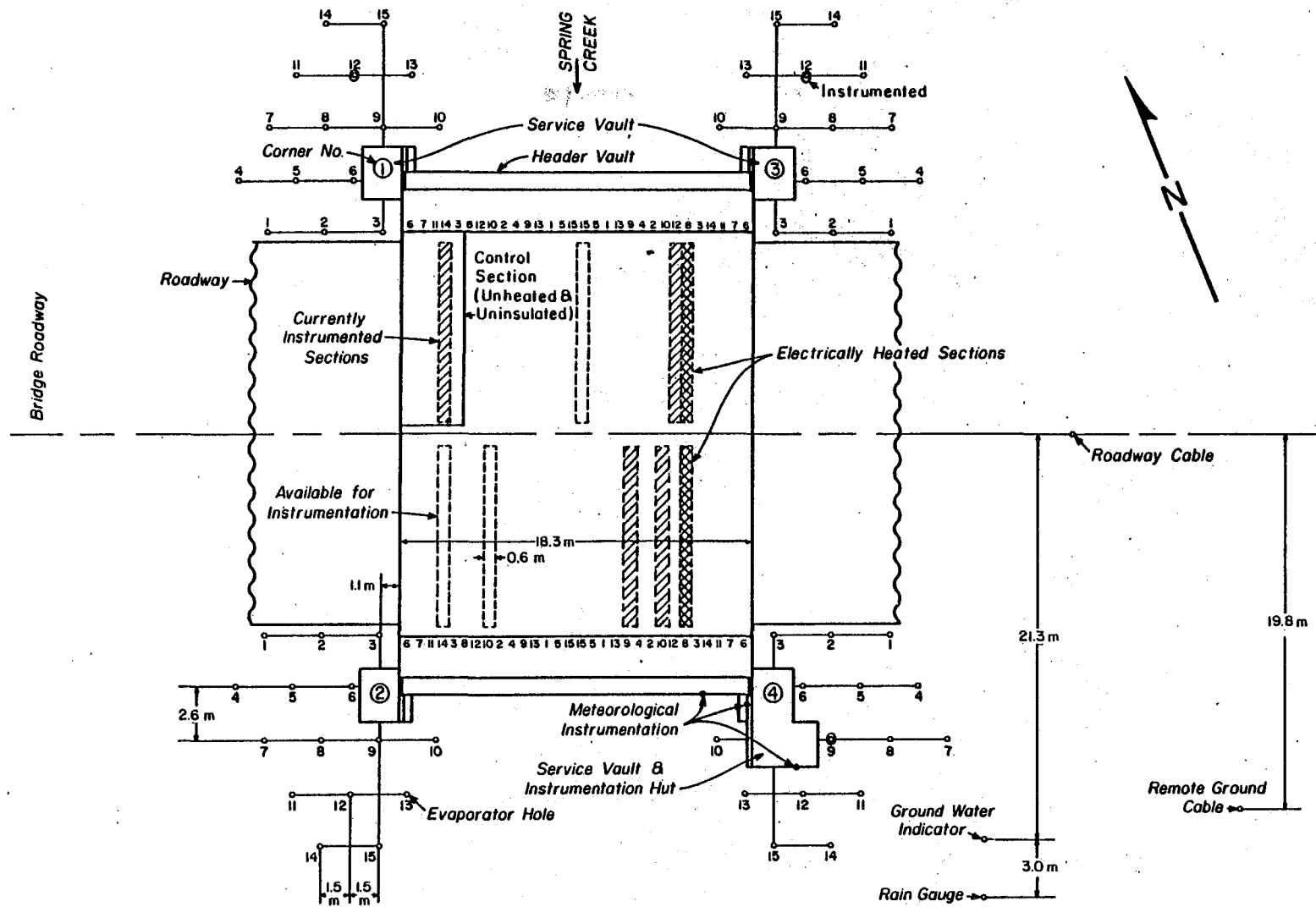


Figure 2.2. Plan View of the Spring Creek Heat Pipe Test Facility.

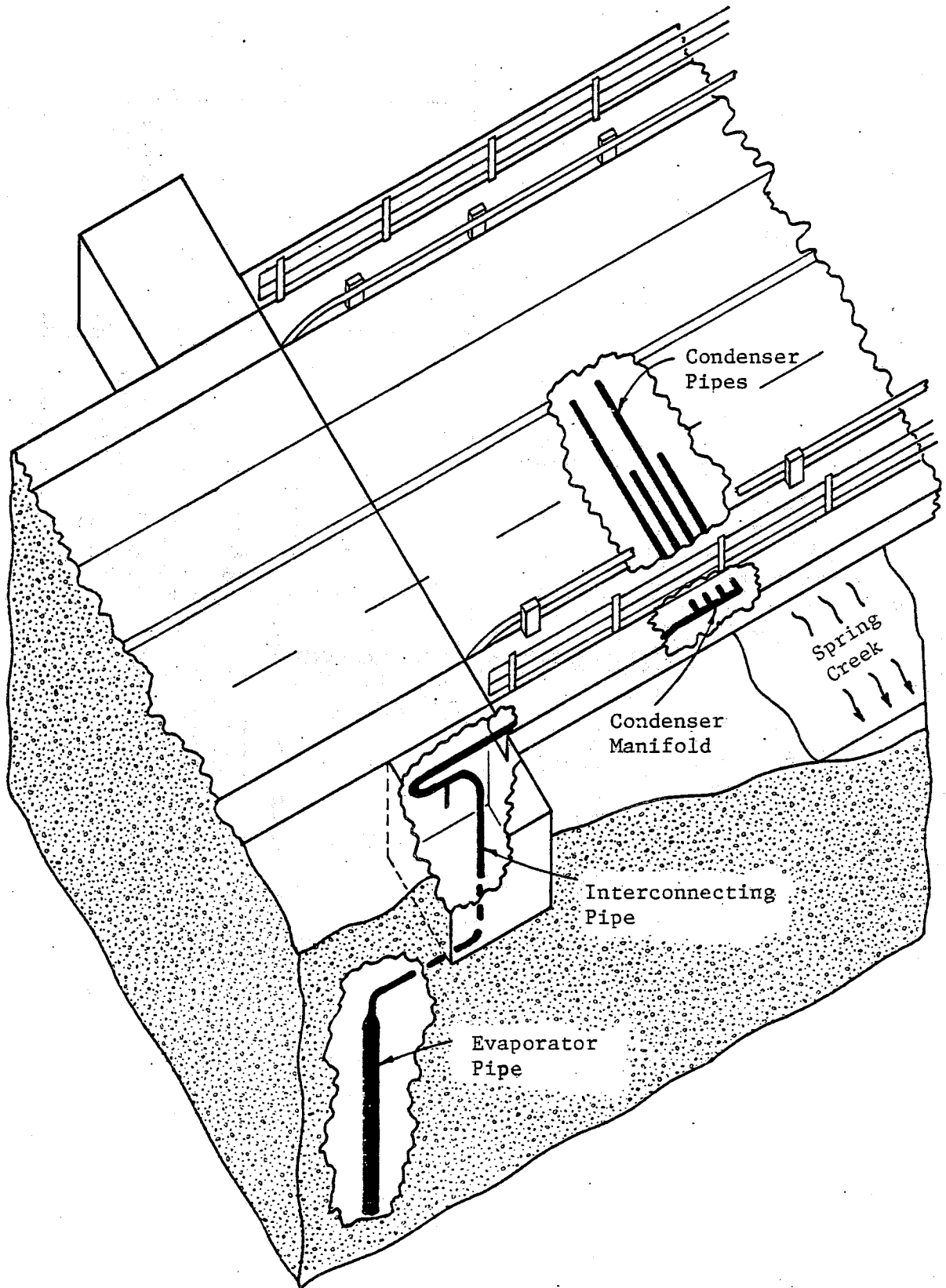


Figure 2.3. Schematic of the Spring Creek Heat Pipe System.

designs had utilized wire springs to increase the wetting of the evaporator walls (8,13,16). The internal surfaces of each heat pipe were grit blasted and cleaned with inhibited trichlorethylene.

The evaporator pipes were butt welded together in 30.5 m (100') lengths with a plug welded in the bottom. After the final pipe butt weld had been completed in the field (Figure 2.4), each evaporator was successively evacuated (Figure 2.5), pressurized with dry nitrogen, leak tested at all welds, temporarily sealed at its top, and inspected for any damage to the external epoxy coating. The evaporators were hoisted into predrilled 20 cm (8") diameter holes and the holes were backfilled with a high thermal conductivity grout (Figures 1.2 and 2.6) to increase the apparent thermal conductance between each evaporator and the surrounding earth. Figure 2.4 shows the temporary plastic casings that were placed in the top 6 m (20') of the evaporator holes to prevent them from caving in. Fifteen evaporator pipes were located on 3 m (10') centers in the ground at each corner of the bridge (Figure 2.2).

The pipes which connected each evaporator to its respective condenser section in the bridge deck were insulated to a 3 m (10') depth to reduce the energy loss to both the air and the cold upper ground levels (Figure 2.6). These connecting pipes and the condensers were all constructed from 1" (2.5 cm) schedule 40 pipe, and a minimum grade of 2% was specified throughout these components to ensure condensate drainage back to the evaporators.

The condenser sections (Figures 1.2 and 2.3) were manufactured by welding four parallel pipes on 15 cm (6") centers to a manifold pipe and sealing the other end of each condenser pipe with a welded plug. The lengths of the condenser pipes alternated between 12.5 m (41') and 6.4 m

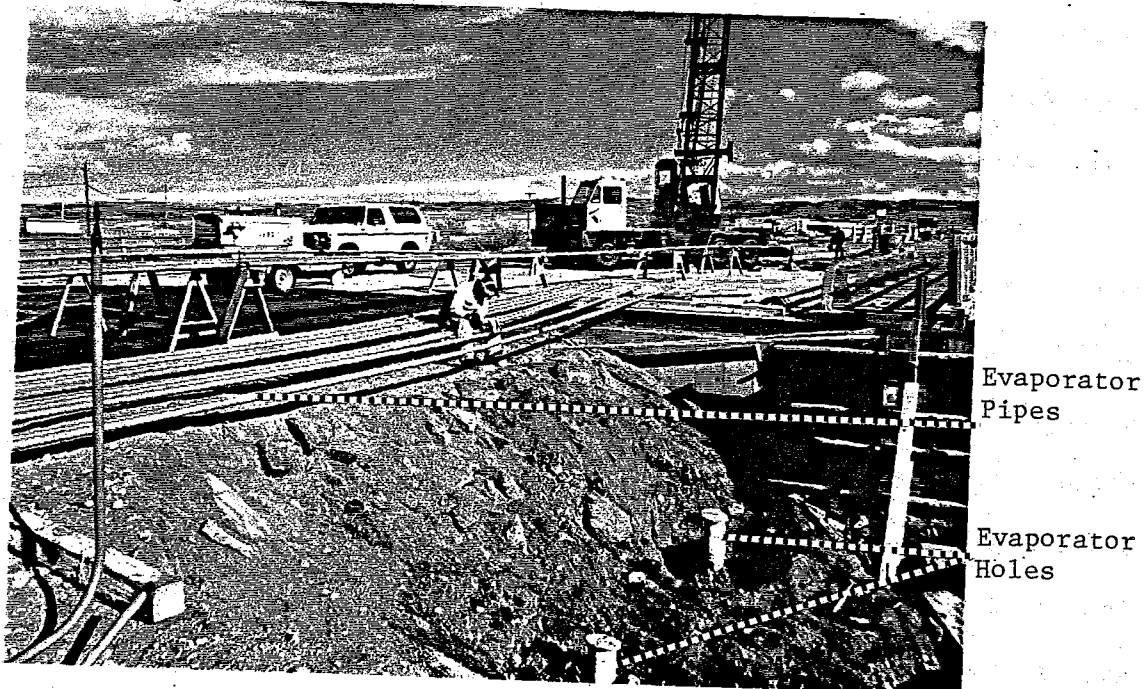


Figure 2.4. Evaporator Pipes Under Construction and Two Evaporator Holes.

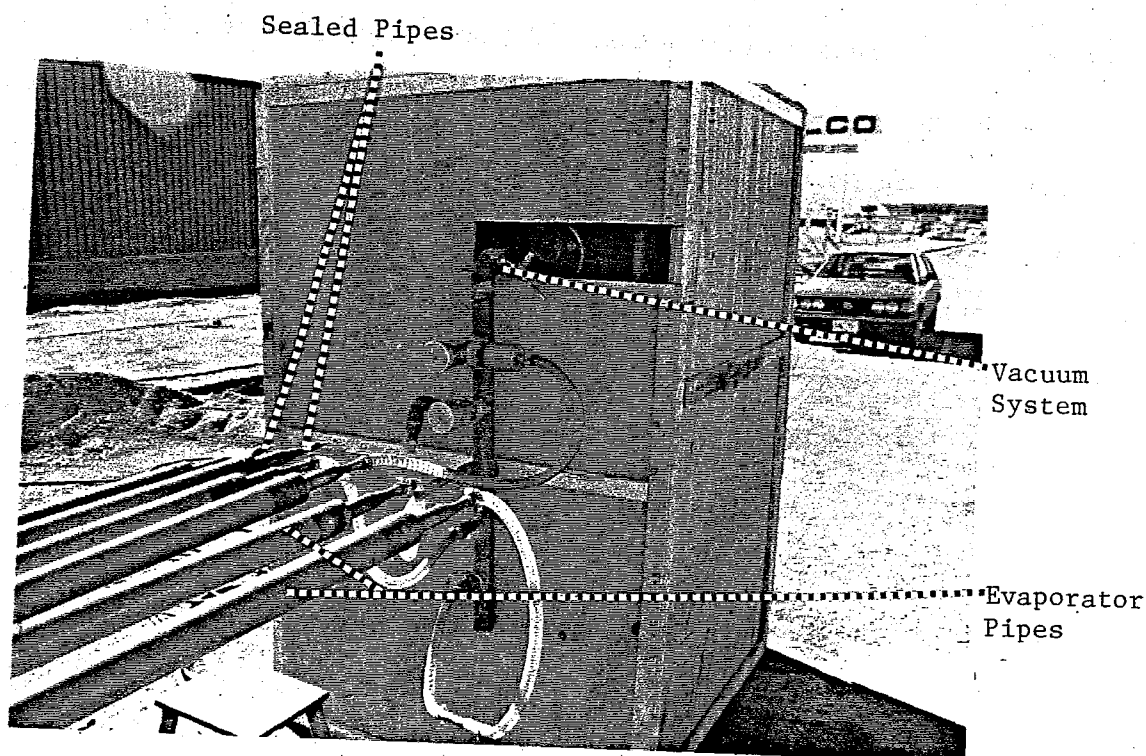


Figure 2.5. Evacuation of Evaporator Pipes at Construction Site.

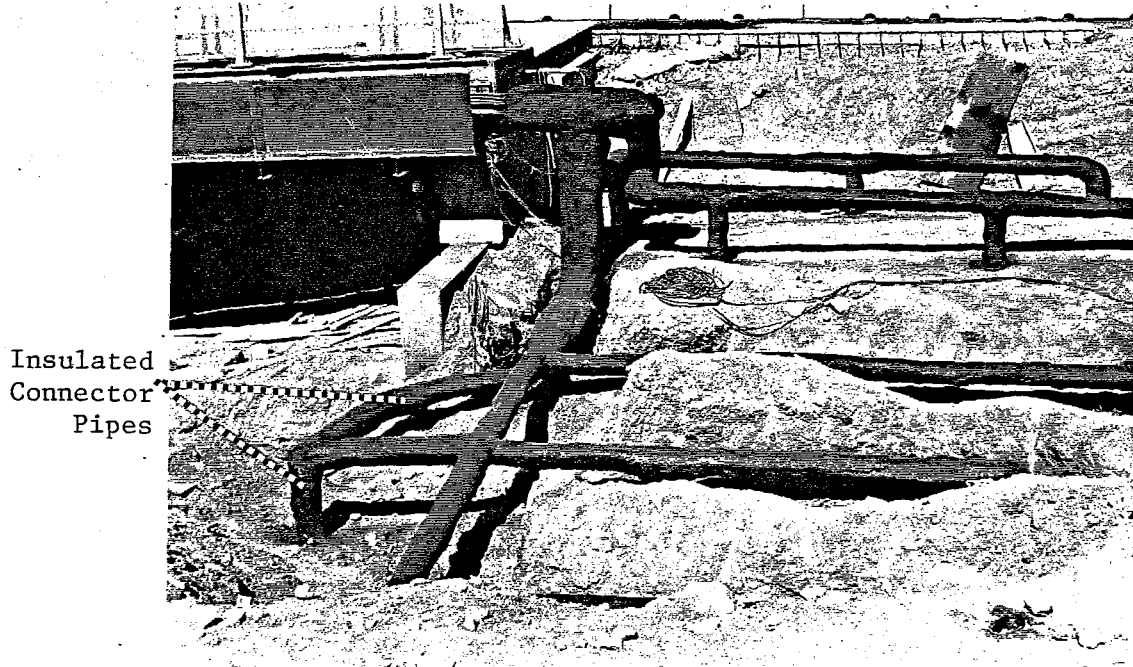
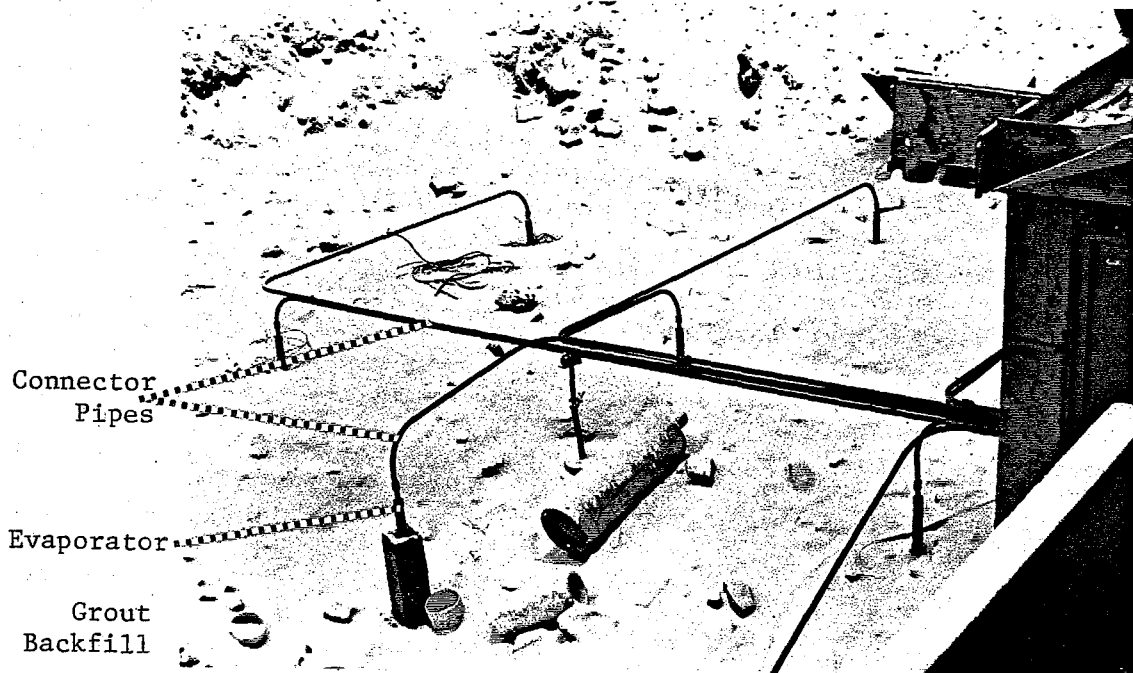


Figure 2.6. Connector Pipes Before and After Insulation.

(21') so that half of the pipes extended from the manifold on the side of the deck to the center line of the bridge, while the other half only extended through the outer traffic lane. The preferential heating of the outer two lanes was a cost cutting measure. Each condenser section heated approximately 7.6 square meters (82 ft<sup>2</sup>) of bridge deck surface area. Figure 2.7 illustrates the positioning of the manifolded condenser sections along the side of the bridge deck prior to the manifolds being foam insulated and enclosed in the header vault. Exposed condenser pipes can be seen extending into the deck from their respective manifolds, along with the connecting pipes that run alongside the bridge between the manifolds and the service vaults located at the corners of the bridge. The connecting pipes from an evaporator and its corresponding condenser were socket welded together with a tee that contained a service nipple to permit the evacuation and ammonia charging of the heat pipe (Figure 2.8). Each heat pipe was charged with 3 kg (6.5 lbs) of ammonia which produced around a 0.3 m (1.0') high liquid level at the bottom of the evaporator to ensure that the ammonia remained in the liquid-vapor state over the operating temperature range of the system.

Examples of the special provisions that are required in the construction of the heat pipe system are presented in Appendix B. These include provisions for the earth work and grouting required in the installation of the evaporators and interconnecting pipes; pipe shop and field fabrication, installation, charging and inspection; and the insulation of the interconnecting pipes.

#### B. Data Acquisition System

Figure 2.9 shows the data acquisition system in a university

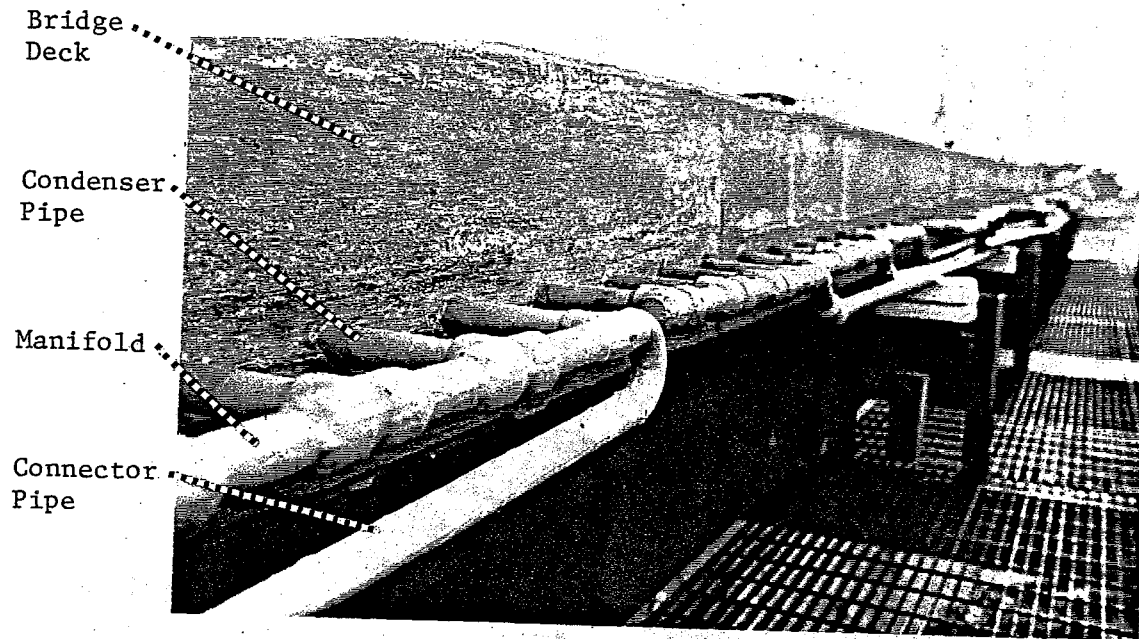


Figure 2.7. Photograph of Condenser Manifolds Prior to Insulation.

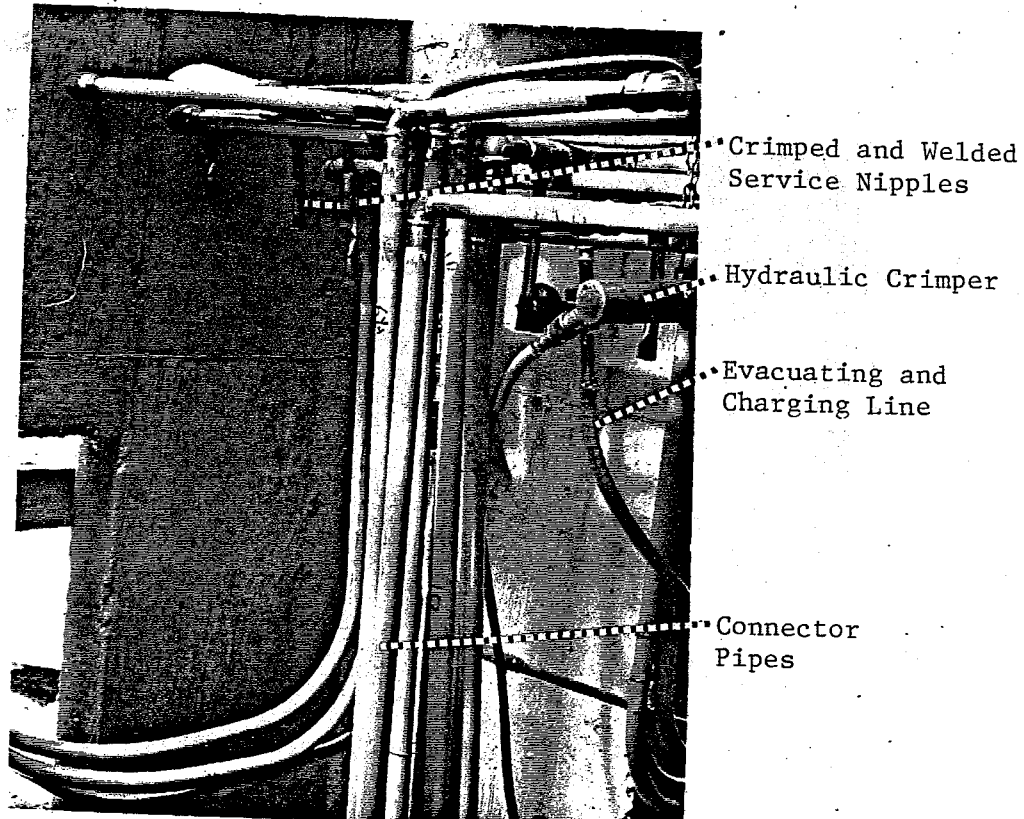


Figure 2.8. Interconnecting Pipes Inside Service Vault.

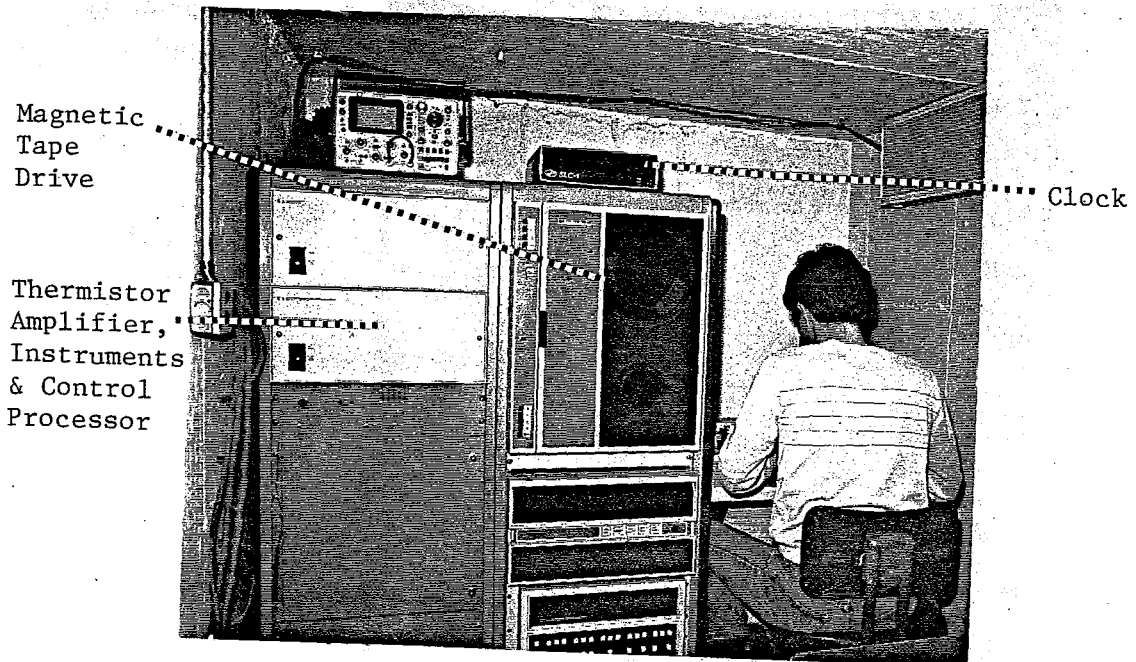
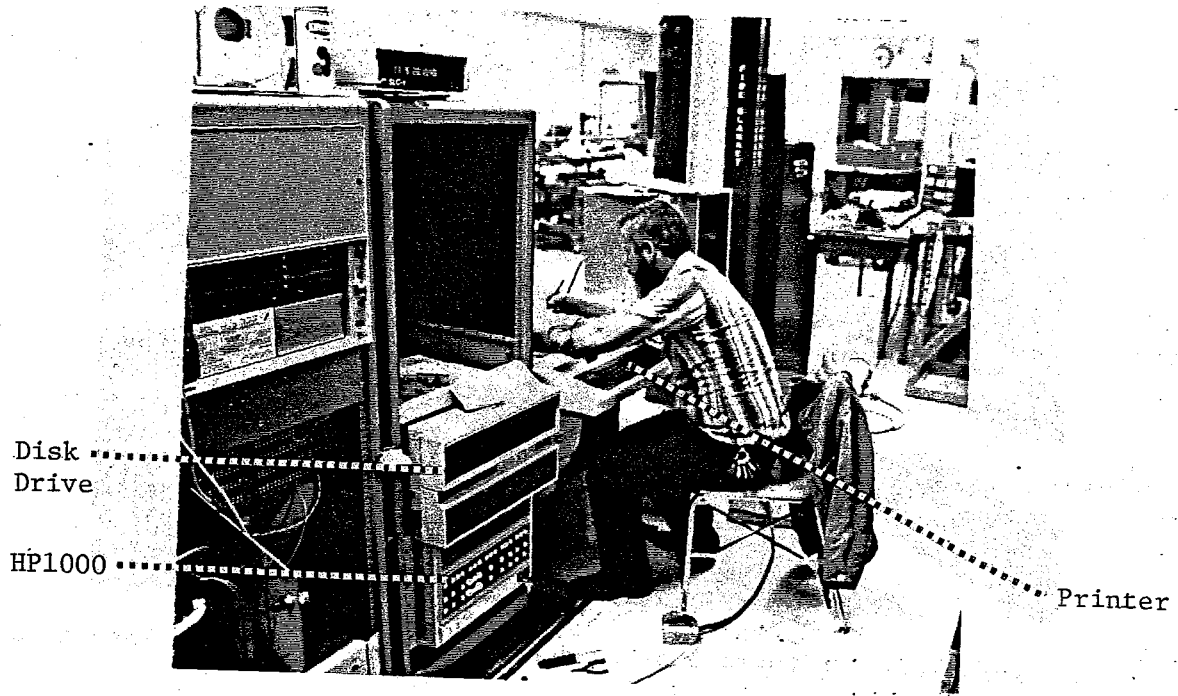


Figure 2.9. Photographs of the Data Acquisition System during its Assembly and in the Instrumentation Vault.

laboratory during its initial assembly and calibration, and in the instrumentation vault at the Spring Creek site. The two computer racks contain a Hewlett-Packard 1000 series programmable computer with a RTE:II software system and a 32K 2100S processor, an H.P. 5M byte disk drive, an H.P. 800 b.p.i. - 9 track tape drive, a power supply, a panel of relay strips to which the 176 thermistor leads from the 24 instrumentation cables were connected, a thermistor amplifier panel, an H.P. extender unit and an H.P. 2240A instrumentation and control processor. The data system also included a Digital Pathway's SLC-1 battery operated back-up clock to aid in the automatic restart of the computer system after a power failure, and a Deckwriter-II terminal for both system programming and monitoring. The system was configured to monitor a maximum of 48 of the 176 temperature sensors that were installed. This report details the heat pipe performance for the period from January 1982 through November 1983 during which the data acquisition system was operational 83% of the time.

### C. Instrumentation

The environment at the Spring Creek facility was characterized by the measurement of ambient air temperature, wind speed, wind direction, solar radiation, relative humidity, barometric pressure, precipitation, and the ground water level. The transducers used to measure these parameters, including their ranges and accuracies, are listed in Table 2.1. Figure 2.10 presents a photograph of the placement of these instruments. All the meteorological instrumentation functioned as intended except for the rain gage and the ground water level which were each erratic at times.

The surface conditions of the bridge deck and the adjacent roadway

TABLE 2.1. METEOROLOGICAL INSTRUMENTATION

Parameters	Sensor	Sensor Range	Sensor Accuracy	Measurement Accuracy
Relative Humidity	General Eastern Model 400-C	0-100%	±0.5%	±0.5%
Solar Radiation	Eppley Labs	0 - 1400 W/m <sup>2</sup>	±1.0%	±14 W/m <sup>2</sup>
Wind Speed	Electric Speed Indicator Model 420C-1-SS	0 - 51.4 m/s	±1.0%	±0.514 m/s
Wind Direction	Electric Speed Indicator Model 420C-R2	0 - 360 degrees	±1.0%	±3.6 degrees
Barometric Pressure	H.E. Sostman Co. Model 2014	48.8 - 65.3 cm. Hg.	±0.1%	±0.165 cm. Hg.
Precipitation	Belfort	0 - 30.5 cm.	±0.25%	±0.08 cm.
Ground Water Level	U.W. constructed	0 - 9.2 m	±1.0%	±0.003 m

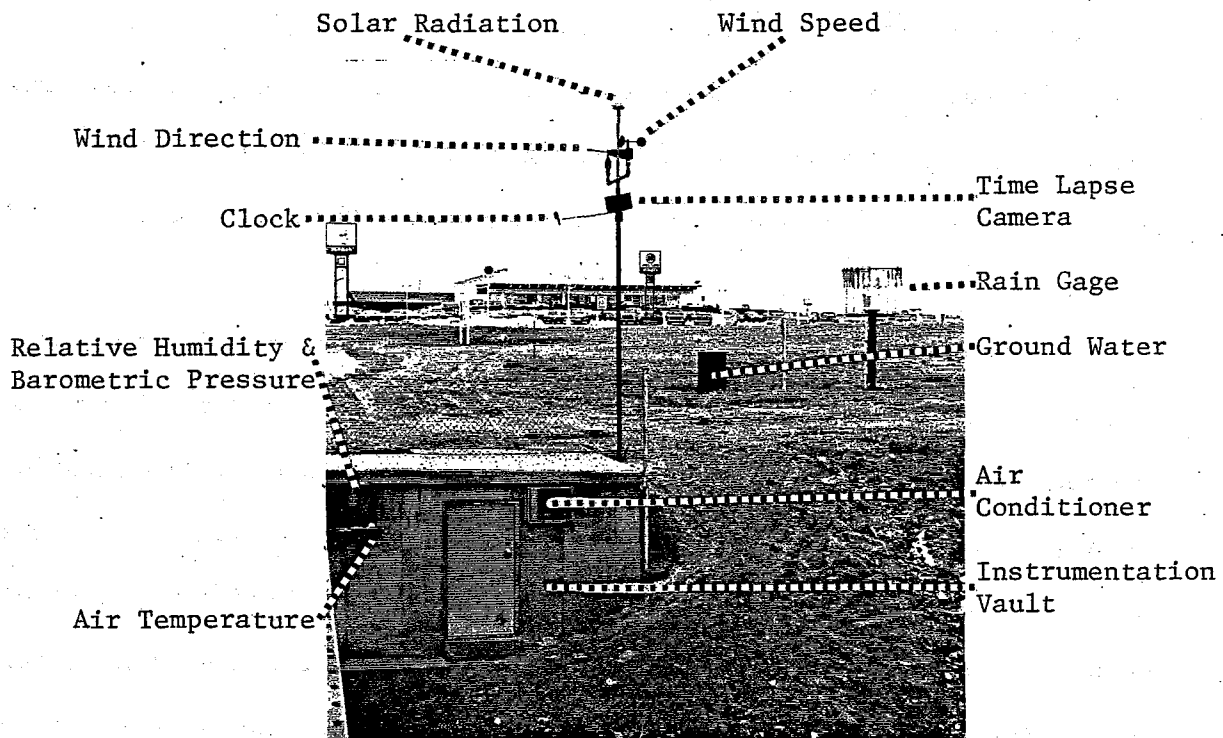


Figure 2.10. Photograph of the Meteorological Instrumentation.

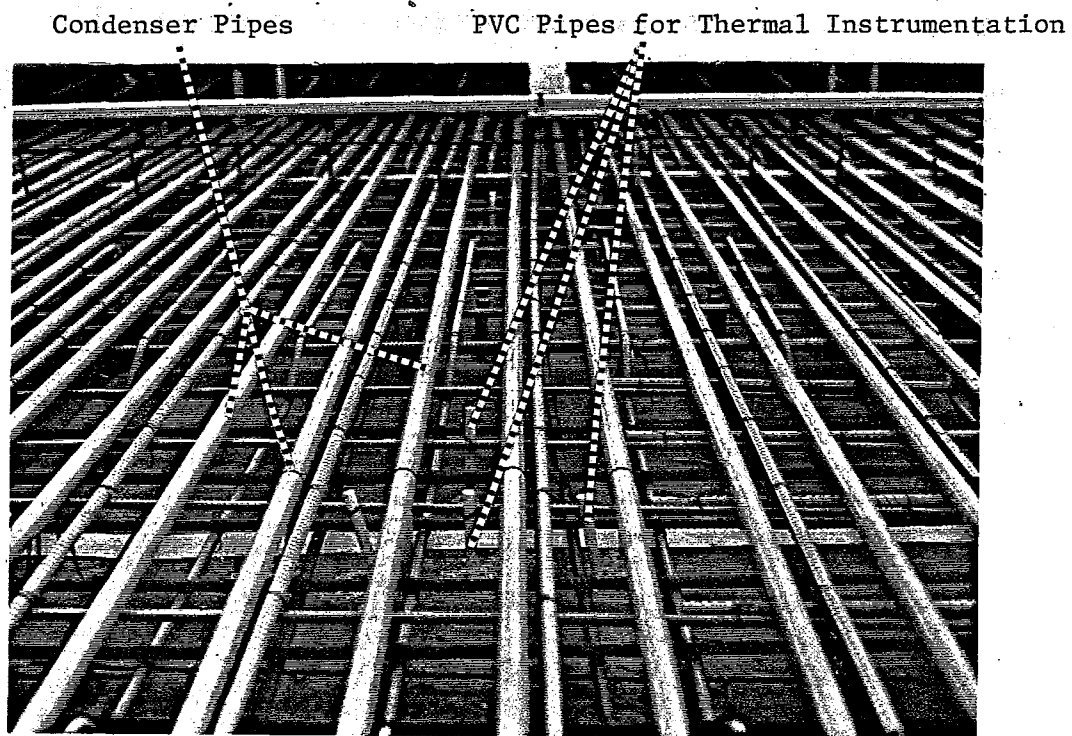


Figure 2.11. Temperature Instrumentation PVC Pipes in Bridge Deck.

were monitored with a time lapse camera which is also pictured in Figure 2.10. One photograph was taken every ten minutes during the daylight hours. Each exposure included an analog clock in the field of view so that the photographic record could be merged with the computer generated record.

To measure the thermal response of the deck, capped PVC pipes were inserted through the bottom of the bridge deck's concrete forms and secured to the rebar (Figure 2.11) at predetermined instrumentation locations prior to the concrete pour. After the construction of the bridge was completed, instrumentation cables were pulled through steel conduit from the various instrumented sites into the instrumentation vault. The PVC caps were then drilled through to the desired depth (Figure 2.12), and a thermistor probe was inserted into each hole and secured in place. These probes were coated with grease to improve their thermal contact with the deck. As depicted in Figure 2.13, temperatures were taken on the top surface, on condenser pipes, on the midplane, and on the bottom surface of the bridge deck.

All temperature measurements at the Spring Creek site were made with YSI 44203 Thermilinear Thermistor Networks<sup>TM</sup>. This is a composite device consisting of resistors and a precision thermistor which produces an output resistance that varies linearly with temperature. An output voltage that is essentially linear with temperature is therefore produced when this network is supplied with a constant and precise current. This voltage is then sampled and recorded by the data acquisition system. One pair of wires on each earth and bridge deck temperature cable was attached to a precision fixed resistor to monitor

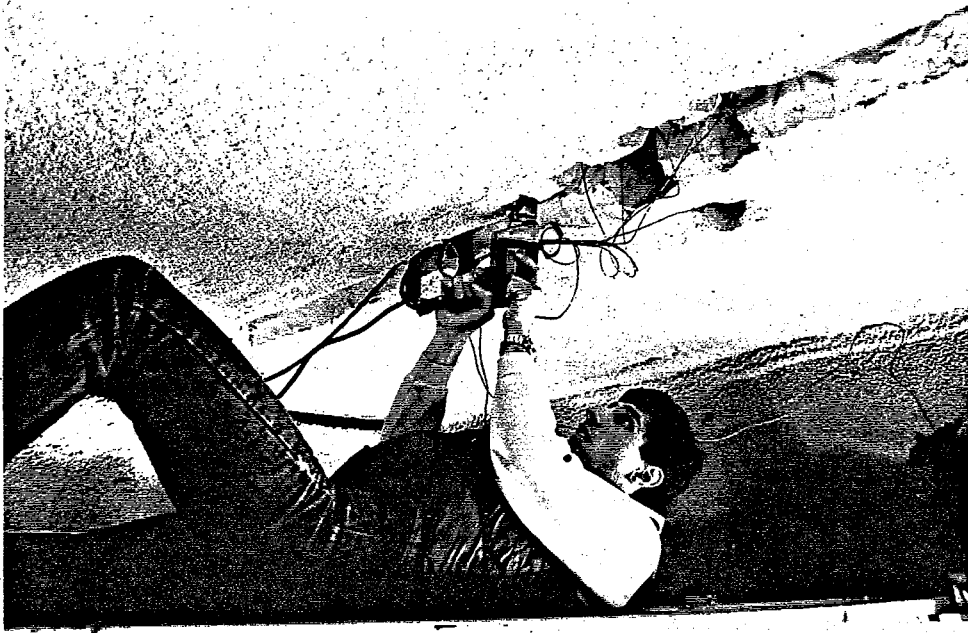


Figure 2.12. Placement of Thermistors in Bridge Deck.

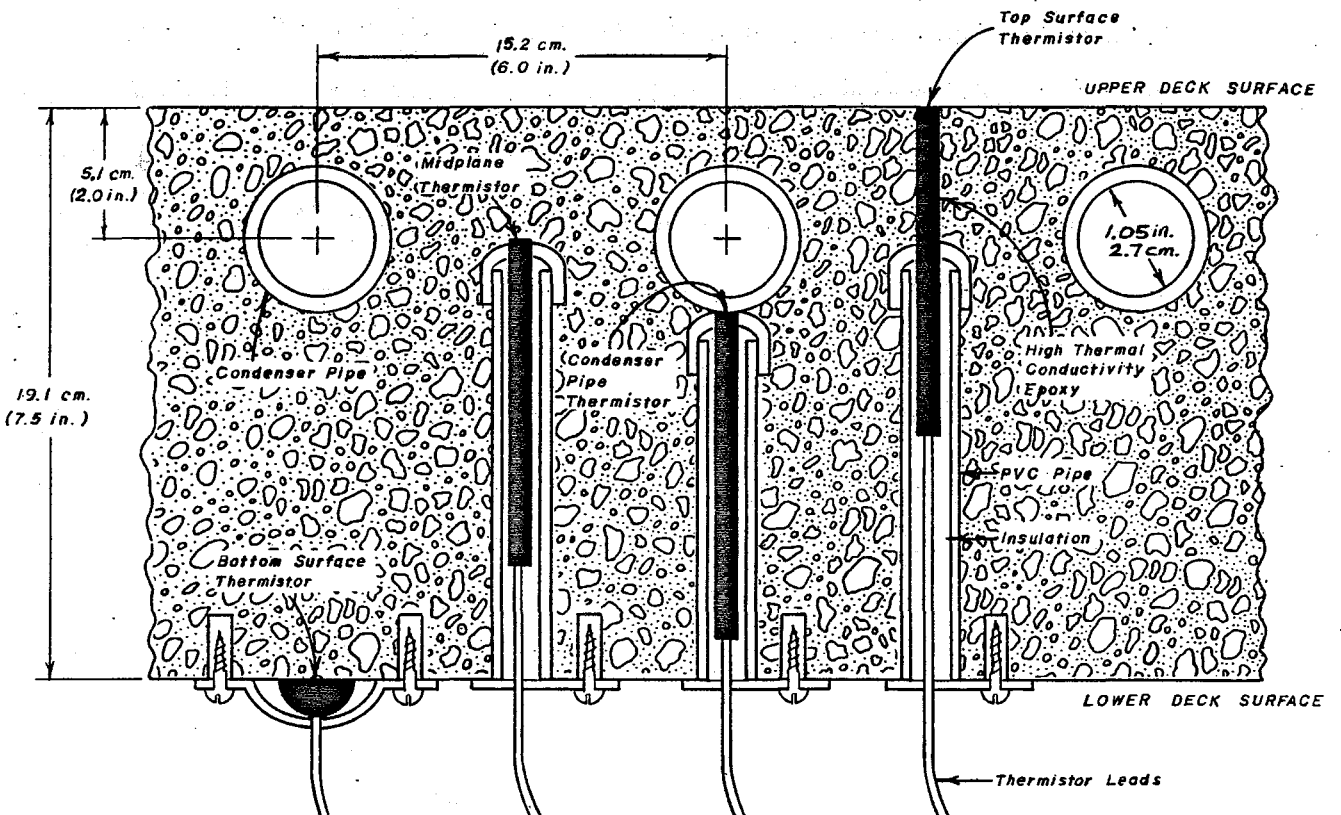


Figure 2.13. Thermistor Locations within the Bridge Deck.

the precision current source, to permit continuous system calibration and to flag problems in a given cable.

Ten 11-pair and seven 3-pair ground instrumentation cables were also constructed to permit the temperature measurement at 118 ground locations. One 11-pair and one 3-pair cable were attached to each of five heat pipe evaporator sections prior to their installation into the ground. The 11-pair cables were designed to measure the evaporator pipe temperatures at locations along the lower 26 meters (85') of the pipe while the 3-pair cables measured temperatures on the upper 4.6 meters (15') of the pipe (Figure 2.14). Although care was taken in installing the instrumented evaporator pipes, the uncontrollable motion of the pressurized concrete grouting nozzle and tube used to backfill the evaporator holes punctured the protective sheath of all the evaporator instrumentation cables. The subsequent penetration of ground water into these cables produced a fluctuating thermistor resistance when measurements were attempted. This eventually caused all of these thermistors to give erroneous measurements. In an effort to ensure the safe installation of instrumentation cables on some evaporators, a 1" (2.5 cm) steel pipe was welded along the length of two evaporator sections (pipe number 12 in corners 1 and 3, Figure 2.2) prior to their installation. Instrumentation cables were installed in these two protective pipes, and the pipes were filled with transformer oil to increase the thermal contact between the encased thermistors and the attached evaporator and the surrounding earth.

Of the remaining ground cables, one 11-pair cable was used to instrument two interconnecting pipes in corner 4 (pipes 8 and 9), while the final two 11-pair and 3-pair cables were used to instrument one

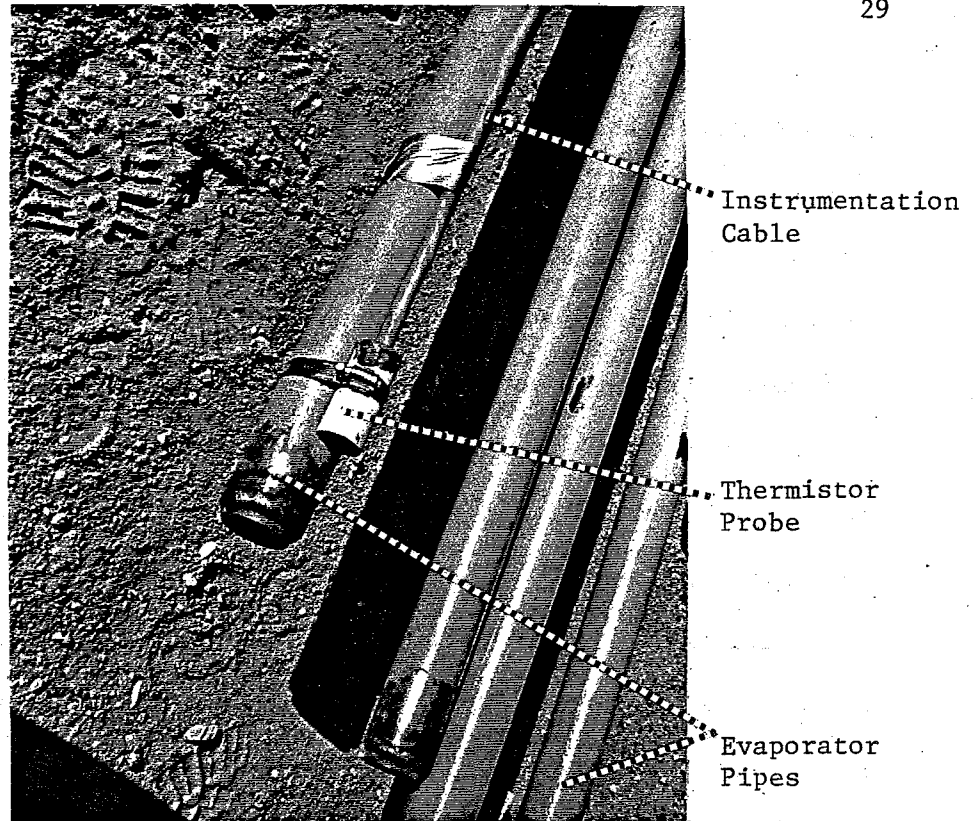


Figure 2.14. Ground Evaporator Pipe with Temperature Instrumentation.

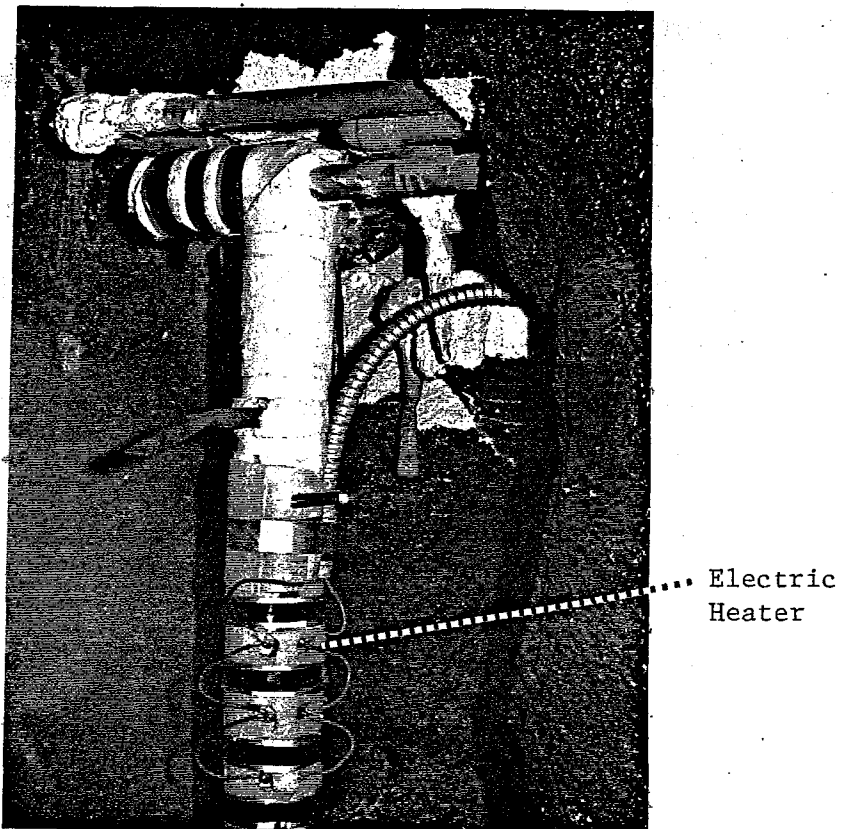


Figure 2.15. Electrically Heated Evaporator.

remote ground location and the ground beneath the center line of the roadway (see Figure 2.2). The procedure used to instrument these last two locations consisted of drilling a 20 cm (8") diameter, 30 meter (100') deep hole into the earth, lowering an instrumentation cable into the hole, and then backfilling it with sand. Temperature probes were positioned near the surfaces of both the ground and the asphalt road. The roadway cable failed when it slipped approximately 1.5 meters (5') due to the backfill sand washing away. The top surface roadway temperatures and field observations indicate that the cave-in occurred on 10/13/82. This situation was corrected on 1/24/83 when the cable was repositioned and the hole was pressure grouted with concrete.

To measure the power transmitted by the ground heat pipes, a section of the interconnecting pipe through the service vault was removed from heat pipe number 8 in corners 3 and 4 (Figure 2.2). A reservoir with three 500 watt pipe heaters was welded to the condenser side of each of these two heat pipes (Figure 2.15). These reservoirs were charged with ammonia and heavily insulated. The computer system monitored the condenser temperatures of these two electrically powered heat pipes and two corresponding earth coupled heat pipes (pipes 12 and 10 in corners 3 and 4, respectively) and minimized the condenser temperature difference between an earth and electric powered pair by controlling the power to the electric heaters. The electric power to each of these electrically powered heat pipes was included in the experimental record as a measure of the power supplied by the ground heat pipes.

### III. SPRING CREEK EXPERIMENTAL RESULTS

Data acquisition was initiated at the experimental facility in January of 1982 and continued through December of 1983. Fifty-five environmental and temperature data channels were digitized and recorded every ten minutes except when system failures and maintenance caused interruptions. Over the two year study period, 83% of the experimental record was obtained and the completeness of this record on a monthly basis is delineated in Table 3.1.

The Laramie winter climate is quite severe since the site elevation is 2208 m (7244') and the latitude is 41°N. Table 3.1 indicates that the average annual air temperatures during the two years monitored in this study were only 5.2°C and 4.7°C respectively while the thirty year average is reported in reference 25 to be 5.9°C. The monthly average air temperatures were below or near freezing for eleven of the twenty-four months. December 1983 had both the coldest average monthly air temperature at -10°C and the coldest instantaneous temperature of -35°C. The temperature difference between the diurnal maximum and minimum temperatures were typically 15°C in January and 17°C in July.

The mean wind speed over the full two years was 3 m/s (6.8 mph) while the average was around 3.2 m/s (7.2 mph) during the significant heating months. The measured prevailing wind direction was from the SSW while the bridge deck orientation is 110°.

Laramie has a dry climate. The measured average winter relative

TABLE 3.1. MONTHLY METEOROLOGICAL PARAMETERS AT THE SPRING CREEK FACILITY.

Month/Year	Ave. Air Temp. (°C)	Ave. Wind Speed (m/s)	Ave. Daily Solar <sub>2</sub> (MJ/m <sup>2</sup> )	Precipitation mm water		% data Recorded**
				Spring Creek	Brees* Field	
1/82	-4.4	3.7	10.0	-	5	84
2	-4.1	3.3	13.5	-	3	99
3	0.6	3.8	16.0	-	9	97
4	3.1	4.0	21.2	-	14	99
5	8.3	3.1	20.1	-	54	85
6	13.3	3.2	23.9	-	20	96
7	18.0	2.8	23.9	-	21	81
8	18.7	2.6	21.5	-	26	79
9	12.2	2.7	15.5	67	42	98
10	4.7	3.3	13.5	14	9	92
11	-2.1	2.9	9.8	-	23	57
12	-6.3	3.1	7.9	-	48	80
1/83	-2.9	2.8	8.5	4	4	97
2	-2.2	2.8	11.7	0	2	76
3	-1.2	3.5	17.5	30	62	85
4	-0.6	2.9	22.3	97	94	97
5	7.0	3.7	23.9	25	32	93
6	12.3	2.6	21.6	66	51	78
7	18.6	2.7	25.3	42	24	84
8	19.7	2.3	21.9	16	31	94
9	16.2	2.9	20.6	10	11	67
10	6.6	2.2	12.2	18	14	51
11	-7.3	3.4	7.5	-	64	41
12	-10.1	2.9	7.9	16	10	79

\* Brees Field Airport, Laramie, Wyoming

\*\* Air temperature, wind speed and solar radiation

humidity at the experimental site was only 21% even though the bridge crosses a small creek that flows throughout the winter. The city's mean annual precipitation is normally 283 mm (11.1") of water with approximately half of this precipitation falling as snow. Because of mechanical problems with the rain gage, the precipitation record that is presented in Table 3.1 is incomplete and some of the monthly entries are possibly inaccurate. For comparison, the precipitation that was measured at Brees Airfield, which is approximately 8 km west of Laramie, is also presented in Table 3.1. The annual precipitation totals that were measured at Brees Field during the two year experiment were 274 and 399 mm of water.

The solar intensity in Laramie is higher than most cities at its latitude because of the predominance of clear, dry skies and its low barometric pressure, 79.1 kPa (11.5 psia). The average daily levels of insolation measured at the site by a horizontal pyranometer (Figure 2.10) are also tabulated in Table 3.1 by month.

The site geology around the evaporators is characterized by reddish brown silt stone bedrock overlaid with 2.3 to 2.7 meters of sandy silt and gravel. The 2.7 to 3.7 meter thick surface layer is composed of silt and silty sand with rock fragments. Two local faults and the resulting fracturing give the bedrock a high permeability to water. The ground water table level varied during the study between 3.2 and 5.7 meters below the surface. Most of the earth encasing the evaporators is therefore saturated which is very beneficial because it increases the ground's thermal conductivity and insures good thermal contact between the ground and the evaporators.

Figure 3.1 presents the measured daily averaged undisturbed ground

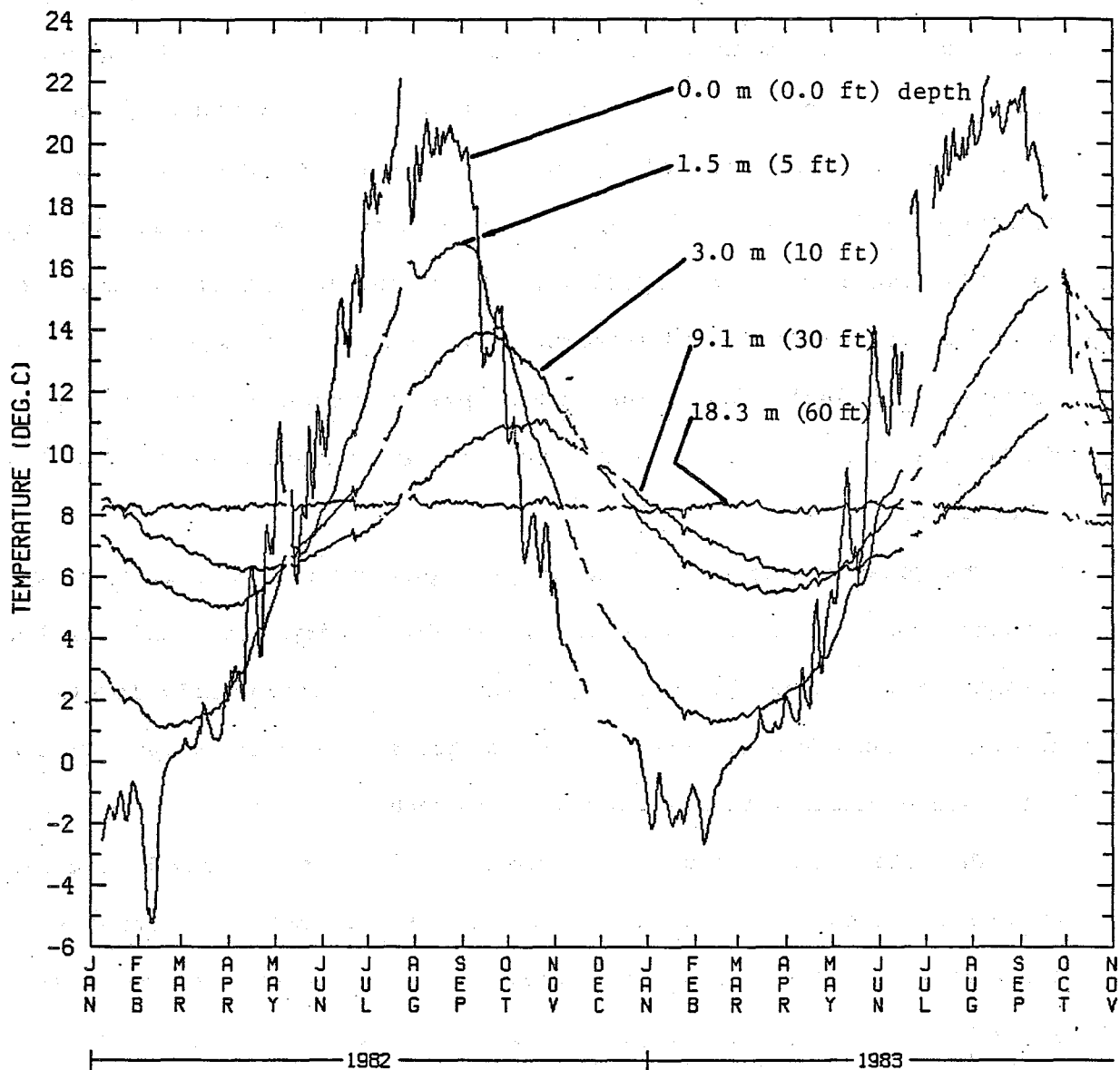


Figure 3.1. Daily Average Remote Ground Temperature Distributions Versus Time.

temperature profile from the surface down to a depth of 18 m (60') over a 23 month period. The three most important points that this figure illustrates are: 1) the ground temperature is essentially constant below 15 meters, 2) this constant ground temperature is only 8°C above freezing, and 3) the warmest ground temperatures occur during the early winter months around the upper portion of an evaporator. As depicted in Figure 1.2, the evaporators were placed approximately 3 m (10') below the ground surface and their connector pipes were insulated to avoid energy losses to the cooler upper ground levels. Table 3.1 indicates that the mean air temperature was below the invariant ground temperature of 8°C for fifteen out of the twenty-four months monitored. The experimental data also supports the rule of thumb that the invariant ground temperature is typically 2 to 3°C above the long-term mean ambient air temperature.

Although the remote ground temperature represents the theoretical temperature potential of the system, the temperature field encasing the evaporator pipes is depressed due to energy extraction. This thermal depression can degrade the system's performance with time, and its magnitude is a complicated function of the amount and rate of energy extraction as well as the evaporator field's thermal recovery over the summer. Figure 3.2 compares the weekly average temperature history of evaporator pipe number 12 in corner 3 (see Figure 2.2) at a 23 m (75') depth to the remote ground temperature at 18 m (60'). This figure also includes the maximum and minimum weekly evaporator temperatures and these data indicate that the evaporator temperature was as much as 10°C below the far field ground temperature and that it fell below the freeze line on several occasions. The significant temperature depression that

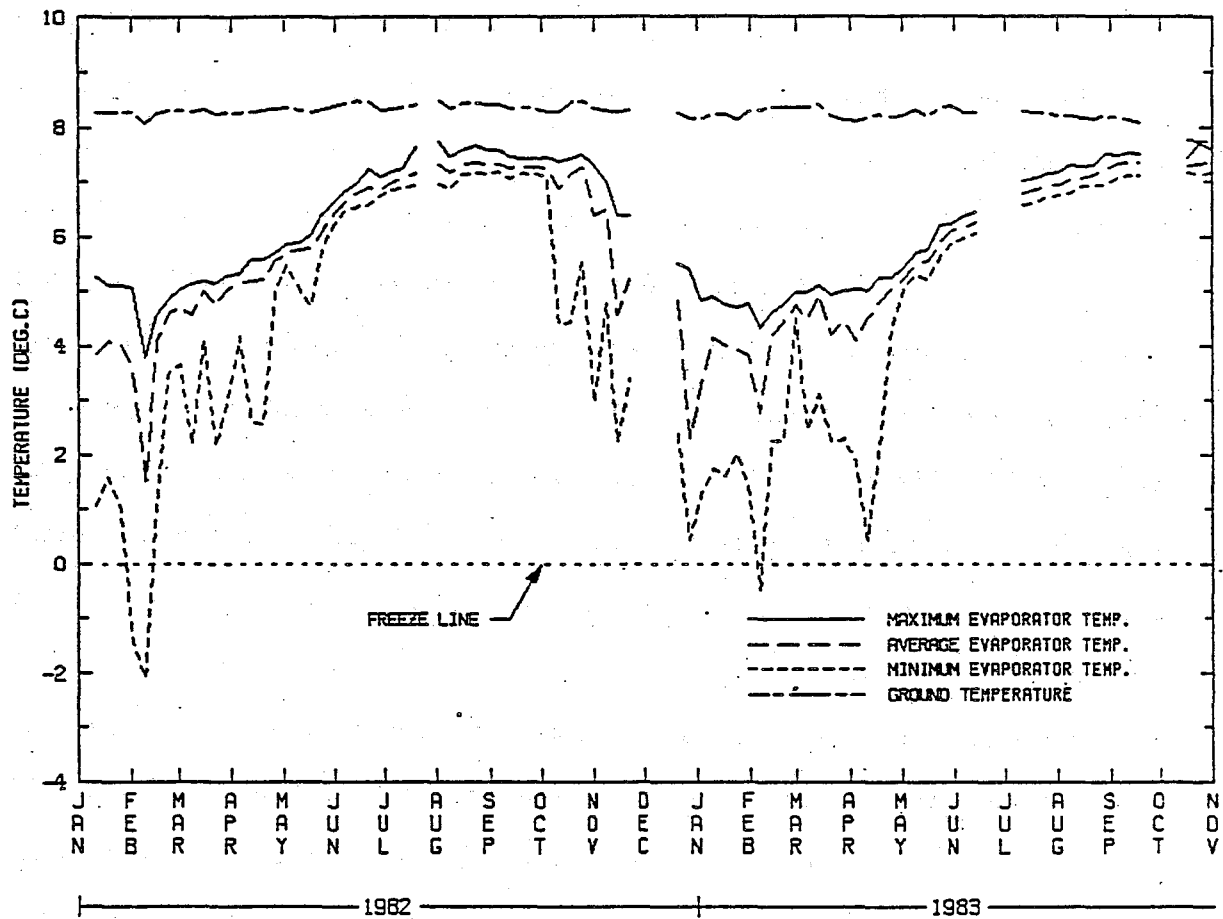


Figure 3.2. Weekly Averaged Evaporator and Ground Temperatures.

occurred in the ground adjacent to the evaporator can be inferred from the maximum evaporator temperature line in this figure since these values were generated during intervals when the heat pipe was not operating. This ground depression reached a maximum value of  $4^{\circ}\text{C}$  in early February of 1982.

The ground heat pipe field recovers in the summer when there is essentially no load applied to the system since the air temperature rarely dropped below the  $8^{\circ}\text{C}$  constant ground temperature. According to Figure 3.2, the ground adjacent to the evaporator returned to within  $1^{\circ}\text{C}$  of the undisturbed ground during the summer of 1982. The same trend appears to be occurring throughout the second summer, but then two problems developed in the fall. First, the remote ground instrumentation began to fail as evidenced by the dropping ground temperature at the end of 1983. This failure is believed to be caused by moisture problems in the instrumentation cables since the thermistors above the water table continued to operate. The second problem is much more serious because Figure 3.2 indicates that the heat pipe that was being monitored failed to turn on in the Fall of 1983. As Figure 3.3 graphically illustrates, failed heat pipes could be readily identified during periods of snow cover (also see Figure 3.7). Surface observations indicated that all the heat pipes were functioning in January 1982, and that approximately twenty of the fifty-five heat pipes that were originally charged with ammonia had totally or partially failed by November of 1983. The malfunctioning heat pipes as enumerated in Figure 2.2 were: pipes 4 and 12 in corner one; pipes 5, 14 and 15 in corner two; pipes 1, 2, 3, 11 and 12 in corner three; and pipes 1, 2, 3, 4, 5, 9, 11, 12, 13 and 15 in corner four. The problem was apparently due to the ground

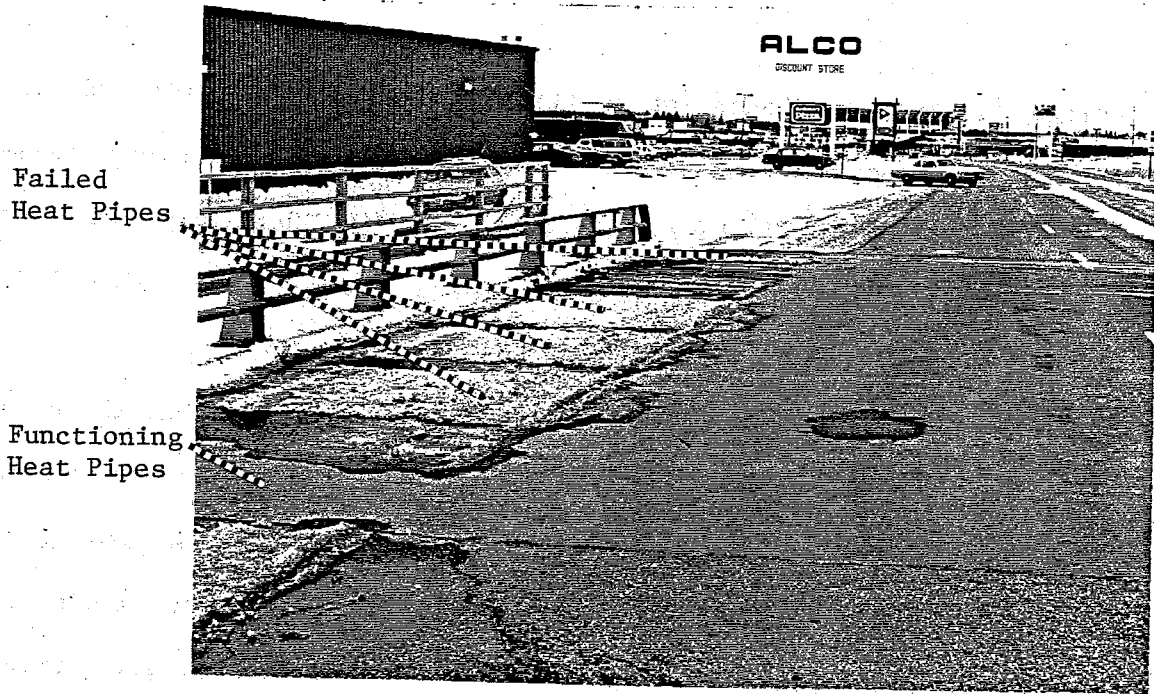


Figure 3.3. Working and Failed Heat Pipes.

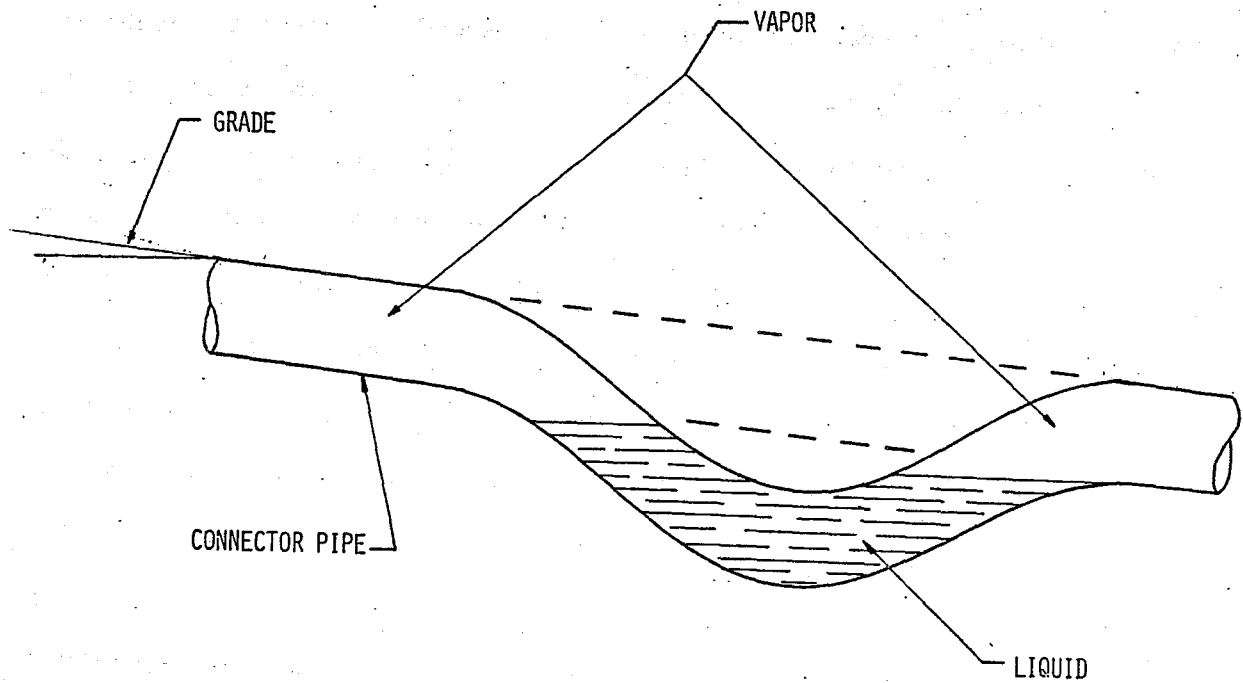


Figure 3.4. Liquid Lock.

connector pipes having an insufficient grade to compensate for nonuniform settling. This caused a liquid lock as depicted in Figure 3.4 to form in some of the connector pipes which prevented any vapor passage and thereby failed these heat pipes. This conclusion was drawn from the fact that most of the failures occurred on the east side where significant vertical displacements between the bridge deck and the service vaults have been observed. The ammonia charges in the five failed heat pipes in corner three were also checked by measuring the time required to vent each of these pipes. This test indicated that all of these failed heat pipes had an adequate charge. The upper portion of these heat pipes were subsequently attached to two water powered evaporators and they all operated properly. This implies that the problem did not involve the connector pipes in the header vaults along the side of the bridge or the condenser fingers.

As a practical construction precaution in future installations, the slope of ground connector pipes must be large enough to tolerate any subsequent settling or any waves that are introduced between the supports during the back filling operation. This precaution was in fact incorporated into the design for the Cheyenne ramps.

Figure 3.5 presents a plot of weekly averaged temperatures on the top surfaces of the heated ( $T_h$ ) and control ( $T_c$ ) sections, as well as the remote ground temperature ( $T_g$ ) at the 18 m (60') depth. Because heating events are of present interest, only situations were considered where the heated surface temperature was below that of the remote ground ( $T_g - T_h > 1^\circ\text{C}$ ). The remote ground temperature represents the maximum temperature that the heated surface can approach during these events, while the difference between the heated and control temperatures

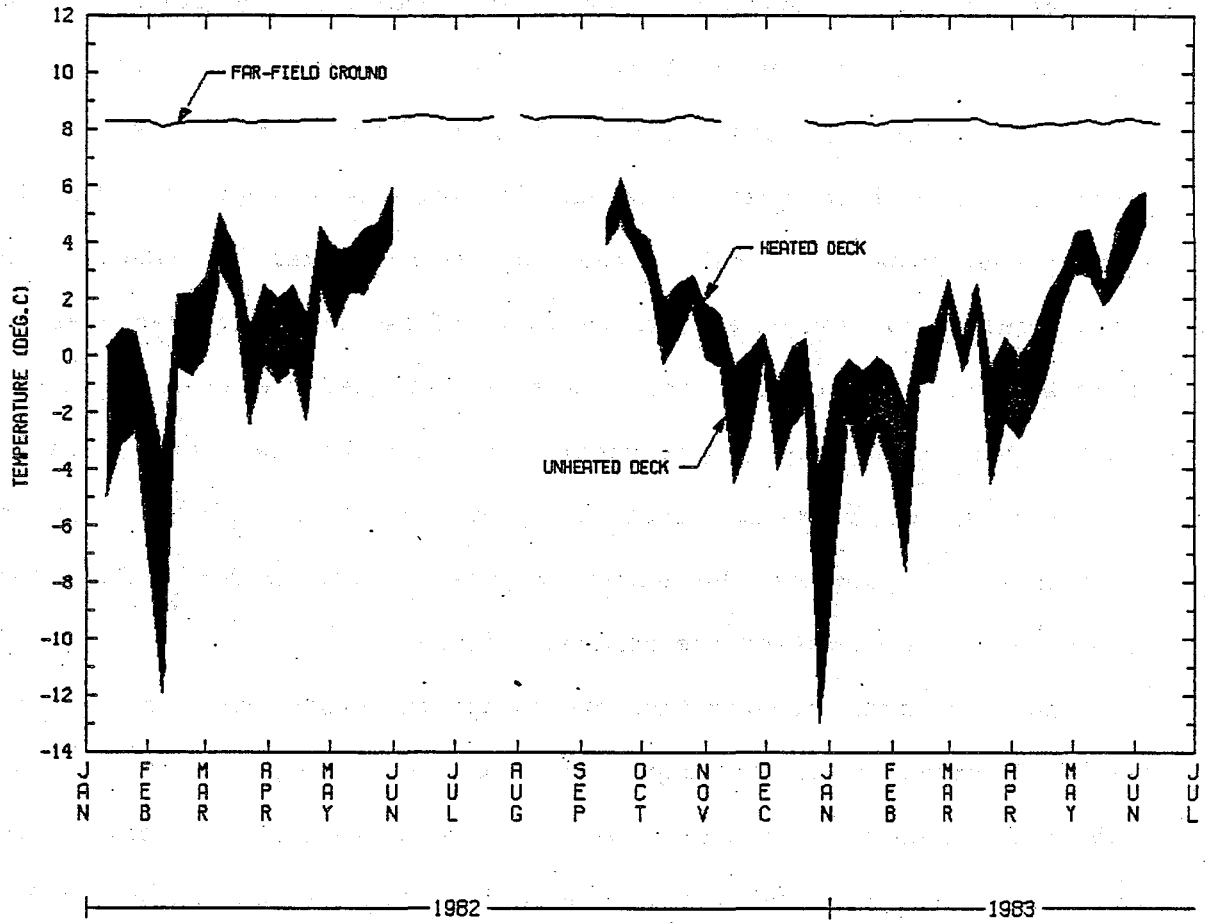


Figure 3.5. Spring Creek Weekly Averaged Heated and Unheated Deck Temperatures During Heating Events.

corresponds to the amount of heating that actually occurred. Weekly averaged temperature increases as high as  $10^{\circ}\text{C}$  ( $18^{\circ}\text{F}$ ) were achieved during the coldest periods.

Figure 3.5 can also be used to obtain a crude prediction of how this heat pipe system would perform in a different location which had a similar ground geology. The invariant far-field ground temperature reflects the ground's steady state response to the seasonal thermal loads that the environment imposes upon it. If these climatic loads are expressed in terms of seasonal effective temperatures, the amplitude of the effective temperatures relative to the respective invariant ground temperature has been found to not vary significantly between locations having similar latitudes. This implies that the thermal performance of a given ground heat pipe system in various climates will be similar if the deck temperature responses are referenced to the corresponding invariant ground temperatures. For example, the ground temperature at the FHWA Fairbank Highway Research Station, where the first ground heat pipe system was tested (8), was found to be approximately  $14^{\circ}\text{C}$  ( $57^{\circ}\text{F}$ ). The performance of the Laramie system in a Virginia climate should be essentially characterized by Figure 3.5 if all the temperatures were increased by  $6^{\circ}\text{C}$  ( $11^{\circ}\text{F}$ ) to account for the warmer ground temperature due to the milder climate. This would obviously have a large impact on the system's snow melting performance since this represents a 75% increase in ground source temperature relative to freezing and a corresponding increase in supplied power. These observations are discussed further in Chapter 5.

Table 3.2 presents the freeze-thaw characteristics recorded over eleven winter months for the top surfaces of the road, control and

TABLE 3.2. SPRING CREEK TOP SURFACE EXPERIMENTAL AND PREDICTED FREEZE-THAW CHARACTERISTICS.

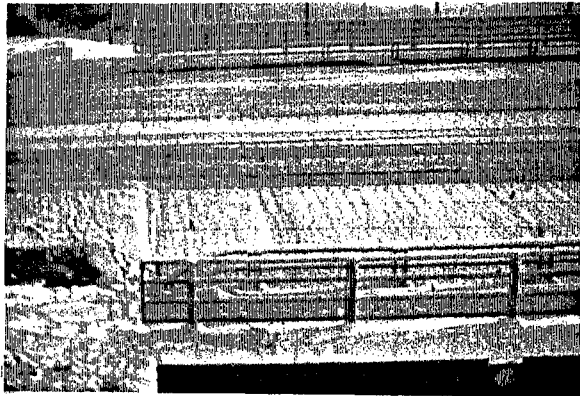
Month	Surface	% Data Present	°C - Days Below 0°C	Time Below 0°C (Days)	Freeze/Thaw Cycles
1/82	Heated		31.1 (29.6)*	11.2 (11.1)*	23 (24)*
	Control	84	115.2 (123.7)	19.9 (18.7)	19 (21)
	Roadway		101.6	18.7	26
2/82	Heated		44.0 (47.6)	10.3 (11.1)	22 (20)
	Control	100	135.5 (143.2)	15.4 (14.4)	22 (16)
	Roadway		130.8	16.9	29
3/82	Heated		5.8 (10.1)	3.2 (5.6)	10 (14)
	Control	98	37.7 (44.2)	9.4 (10.7)	24 (28)
	Roadway		29.6	9.5	26
4/82	Heated		6.5 (6.8)	3.1 (3.9)	12 (11)
	Control	100	25.2 (26.7)	6.0 (6.2)	17 (17)
	Roadway		15.4	4.9	18
10/82	Heated		3.3 (0.6)	2.7 (1.2)	10 (6)
	Control	93	14.3 (13.2)	4.9 (5.5)	15 (13)
	Roadway		-	-	-
11/82	Heated		11.0 (10.2)	6.6 (5.3)	17 (11)
	Control	57	46.9 (55.5)	11.6 (11.0)	16 (17)
	Roadway		-	-	-
12/82	Heated		47.6 (64.6)	15.4 (15.6)	21 (24)
	Control	80	146.3 (172.7)	20.4 (20.1)	14 (14)
	Roadway		-	-	-
1/83	Heated		41.1 (39.5)	16.3 (16.6)	38 (30)
	Control	97	116.0 (110.4)	21.7 (20.5)	23 (24)
	Roadway		-	-	-
2/83	Heated		29.0 (35.0)	10.7 (11.7)	31 (25)
	Control	96	88.2 (85.2)	15.9 (15.2)	22 (25)
	Roadway		78.8	16.7	35
3/83	Heated		14.4 (20.6)	6.5 (8.4)	17 (20)
	Control	85	39.7 (51.4)	10.4 (11.4)	22 (24)
	Roadway		25.0	9.8	25
4/83	Heated		12.4 (19.6)	4.9 (6.3)	16 (14)
	Control	98	38.4 (50.7)	9.5 (8.7)	14 (18)
	Roadway		27.6	8.9	16
Totals:		Heated	246.2 (284.2)	90.9 (96.8)	217 (199)
		Control	803.4 (876.9)	145.1 (142.4)	208 (217)

\*Predicted values are enclosed in parentheses.

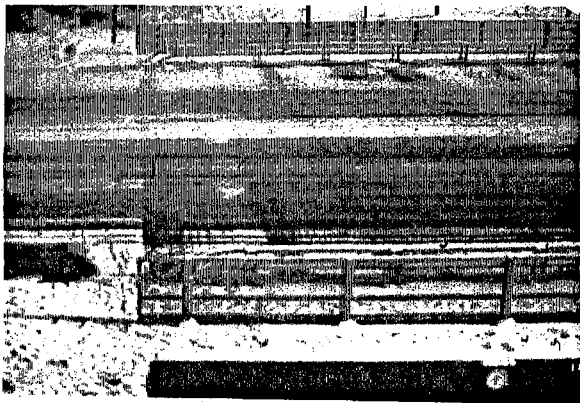
heated instrumented sections (Figure 2.2). The data for both the control and heated bridge sections were from the outer two lanes which contained the 15 cm (6") condenser spacing and where there was little traffic. The predicted values listed in this table are from simulations which are described in Chapter 5. Because of the low ground temperature, the heat pipe system reduced the frozen time of the heated section by only 37% relative to the unheated control and the °C-days below freezing by 69%. The heating system was found to be more than capable of preventing preferential freezing of the deck relative to the roadway which was the system's main design criterion. The heating reduced the deck's frozen time relative to the road by 42% and the corresponding degree-days below freezing was reduced by 65%.

The time lapse movie camera shown in Figure 2.10 provided the film record of the heat pipe system performance in terms of snow melting. Figure 3.6 presents an example of this photographic record during a minor snow event along with the corresponding ambient air and bridge surface temperatures. This particular sequence is interesting because it illustrates several characteristics of low powered heating systems. The influence of traffic is demonstrated since the heated deck had very little advantage in this case over either the unheated control or the road in the center two lanes which are utilized by all the traffic. This is not true for the outer two nontraffic lanes where the heated sections cleared demonstrably faster. The last picture in this sequence in fact indicates that the unheated control and the failed heat pipe sections in the outer two lanes are preferentially snow covered relative to the road. The corresponding temperature plot depicts a typical melting event in which the surface temperature remains between 1° and 2°C during the

7:00

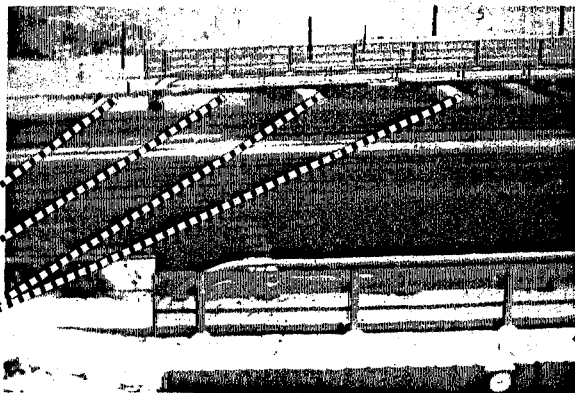


8:30



9:15

Road  
Control  
Failed  
Heat  
Pipes



10:00

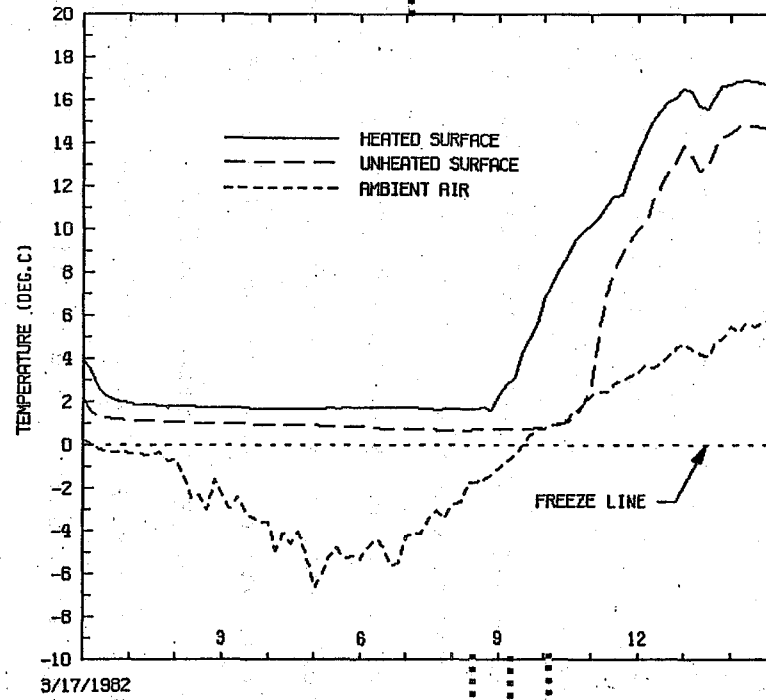
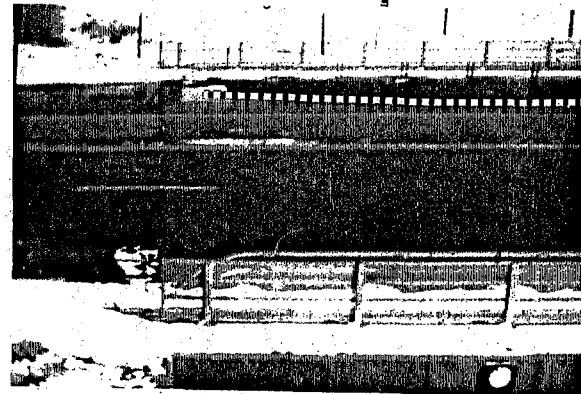


Figure 3.6. Spring Creek Snow Melting Sequence.

phase change period.

Figure 3.7 gives an example where both the road and the unheated control are covered with ice while the heated deck is dry. The snow cover near the rail was pushed there by a snow plow.

To characterize the snow melting performance of the system, specific observation sections were established on both the heated and control portions of the bridge and on the adjacent roadway as denoted in Figure 3.8. The film record from the movie camera was then used to characterize the surface conditions of these designated sections in terms of whether they were dry, wet, slush covered, partially snow covered or totally snow covered.

The classification of surface conditions from this film record was obviously somewhat subjective but a reasonable comparison in terms of snow cover duration was obtained between the sections. Table 3.3 summarizes some of this information on a monthly basis over fifteen winter months for the north non-traffic lane. These data indicate that the heat pipes reduced the periods with snow and ice cover by approximately 50% relative to the unheated control and by 47% relative to the road in the non-traffic lanes. Table 3.4, which presents the same information for the two traffic lanes, shows that the snow and ice duration on these heated sections was only reduced by 25% relative to both the road and control. The reduced effectiveness of the heat pipes on the traffic lanes is caused by the condenser spacing in the inner lanes being twice the condenser spacing in the outer lanes, and by the influences of traffic and snow plows.

The evaluation of the Spring Creek system in terms of heat transfer parameters is performed in Chapter 5. Additional experimental results

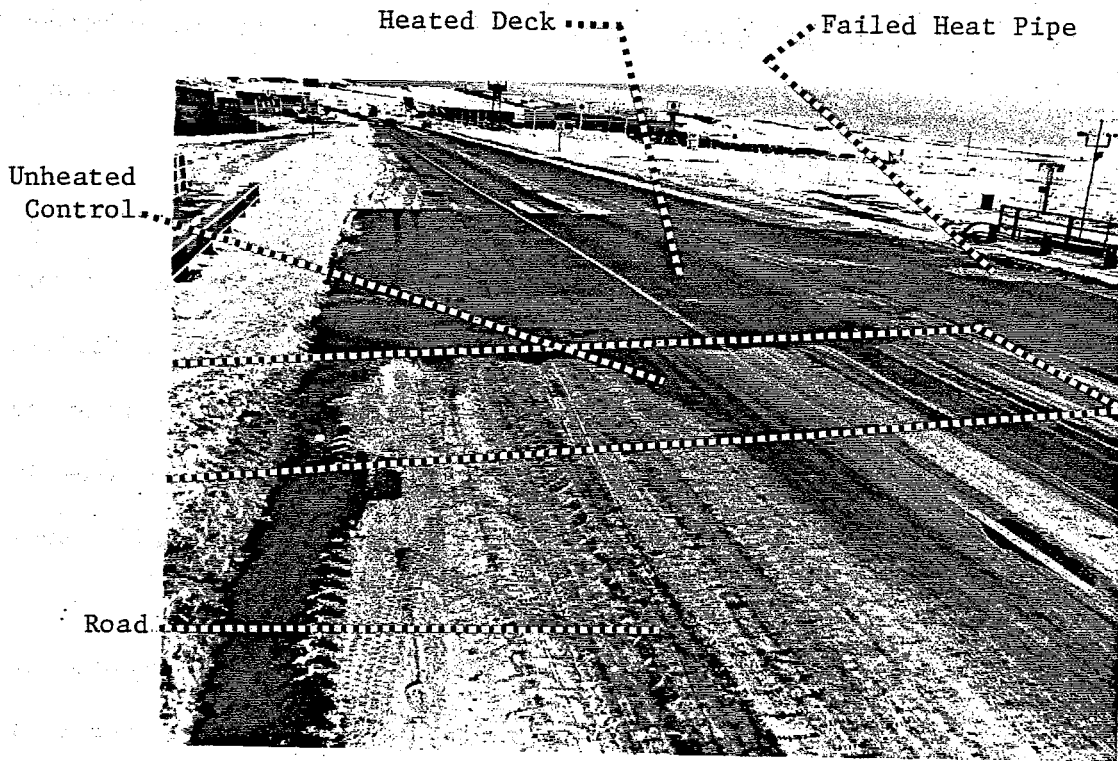


Figure 3.7. Clear Heated Deck and Iced Covered Road and Control.

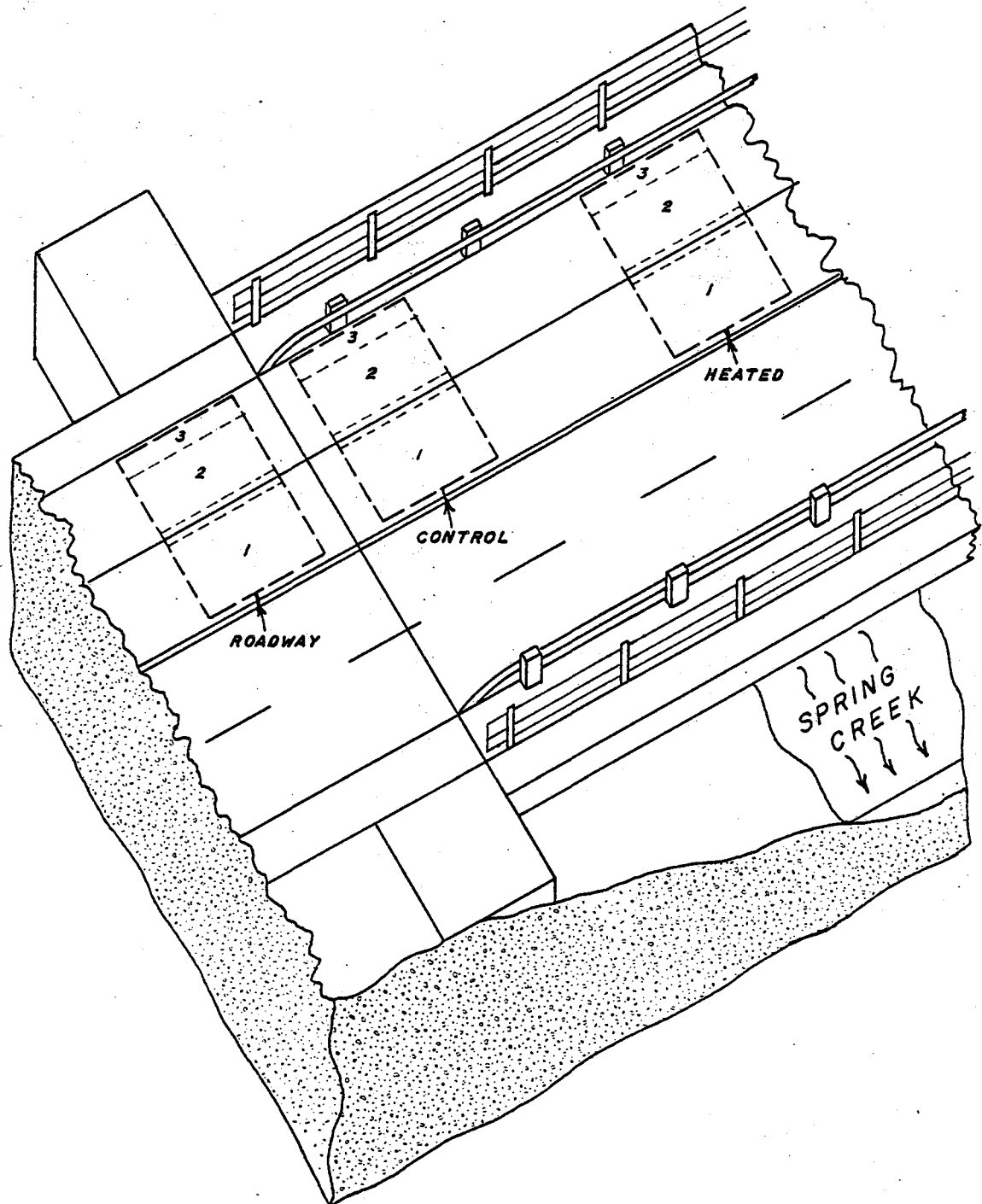


Figure 3.8. Observation Sections Used in Photographic Record.

TABLE 3.3. SPRING CREEK NON-TRAFFIC LANE SURFACE CONDITIONS.

Month	Surface	% Data Present	Clear (Hours)	Wet/Slush (Hours)	Ice (Hours)	Snow (Hours)
1/82	Heated		184.5	19.0	7.5	48.0
	Control	84	141.0	15.5	13.0	89.5
	Roadway		141.5	14.5	1.5	101.5
2/82	Heated		273.5	6.0	0.0	26.0
	Control	100	220.5	4.0	0.0	80.5
	Roadway		240.5	1.0	0.0	63.5
3/82	Heated		315.5	24.5	2.0	15.0
	Control	100	308.5	23.5	2.5	22.5
	Roadway		316.5	19.5	0.5	20.5
4/82	Heated		56.5	1.0	4.0	1.0
	Control	17	57.0	0.0	4.5	1.0
	Roadway		56.5	1.5	3.5	1.0
10/82	Heated		51.5	3.5	0.0	0.0
	Control	17	51.0	4.0	0.0	0.0
	Roadway		51.0	4.0	0.0	0.0
11/82	Heated		242.5	25.0	0.0	50.5
	Control	100	199.5	20.0	0.0	98.5
	Roadway		199.5	20.0	0.0	98.5
12/82	Heated		190.5	11.5	9.5	106.0
	Control	100	103.0	35.0	41.5	138.0
	Roadway		103.0	35.0	41.5	138.0
1/83	Heated		290.5	6.5	0.0	13.0
	Control	100	210.0	28.0	40.0	32.0
	Roadway		210.0	30.0	40.0	30.0
2/83	Heated		282.0	21.5	2.0	13.5
	Control	100	210.5	33.0	50.5	25.0
	Roadway		213.0	27.5	54.0	24.5
3/83	Heated		246.0	76.5	6.0	43.5
	Control	100	190.0	74.0	10.0	98.0
	Roadway		215.0	66.0	1.0	90.0
4/83	Heated		231.5	50.0	2.5	63.0
	Control	93	210.0	56.0	0.5	90.5

TABLE 3.3 (CONTINUED).

Month	Surface	% Data Present	Clear (Hours)	Wet/Slush (Hours)	Ice (Hours)	Snow (Hours)
10/83	Heated		68.0	0.0	0.0	0.0
	Control	23	68.0	0.0	0.0	0.0
	Roadway		68.0	0.0	0.0	0.0
11/83	Heated		203.0	46.0	15.5	58.0
	Control	100	129.0	45.0	27.5	121.0
	Roadway		151.0	33.0	16.5	122.0
12/83	Heated		127.0	65.5	52.5	44.5
	Control	100	97.5	43.5	40.5	108.0
	Roadway		105.0	36.0	41.5	107.0
1/84	Heated		154.5	9.5	22.0	32.0
	Control	77	71.5	6.5	34.5	105.5
	Roadway		64.0	18.5	17.5	118.0
Totals:		Heated	2916.5	366.0	123.5	514.0
		Control	2267.0	388.0	265.0	1000.0
		Roadway	2357.0	361.5	218.0	983.5

Note: Times are based on digitized film results during daylight.

TABLE 3.4. SPRING CREEK SURFACE CONDITIONS ON TRAFFIC LANES.

Month	Surface	Clear (Hours)	Wet/Slush (Hours)	Ice (Hours)	Snow (Hours)
1/82	Heated	205.5	30.0	11.0	12.5
	Control	179.0	34.5	33.0	12.5
	Roadway	172.5	40.5	33.5	12.5
2/82	Heated	293.0	4.0	8.0	0.0
	Control	294.0	2.5	8.5	0.0
	Roadway	294.0	2.5	8.5	0.0
3/82	Heated	322.5	25.0	3.0	6.5
	Control	322.0	24.5	4.0	6.5
	Roadway	323.0	24.5	3.0	6.5
4/82	Heated	56.5	2.0	3.0	1.0
	Control	56.0	2.0	4.5	0.0
	Roadway	58.0	1.0	3.5	0.0
10/82	Heated	51.5	4.0	0.0	0.0
	Control	51.0	4.0	0.0	0.0
	Roadway	51.0	3.5	0.0	0.0
11/82	Heated	243.5	37.5	2.5	34.5
	Control	231.0	48.5	2.0	36.5
	Roadway	231.0	48.5	2.0	36.5
12/82	Heated	200.5	26.5	27.0	63.5
	Control	180.0	22.5	59.0	56.0
	Roadway	176.0	22.5	63.0	56.0
1/83	Heated	293.5	11.5	2.5	2.5
	Control	245.0	38.0	25.0	2.0
	Roadway	245.0	38.0	25.0	2.0
2/83	Heated	289.0	15.5	2.0	12.5
	Control	285.0	17.5	2.0	14.5
	Roadway	285.0	17.5	2.0	14.5
3/83	Heated	240.0	72.5	15.0	44.5
	Control	235.0	78.5	14.5	44.0
	Roadway	235.0	77.5	14.5	45.0
4/83	Heated	210.5	72.5	5.0	59.0
	Control	211.5	77.0	2.5	56.0
	Roadway	215.5	78.0	4.5	49.0
10/83	Heated	68.0	0.0	0.0	0.0
	Control	68.0	0.0	0.0	0.0
	Roadway	68.0	0.0	0.0	0.0
11/83	Heated	196.0	46.5	14.0	66.0
	Control	197.0	39.5	16.0	70.0
	Roadway	197.0	39.5	16.0	70.0

TABLE 3.4 (CONTINUED).

Month	Surface	Clear (Hours)	Wet/Slush (Hours)	Ice (Hours)	Snow (Hours)
12/83	Heated	80.0	48.0	48.0	113.5
	Control	33.0	56.0	63.5	137.0
	Roadway	21.5	55.5	71.0	141.5
1/84	Heated	140.5	25.0	25.0	27.5
	Control	52.0	33.0	48.0	85.0
	Roadway	47.0	29.0	32.0	110.0
Totals:	Heated	2890.5	420.0	166.0	443.5
	Control	2639.5	478.0	282.5	520.0
	Roadway	2619.5	478.5	278.5	543.5

Note: Times are based upon daylight film record.

can also be found in that chapter.

In summary, the Spring Creek system demonstrated that large heat pipes for bridge decks can be field constructed as long as careful consideration is given to cleaning, welding and the maintenance of proper grades on the pipes. The working heat pipes prevented any preferential freezing of the heated deck relative to the road, and they performed a reasonable amount of snow melting in the section with the 15.2 cm (6") condenser spacing when one takes into account the very low ground temperature and the severe climate. In a milder climate, the snow melting capability of the heat pipes would have been much more substantial.

#### IV. SYBILLE CANYON HEAT PIPE FACILITY

The second data base that is utilized in this report was generated by a heat pipe system that was installed in a portion of a bridge over Sybille Creek on Wyoming State Highway Number 34 near Laramie. Only a brief description of this facility and the performance of these ground heat pipes will be presented in this chapter since this information is documented in reference 15. The Sybille Creek facility has an elevation of 1820 m (5960') which is 380 m lower than Laramie's elevation. The layout of this facility's fifteen heat pipes and associated instrumentation is given in Figure 4.1. Twelve of the heat pipes are 24.4 m (80') long with 4.9 m (16') embedded in the deck, while the other three pipes are 6.4 m (21') long and were electrically powered for short periods during the experiment. The heat pipes were fabricated from seamless, cold rolled, low carbon steel tubing with an outside diameter of 2.54 cm (1") and a 0.3 cm (0.125") wall thickness. The heat pipes were installed in the ground on 10/29/76 in 15 cm (6") diameter holes on 1.2 m (4') centers (Figure 4.1) and the holes were backfilled to 3 m (10') of the surface with drilling mud (bentonite). A removable insulation was placed in the upper 3 meters of the hole so that the mud levels could be periodically checked. The condenser sections of the heat pipes were bent into the bridge forms on 15 cm (6") centers in December of 1976 and the deck was poured.

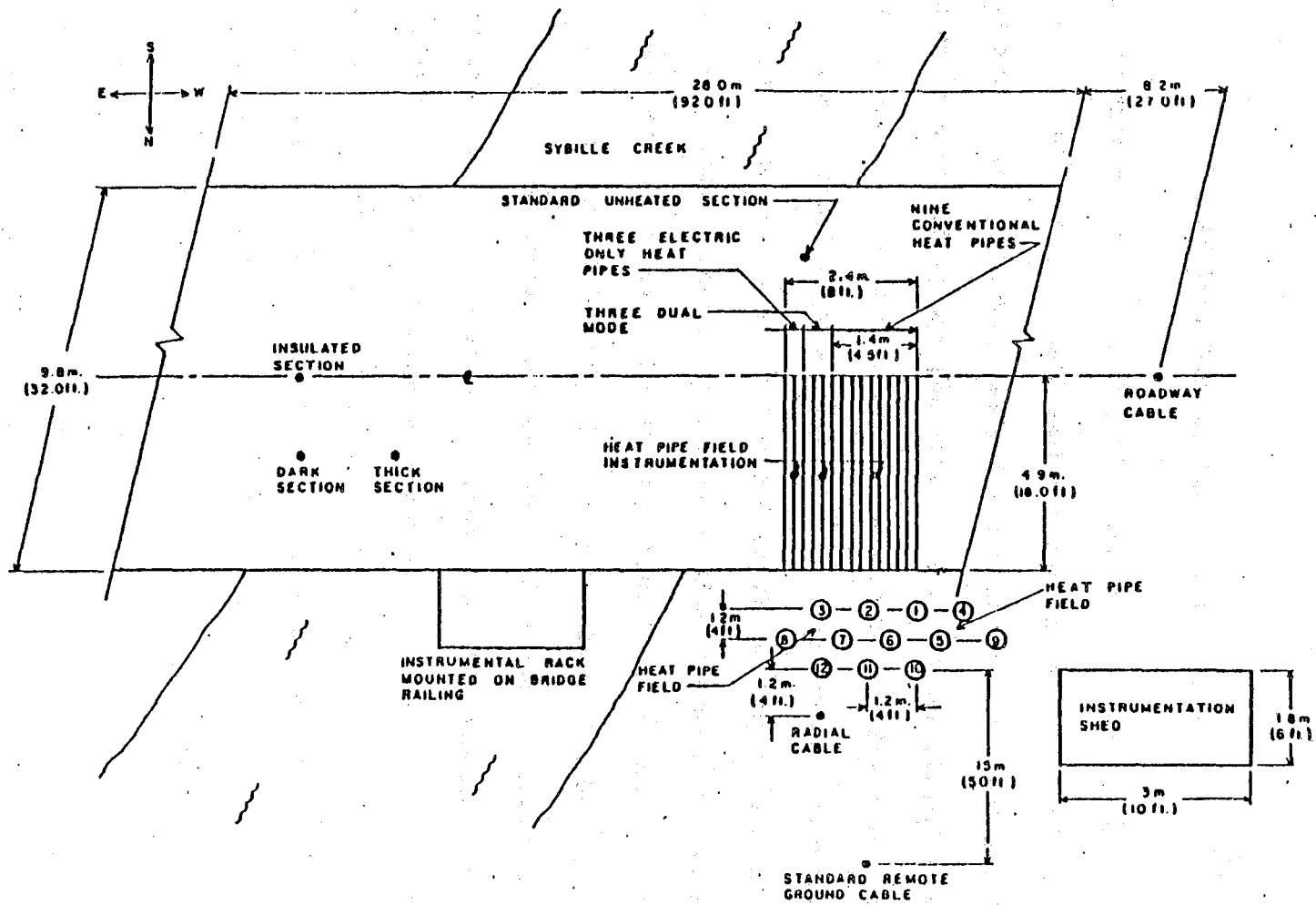


Figure 4.1. Sybille Creek Experimental Facility.

Unfortunately some of the formwork in the immediate vicinity of the heat pipes slipped during the pour, which caused both the thickness of the deck in the heated section to vary between 15 and 18 cm (5.8 and 7.1") and the concrete cover above the condenser pipes to vary from around 1.6 to 4.8 cm (0.6 to 1.9"). This created some difficulty in characterizing the bridge deck in terms of the two dimensional geometry that is required in the thermal model of the bridge deck.

A serious geometric problem also occurred in characterizing the drilling mud height in the evaporator holes since the mud level in some of the holes fell during the study. The mud depth encasing the two evaporator pipes that are utilized in this report (evaporator pipes 6 and 8 in Figure 4.1) was initially 13.4 m (44') going into the 1977/78 winter and was 10 m (33') with 2 m (7') of water above the drilling mud at the conclusion of the 1978/79 winter. In simulating the thermal performance of these two heat pipes, a constant effective evaporator length of 12.2 m (40') was assumed. This experience demonstrates that caution must be exercised in backfilling evaporator holes with drilling mud in fractured or porous terrains. Even if the drilling mud that is lost due to seepage is replaced by water, the system's performance should degrade since the thermal conductivity of water is approximately one half that of saturated bentonite. Drilling mud was also utilized at the Fairbank Highway Research Station (8) and at Oak Hill, West Virginia (16) but the mud levels at these two demonstration sites were never monitored.

Figure 4.2 is a picture of the site right after the deck was poured and before the adjacent road was completed. The heated portion of the

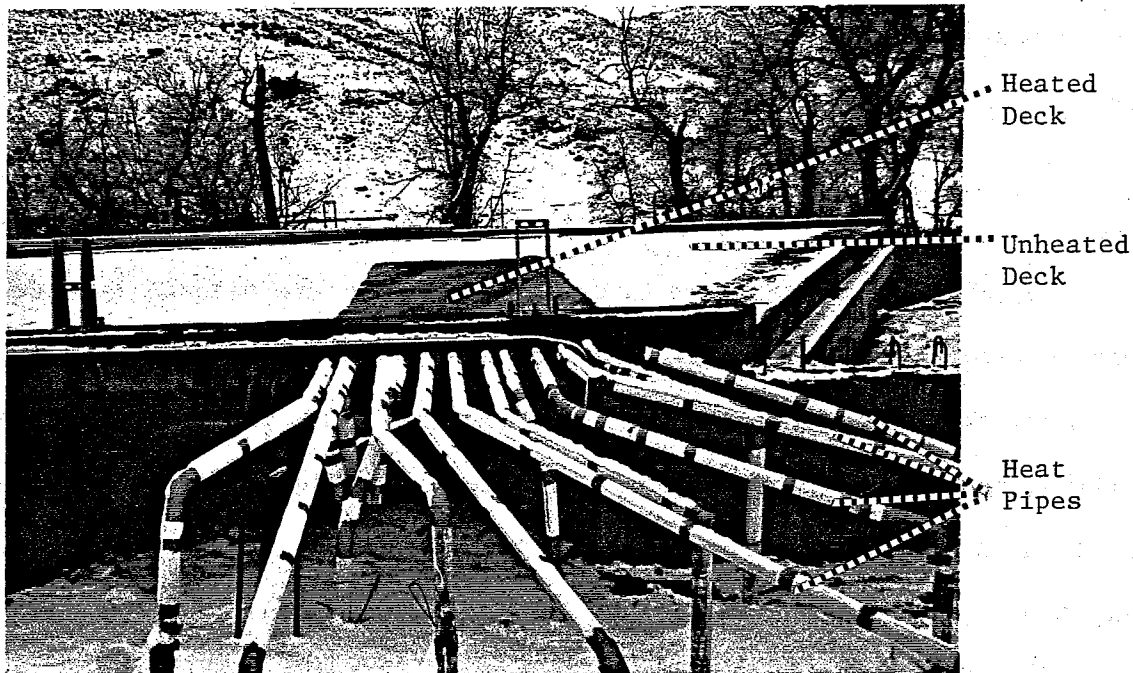


Figure 4.2. Sybille Creek Heat Pipe Facility.

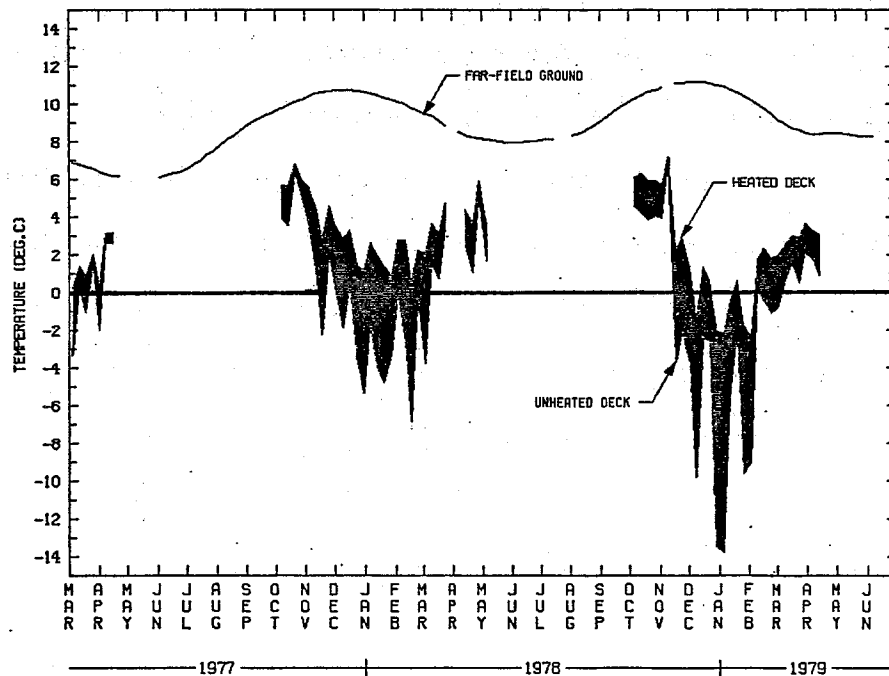


Figure 4.3. Sybille Creek Weekly Averaged Heated and Unheated Deck Temperatures during Heating Events.

deck is clearly outlined in this picture by the unmelted snow around it. The sections of heat pipes that were exposed to the air were insulated with 7.6 cm (3") of fiberglass pipe insulation which was wrapped with a thin plastic covering in an attempt to protect the insulation from the elements but, in spite of this, most of the insulation became damp. This exposed section was approximately 2.9 m (9.5') in length for heat pipes number 6 and 8. The bottom of the heated section of deck was insulated with 10 cm (4") of closed cell insulation.

Data acquisition was initiated on 2/15/77 and continued through June of 1979. A one minute sample rate was utilized so that line noise could be filtered. Over the 2-1/3 year study period, the data acquisition system performed satisfactorily 92% of the time. The monthly meteorological record during this period is presented in Table 4.1. This record indicates that Sybille's climate was significantly milder than the one recorded for Laramie in that the mean annual air temperatures were 7.6°C and 6.7°C (46° and 44°F) for the two consecutive years. The second year had the more severe winter with monthly averaged air temperatures of only -7.2°C and -9.6°C (19° & 15°F) for the months of December and January respectively which were 6°C and 4.8°C (11° & 9°F) colder than the corresponding temperatures from the previous year. The solar radiation record for these two very cold months indicate that there was also less cloud cover in the second year. The monthly averaged wind speeds during these two Januaries were 7.9 m/s (18 mph) and 7.2 m/s (16 mph) and represented the maximum of the monthly averages. The prevailing wind direction in this canyon was essentially parallel to the bridge.

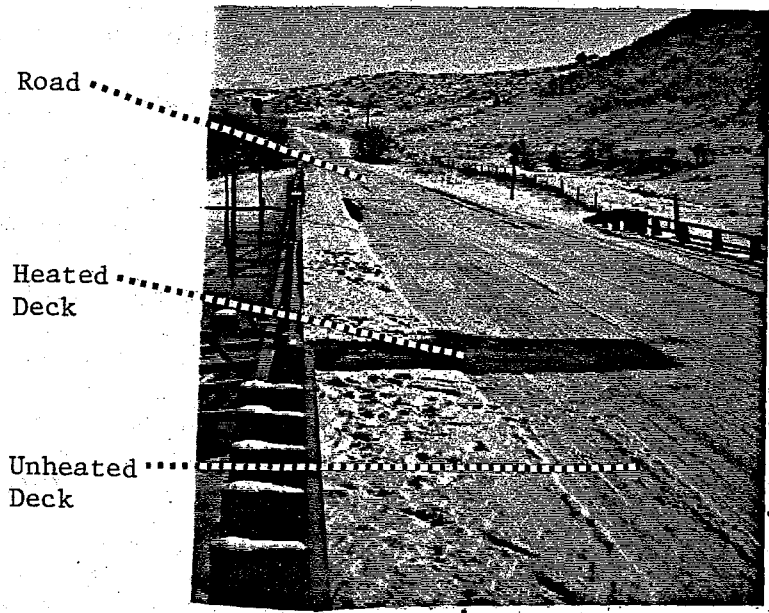
TABLE 4.1 MONTHLY METEOROLOGICAL RECORD AT THE SYBILLE CREEK FACILITY.

Month/Year	Ave. Air Temp. (°C)	Ave. Wind Speed (m/s)	Ave. Daily Solar (MJ/m <sup>2</sup> )
3/77	-1.6	4.2	16.0
4	6.5	2.1	19.0
5	12.3	2.6	21.0
6	19.3	2.0	24.2
7	20.3	2.3	22.3
8	17.4	2.2	19.3
9	15.7	3.7	18.4
10	9.1	5.5	14.8
11	2.2	5.2	9.0
12	-1.2	6.4	6.3
1/78	-4.8	7.9	7.3
2	-3.5	3.8	11.8
3	2.1	4.1	16.1
4	5.7	4.2	16.3
5	9.6	3.6	20.6
6	17.1	2.8	25.1
7	21.1	-	24.6
8	17.5	2.2	20.4
9	15.6	3.2	19.5
10	8.4	4.6	13.8
11	1.4	5.2	8.8
12	-7.2	6.7	6.7
1/79	-9.6	7.2	8.1
2	-1.7	5.0	12.4
3	1.2	4.7	15.1
4	7.0	4.7	20.9
5	9.5	3.0	20.6
6	14.0	2.7	25.7

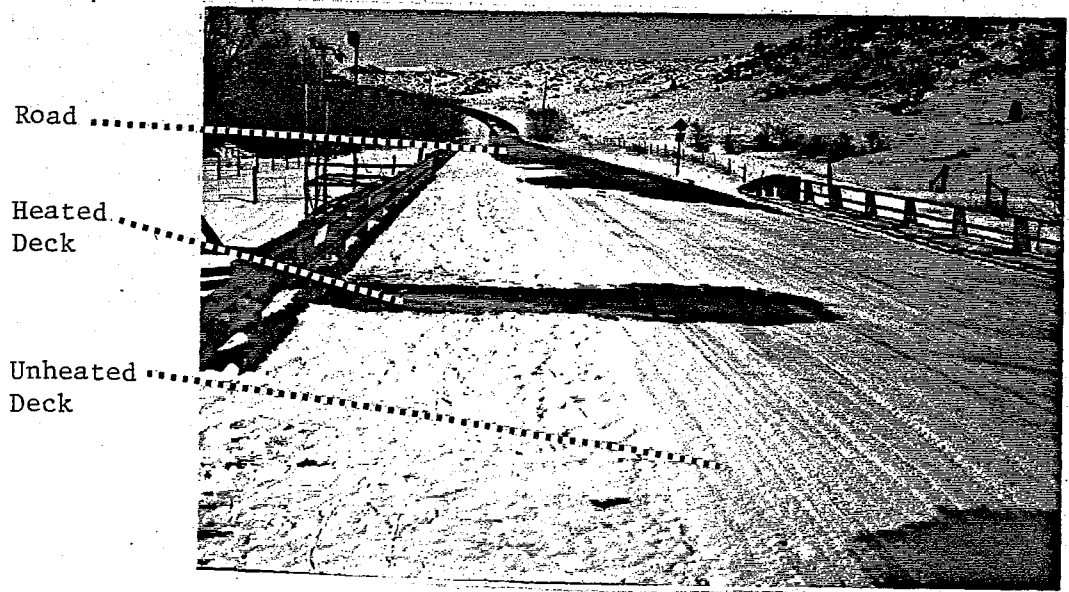
A comparison between the heated deck and the unheated control section is presented in Figure 4.3 in terms of weekly averaged surface temperatures during events when the heated deck temperature ( $T_h$ ) was at least  $1^\circ\text{C}$  below the 12 m (40') far field ground temperature ( $T_g$ ). This figure indicates that the heat pipe system was capable of maintaining the weekly average heated surface temperature above freezing during the first year. The severe second winter froze this section for an extended period of time even though its weekly average temperature was as much as  $12^\circ\text{C}$  ( $22^\circ\text{F}$ ) above the average temperature of the unheated control.

During the coldest four months, the heated deck was on the average  $4.4^\circ\text{C}$  ( $8^\circ\text{F}$ ) warmer than the unheated control in the first year and  $4.9^\circ\text{C}$  ( $9^\circ\text{F}$ ) in the second year. Table 4.2 indicates that this resulted in a consecutive yearly reduction of 75% and 54% in the total time the heated surface was frozen as compared to the control. The control surface was preferentially frozen with respect to the road for an approximate total time of six days during the first winter and ten days in the second winter. The heated surface was never preferentially frozen with respect to the road. The degree-days below  $0^\circ\text{C}$  of the heated surface was reduced relative to the unheated control by 92% in the first year and by 82% during the second winter.

Figure 4.4 presents a sequence of photographs that depicts the operation of this system during a snow melting event. The first photo shows an event where both the road and unheated deck are snow covered and the heated deck is clear. The second photo indicates that the road clears the next day while the unheated deck is still covered with packed snow. Table 4.3 summarizes the snow cover duration for the various



a. November 25, 1978 - noon until sunset



b. November 26, 1978 - noon

Figure 4.4. Sybille Creek Snow Melting Sequence.

TABLE 4.2. SYBILLE TOP SURFACE EXPERIMENTAL AND PREDICTED SURFACE FREEZE-THAW CHARACTERISTICS.

Month	Surface	% Data Present	°C - Days Below 0°C		Time Below 0°C (Days)		Freeze/Thaw Cycles
3/77	Heated	95	11.1	(4.8)*	7.0	(3.9)*	29 (13)*
	Control		47.7	(46.2)	11.8	(10.2)	29 (24)
4/77	Heated	85	0.0	(0.0)	0.4	(0.7)	8 (2)
	Control		4.6	(10.5)	3.2	(3.6)	5 (8)
10/77	Heated	100	0.0	(0.0)	0.0	(0.0)	0 (0)
	Control		2.6	(1.9)	1.2	(1.1)	4 (4)
11/77	Heated	99	3.7	(5.0)	1.5	(1.7)	3 (5)
	Control		40.9	(52.3)	10.0	(10.7)	29 (17)
12/77	Heated	100	7.6	(14.7)	4.8	(8.0)	16 (18)
	Control		93.9	(103.3)	18.4	(16.5)	25 (20)
1/78	Heated	100	10.4	(62.2)	7.3	(19.5)	26 (24)
	Control		139.6	(175.2)	24.6	(24.3)	20 (18)
2/78	Heated	100	7.5	(27.2)	4.7	(11.8)	18 (25)
	Control		86.6	(112.6)	17.0	(17.7)	18 (25)
	Roadway		63.4		16.9		32
3/78	Heated	95	3.3	(11.0)	1.9	(4.2)	9 (11)
	Control		35.1	(44.0)	6.4	(7.7)	13 (18)
	Roadway		17.8		4.4		13
4/78	Heated	81	0.0	(0.0)	0.0	(0.2)	0 (1)
	Control		2.7	(3.3)	2.0	(2.1)	10 (11)
	Roadway		0.0		0.0		2
1st Winter Totals:	Heated		32.5	(120.1)	20.2	(45.4)	72 (84)
	Control		401.4	(402.6)	79.6	(80.1)	119 (113)
	Roadway		-	-	-	-	-

TABLE 4.2 (CONTINUED)

Month	Surface	% Data Present	°C - Days Below 0°C		Time Below 0°C (Days)		Freeze/Thaw Cycles
10/78	Heated		0.0	(0.0)	0.0	(0.0)	0 (0)
	Control	91	2.7	(4.3)	1.7	(2.1)	7 (10)
	Roadway		0.0		0.1		2
11/78	Heated		0.5	(0.9)	1.1	(1.2)	9 (9)
	Control	77	47.4	(56.3)	11.4	(11.0)	13 (15)
	Roadway		24.5		9.9		18
12/78	Heated		33.9	(74.3)	14.5	(19.3)	25 (21)
	Control	100	215.4	(239.0)	24.5	(24.4)	18 (15)
	Roadway		164.4		24.9		25
1/79	Heated		61.4	(142.8)	19.2	(25.5)	26 (22)
	Control	100	279.7	(303.2)	27.3	(27.9)	15 (10)
	Roadway		250.2		28.2		15
2/79	Heated		18.7	(33.2)	9.9	(12.1)	28 (22)
	Control	98	78.1	(84.4)	14.5	(15.7)	23 (23)
	Roadway		58.7		14.8		27
3/79	Heated		3.1	(9.8)	2.5	(6.1)	9 (19)
	Control	98	22.1	(37.0)	6.5	(10.2)	18 (24)
	Roadway		9.5		4.3		14
4/79	Heated		0.2	(2.5)	0.4	(2.3)	3 (6)
	Control	100	5.8	(10.6)	2.5	(3.8)	8 (9)
	Roadway		0.7		0.7		5
2nd Winter Totals:	Heated		117.8	(263.5)	47.6	(66.5)	100 (99)
	Control		651.2	(734.8)	88.4	(95.1)	102 (106)
	Roadway		508		82.9		106

\*Predicted values are enclosed in parentheses.

TABLE 4.3. MONTHLY PRECIPITATION AND SNOW COVER DURATION.

Month/Year	Frozen Precip.* (mm water)	Snow Cover Duration (Hours)		
		Heated	Control	Road
10/77	5		3.1	2.2
11	6	34.1	63.7	60.7
12	13	61.5	133.0	149.9
1/78	27	173.6	260.6	272.2
2	26	36.3	110.7	66.0
3	21	20.0	56.8	52.6
4	4	2.9	7.2	7.2
Total:	102	328.4	635.1	610.8
10/78	49	0	69	5.6
11	11	18.0	52.6	28.3
12	34	238.4	291.2	291.4
1/79	13	305.7	330.4	324.3
2	3	12.5	35.5	12.5
3	35	19.0	73.5	56.4
4	15	1.4	21.9	8.5
5	19	0	13.5	2.9
Total:	179	595.0	824.6	729.9

\* Frozen precipitation data obtained from U.S. Fish & Wildlife Service Research Station in Sybille Canyon.

surfaces over the two winters. The heat pipe system reduced the snow cover duration relative to the control by 48% during the first winter but the reduction in the second winter was only 28% due to the very cold and snowy months of December and January. All the surfaces remained snow packed over a significant part of these two months.

Figure 4.5 tracks the thermal response of the evaporator relative to the ground temperature at a depth of 12 m (40'). The undisturbed ground at this site still has a significant cyclic temperature amplitude at 12 m whereas the amplitude had essentially damped out by 15 m at the Spring Creek site (see Figure 3.1). The average temperature and amplitude of this 12 m deep thermal wave is approximately 9.3°C and 1.3°C respectively during the first winter but there appears to be a significant variation in these values over the two seasons monitored. This variance of the far field ground temperature with time and over the depths of the exposed evaporators obviously had a strong influence on the performance of this system whereas these effects were minor at the Spring Creek facility.

The question of whether the temperature in the heat pipe field recovers to its undisturbed value was not answered by the data taken over twenty-eight months. Figure 4.5 appears to indicate that there is a recovery problem but spot checks that were made after 6/79 implied that the heat pipe field did recover. The weekly averaged evaporator temperatures fell below 0°C on several occasions in 1979 and the drilling mud began to freeze as can be seen in Figure 4.5 by the constant minimum evaporator temperature for a period of time in January.

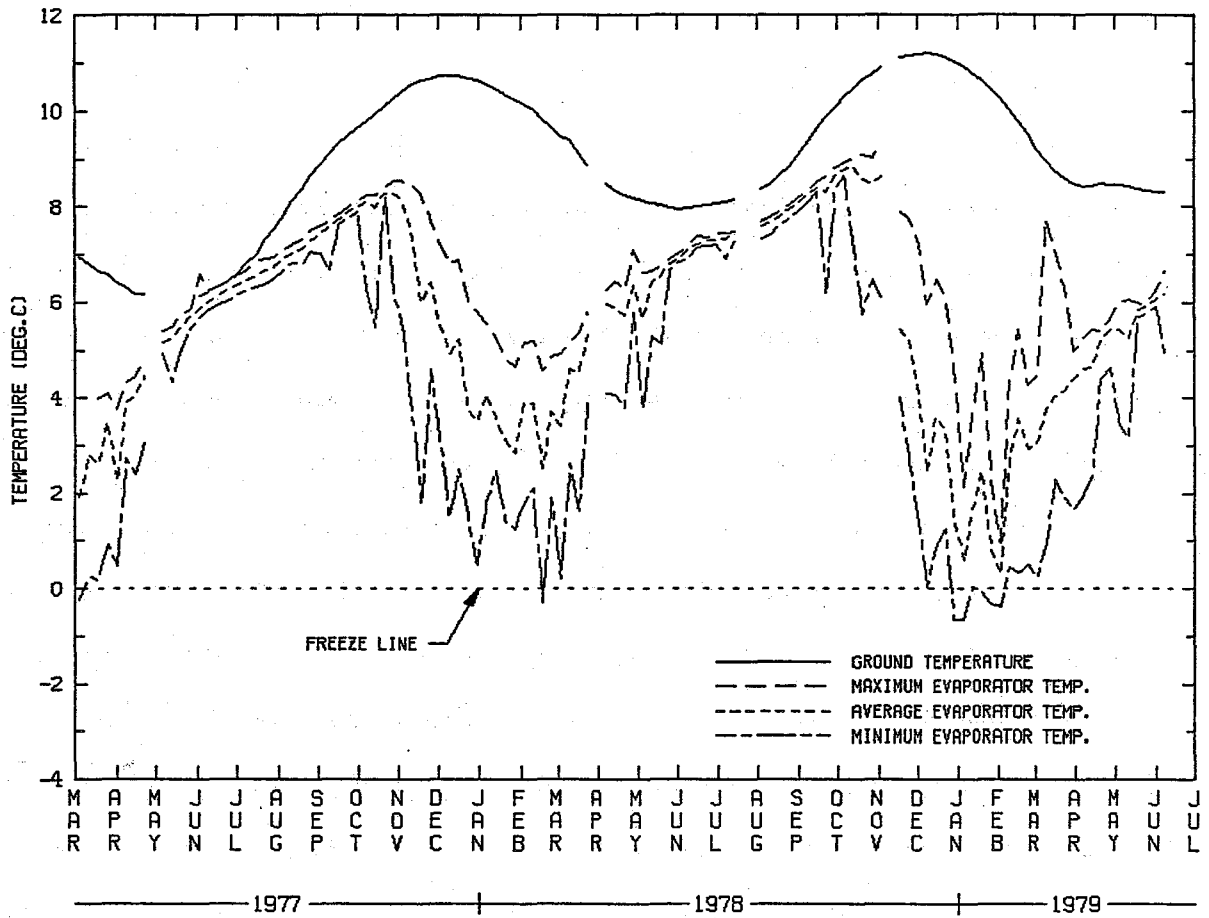


Figure 4.5. Weekly Averaged Experimental Ground and Evaporator Temperatures at Sybille (12 m).

## V. HEAT TRANSFER MODEL

### A. General Description

The ultimate goal of this research project was to formulate a design procedure for bridge heat pipe systems that could be utilized by state, county and city design and construction engineers. This was obviously a very formidable task. The first step in this program had to be the development of a numerical model that was comprehensive enough to accurately handle the complex and dynamic interactions between the heat pipes, the deck, the ground and the environment while remaining simple enough to permit numerous multi-year simulations. The next step entailed the validation of the thermal model against the experimental data that was obtained from the two experimental prototype installations. The final step involved parametric studies to determine the influence that various ground and system parameters have on the thermal performance of the heat pipe system. Many simulations were performed since the essential features of the heat pipe system had to be characterized in enough detail that dependable design algorithms could be formulated. The above heat transfer model, its validation, and the results of the parametric studies are discussed in this chapter.

A schematic of the heat transfer system that was modeled is depicted in Figure 5.1. The model was divided into the following major heat transfer components:

- 1) Heat transfer within the deck.

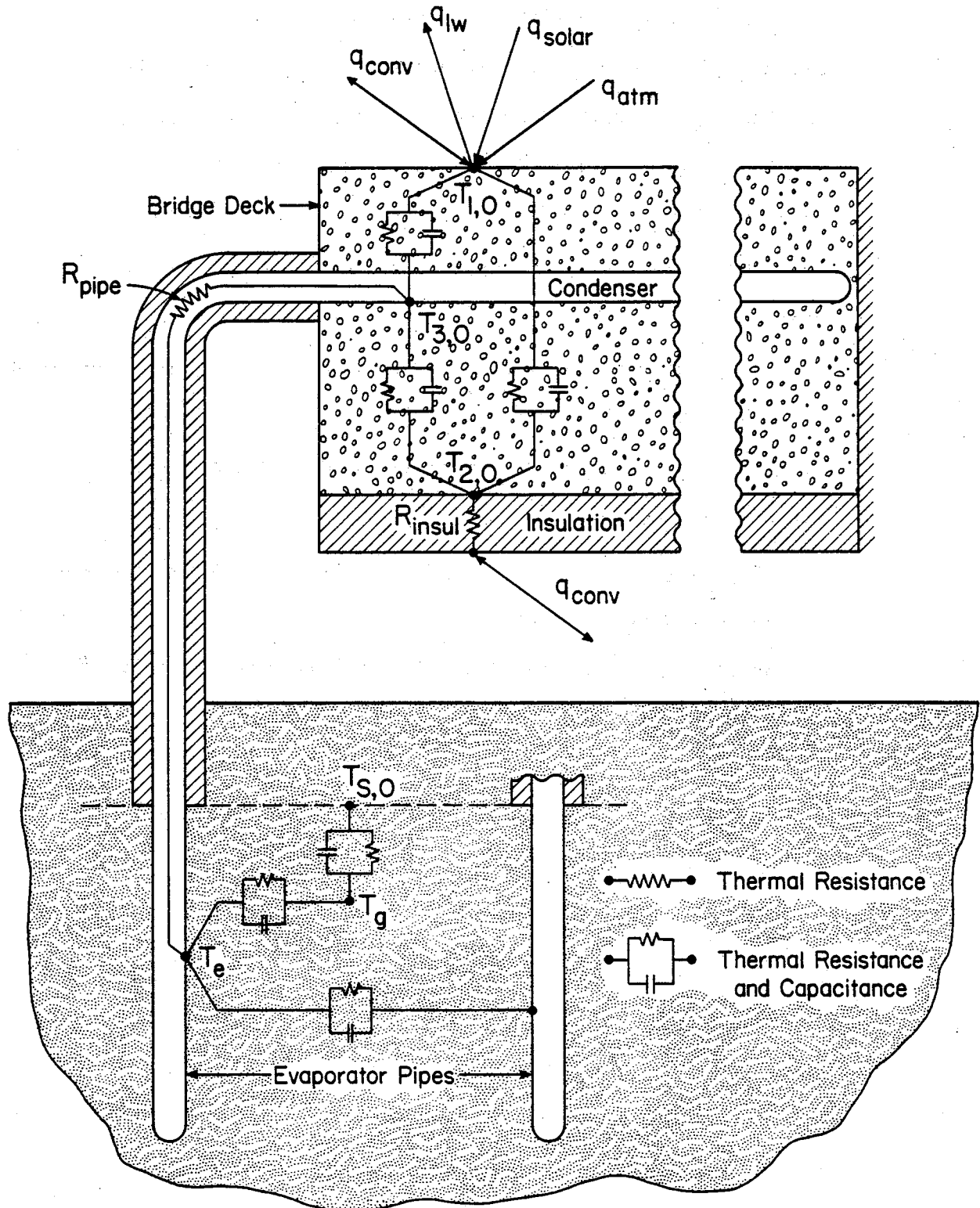


Figure 5.1. Heat Transfer Schematic.

- 2) Thermal interaction between the transient environment and the top and bottom surfaces of the bridge deck.
- 3) Heat transfer from the ground to an evaporator pipe.
- 4) Thermal interaction between the evaporator pipes.
- 5) Transient far-field ground temperature distribution.

Because of the complex nature of the system, it was necessary to make certain major simplifying assumptions at the outset. These included:

- 1) Homogeneous and constant thermal properties in both the ground and deck.
- 2) Conduction dominated heat transfer in the ground.
- 3) Dry surface conditions.
- 4) Perfect insulation on the connecting pipe between evaporator and condenser sections.
- 5) Surface temperatures of the top and bottom of the deck, condenser pipe, and the evaporator pipe are only functions of time.
- 6) Clear sky.

The boundary conditions for this problem are time-dependent, involve both infinite and finite coordinates and are non-linear in the case of the bridge deck due to radiative and convective heat transfer. The environmental parameters that are required to specify these boundary conditions are the ambient air temperature, pressure and velocity; incident solar radiation and (although not strictly independent of the previous parameters) the ground temperature at some depth.

Under the assumption of constant thermal properties, the governing differential heat transfer equation is

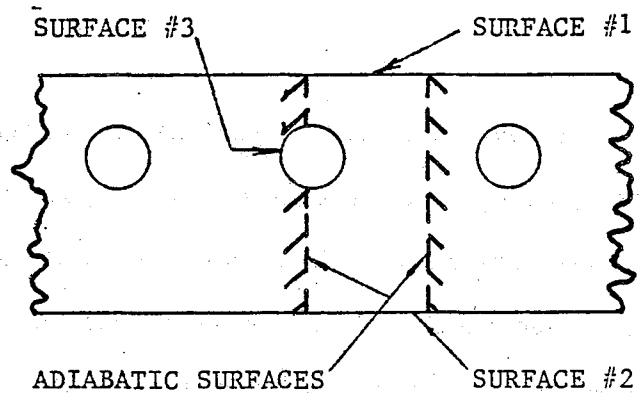
$$\frac{\partial T}{\partial t} = \alpha \nabla^2 T \quad (5.1)$$

This equation is linear and the principle of superposition can be utilized. The response factor technique is a powerful form of this principle which was originally developed to numerically handle the transient thermal behavior of one dimensional systems in a very efficient manner with respect to computer time (26). For this reason it is currently being used in programs that model the heat transfer through the outer envelope and interior walls of large buildings (27). The response factors that were developed in this research for bridge decks with embedded condenser pipes and for ground evaporator pipes appear to be one of the first examples where this method has been employed to solve problems with complex two dimensional geometries. The response factor model that was developed in this research was capable of accurately simulating the thermal behavior of the heat pipe system at one hour intervals over a two year period and only utilized around one minute of cpu time on a CDC Cyber 760.

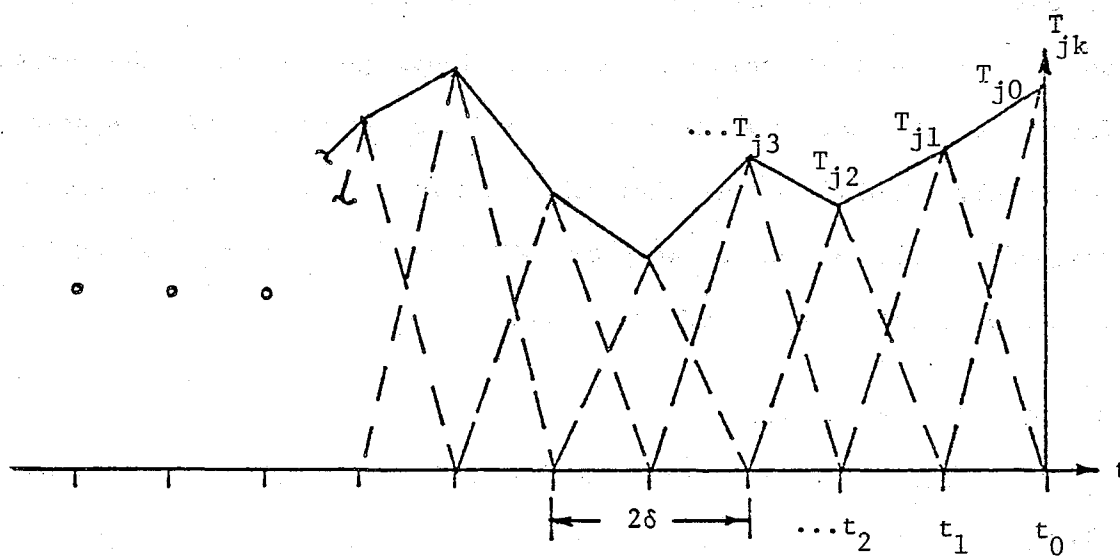
#### B. Deck Response Factors

The determination of response factors for complex geometries can be difficult. The details of the procedure that was used to calculate the response factors for a deck with embedded heat pipes are delineated in references (19) and (21) and only a brief description is included here.

In the heated deck depicted in Figure 5.2, the temperatures of the top surface (#1), the bottom surface (#2), and the outer surface of the condenser pipe (#3) are all assumed to be only functions of time while the other two boundary surfaces are adiabatic due to the symmetry of the



a. Surface Designation for Heated Deck



b. Linear Representation of Surface Temperature History

Figure 5.2. Deck Surface Designation and Temperature History Representation.

condenser pipes. The heat transfer through each of the isothermal surfaces at any given time can be written as a function of the temperature histories of the three numbered surfaces. The classical form of the response factor method replaces the three continuous surface temperature records with discrete values taken at equal time intervals and assumes a linear temperature variation with time between each temperature record (see Figure 5.2). The power  $\dot{Q}_i$  through one of the surfaces  $i$  ( $i = 1, 2$  or  $3$ ) can then be calculated from an infinite series in terms of this temperature record  $T_{jk}$  for the three surfaces ( $j=1, 2$  or  $3$ )

$$\frac{\dot{Q}_{i,k=0}}{A_i} = \sum_{j=1}^3 \sum_{k=0}^{\infty} X_{ijk} T_{jk} \equiv q_{i,0} \quad (5.2)$$

where  $k$  is the number of time intervals back in time, and  $X_{ijk}$  is the response factor. These response factors represent the power through surface  $i$  due to a triangular temperature pulse on surface  $j$  of unit magnitude which is centered  $k$  time intervals back in time and has a time duration which is twice the surface temperature time interval  $\delta$ .

An interesting feature of response factors in finite geometries is that the ratio of succeeding response factors approaches a constant, defined as the common ratio (CR), after a certain number of terms  $k=N$ . In this case a modified response factor  $X'_{ijk}$  may be defined which truncates the above infinite series to the following finite summation:

$$\dot{Q}_{i,k=0} = A_i \sum_{j=1}^3 \sum_{k=0}^N X'_{ijk} T_{jk} + CR \cdot \dot{Q}_{i,k=1} \quad (5.3)$$

where  $\dot{Q}_{i,k=1}$  represents the instantaneous power through surface  $i$  at the

previous time step ( $k = 1$ ).

A one hour time interval was used in the above equations since this is the normal recording rate utilized by the U. S. Weather Bureau for their weather and solar tapes. Only six sets of response factors were required,  $N=5$ , in the above series for the two heated deck configurations that were investigated in this study.

Heated deck response factors were evaluated through the use of a finite element package (28) to numerically integrate the differential heat transfer equation. In the case of an unheated deck, the deck geometry is one dimensional which allows the response factors to be determined analytically (26).

In order to evaluate the current ( $k=0$ ) surface temperature  $T_{j,0}$ , the above response factor representation of the conductive heat transfer through each surface was utilized in a surface energy balance. In the case of the top surface, the surface conductive heat flux is equal to the sum of the four environmental modes of heat transfer depicted in Figure 5.1; solar radiation ( $q_{\text{solar}}$ ), long-wave atmospheric radiation ( $q_{\text{atm}}$ ), long-wave radiation from the deck ( $q_{\ell w}$ ), and convective heat transfer ( $q_{\text{conv}}$ ). That is,

$$\begin{aligned} \sum_{j=1}^3 \sum_{k=0}^N X'_{1jk} T_{jk} + CR \cdot q_{1,k=1} &= \alpha_{\text{sw}} q_{\text{solar}} + \alpha_{\ell w} q_{\text{atm}} + q_{\ell w} + q_{\text{conv}} \\ &= \alpha_{\text{sw}} q_{\text{solar}} + \alpha_{\ell w} \epsilon_{\text{air}} \sigma T_{\text{air}}^4 \\ &\quad - \epsilon_{\ell w} \sigma T_{1,0}^4 - h_u (T_{1,0} - T_{\text{air}}) \end{aligned} \quad (5.4)$$

which contains not only the unknown upper surface temperature  $T_{1,0}$  but also  $T_{2,0}$  and  $T_{3,0}$  in the summation term on the left. The remainder of

the temperatures given in the summation are previous temperatures ( $k \geq 1$ ) which are known values.

The bottom surface energy balance was performed in a similar manner except that radiation terms were neglected. The energy balance for an insulated bottom where  $u_{\text{insul}} \ll h_{\ell}$  is:

$$\sum_{j=1}^3 \sum_{k=0}^N X'_{2jk} T_{jk} + CR \cdot q_{2,k=1} = -u_{\text{insul}} (T_{2,0} - T_{\text{air}}) \quad (5.5)$$

and the corresponding energy balance for an uninsulated bottom is:

$$\sum_{j=1}^3 \sum_{k=0}^N X'_{2jk} T_{jk} + CR \cdot q_{2,k=1} = -h_{\ell} (T_{2,0} - T_{\text{air}}) \quad (5.6)$$

The environmental heat transfer correlations that were utilized in this study are presented in Table 5.1.

The final deck energy balance is performed at the condenser pipe surface,

$$\sum_{j=1}^3 \sum_{k=0}^N X'_{3jk} T_{jk} + CR \cdot q_{3,k=1} = \dot{Q}_3 / A_{\text{cond}} \quad (5.7)$$

where  $\dot{Q}_3$  is the condenser power and  $A_{\text{cond}}$  is the total condenser pipe area. Since  $\dot{Q}_3$  is unknown, a fourth equation which considers the heat transfer from the ground is required.

In the case of an unheated deck, only the upper and lower surface energy balances are required and the  $j$  summation in these two equations would only be to two.

### C. Isolated Evaporator Model

The most challenging of the heat pipe components to model is

TABLE 5.1. ENVIRONMENTAL HEAT TRANSFER CORRELATIONS

<u>Term</u>	<u>Definition</u>	<u>Correlation</u>	<u>Reference</u>
$\epsilon_{\text{air}}$	Atmospheric long-wave emissivity	$0.70 + 5.95 \times 10^{-5} e_o e^{(1500/T_{\text{air}})}$ <p><math>e_o</math> = Partial pressure of air (mB)  <math>T_{\text{air}}</math> = Air temperature (K)</p>	31
$h_u$ (W/m <sup>2</sup> °C)	Top surface convective film coefficient	$T_m^{0.3} V^{0.7} + 0.68  T_{1,0} - T_{\text{air}} ^{0.3}$ <p><math>T_{1,0}</math> = Surface Temperature (K)  <math>T_{\text{air}}</math> = Air Temperature (K)  <math>T_m = (T_{1,0} + T_{\text{air}})/2</math> (K)  <math>V</math> = Wind speed (m/sec)</p>	32
$h_l$ (W/m <sup>2</sup> °C)	Bottom surface convective film coefficient	$64.6/T_m^{1/2} + 22.2V^{.728}/T_m^{.591}$ <p><math>T_m = (T_{2,0} + T_{\text{air}})/2</math> (K)  <math>V</math> = Wind speed (m/sec)</p>	33

obviously the evaporator because of its many inherent complexities. The heat pipe field gives the semi-infinite ground a complicated geometry. The thermal conductance between the evaporators and the ground varies with time because of persistent residual temperature fields that are induced into the ground when energy is extracted by the heat pipes. The far field ground temperature distribution adjacent to the evaporators may itself vary with depth and time.

The interest in the design of vertical and horizontal heat exchangers has recently increased because of its heat pump applications which were initially investigated in the 1950's. Reference 29 presents a historical review of the various methodologies that have been utilized in the design of ground heat exchangers. The simplest of these methods assumes that a quasi-static condition is approached sometime after energy extraction commences which implies that a steady state analysis is applicable. The steady state thermal conductance between the evaporator and the ground is the minimum value that the transient conductance can approach but the results from this and other research indicates that the steady state value is excessively conservative.

Most of the recent ground models utilize either a finite difference or a finite element formulations which have limited utility because of the prohibitive expense involved in setting up and running many of these models. Even though these types of models can accurately handle the more general situations such as inhomogeneous properties, there are some very confining limitations on the physical size and the time interval that can be simulated. In some respects many of these totally numerical models are the antithesis of the steady state analytical model since they assume that the evaporators can be characterized by the short term

response of relatively small ground systems. The steady state analysis on the other hand calculates the maximum long term thermal impact that the evaporators can induce upon the infinite ground.

Ingersoll's (30) classical ground heat exchanger theory was built around the thermal response of the ground to infinitely long Kelvin line sources with time dependent strengths. Since this theory has the capacity to efficiently handle long-term transient responses in an infinite medium, the evaporator response functions were based upon a finite length version of Ingersoll's model. As shown in Figure 5.3, the evaporator pipe was represented by a line source that was twice the evaporator's length. The plane of symmetry through the line source represents an adiabatic plane. This provides a somewhat conservative but simple boundary condition for the ground plane across the top of the evaporator. The ground is assumed to be homogeneous with a thermal conductivity  $K_g$  and a thermal diffusivity  $\alpha_g$ , and to have a zero initial gage temperature when the line source is pulsed with a constant power per unit length for a time duration  $\delta_k$ . The temperature on the adiabatic plane at a distance  $R_e$  from the line source due to a train of past rectangular power pulses  $\dot{Q}_{pk}$  is given by

$$T_e - T_g = - \sum_{k=0}^{\infty} W_{ak} \dot{Q}_{pk} \quad (5.8)$$

where

$$W_{ak}(t_k, \delta_k) = \frac{1}{2\pi K_g l_p} \int_0^1 \frac{\operatorname{erf} \frac{1}{2} \left[ \frac{\zeta^2 + r_e^2}{\tau_k} \right]^{1/2} - \operatorname{erf} \frac{1}{2} \left[ \frac{\zeta^2 + r_e^2}{\tau_{k+1}} \right]^{1/2}}{(r_e^2 + \zeta^2)^{1/2}} d\zeta \quad (5.9)$$

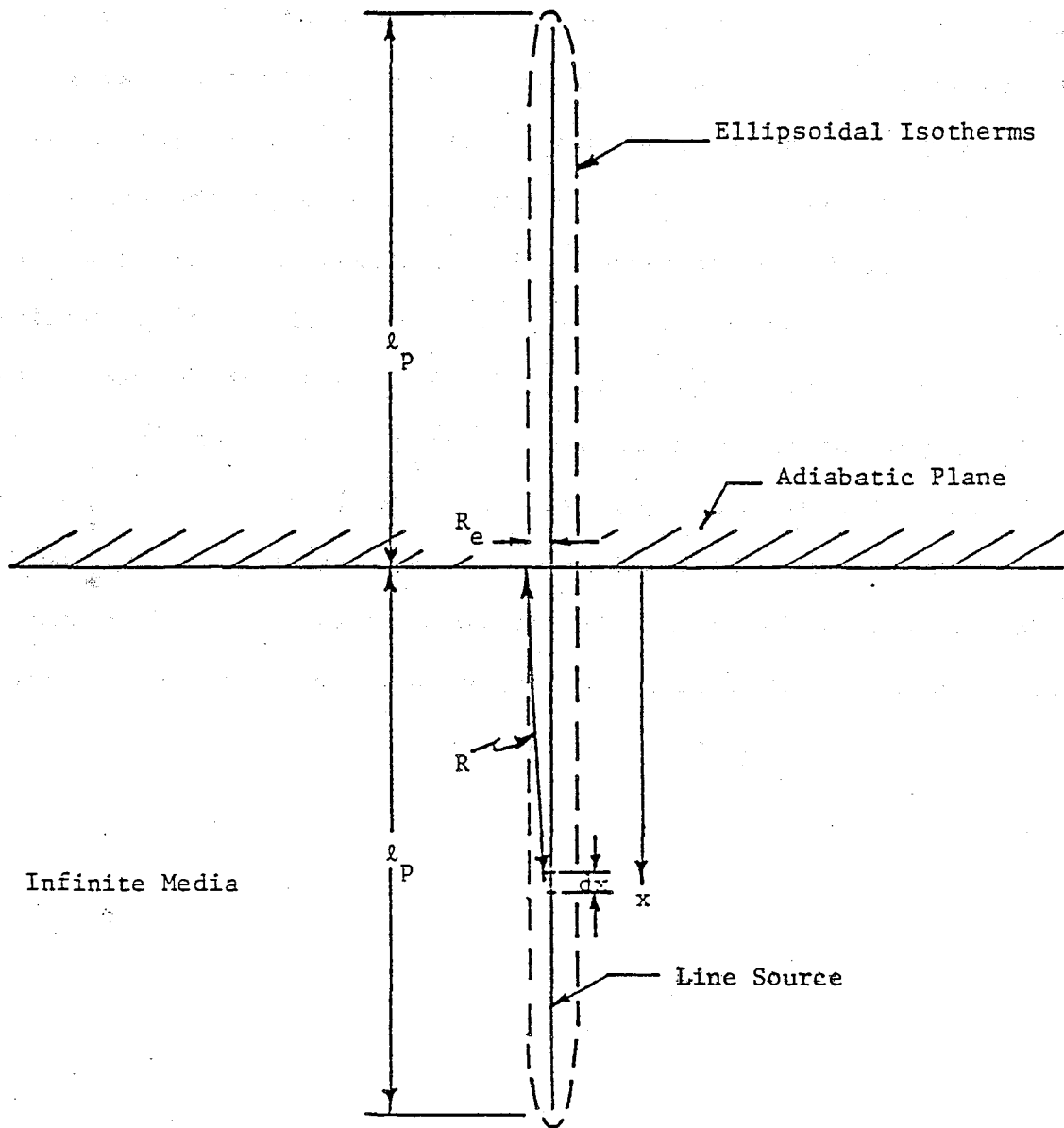


Figure 5.3. Line Source Representation of the Evaporator Pipe.

and

$$\tau \equiv \frac{\alpha_g t}{\lambda_p^2}, \quad \zeta \equiv \frac{x}{\ell_p} \quad \text{and} \quad r_e \equiv \frac{R_e}{\ell_p}.$$

The isothermals surrounding the line source are ellipsoids but they closely approximate the thermal profile surrounding an isothermal pipe with a large length to diameter ratio. The effective radius  $R_e$  that appears in the above response factor equation was determined by matching the steady state conductance obtained from an ellipsoidal model to the steady state line source conductance. The ellipsoidal representation of the cylindrical evaporator in a backfilled hole is presented in Figure 5.4, where the difference between cylindrical and elliptical geometries is greatly exaggerated for purposes of illustration. The ellipsoidal geometry was determined by matching the volumes and surface areas of the cylindrical evaporator pipe and its corresponding elliptical model along with the outer surface areas of the backfilled holes in the two coordinate systems. The steady state conductance for the ellipsoidal model was obtained by solving the appropriate one-dimensional conductive heat transfer equation in prolate spheroidal coordinates which, after some simplification, renders the result

$$U_{eg} \approx \frac{2.162\pi K_b \ell_p}{\ln\left(\frac{3.670\ell_p}{d_{eo}}\right) + \left(\frac{K_b}{K_g} - 1\right) \cdot \ln\left(\frac{3.670\ell_p}{d_h}\right)} \quad (5.10)$$

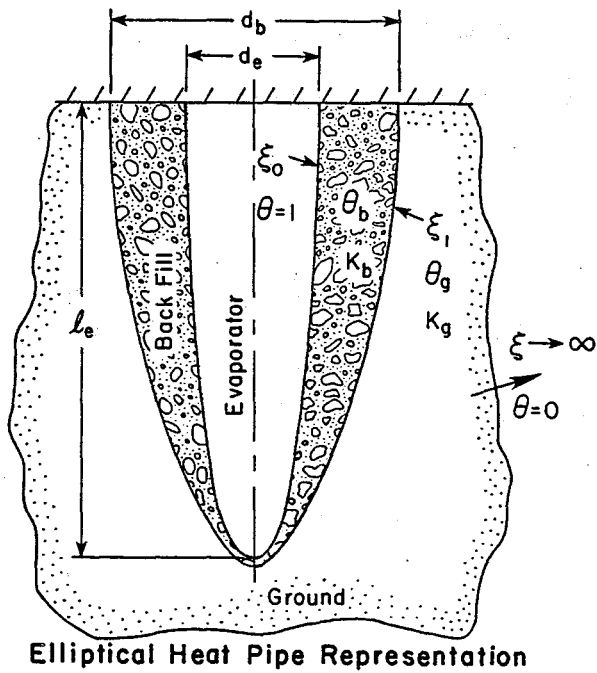
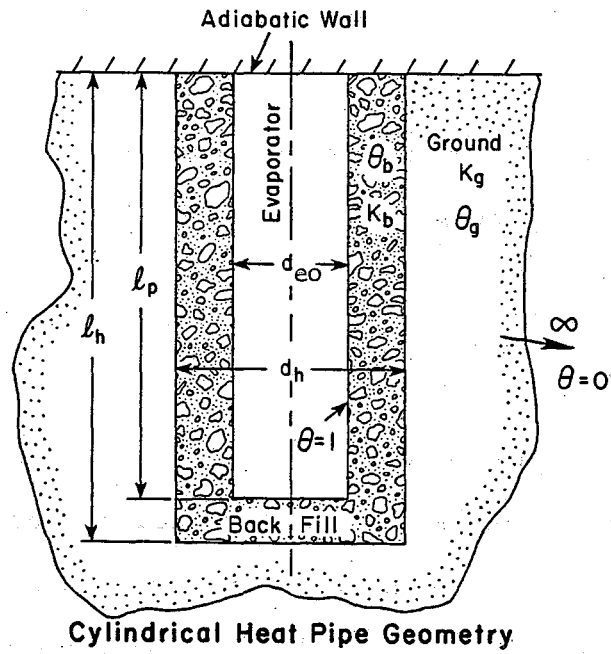


Figure 5.4. Evaporator Pipe-Backfill Geometry.

while the conductance of the line source under steady state conditions reduces to:

$$U_s \approx \frac{2.162\pi K_g \ell_p}{\ln\left(\frac{2.162\ell_p}{R_e}\right)} \quad (5.11)$$

The effective radius of the ellipsoidal representation of the evaporator pipe-backfill combination is therefore given by:

$$R_e = 2.162\ell_p e^{-2.162\pi K_g \ell_p / U_{eg}} \quad (5.12)$$

#### D. Evaporator Pipe Interaction

The interaction between evaporators can be very significant. The line source model was again utilized to calculate the average temperature response of evaporator "i" to a previous power pulse of unit magnitude along an adjacent evaporator "j". (Figure 5.5). This response factor  $W_{jk}$  is given by the expression:

$$W_{jk}(t, \delta_k) = \frac{1}{4\pi K_g \ell_p} \int_{-1}^1 \int_0^1 \frac{\operatorname{erf}\frac{1}{2}\left[\frac{(\zeta-\mu)^2 + r_{ij}^2}{\tau_k}\right]^{\frac{1}{2}} - \operatorname{erf}\frac{1}{2}\left[\frac{(\zeta-\mu)^2 + r_{ij}^2}{\tau_{k+1}}\right]^{\frac{1}{2}}}{[(\zeta-\mu)^2 + r_{ij}^2]^{\frac{1}{2}}} d\zeta d\mu \quad (5.13)$$

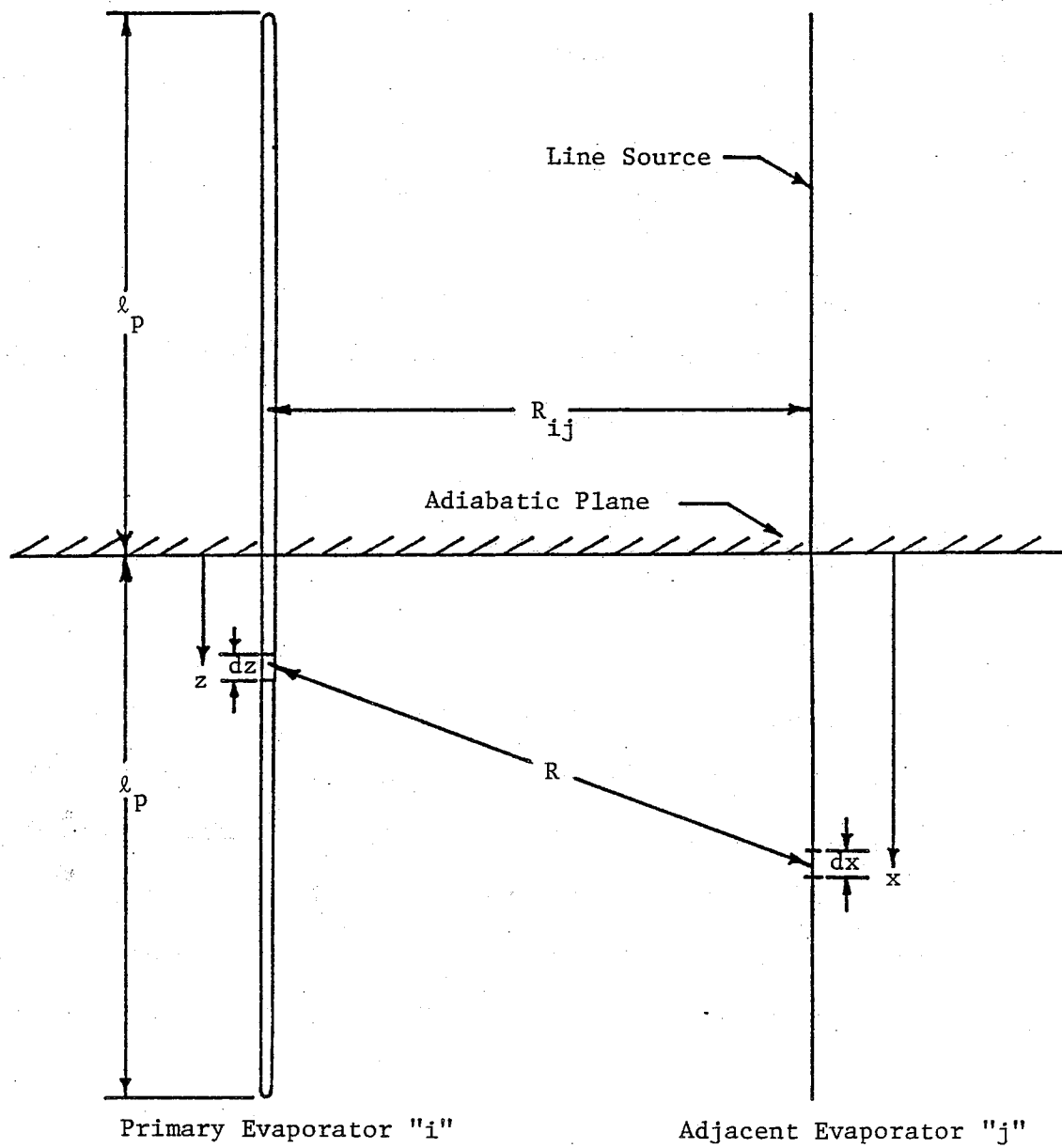


Figure 5.5. Evaporator Pipe Interaction Geometry.

where the power pulse occurred between the times  $t_k$  and  $t_{k+1}$  and the dimensionless quantities are defined as:

$$\tau \equiv \frac{\alpha t}{l_p^2} \quad \zeta \equiv \frac{x}{l_p} \quad \mu \equiv \frac{z}{l_p} \quad r_{ij} \equiv \frac{R_{ij}}{l_p}$$

The evaporator temperature change due to the energy extraction history of the primary evaporator pipe and all  $N_s$  surrounding evaporator pipes is therefore given by the expression:

$$T_e - T_g = - \sum_{k=0}^{\infty} W_{ak} \dot{Q}_{pk} - \sum_{j=1}^{N_s} \sum_{k=0}^{\infty} W_{jk} \dot{Q}_{jk} \quad (5.14)$$

where  $\dot{Q}_{pk}$  is the power extraction by the primary evaporator pipe. The response factors  $W_{jk}$  are each evaluated with the appropriate separation distance  $R_{ij}$  between the primary and  $j$ th adjacent evaporator and  $\dot{Q}_{jk}$  is the power extracted by evaporator pipe  $j$  over time interval  $k$ .

It was assumed that all evaporator pipes extract energy from the ground at approximately the same rate,  $\dot{Q}_{pk}$ , which simplifies the previous equation to

$$T_e - T_g = \sum_{k=0}^{\infty} W_k \dot{Q}_{pk} \quad (5.15)$$

where

$$W_k \equiv -W_{ak} - \sum_{j=1}^{N_s} W_{jk} \quad (5.16)$$

The above terms in the series have a limiting common ratio of one, which has the theoretical implication that the series may not converge. In this case, the series does converge very slowly which has the practical implication that the ground has an extremely long memory. To accurately but efficiently handle these long ground energy extraction records, power pulses of arbitrary duration  $\delta_k$  were utilized. This permitted the energy extraction record to be represented by pulses of increasing duration as time increased, but also entailed the calculation of variable time length response factors.

#### E. Far-Field Ground Temperature

The temperature change at the effective radius of the evaporator as given by Equation 5.15 assumes a time-independent and uniform far-field ground temperature  $T_g$ , but the ground temperature can vary significantly due to annual and diurnal temperature cycles (see Figures 3.1 and 4.5). It will be assumed that the evaporator pipe temperature floats with the average far-field ground temperature along its length. This implies that the same amount of energy enters the heat pipe field from above as does the far-field ground. This is a conservative assumption since more energy would be conducted into the heat pipe grid due to its locally depressed temperature field.

A simplified but often used approximation is to assume the surface temperature cycles to be harmonic functions of time. The surface cycles are not, however, sinusoidal or consistent from year to year and a more accurate model was developed using response factors. Figure 5.6 presents the response factor representation for the surface temperature

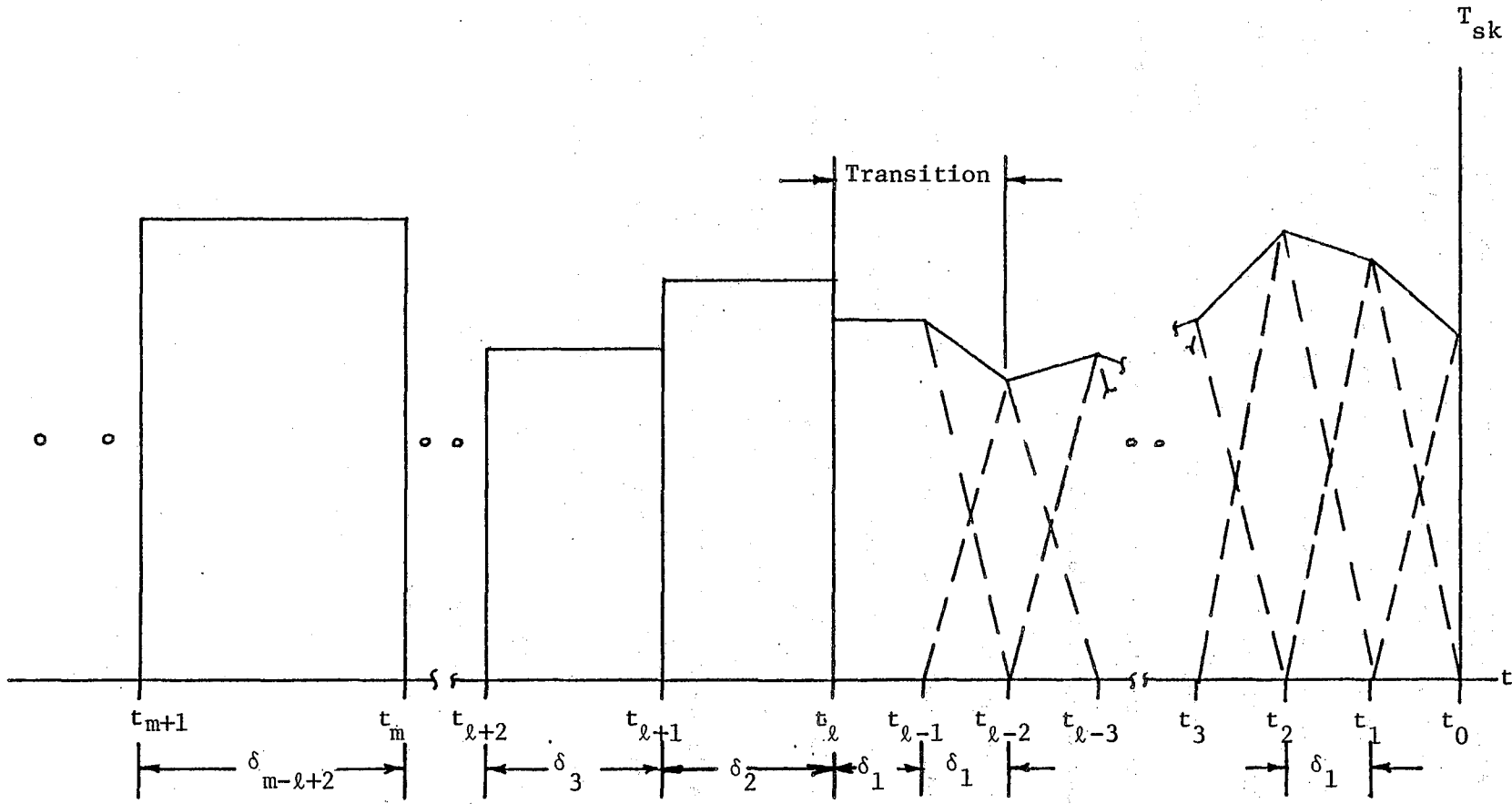


Figure 5.6. Discrete Representation of the Ground Surface Temperature History.

(or the temperature at any given depth in the soil) that was utilized in this analysis. The older data were again represented by time averaged rectangular pulses of increasing duration but, unlike the evaporator analysis, the thermal record near time equal zero was approximated with triangular pulses. This required the calculation of a special response factor that permitted the transformation from triangular to rectangular temperature pulses (see Figure 5.7).

The response function representation of the far field ground temperature at depth D is:

$$T_D = \sum_{k=0}^{\infty} Z_k T_{sk} \quad (5.17)$$

where  $T_{sk}$  is the temperature record on some reference ground plane and  $Z_k$  is the temperature rise at a depth D due to a unit temperature pulse on the reference plane at time  $t_k$ . The response functions for the triangular pulses shown in Figures 5.6 and 5.7 are obtained by considering the response of a semi-infinite solid with an initial reference temperature of zero to a ramp temperature change on the reference or surface plane.

$$T_s(t) = Ct$$

The temperature at a depth D below the reference plane is given by (34):

$$T_D = Ct \left[ \left( 1 + \frac{D^2}{2\alpha t} \right) \operatorname{erfc} \left( \frac{D}{2(\alpha t)^{1/2}} \right) - \frac{D}{(\pi\alpha t)^{1/2}} \exp(-D^2/4\alpha t) \right] \quad (5.18)$$

$$\equiv f_1(C, M, t)$$

where  $M = D^2/2\alpha$ . This implies that the first response factor at  $t = \delta_1$  is:

$$Z_0 = f_1(1/\delta_1, M, \delta_1) \quad (5.19)$$

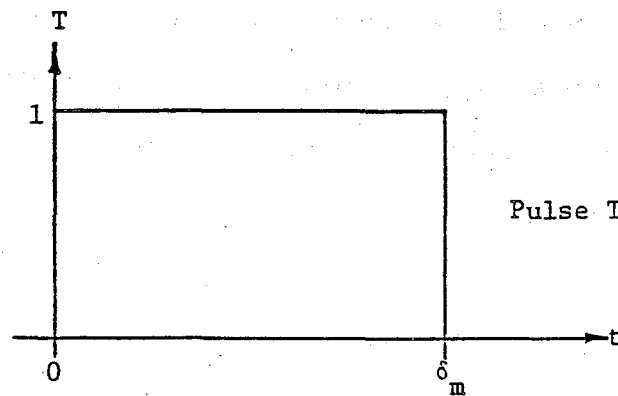
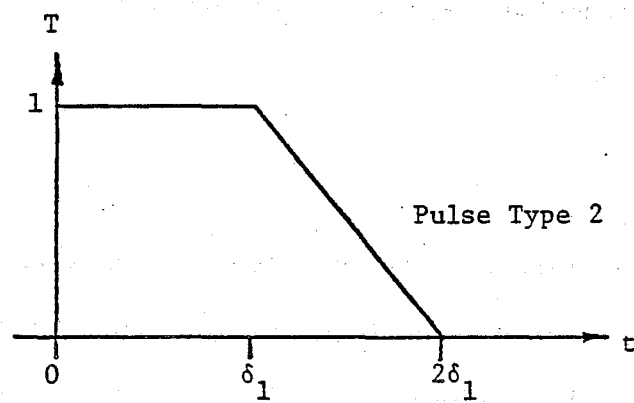
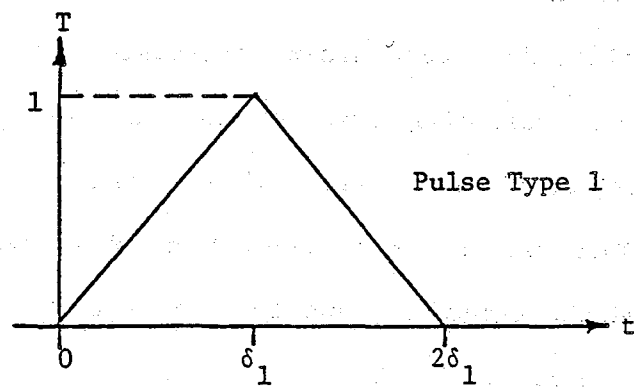


Figure 5.7. Temperature Pulses Used to Evaluate Z Response Factors.

The second response factor is the temperature rise due to pulse type 1 (see Figure 5.7) at  $t=2\delta_1$ :

$$Z_1 = f_1(1/\delta_1, M, 2\delta_1) - f_1(2/\delta_1, M, \delta_1) \quad (5.20)$$

The remainder of the response factors due to unit triangular temperature pulses for  $2\delta_1 < t < t_\ell$  (see Figure 5.6) are:

$$Z_k = f_1(1/\delta_1, M, (k+1)\delta_1) - f_1(2/\delta_1, M, k\delta_1) + f_1(1/\delta_1, M, (k-1)\delta_1) \quad (5.21)$$

$2 \leq k \leq \ell - 2$

Under the same initial conditions, if the surface is subjected to a step change in temperature of magnitude B, then the temperature at a depth D below the surface plane is given by (34):

$$T_D = B \cdot \operatorname{erfc}\left(\frac{D^2}{4\alpha t}\right) \quad (5.22)$$

$$\equiv f_2(B, M, t)$$

The transition response factor is therefore given by:

$$Z_{\ell-1} = f_2(1, M, \ell\delta_1) - f_1(1/\delta_1, M, (\ell-1)\delta_1) + f_1(1/\delta_1, M, (\ell-2)\delta_1) \quad (5.23)$$

and the rectangular response factors by:

$$Z_m = f_2(1, M, t_m + \delta_{m-\ell+2}) - f_2(1, M, t_m) \quad m \geq \ell \quad (5.24)$$

where

$$t_m = (\ell - 1)\delta_1 + \sum_{n=1}^{m-\ell+1} \delta_n \quad (5.25)$$

The average far-field ground temperature along the length of the evaporator pipe can be obtained from an average ground response factor:

$$T_g = \sum_{k=0}^{\infty} Z'_k T_{sk} \quad (5.26)$$

where

$$Z'_k = \frac{1}{D_\ell - D_o} \int_{D_o}^{D_\ell} Z_k(x) dx \quad (5.27)$$

and  $D_o$  and  $D_\ell$  are the depths corresponding to the top and bottom of the evaporator respectively. Equation 5.27 was evaluated numerically using trapezoidal integration.

Equations 5.15 and 5.26 may now be combined to provide the fourth energy balance equation necessary to evaluate the heat pipe system:

$$T_{3,0} = \dot{Q}_{p,0} (W_0 - R_{\text{pipe}}) + \sum_{k=1}^{\infty} W_k \dot{Q}_{pk} + \sum_{k=0}^{\infty} Z'_k T_{sk} \quad (5.28)$$

where the term  $R_{\text{pipe}}$  is included in the energy balance to account for the thermal resistance of the heat pipe and is given by:

$$R_{\text{pipe}} = \frac{\ln(d_{eo}/d_{ei})}{2\pi K_e \ell_p} + \frac{\ln(d_{co}/d_{ci})}{2\pi K_c \ell_c} + \frac{1}{\pi d_{ei} \ell_p h_e} + \frac{1}{\pi d_{ci} \ell_c h_c} \quad (5.29)$$

The terms  $h_e$  and  $h_c$  correspond to the evaporative and condensing film coefficients in the heat pipe. Experimentally based estimates of their values were utilized since appropriate correlations were not readily available or required in this analysis. Equation 5.28 contains two unknowns; the current heat pipe power ( $\dot{Q}_{p,0}$ ) and the current condenser

pipe temperature ( $T_{3,0}$ ).

#### F. Numerical Model

A computer program was developed to simulate the performance of the heat pipe system using the four surface energy balance equations developed in the previous three sections.

- 1) Top deck surface (Surface 1, Figure 5.2, Equation 5.4)
- 2) Bottom deck surface (Surface 2, Figure 5.2, Equation 5.5 or 5.6)
- 3) Condenser pipe surface (Surface 3, Figure 5.2, Equation 5.7)
- 4) Evaporator pipe surface (Equation 5.28)

The above four equations are summarized in Table 5.2. This represents a system of four equations with the following unknowns:

- 1)  $T_{1,0}$  - The current top surface temperature
- 2)  $T_{2,0}$  - The current bottom surface temperature
- 3)  $T_{3,0}$  - The current condenser surface temperature
- 4)  $Q_{p,0}$  - The current heat pipe power

These equations, which are non-linear due to the top surface energy balance, were solved using Newton-Raphson iteration. Because of the nature of a gravity-operated heat pipe, the heat pipe power can never be negative. When the above set of equations produced a negative value, the power was defined to be zero at that particular time and the system of equations was reduced from four to three. For the case of an unheated deck, only the top and bottom surface equations had to be solved to obtain  $T_{1,0}$  and  $T_{2,0}$ .

Special accommodations were made in the program for the ground response factors. A subroutine was developed to perform the time averaging of the  $Q_{pk}$  (heat pipe powers) and  $T_{sk}$  (the far-field ground

TABLE 5.2. SURFACE ENERGY BALANCES

<u>Energy Balance</u>	<u>Simulation Type</u>
<u>Top Surface</u>	
$\sum_{j=1}^{NS} \sum_{k=0}^N X'_{1jk} T_{jk} + CR \cdot q_{1,1} = \alpha_{sw} q_{solar} + \alpha_{lw} \epsilon_{air} \sigma T_{air}^4 - \epsilon_{lw} \sigma T_{1,0}^4 - h_u (T_{1,0} - T_{air})$	
<u>Bottom Surface</u>	
$\sum_{j=1}^{NS} \sum_{k=0}^N X'_{2jk} T_{jk} + CR \cdot q_{2,1} = -u_{insul} (T_{2,0} - T_{air})$	Insulated
$\sum_{j=1}^{NS} \sum_{k=0}^N X'_{2jk} T_{jk} + CR \cdot q_{2,1} = -h_l (T_{2,0} - T_{air})$	Air-Coupled
<u>Condenser Surface</u>	
$\sum_{j=1}^{NS} \sum_{k=0}^N X'_{3jk} T_{jk} + CR \cdot q_{3,1} = \dot{Q}_3 / A_{cond}$	Heated Deck
<u>Evaporator Surface</u>	
$T_{3,0} = \dot{Q}_{p,0} (W_0 - R_{pipe}) + \sum_{k=1}^{\infty} W_k \dot{Q}_k + \sum_{k=0}^{\infty} Z'_k T_{sk}$	Heated Deck
<u>Assumption 4</u>	
$\dot{Q}_{3,0} = \dot{Q}_{p,0}$	

temperatures at a depth D). For simplicity, only hourly, daily, and monthly (30 days) time intervals were considered. Based on the results of several test cases to determine appropriate transition times, the  $W_k$  and  $Z'_k$  response factors were calculated for 100 hour, 100 day, and 100 month time intervals. An attempt was made to account for initial conditions by initializing the  $T_{si}$  (ground temperatures) array with a nominal temperature sinusoid having a period of 1 year.

#### G. Model Validation

A test of the model was made by simulating the performance of the Sybille and Spring Creek bridge systems using the computer data bases generated during these experiments. A necessary first step was to place the data for these sites on a continuous basis with a one hour time interval between data sets. Approximately 6% of the data at Sybille and 17% of the data at Spring Creek within the monitored time intervals were missing. Short gaps (less than six hours) were filled with linearly interpolated data while longer gaps were filled with data from adjacent time periods.

The principal system parameters that were utilized in these two simulations are delineated in Table 5.3. The concrete and ground thermal properties were measured in the laboratory. The values that are listed for deck thickness and the embedded condenser depth are estimated average values in the case of Sybille because of the variations that existed throughout the heated deck. The alternating condenser lengths of the Spring Creek System pictured in Figure 1.2 were handled by calculating the condenser length per evaporator  $\ell_c$  that a system with a uniform 15 cm (6") condenser spacing would require to produce the same

TABLE 5.3. SYBILLE AND SPRING CREEK SYSTEM PARAMETERS.

<u>Parameter</u>	<u>Sybillie</u>	<u>Spring Creek</u>
$K_{\text{conc}}$ (W/m°C)	1.8	2.1
$(\rho c)_{\text{conc}}$ (J/m <sup>3</sup> °C)	2.06x10 <sup>6</sup>	2.16x10 <sup>6</sup>
$\epsilon_{\text{lw}} = \alpha_{\text{lw}}$	0.85	0.85*
$\alpha_{\text{sw}}$	0.60	0.60*
b (m)	0.1524	0.1524
h (m)	0.0349	0.0548
H (m)	0.1588	0.2096
$d_{\text{co}}$ (m)	0.0254	0.0334
$d_{\text{ci}}$ (m)	0.0191	0.0266
$\lambda_{\text{c}}$ (m)	4.877	40.5
$h_{\text{c}}$ (W/m <sup>2</sup> °C)	7.95x10 <sup>3</sup>	7.95x10 <sup>3</sup>
$K_{\text{g}}$ (W/m°C)	1.21	2.1
$K_{\text{b}}$ (W/m°C)	0.80	2.0
$\alpha_{\text{g}}$ (m <sup>2</sup> /sec)	5.6x10 <sup>-7</sup>	1.0x10 <sup>-6</sup>
$d_{\text{h}}$ (m)	0.1524	0.2032
$d_{\text{eo}}$ (m)	0.0254	0.0603
$d_{\text{ei}}$ (m)	0.0191	0.0493
$\lambda_{\text{p}}$ (m)	12.19	30.48
$u_{\text{insul}}$ (W/m <sup>2</sup> °C)	0.4	0.4
$h_{\text{e}}$ (W/m <sup>2</sup> °C)	2.04x10 <sup>3</sup>	2.04x10 <sup>3</sup>
$K_{\text{c}}$ (W/m°C) = $K_{\text{e}}$	45.	45.

\* assumed to be the same as the corresponding value for Sybillie

steady state heat transfer as the actual system. This equality is given by the expression:

$$S_1 K_{\text{conc}} \ell_c = 4S_1 K_{\text{conc}} \ell_1 + 2S_2 K_{\text{conc}} (\ell_2 - \ell_1) \quad (5.30)$$

where  $S_1$  and  $S_2$  are the shape factors for the Spring Creek condenser pipes on 15.2 cm (6") and 30.5 cm (12") spacings respectively (see Figure 6.7), and  $\ell_1$  and  $\ell_2$  are the shorter and longer condenser pipe lengths respectively.

A plan view of the Sybille and Spring Creek evaporator pipe fields is presented in Figure 5.8 and the primary evaporators that were simulated are also denoted. These primary evaporator pipes were chosen on the basis of available experimental temperature data.

Figure 5.9 compares the predicted and experimental Sybille bridge responses of both the heated and unheated bridge sections over a week in December, 1977. This figure presents a representative example of the model's performance over a large range of temperatures and during periods with and without snow cover. The duration of the daily snow cover above the heated and unheated sections are also denoted on Figure 5.9. The unheated deck simulation indicates that the model can accurately handle the dynamic interactions between a dry deck and the environment, but not the behavior of a snow covered deck. This inaccuracy is of course expected since the predicted values are all based upon the assumption of dry surface conditions. The close agreement between the predicted and measured freeze-thaw characteristics of the unheated section which are tabulated in Table 4.2, likewise attest to this model's accuracy.

The heated deck simulation also shows the same excellent agreement

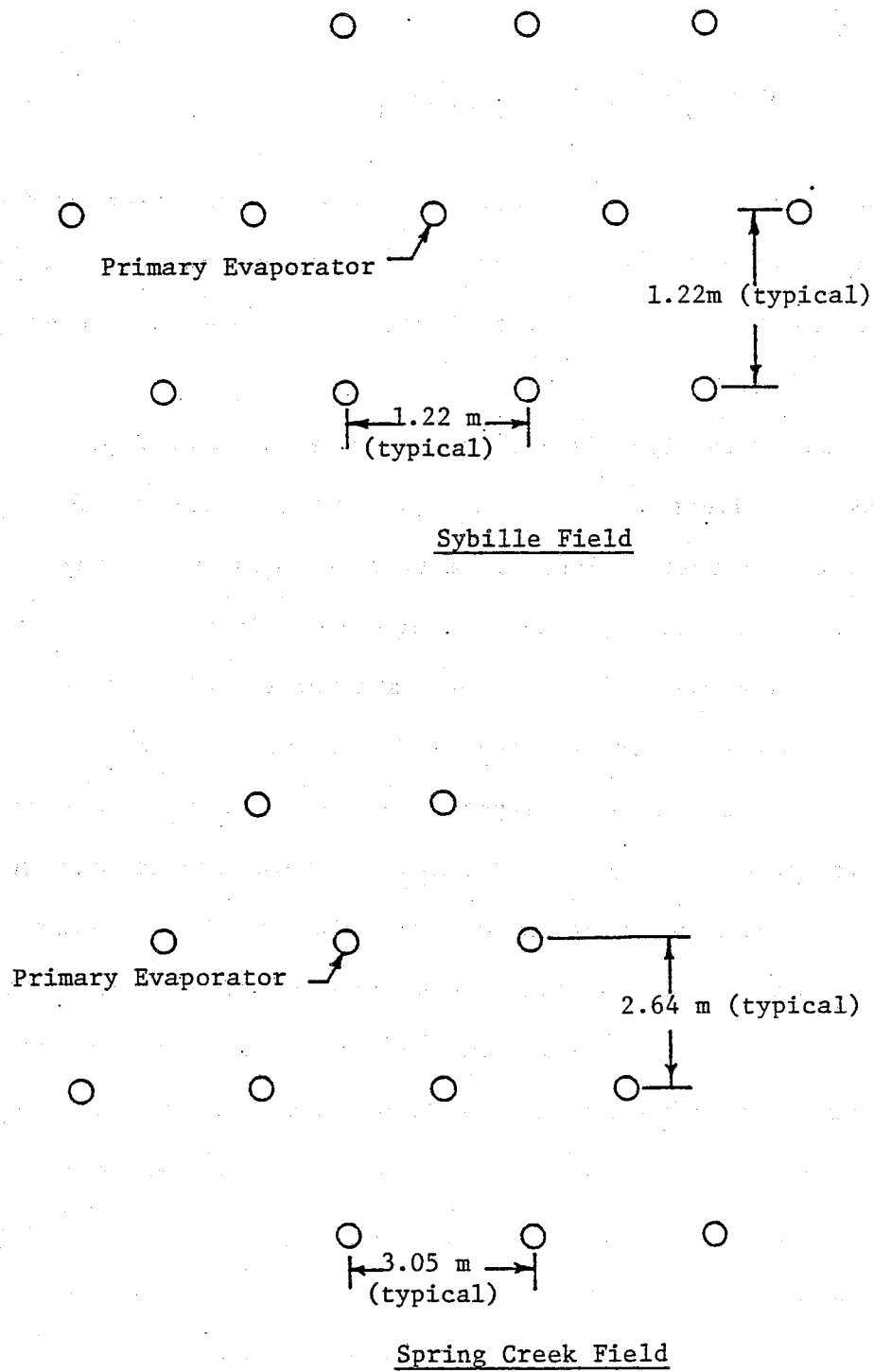
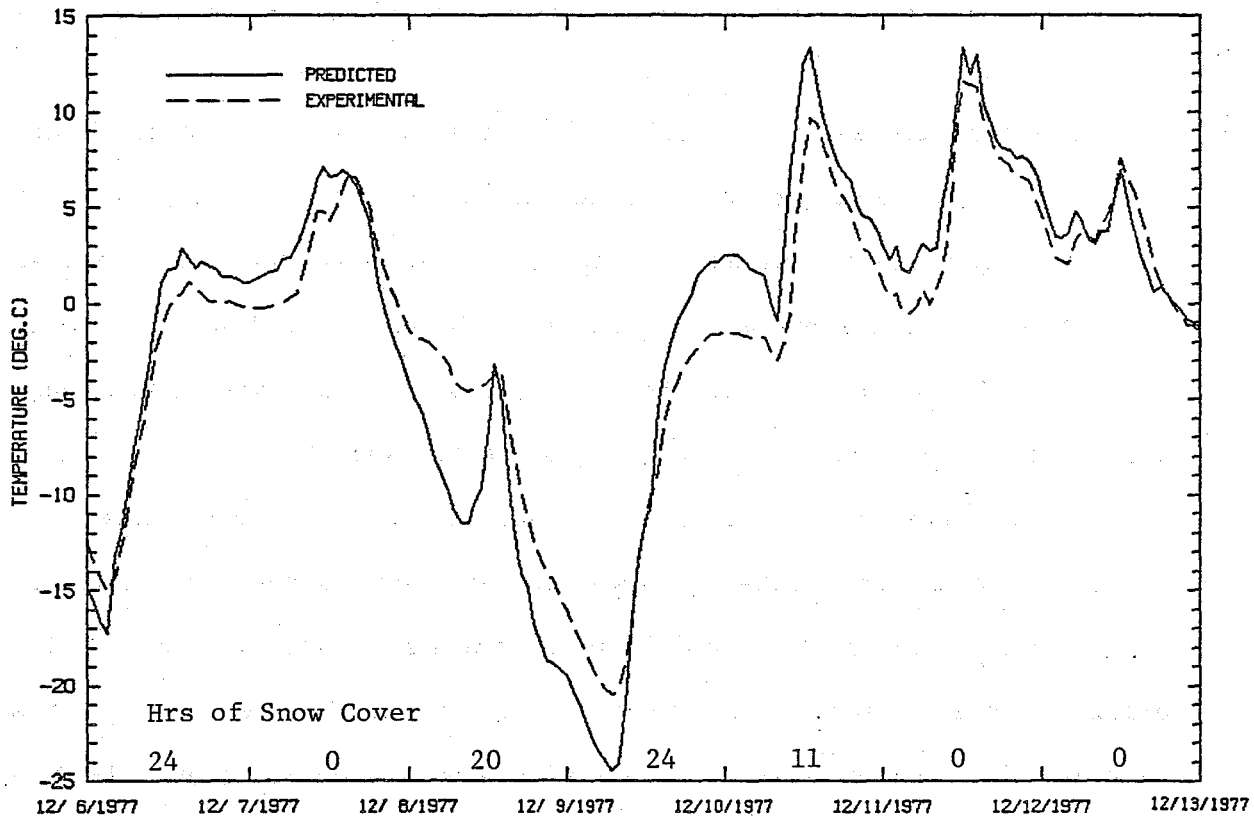
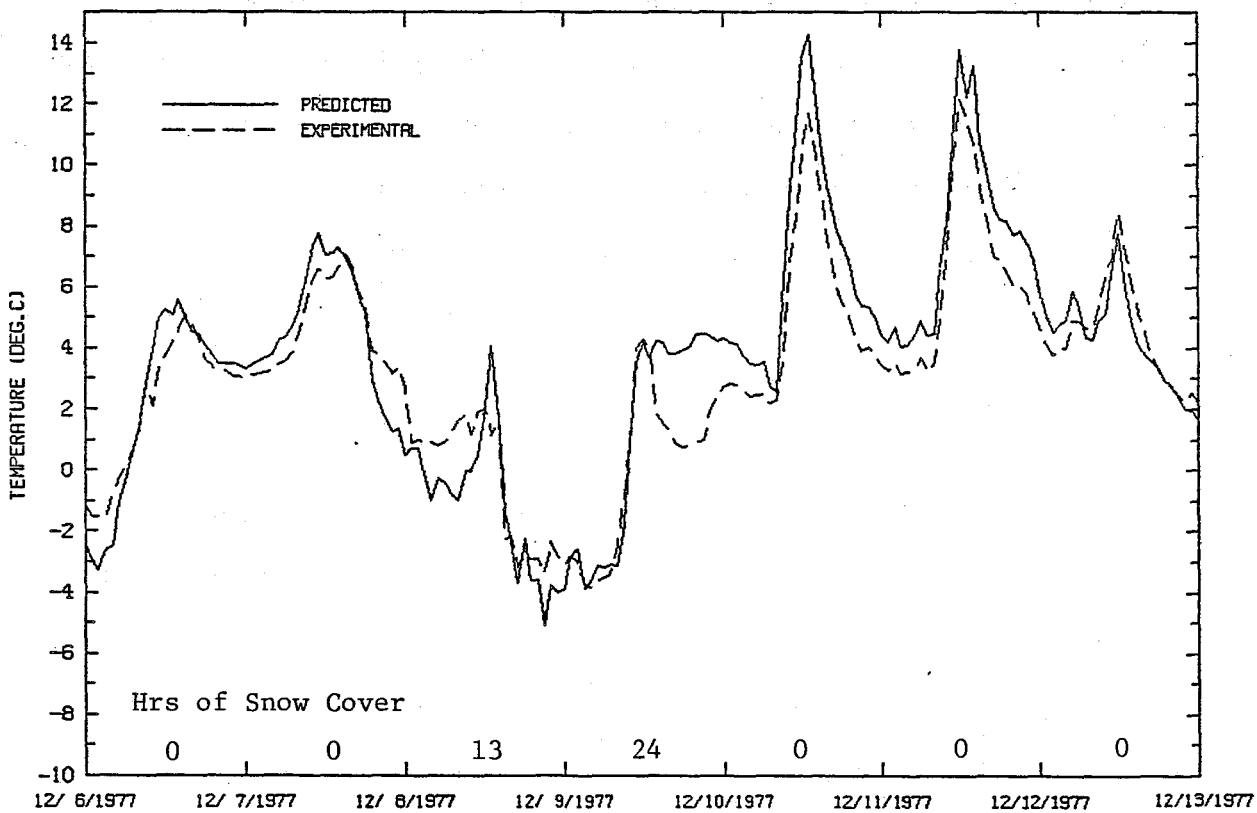


Figure 5.8. Sybille and Spring Creek Evaporator Fields.



A. Unheated Deck



B. Heated Deck

Figure 5.9. Predicted/Experimental Heated and Unheated Sybille Top Surface Temperatures.

with the experimental data during the clear deck conditions in Figure 5.9, but the predicted heated surface temperatures were generally lower than the experimental values over the winter months. Table 4.2 displays this trend since the predicted reductions in the heated deck's frozen time and °C-Days frozen over the two years are 36% and 66% respectively while the corresponding measured values are 60% and 86%.

The Sybille Canyon simulation proved to be more conservative than desired, but the heat pipe system's dynamic performance was obviously characterized accurately enough that it could have been utilized in its original design. The reason for the degree of conservatism in this particular simulation is not totally understood. The heat pipe model was formulated to be somewhat conservative because of the adiabatic boundary condition that was placed through the top of the evaporators, but there are probably other contributing factors. Many uncertainties in the experiment itself exist such as the nonuniform dimensions in the heated deck section and the accuracy of some of the experimental data -- especially the ground and evaporator temperatures.

Figure 5.10 compares the weekly averaged experimental temperatures from a thermistor that was placed on the outer surface and near the bottom of an evaporator pipe to the predicted average temperature of the evaporator. This figure shows that the predicted evaporator temperatures are notably below the experimental values during the second half of the heating seasons, except during the spring of 1977 which is only an artifact of the assumed initial values and should, therefore, be ignored. The ground depression is influenced by such natural phenomena as water movement and nonuniformities of ground properties which this

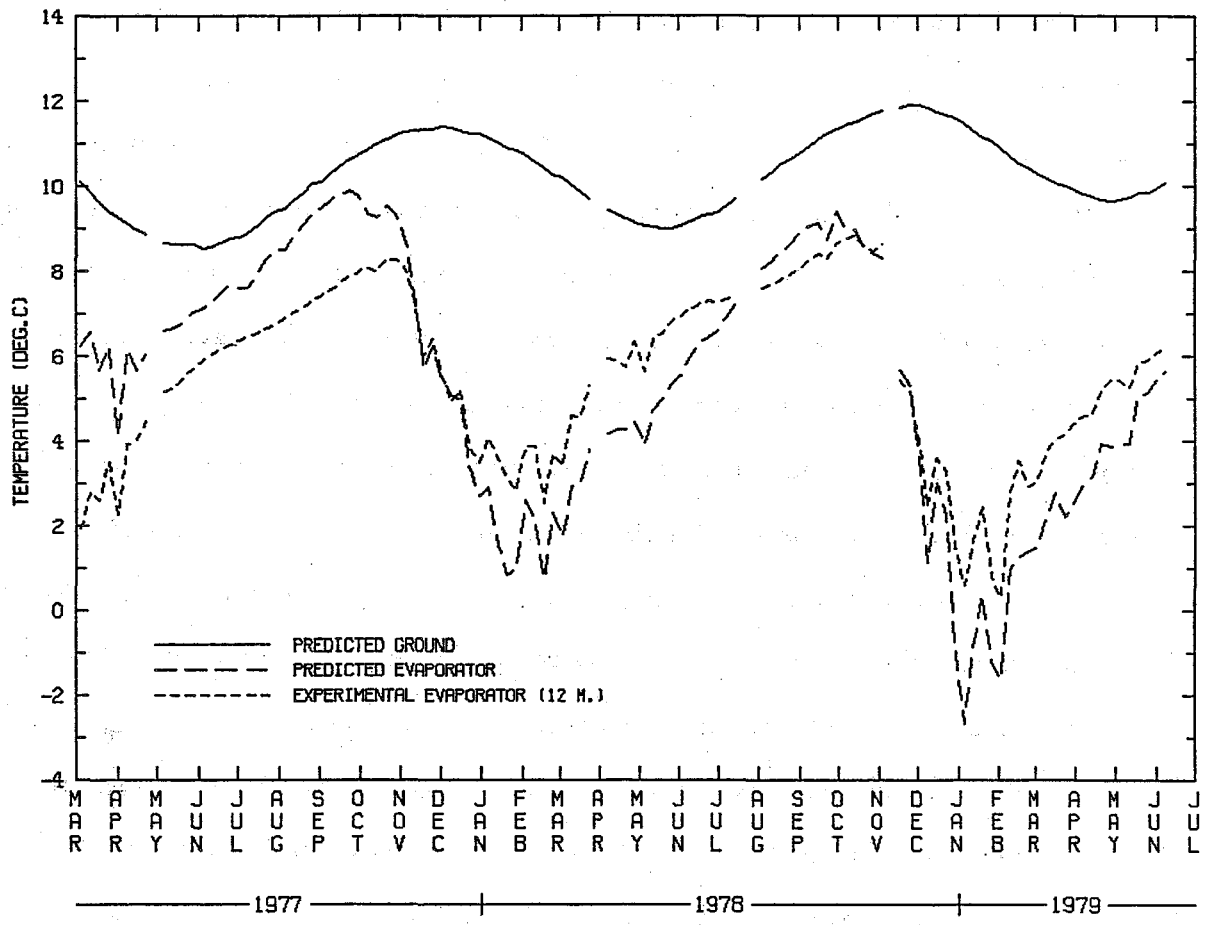


Figure 5.10. Predicted/Experimental Weekly Averaged Evaporator Temperatures at Sybille. Interactive Model.

model cannot handle even if these properties could be quantified. The significant variation of the drilling mud and water levels in the evaporator holes caused the characterization of the evaporator geometry and the backfill lumped thermal conductivity to be somewhat problematical. Defining the effective far field ground temperature was also difficult since the amplitude of the thermal wave was as high as 2.5°C, 12 m (40') in the ground. The predicted ground temperature that is plotted in Figure 5.10 is the mean far field ground temperature over the length of the evaporator. This temperature was calculated from the 3 m (10') experimental ground record and equation 5.26. The evaporator temperature is assumed to float with this effective ground temperature. The evaporator math model is based upon a uniform far field ground temperature which is a good approximation for most locations at depths below 3 m (10'). The effect that these large amplitude thermal waves had on the thermal model's accuracy was not investigated.

Much of the thermal depression of the ground surrounding an evaporator is caused by the other evaporators. An indication of the magnitude of this interaction can be obtained by comparing the predicted response of the Sybille evaporators in Figure 5.10 to the predicted response of an isolated evaporator which is presented in Figure 5.11.

To summarize, the heat pipe model predictions concerning the dynamic performance of the Sybille Canyon system were too conservative, but the results are quite reasonable when one considers all the complexities, uncertainties and simplifications that were involved.

The Spring Creek test proved to be a much more controlled experiment when compared to the Sybille Canyon test which is probably

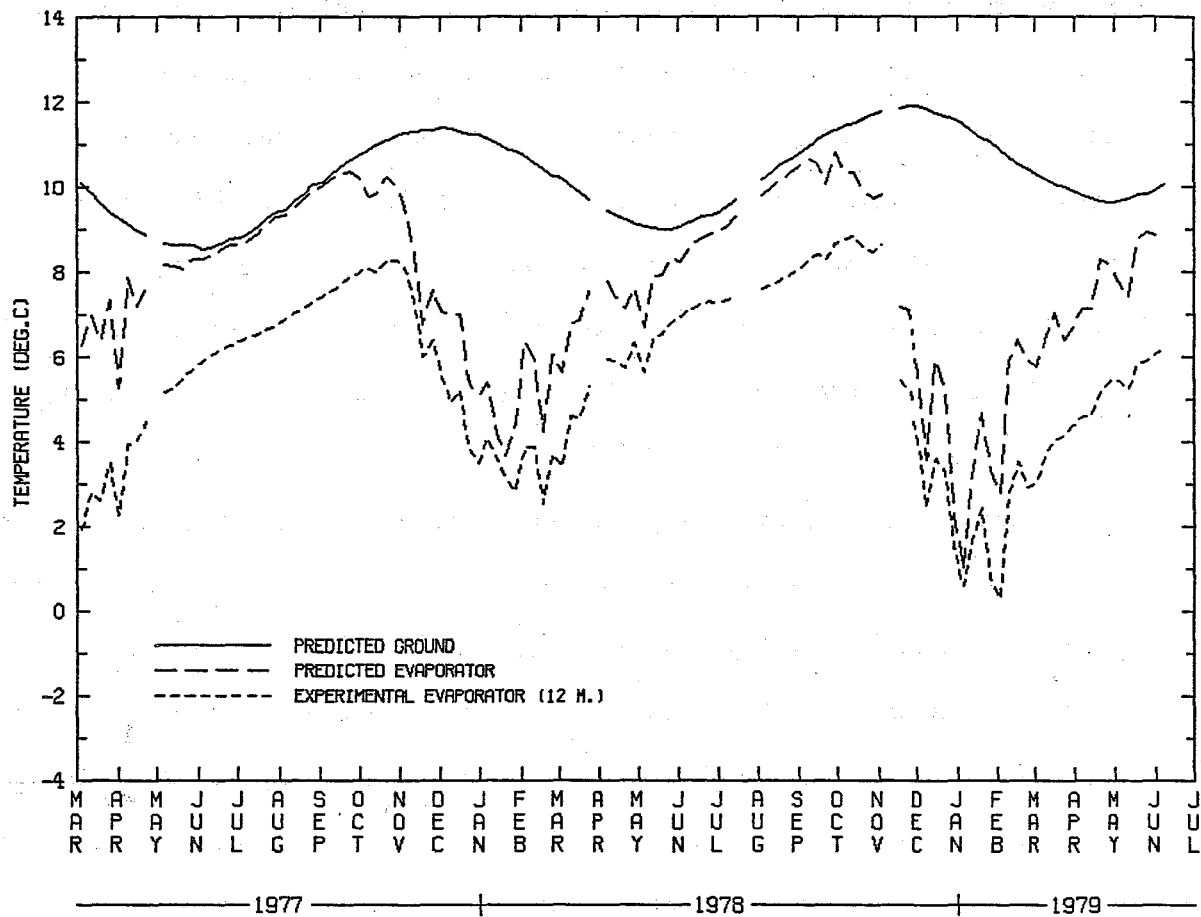
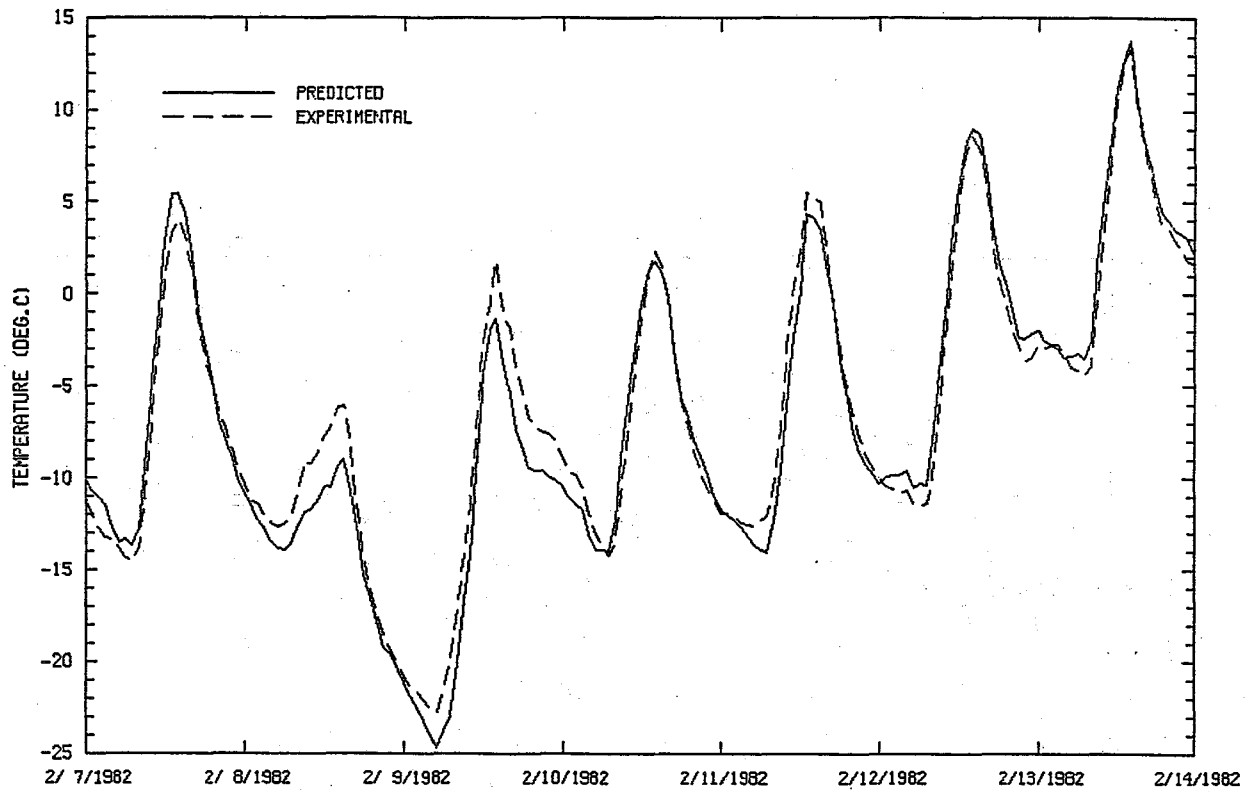


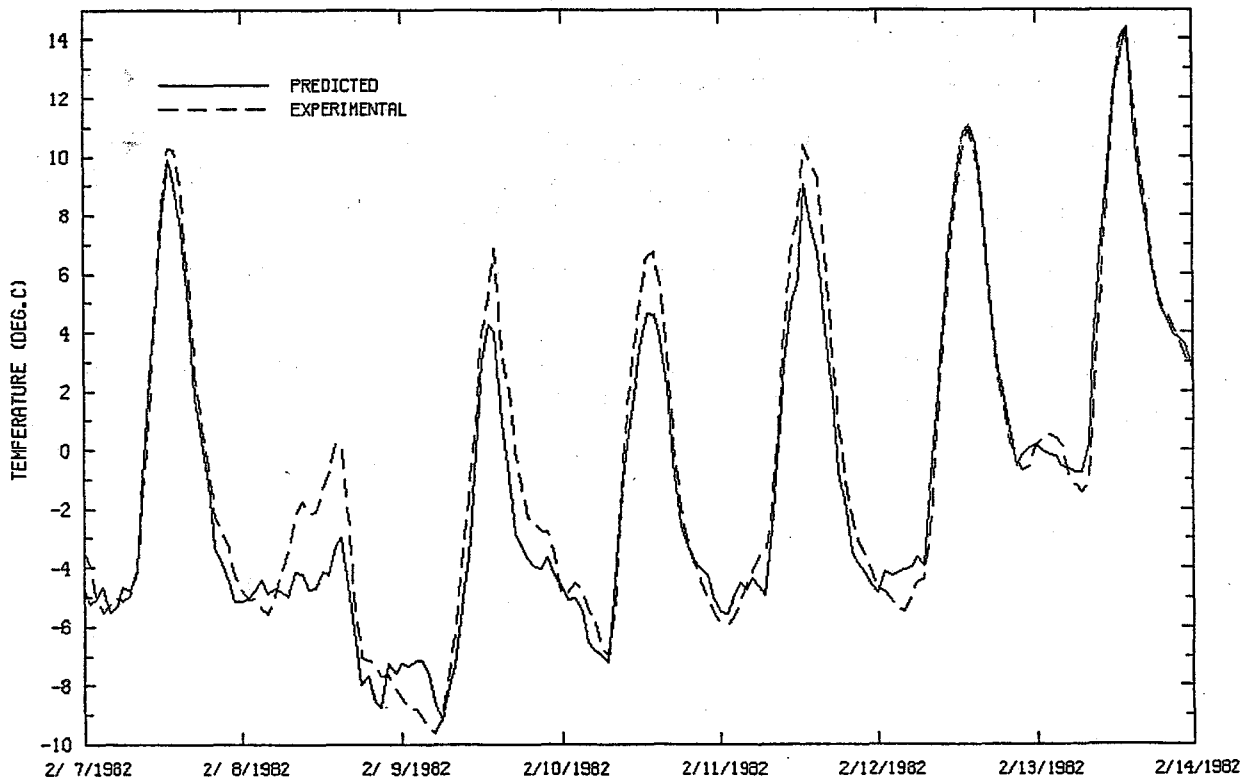
Figure 5.11. Predicted/Experimental Weekly Averaged Evaporator Temperatures at Sybille. Isolated Model.

responsible for some of the improved agreement between the predicted and experimental results. Figure 5.12 compares a typical simulation of the Spring Creek heated and unheated top surface temperatures to the corresponding experimental values. This figure indicates that there was excellent agreement between the experimental and predicted values over a large temperature range and that the heat pipe system increased the heated surface temperature by as much as 15°C during this particular week. The simulation of another time period is also plotted in Figure 5.15. The surface freeze characteristics which are detailed in Table 3.2 were also reasonably well predicted for both the heated and unheated surfaces.

Figure 5.13 compares the experimental temperatures that were recorded by two probes next to the evaporator at two different depths and the predicted average temperature of the evaporator pipe. The simulation was based upon a twelve evaporator field since pipes 1, 2 and 3 in corner 3 (see Figure 2.2) had malfunctioned by the second winter. The predicted evaporator temperature remained below the experimental values throughout this simulation with a major divergence occurring in the 1982-83 winter. Part of this depression may be the result of the model underpredicting the ground's thermal recovery during the summer, but it appears that the gradual failures of the two remaining heat pipes with functioning evaporator thermal instrumentation was the essential cause of this divergence. These failures are believed to be due to the formation of liquid locks in the interconnecting pipes which are discussed in Chapter 3. Figure 5.13 shows that the coldest measured weekly averaged evaporator temperature occurred during the first winter even



A. Unheated Deck



B. Heated Deck

Figure 5.12. Predicted/Experimental Heated and Unheated Spring Creek Top Surface Temperatures.

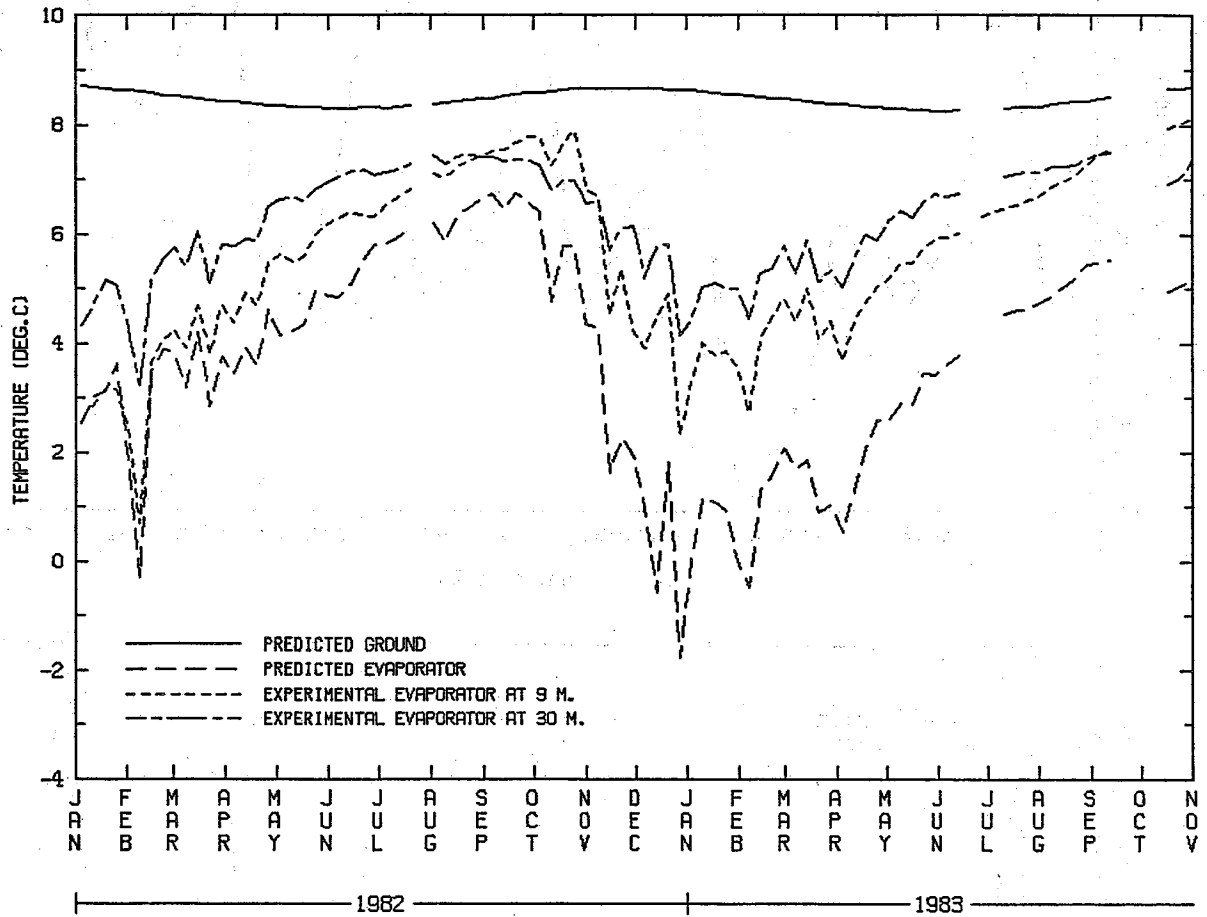


Figure 5.13. Predicted/Experimental Weekly Averaged Evaporator Temperatures at Spring Creek. Interactive Model.

though the coldest monthly air (see Table 3.1) and predicted evaporator temperatures occurred during the second winter. This indicates that the performance of these heat pipes were declining. The influence of the evaporator interactions at this site can be obtained by comparing the predicted response of an isolated model (Figure 5.14) to the response of the heat pipe field (Figure 5.13). The experimental values are significantly above the isolated model predictions for a long period in the second year, which is also a consequence of the heat pipe's gradual failure.

An attempt was made to measure the ground heat pipe power with an electrically powered heat pipe (Figure 2.15) by matching respective condenser temperatures in the region with 30 cm (12") condenser spacing (Figure 2.3). Table 5.4 tabulates the monthly electrical energy consumed by the electric heaters and the values predicted by the ground heat pipe model and the deck response factors. The latter calculation utilizes the experimental temperature record for the top surface, condenser pipe and bottom surface (see Figure 5.2 and Equation 5.3). The results of this experiment show that the model's prediction was on the average only 17% below the measured values while the deck response factors calculations were 20% higher. Figure 5.15 indicates that the best agreement between predicted and measured heat pipe powers occurred during the major events when the 1500 W heater did not have to cycle as much.

In summary, the Spring Creek experimental record indicates that the ground heat pipe model's predictions of the freeze-thaw characteristics of the heated deck (Table 3.2) and the ground energy extraction (Table 5.4) were reasonably accurate on the conservative side. Similar results

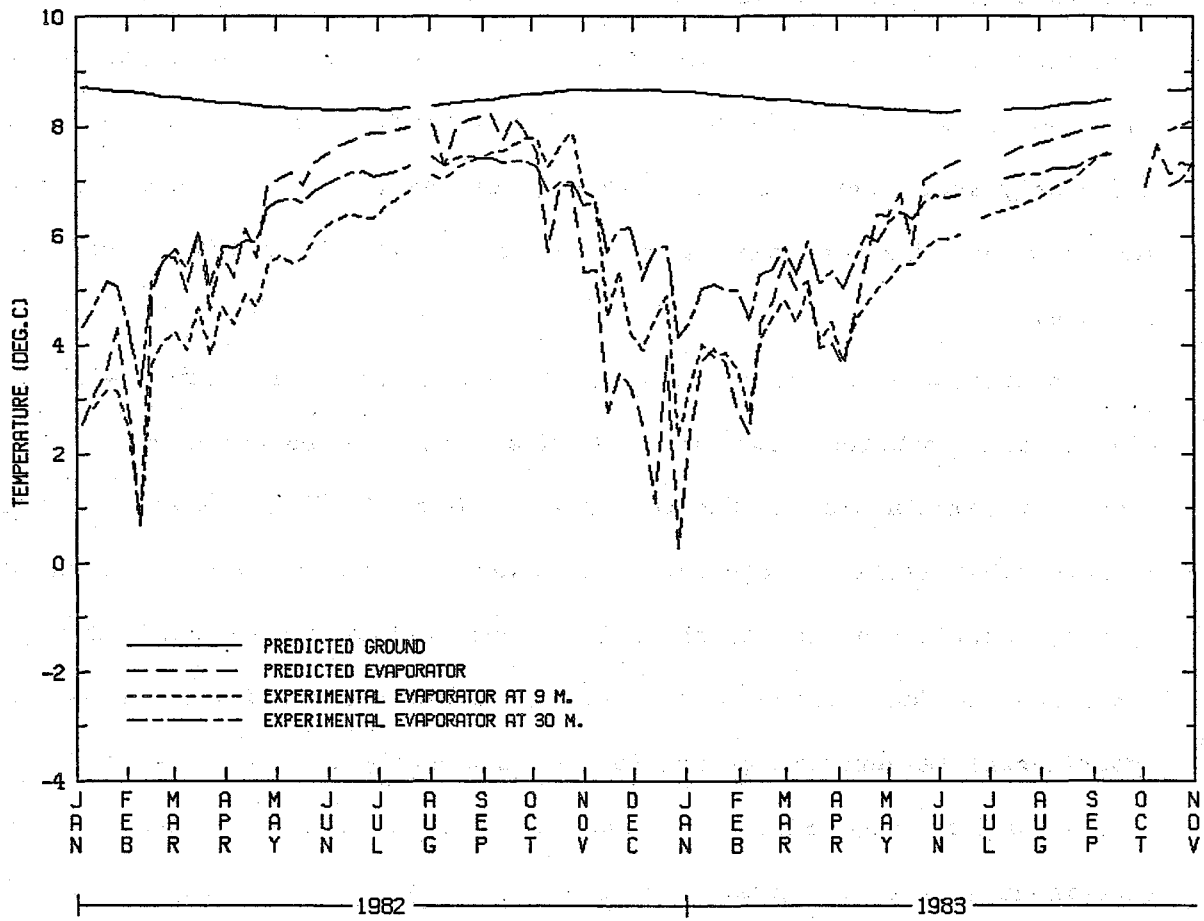
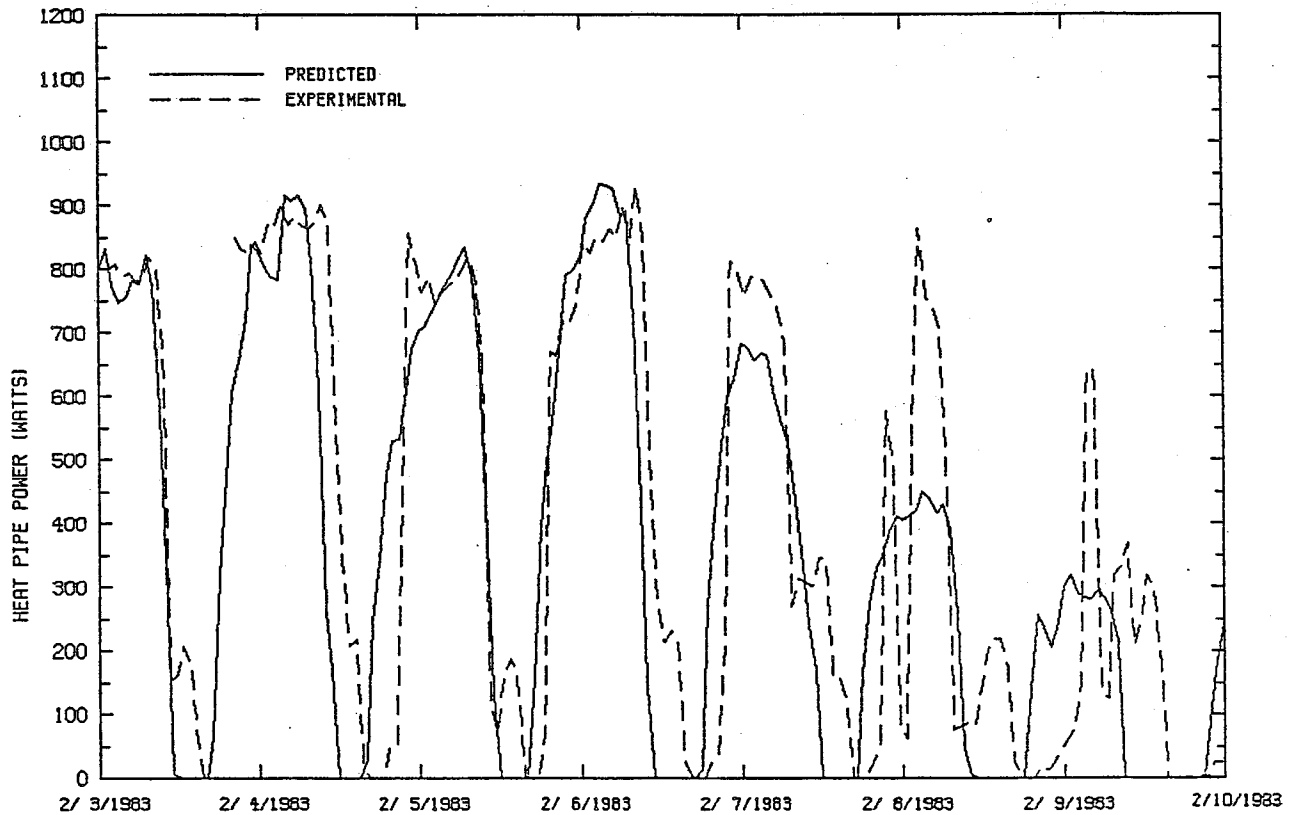
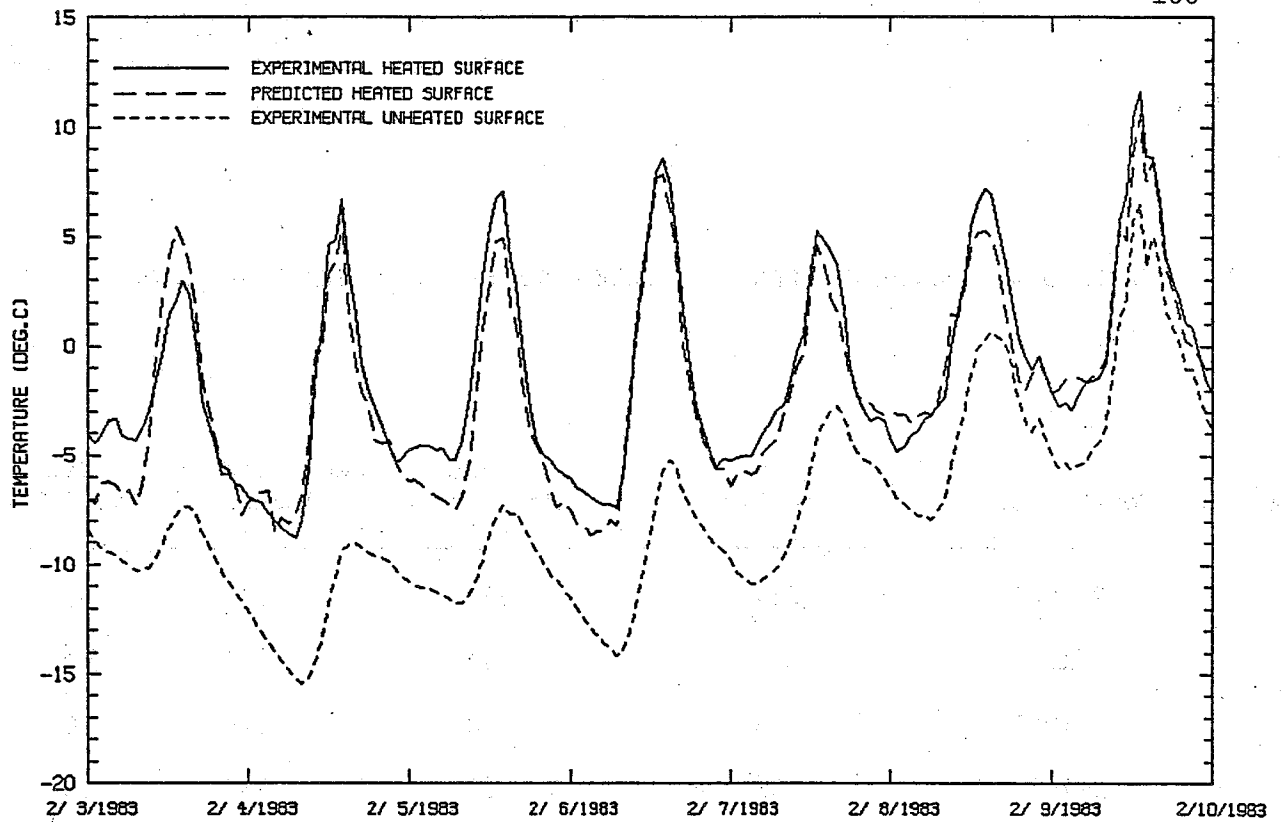


Figure 5.14. Predicted/Experimental Weekly Averaged Evaporator Temperatures at Spring Creek. Isolated Evaporator.

TABLE 5.4. MONTHLY ENERGY EXTRACTED PER SPRING CREEK EVAPORATOR

Month/Year	Electric Heaters (MJ)	Model Prediction (MJ)	Deck Response Factors (MJ)	% Data Available
12/1982	854	830	1097	65
1/1983	660	611	964	80
2/1983	493	388	586	60
3/1983	401	257	367	53
4/1983	220	91	144	26



5.15. Comparison of Measured and Predicted Heat Pipe Powers at Spring Creek.

were obtained for the Sybille Canyon system. Since these two heat pipe systems were geometrically and thermally dissimilar, the validity of the model has been substantiated.

#### H. Parametric Studies

One of the primary purposes of developing the computer model was to be able to characterize system performance as a function of the significant system variables. Numerous parametric studies were performed to accomplish this goal. In all these studies, the predicted system performance over the second year of operation was used to characterize each system because long term simulations indicated that there was little degradation in performance after the second year, and the model appears to underpredict thermal recovery during the summer. The segment of the environmental record which covered a complete year that began in the spring was cycled twice in these two year parametric studies.

Figure 5.16 shows the sensitivity of the Spring Creek system performance to variation in key system parameters. The performance was defined in terms of the total annual energy extracted from the ground per evaporator and the system parameters which were varied were  $U_{\text{system}}$ ,  $\alpha_g$ ,  $K_g$ ,  $R_e$ , and  $\ell_p$ .  $U_{\text{system}}$  is defined as the thermal conductance from the outside wall of the evaporator pipe to the ambient air

$$U_{\text{system}} = 1 / \left[ \frac{1}{h_u A_{\text{deck}}} + \frac{1}{SK_{\text{conc}} \ell_c} + R_{\text{pipe}} \right] \quad (5.31)$$

where  $A_{\text{deck}}$  is the deck area associated with one heat pipe and  $S$  is the steady-state shape factor of the heated deck (see Figures 6.5, 6.6 and 6.7). This parameter characterizes that part of the system's thermal

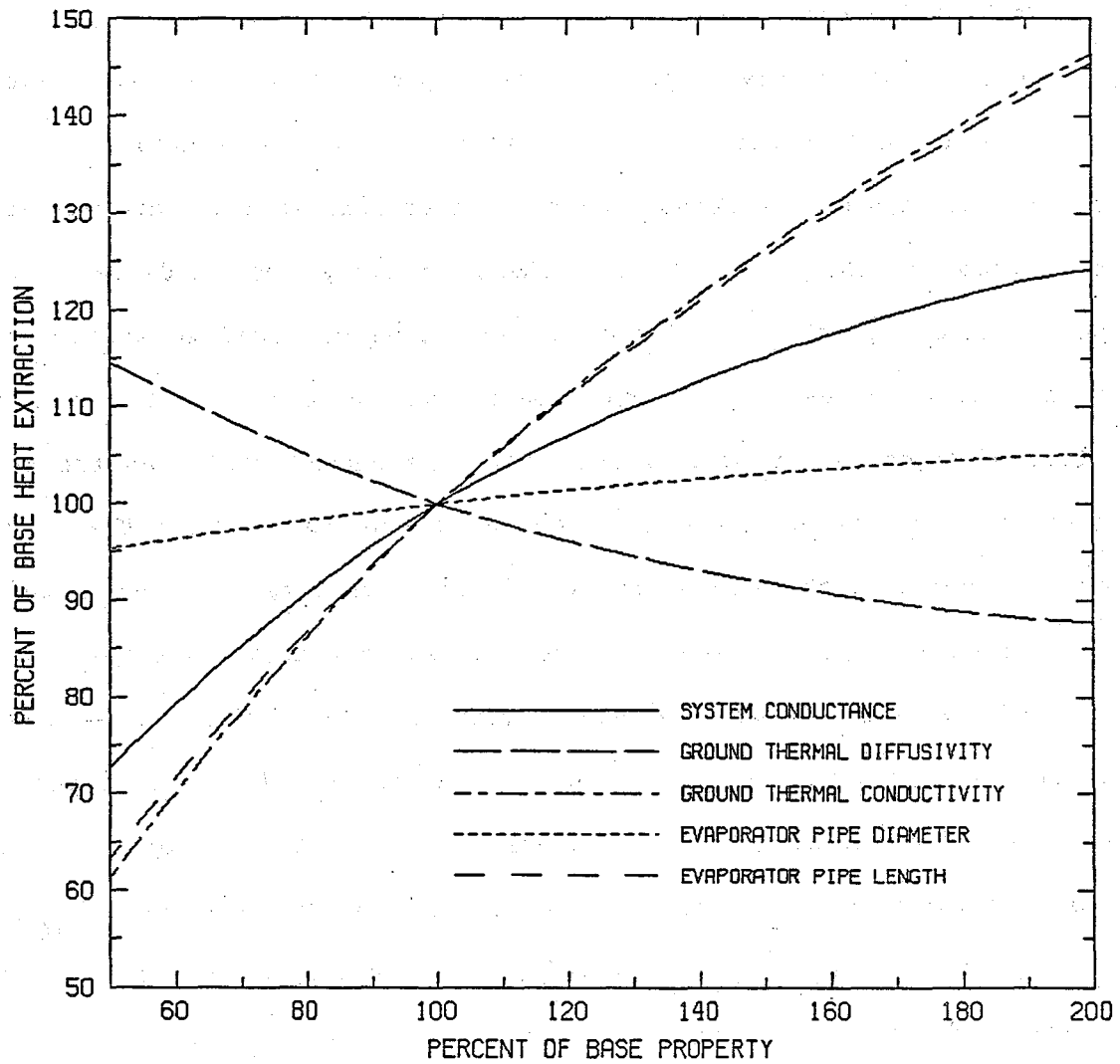


Figure 5.16. Percent Change of Base Energy Extraction at Spring Creek as a Function of Various System Parameters.

conductance which is not associated with the ground. For purposes of gross characterization, the transient behavior of the deck and heat transfer through the insulation are not included in this variable, although the simulations did not neglect them. An average top surface film coefficient was used and was determined from the data to be  $\sim 12$   $W/m^2 \cdot ^\circ C$ . The results of this parametric study, Figure 5.16, indicated that a smaller evaporator pipe diameter could have been employed with little loss in performance.

The essential heat transfer parameter to be characterized is the conductance between the ground and the heated deck surface. If the system were to operate at steady-state conditions, then the relation

$$q_s = u_{ss} (T_g - T_{surf}) \quad (5.32)$$

would be valid, where  $q_s$  is the top surface heat flux and  $u_{ss}$  is the steady-state specific thermal conductance between the ground and bridge top surface. A system's steady state conductance can be uniquely determined but this value only represents a lower limit on the conductance due to the transient nature of the heat transfer process--especially in the ground. A dynamic conductance between the ground and bridge surface can be defined as follows:

$$u_{dyn} \equiv \frac{q_s}{T_g - T_{surf}} \quad , \quad \text{when} \quad \begin{cases} q_s > 0 \\ T_g > T_{surf} \end{cases} \quad (5.33)$$

This quantity varies during each heating event and over the heating

season. It has been found, however, that the dynamic conductance was reasonably constant over that portion of a single event where the heat pipe power was significant. A daily average conductance was therefore defined using heat pipe power  $\dot{Q}_3$  as a weighting function:

$$\bar{u}_{\text{dyn}} \equiv \frac{\sum_{i=1}^{24} (\dot{Q}_3 u_{\text{dyn}})_i}{\sum_{i=1}^{24} (\dot{Q}_3)_i} \quad (5.34)$$

where values are calculated on an hourly basis. These daily values were then averaged in 30 day blocks and the characteristic dynamic specific conductance was defined as the minimum of these 30 day averages:

$$\bar{u} \equiv \min \left[ \frac{1}{30} \sum_{j=1}^{30} (\bar{u}_{\text{dyn}})_j \right] \quad (5.35)$$

This minimum value will provide a conservative estimate of the dynamic conductance during most of the winter. The predicted monthly averaged dynamic conductance plus and minus one standard deviation are plotted for the Sybille and Spring Creek systems in Figures 5.17 and 5.18. The dynamic behavior of both these systems are quite similar in that their monthly averaged dynamic conductances approach constant values which are significantly higher than their respective steady state conductance  $u_{\text{ss}}$ . The primary environmental parameter that influences the value of  $\bar{u}$  is obviously the air temperature record. To obtain an estimate of the magnitude of this influence, two simulations of the Spring Creek system were made in which the differences between the hourly air temperatures

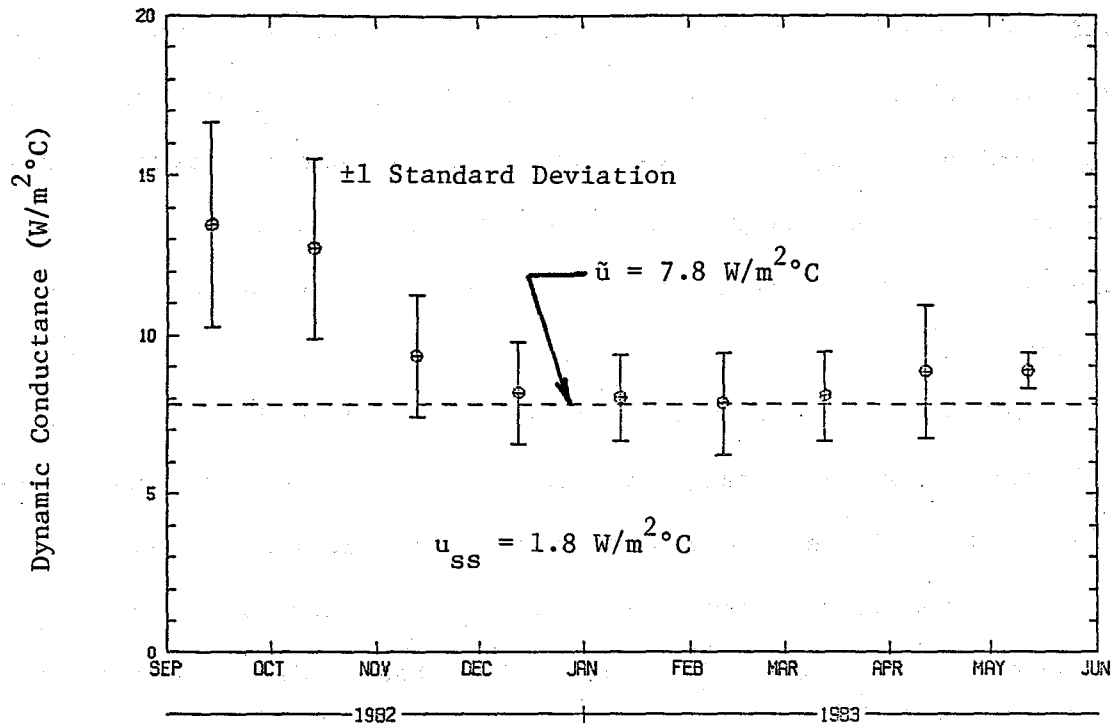


Figure 5.17. Monthly Averaged Ground to Surface Conductance for Spring Creek.

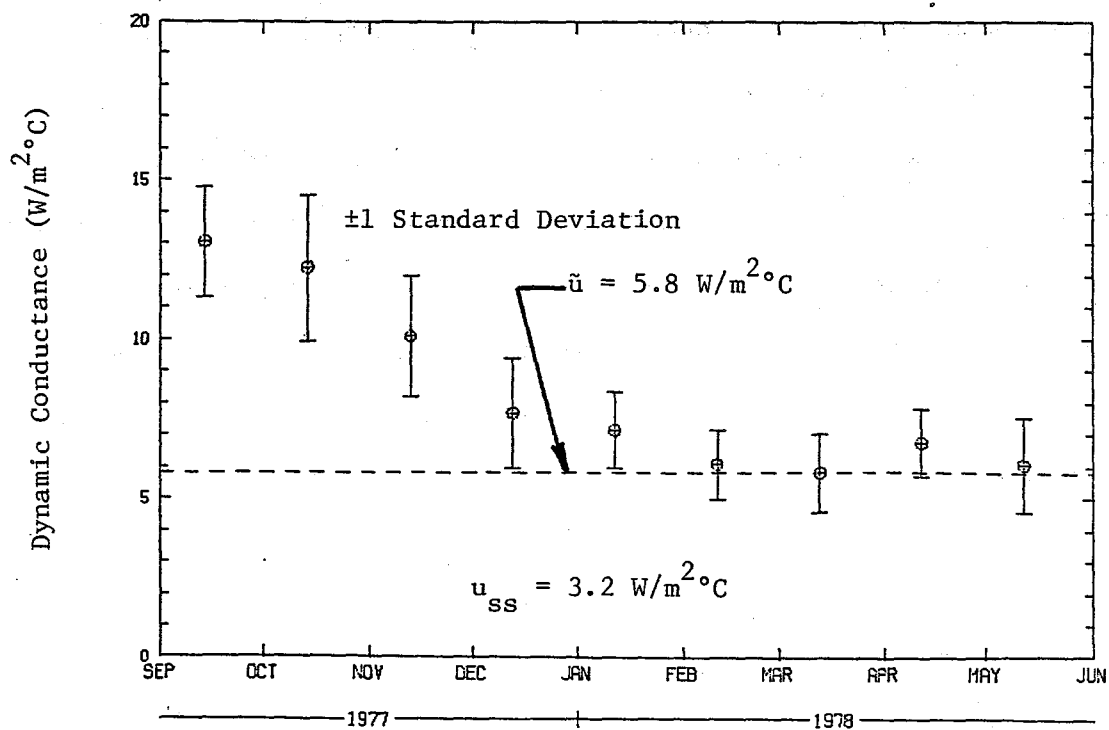


Figure 5.18. Monthly Averaged Ground to Surface Conductance for Sybille.

and their yearly average were consecutively increased and decreased by 20%. The values of  $\bar{u}$  calculated from these simulations were within 3% of the base value. This indicates that the environment at a particular site in the continental United States should have a weak influence on  $\bar{u}$ , whereas the local environment essentially specifies the far field ground temperature,  $T_g$ .

Twenty-five computer simulations were performed which systematically varied the significant thermal and geometric parameters of the heat pipe system. Table 5.5 tabulates this information in terms of the geometric and thermal parameters that were varied and the resulting principal conductances. These data formed the bases for determining an empirical correlation of  $\bar{u}$  that can be utilized in the design algorithm. Figure 5.19 presents the results of this study which correlates the dynamic conductance in terms of the steady state system conductance  $u_{ss}$ , field conductance  $U_{field}$ , evaporator to deck surface conductance  $U_{es}$  and Fourier modulus  $\tau$ . The procedure required to calculate each of these terms is presented in Chapter 6. Despite the complexity of the system, Figure 5.19 indicates that the recommended empirical correlation collapses essentially all the simulation results in a manner that produces an accurate or a conservative estimate of the minimum dynamic conductance  $\bar{u}$ . The only major discrepancy to this trend occurred in the Sybille Creek case ( $\sqrt{\tau} \times 100 = 34$  in Figure 5.19) where the proposed empirical correlation gives a significantly larger value than the theoretical value. Table 4.2 shows that the measured performance of the Sybille Creek system was notably superior to its theoretically predicted performance.

TABLE 5.5. PARAMETRIC STUDIES OF DYNAMIC CONDUCTANCE

Simulation*	$\sqrt{\tau}$ x 100	$U_{es}$ (W/°C)	$U_{field}$ (W/°C)	$A_{deck}$ (m <sup>2</sup> )	$U_{ss}$ (W/°C) [ $u_{ss}$ (W/m <sup>2</sup> °C)]	$\tilde{U}$ (W/°C) [ $\tilde{u}$ (W/m <sup>2</sup> °C)]	$(\rho c)_g$ (J/m <sup>3</sup> °C) x 10 <sup>6</sup>
<u>Spring Creek</u>							
Standard	18.41	204.8	11.6	6.2 **	11.0 (1.78)	48.3 (7.8)	2.1
$U_{sys}$ ( $\lambda_c = 87$ m)	18.41	427.0	11.6	13.3	11.3 (0.85)	68.6 (5.2)	2.1
$U_{sys}$ ( $\lambda_c = 19.6$ m)	18.41	100.5	11.6	3.0	10.4 (3.5)	34.4 (11.5)	2.1
$\alpha_g = 2 \times 10^{-6}$ m <sup>2</sup> /s	26.04	204.8	11.6	6.2	11.0 (1.78)	42.2 (6.8)	1.05
$\alpha_g = .5 \times 10^{-6}$ m <sup>2</sup> /s	13.02	204.8	11.6	6.2	11.0 (1.78)	56.5 (9.2)	4.2
$k_g = 4.2$ W/m°C	18.41	204.8	23.1	6.2	20.8 (3.4)	69.2 (11.2)	4.2
$k_g = 1.05$ W/m°C	18.41	204.8	5.8	6.2	5.6 (0.91)	33.2 (5.4)	1.05
$R_e = 6.65 \times 10^{-2}$ m	18.41	204.8	11.8	6.2	11.2 (1.81)	49.5 (8.0)	2.1
$R_e = 1.66 \times 10^{-2}$ m	18.41	204.8	10.6	6.2	10.1 (1.63)	47.1 (7.6)	2.1
$\lambda_e = 60.96$ m	9.21	207.5	18.8	6.2	17.2 (2.8)	68.6 (11.1)	2.1
$\lambda_e = 15.24$ m	36.83	199.5	7.4	6.2	7.1 (1.16)	33.9 (5.5)	2.1

TABLE 5.5 (CONTINUED)

Simulation*	$\sqrt{\tau}$ x 100	$U_{es}$ (W/°C)	$U_{field}$ (W/°C)	Area (m <sup>2</sup> )	$U_{ss}$ (W/°C) [ $u_{ss}$ (W/m <sup>2</sup> °C)]	$\bar{U}$ (W/°C) [ $\bar{u}$ (W/m <sup>2</sup> °C)]	$(\rho c)_g$ (J/m <sup>3</sup> °C) x 10 <sup>6</sup>
Isolated Evaporator $l_c = 20.3$ m	18.41	104.0	53.5	3.2	35.3 (11.2)	51.6 (16.3)	2.1
$l = 15.12$ m, $l_c^e = 20.3$ m	37.12	102.6	7.4	3.2	6.9 (2.2)	24.3 (7.7)	2.1
$l = 60.96$ m, $l_c^e = 20.3$ m	9.21	104.7	18.8	3.2	15.9 (5.0)	46.8 (14.8)	2.1
$k = 1.05$ W/m°C, $l_c^g = 20.3$ m	18.41	104.0	5.8	3.2	5.5 (1.74)	23.4 (7.4)	1.05
$k = 4.20$ W/m°C, $l_c^g = 20.3$ m	18.41	104.0	23.1	3.2	18.9 (6.0)	4.75 (15.0)	4.2
$U_{sys} = 13.55$ W/°C, $l_c^{sys} = 10.1$ m	18.41	52.1	11.6	1.6	9.5 (6.1)	24.0 (15.5)	2.1
$\alpha_g = 5.2 \times 10^{-6}$ m <sup>2</sup> /s	41.99	204.8	11.6	6.2	11.0 (1.78)	36.1 (5.8)	.40
$l_e = 15.24$ m $\alpha = 4.7 \times 10^{-6}$ m <sup>2</sup> /s	79.84	199.5	7.4	6.2	7.1 (1.16)	22.0 (3.6)	.45
$l = 60.96$ m $l_c^e = 112.7$ m	9.21	564	18.8	17.18	18.2 (1.06)	101.7 (5.9)	2.1
80% $T_\infty$ range	18.41	204.8	11.6	6.2	11.0 (1.78)	49.8 (8.1)	2.1
120% $T_\infty$ range	18.41	204.8	11.6	6.2	11.0 (1.78)	47.1 (7.6)	2.1

TABLE 5.5 (CONTINUED)

Simulation*	$\sqrt{T}$ x 100	$U_{es}$ (W/°C)	$U_{field}$ (W/°C)	Area (m <sup>2</sup> )	$U_{ss}$ (W/°C) [ $u_{ss}$ (W/m <sup>2</sup> °C)]	$\bar{U}$ (W/°C) [ $\bar{u}$ (W/m <sup>2</sup> °C)]	$(\rho c)_g$ (J/m <sup>3</sup> °C) x 10 <sup>6</sup>
<u>Sybilie</u>							
Standard	34.45	26.2	2.6	0.74	2.4 (3.2)	4.3 (5.8)	2.2
Spring Creek Environment	34.45	26.2	2.6	0.74	2.4 (3.2)	4.8 (6.5)	2.2
$\alpha_g = 3 \times 10^{-6} \text{ m}^2/\text{s}$	79.75	26.2	2.6	0.74	2.4 (3.2)	3.8 (5.1)	.403

\*See Table 5.3 for base case values; parameters listed in this column denote the variation.

\*\*See Table 6.1A.



In summary, a heat transfer analysis of the ground-heat pipe-bridge deck-environment dynamic interactions has been developed and demonstrated to be both accurate on the conservative side, and computationally efficient. This model permitted the performance of a large parametric study which generated the data base that was used to formulate a practical empirical design algorithm for ground heat pipes in bridges.

## VI. DESIGN MANUAL

This chapter presents a design procedure that is recommended for bridge decks that are heated by ground heat pipes, discusses the surface heating and snow control potential of these systems, gives a worked illustration, and includes example construction specifications.

### A. Thermal Design Procedure

The thermal design of the ground heat pipe system is based on the minimum monthly averaged dynamic conductance  $\bar{u}$  between the far field ground and the top surface of the bridge. Once this conductance is known, the minimum statistical specific power  $q_s$  ( $W/m^2$ ) that is delivered to the heated bridge surface during a significant heating event should be

$$q_s = \bar{u}(T_g - T_{surf}) \quad (6.1)$$

where  $T_{surf}$  is the heated surface temperature and  $T_g$  is the characteristic temperature of the far-field ground. This dynamic conductance is a function of the deck and heat pipe system geometry and the thermal properties of the deck, heat pipe system, and the earth in the evaporator field.

Table 6.1 and Figure 6.1 delineate the required geometric design parameters. Note that  $l_c$  represents the total length of the condenser pipe that is connected to each evaporator pipe.  $N_e$  is the number of evaporator pipes in close proximity to each other. For example,  $N_e$  is

TABLE 6.1. REQUIRED GEOMETRIC DESIGN PARAMETERS (See Figure 6.1)

Symbol	Description	Recommended Units
<u>Bridge Deck</u>		
$A_{\text{deck}}$	Deck surface area associated with each evaporator pipe: $A_{\text{deck}} = \ell_c \cdot b$	$\text{m}^2$
H	Thickness of bridge deck	m
<u>Condenser Pipes</u>		
b	Spacing between condenser pipes	m
$d_{\text{ci}}$	Inside diameter of condenser pipe	m
$d_{\text{co}}$	Outside diameter of condenser pipe	m
h	Distance from top surface to center of condenser pipes	m
$\ell_c$	Total length of condenser pipe connected to each evaporator pipe	m
<u>Evaporators</u>		
$d_{\text{ei}}$	Inside diameter of evaporator pipe	m
$d_{\text{eo}}$	Outside diameter of evaporator pipe	m
$d_{\text{h}}$	Diameter of the backfilled evaporator hole	m
$\ell_p$	Length of evaporator pipe	m
$N_e$	Number of evaporator pipes in each heat pipe field	-
$R_s$	Characteristic separation distance between evaporator pipes	m

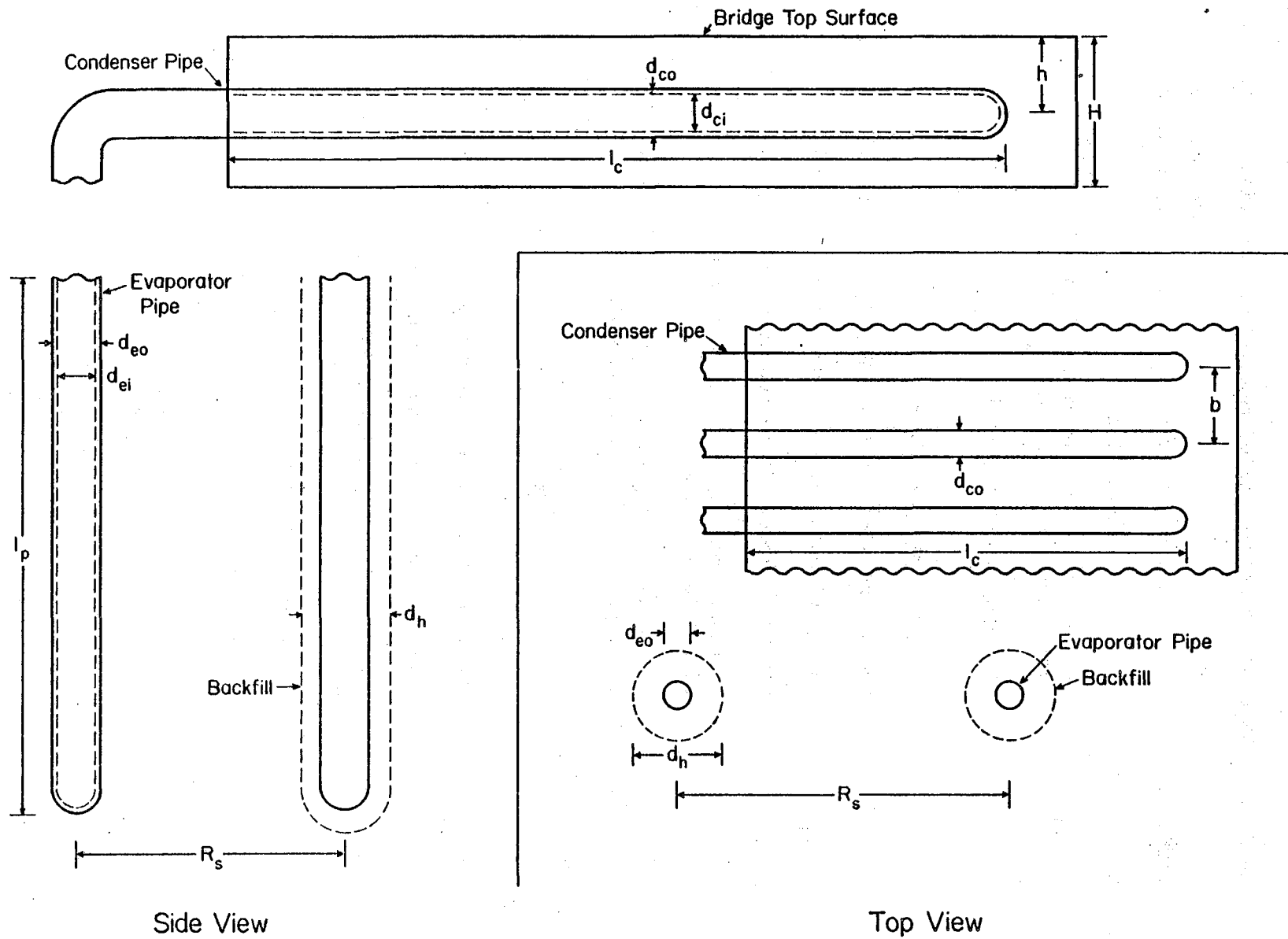


Figure 6.1 . Schematic Illustration of Required Geometric Design Parameters.

fifteen at the Spring Creek facility where a quarter of the sixty evaporator pipes were placed at each corner of the structure.

Table 6.2 tabulates the required thermodynamic properties. The values of the condensing and evaporative film coefficients ( $h_c$  and  $h_e$ ) have not been accurately measured to date, and the values given are best estimates for ammonia.  $\bar{u}$ , however, is not particularly sensitive to these two parameters. Table 6.3 presents some representative soil properties but it is imperative that actual soil properties be utilized in any final design calculations. The magnitude of  $K_g$  and  $(\rho c)_g$  increase with moisture content. If possible, evaporators should be placed below the water table for the above reason, but it also minimizes the thermal contact resistance between the soil and the grout embedding an evaporator. The thermal conductivity ( $K_{conc}$ ) of concrete bridge decks varies from 1 to 2 W/m°C depending on concrete type and aggregate content and size. In general, the concrete and aggregate should have the highest thermal conductivities available, and the aggregate should be as large as codes allow.

The above geometric and thermodynamic parameters are used to calculate the component steady-state resistances that are listed in Table 6.4 and schematically depicted in Figure 6.2. These component resistances are combined in the manner shown in Table 6.5 to form the steady state sub-system resistances  $R_{es}$ ,  $R_{field}$ , and the total system specific steady-state conductance  $u_{ss}$  between the far field ground and the heated deck surface.  $u_{ss}$  represents the minimum theoretical specific conductance that the system could ever produce.

Finally,  $\bar{u}$  is determined from Figure 6.4 as a function of the

TABLE 6.2. REQUIRED THERMAL DESIGN PARAMETERS

<u>Symbol</u>	<u>Description</u>	<u>Recommended Units</u>	<u>Value</u>
$h_c$	Condensing film coefficient	$W/m^2 \text{ } ^\circ C$	$\sim 8 \times 10^3$
$h_e$	Evaporative film coefficient	$W/m^2 \text{ } ^\circ C$	$\sim 2 \times 10^3$
$K_b$	Thermal conductivity of the evaporator hole backfill	$W/m \text{ } ^\circ C$	
$K_c$	Thermal conductivity of the condenser pipe	$W/m \text{ } ^\circ C$	
$K_{conc}$	Thermal conductivity of the bridge deck concrete	$W/m \text{ } ^\circ C$	
$K_e$	Thermal conductivity of the evaporator pipe	$W/m \text{ } ^\circ C$	
$K_g$	Thermal conductivity of the ground (see Table 6.3 for approximate values)	$W/m \text{ } ^\circ C$	
$(\rho c)_g$	Heat capacitance of the ground (see Table 6.3 for approximate values)	$J/m^3 \text{ } ^\circ C$	
S	Deck shape factor (37), (see Figures 6.5-6.7)		
$\tau$	The Fourier modulus of the ground evaporator pipe based on 1 year		
			$\tau = \frac{(3.15 \times 10^7 \text{ s}) K_g}{(\rho c)_g l_p^2}$
$T_g$	Average far-field ground temperature along the length of the evaporator pipe	$^\circ C$	

TABLE 6.3. THERMOPHYSICAL PROPERTIES OF VARIOUS SOILS

Soil Designation	Corps of Engineers Class	% Moisture Content	Density (kg/m <sup>3</sup> )	Specific Heat Capacity (J/kg°C)	Thermal Conductivity K <sub>g</sub> (W/m°C)	Heat Capacitance (ρc) <sub>g</sub> (J/m <sup>3</sup> °C)
Crushed Granite <sup>35</sup>	SW	4	1730	860	1.1	1.5x10 <sup>6</sup>
Graded Pure Silica Sand <sup>35</sup>	SP	4	1730	820	2.0	1.4x10 <sup>6</sup>
Sand <sup>35</sup>	SW	4	1730	910	0.9-1.6	1.6x10 <sup>6</sup>
Silt Loam <sup>35</sup>	ML	10	1730	1050-1080	1.0-1.3	1.8-1.9x10 <sup>6</sup>
Sybille	-	2	2300	910	1.2	2.1x10 <sup>6</sup>
Spring Creek	-	5	2500	840	2.1	2.1x10 <sup>6</sup>

TABLE 6.4. STEADY-STATE COMPONENT THERMAL RESISTANCES ( $^{\circ}\text{C}/\text{W}$ )  
(SEE FIGURE 6.2)

<u>Symbol</u>	<u>Description</u>	<u>Equation</u>
$R_{\text{conc}}$	Deck resistance	$[SK_{\text{conc}}\ell_c]^{-1}$
$R_{\text{cp}}$	Resistance of the condenser pipe	$\frac{\ln(d_{\text{co}}/d_{\text{ci}})}{2\pi K_c \ell_c}$
$R_c$	Condensing resistance	$(\pi d_{\text{ci}} \ell_c h_c)^{-1}$
$R_{\text{evap}}$	Evaporative resistance	$(\pi d_{\text{ei}} \ell_p h_e)^{-1}$
$R_{\text{ep}}$	Resistance of the evaporator pipe	$\frac{\ln(d_{\text{eo}}/d_{\text{ei}})}{2\pi K_e \ell_p}$
$R_{\text{eg}}$	Resistance between an isolated evaporator and the ground	$R_{\text{eg}} \approx \frac{\ln\left(\frac{3.67\ell_p}{d_{\text{eo}}}\right) + \left(\frac{K_b}{K_g} - 1\right) \ln\left(\frac{3.67\ell_p}{d_h}\right)}{2.162\pi K_b \ell_p}$
$R_I$	Resistance due to evaporator pipe interactions (see Figure 6.3)	$(R_I K_g \ell_p) / (K_g \ell_p)$

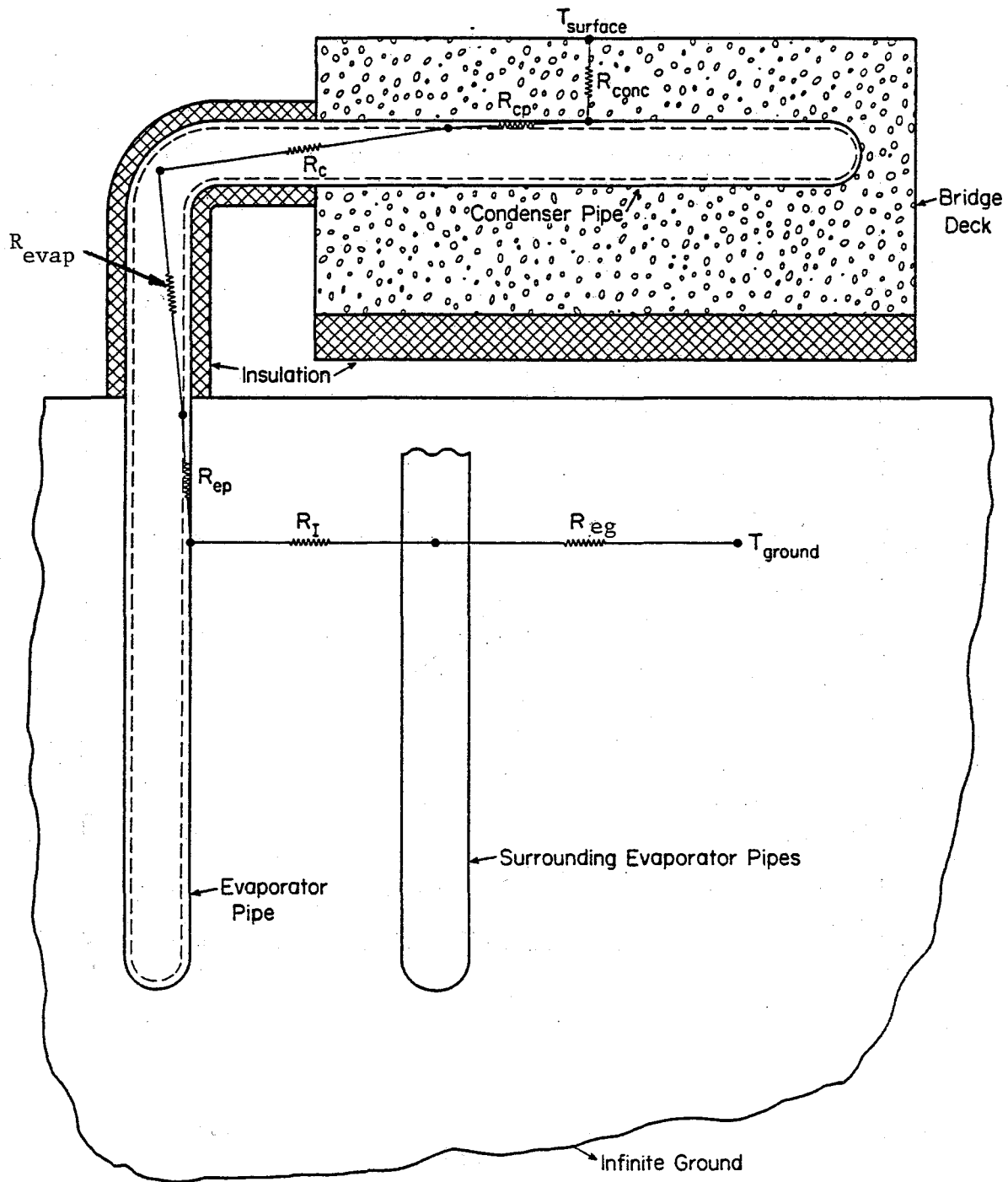


Figure 6.2. Schematic Illustration of Steady-State Thermal Resistances.

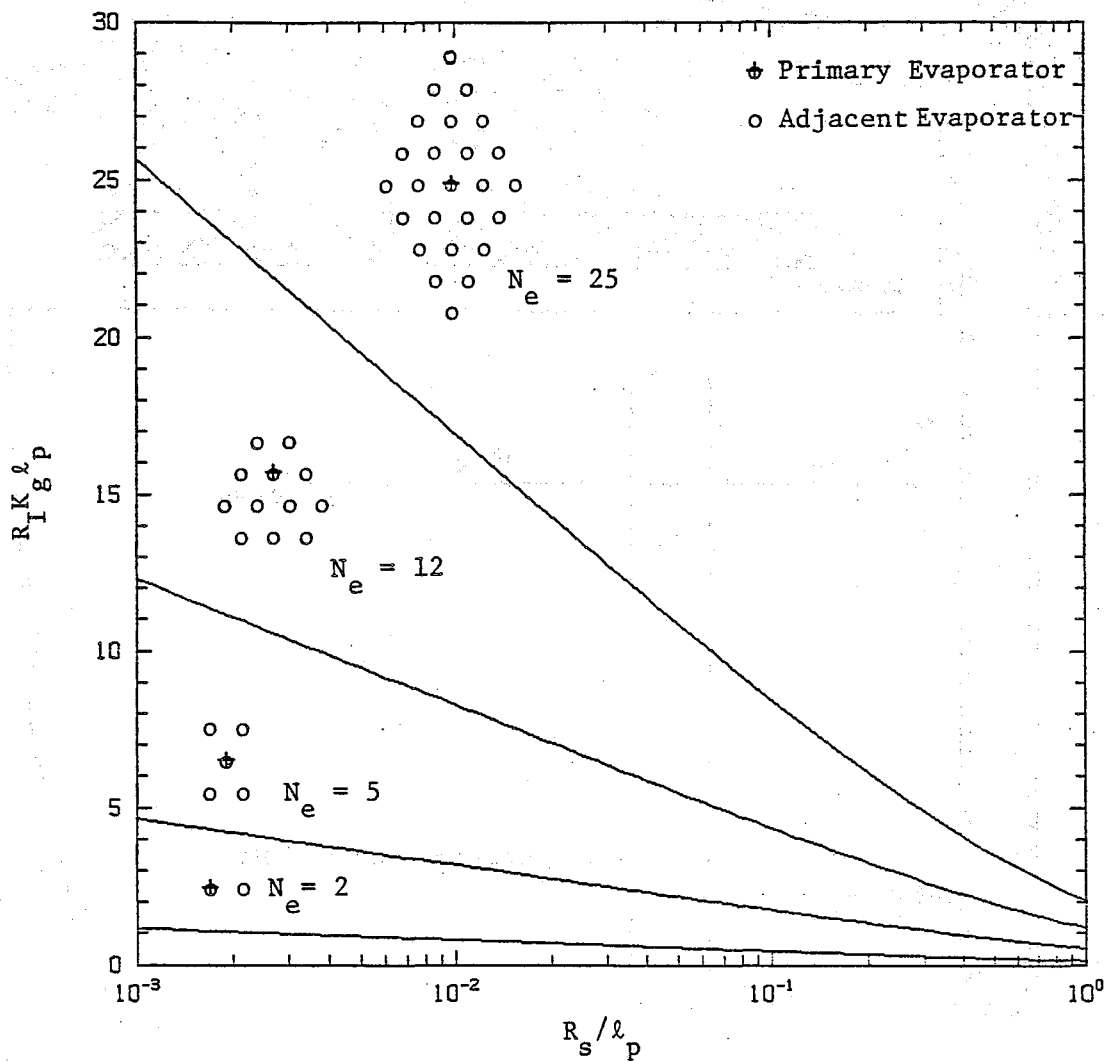


Figure 6.3. Non-Dimensional Interaction Resistance for Various Evaporator Field Geometries.

TABLE 6.5. STEADY-STATE SUBSYSTEM RESISTANCES AND STEADY-STATE AND DYNAMIC SYSTEM CONDUCTANCES.

<u>Symbol</u>	<u>Description</u>	<u>Equation</u>	<u>Recommended Units</u>
$R_{es}$	Resistance between the evaporator pipe and the bridge top surface	$R_{conc} + R_{cp} + R_c + R_{evap} + R_{ep}$	$^{\circ}\text{C}/\text{W}$
$R_{field}$	Resistance between the far-field ground and the evaporator	$R_{eg} + R_I$	$^{\circ}\text{C}/\text{W}$
$U_{ss}$	Steady-state conductance between the ground and the bridge top surface	$[R_{es} + R_{field}]^{-1}$	$\text{W}/^{\circ}\text{C}$
$u_{ss}$	Steady-state specific conductance between the ground and the bridge top surface	$U_{ss}/A_{deck}$	$\text{W}/\text{m}^2\text{C}$
$\ddot{u}$	Dynamic specific conductance between the ground and the bridge top surface	See Figure 6.4	$\text{W}/\text{m}^2\text{C}$

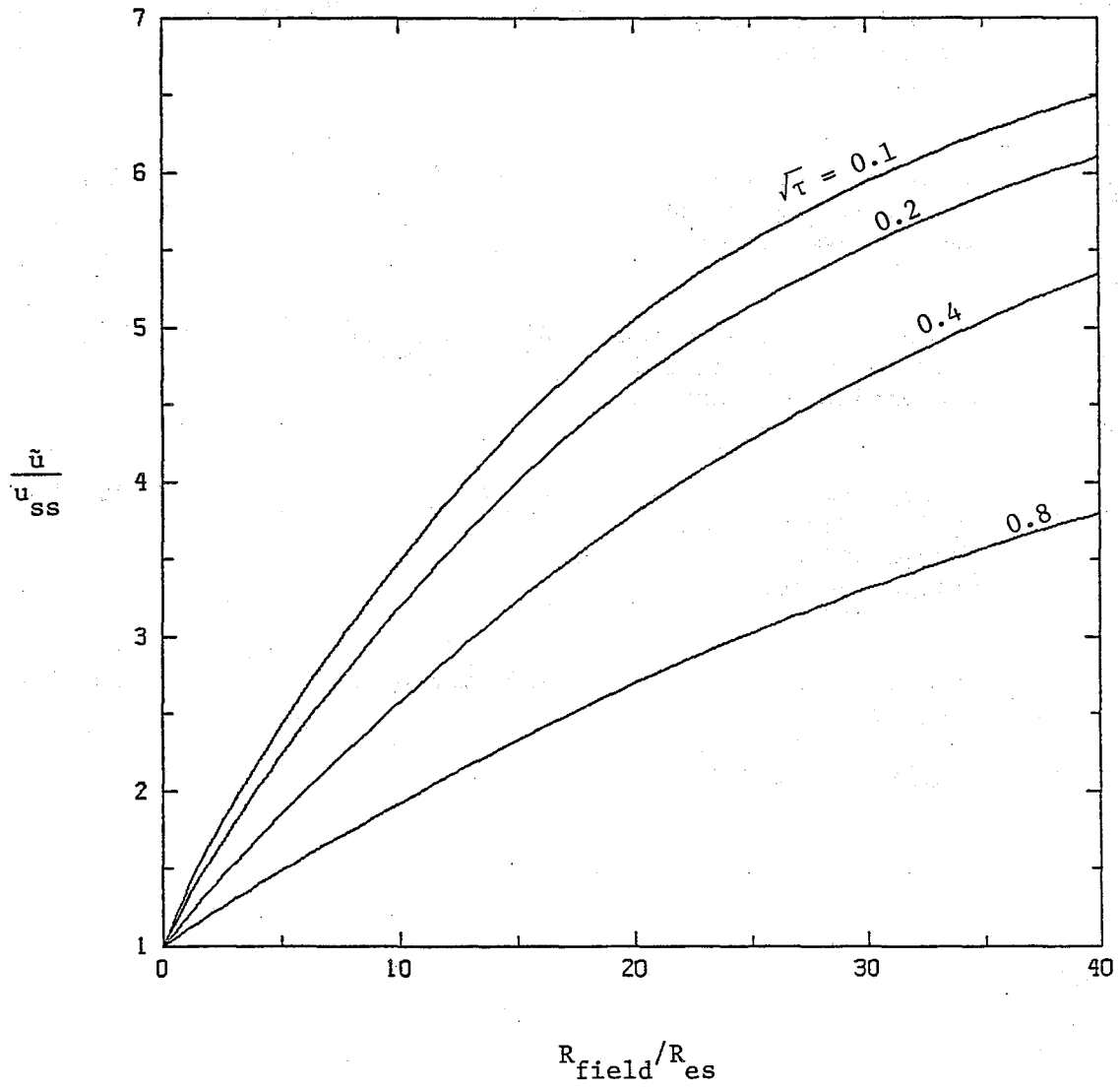


Figure 6.4. Dynamic Ground to Surface Conductance.

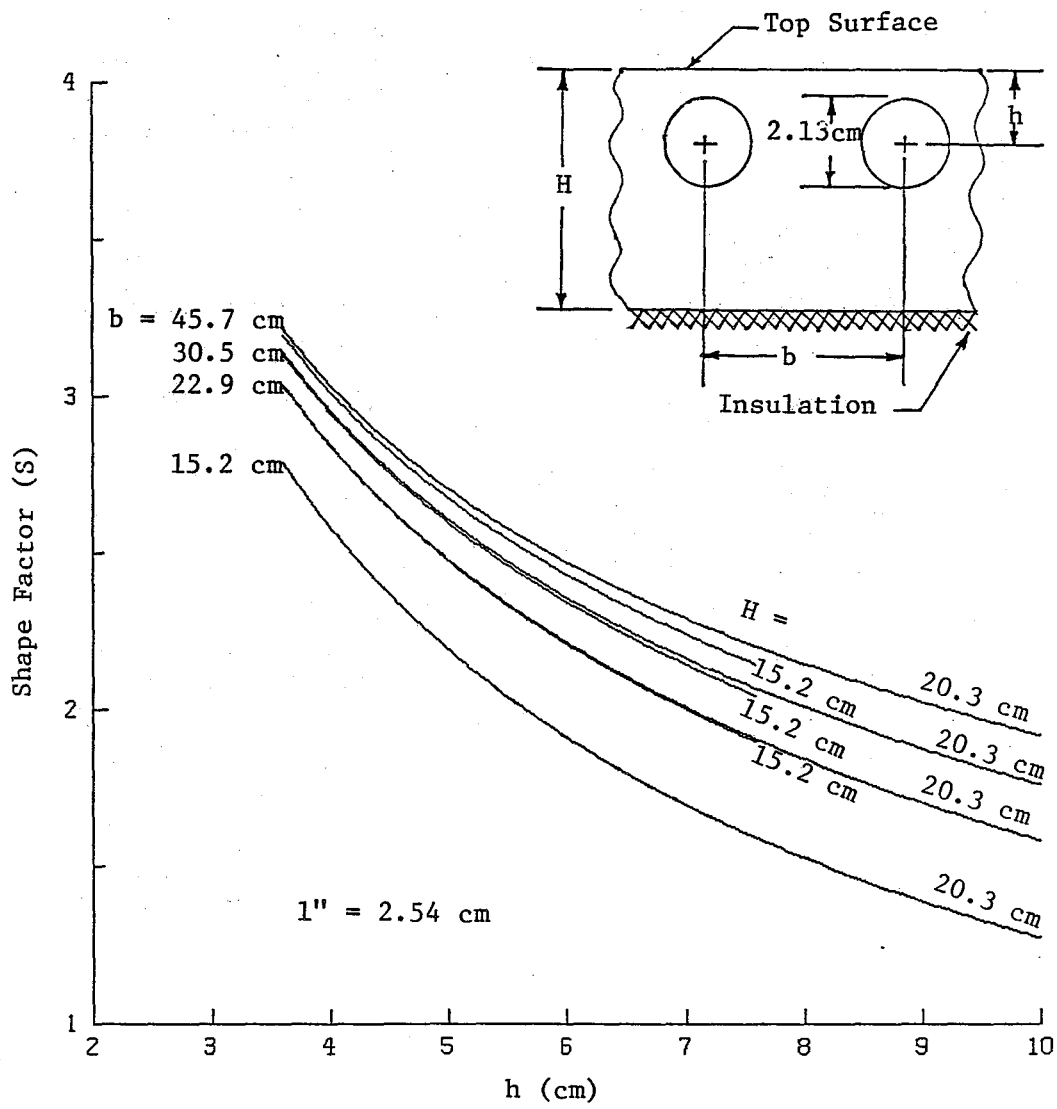


Figure 6.6. Shape Factor for a 1/2" Standard Embedded Pipe  
 ( $d_{co} = 2.13 \text{ cm}$ )

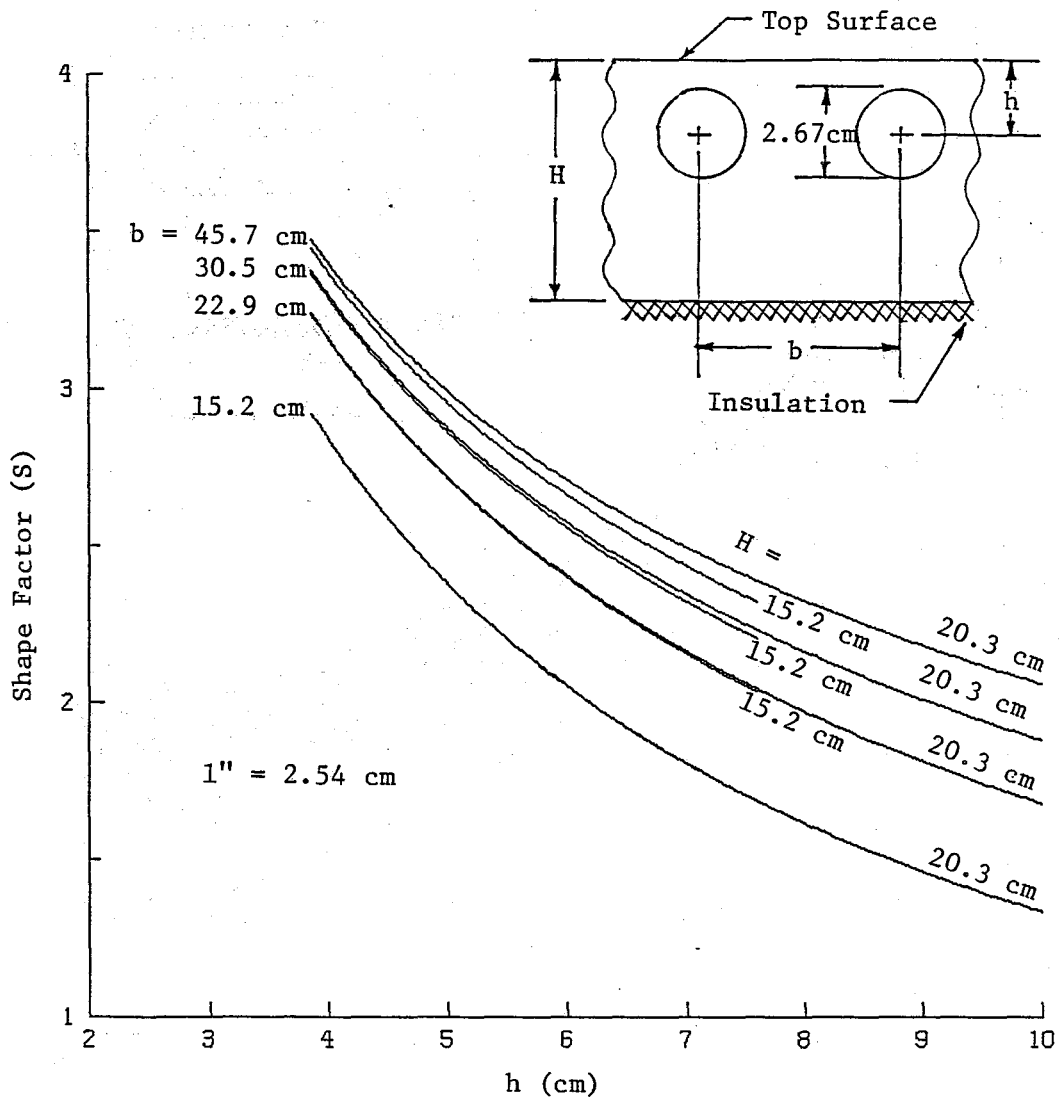


Figure 6.6. Shape Factor for a 3/4" Standard Pipe  
 ( $d_{co} = 2.67$  cm)

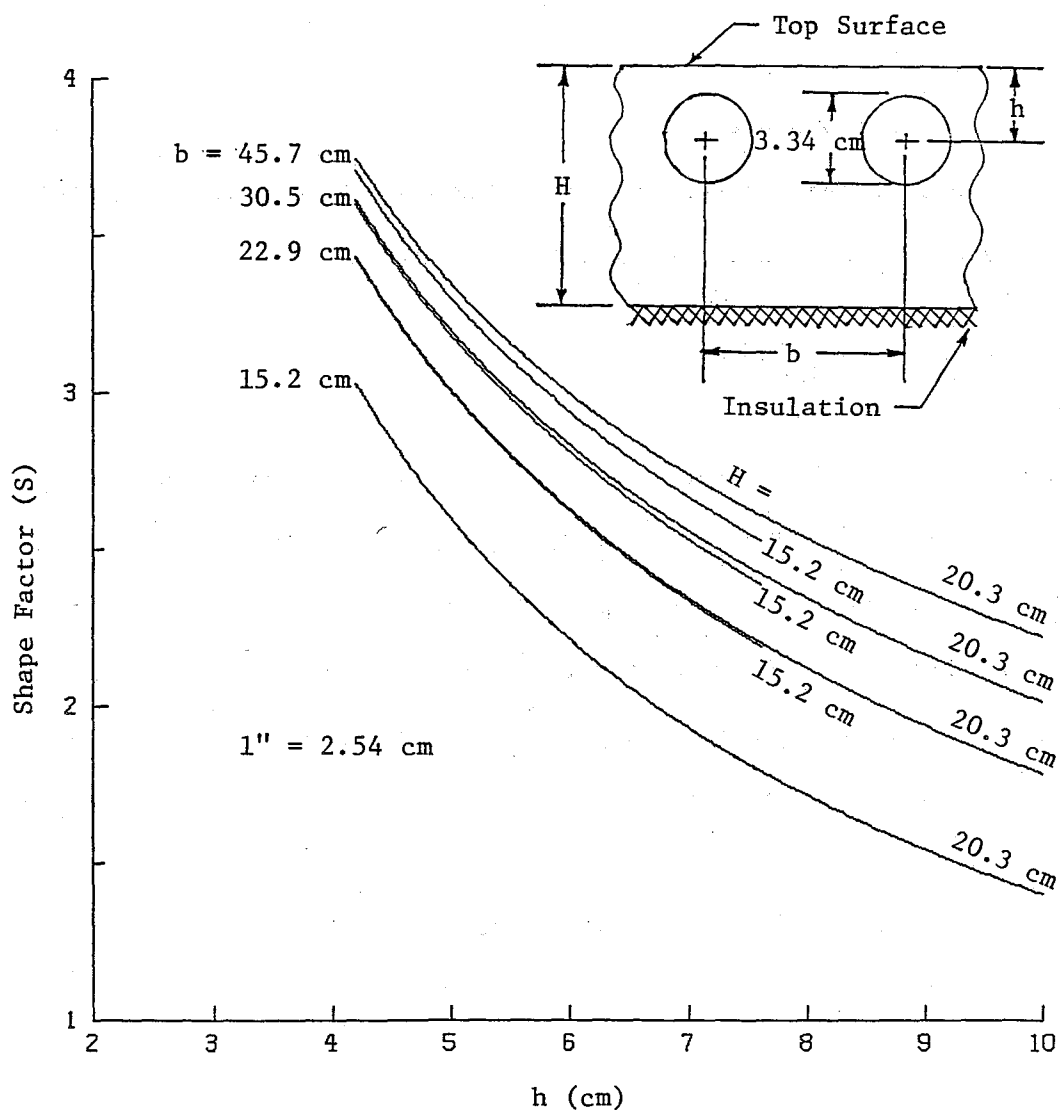


Figure 6.7. Shape Factor for a 1" Standard Embedded Pipe  
( $d_{co} = 3.34$  cm).

previously calculated parameters:  $R_{es}$ ,  $R_{field}$ ,  $u_{ss}$  and the Fourier modulus  $\tau$ . A parameter which has been assumed constant in the calculation of  $\bar{u}$  is the heat capacitance of the bridge deck. The value of  $(\rho c)_{deck}$  was essentially the same for both the Sybille and Spring Creek systems ( $2.1 \times 10^6 \text{ J/m}^3 \text{ } ^\circ\text{C}$ ) and it is assumed that this value would be characteristic of future designs.

#### B. System Performance

The expected top surface heat flux when the system is melting snow or ice can be calculated by using the relation

$$q_{melt} = \bar{u}(T_g - 1^\circ\text{C}) \quad (6.2)$$

where  $1^\circ\text{C}$  is used for the heated surface temperature since values around  $1^\circ\text{C}$  are typically observed during snow melting events (see Figure 3.6).  $T_g$ , the average far-field ground temperature across the evaporator depths during the heating season, should be measured at the site in question but the average ground temperature is generally a few  $^\circ\text{C}$  above the average annual air temperature.

The value of  $q_{melt}$  calculated by equation 6.2 is the predicted minimum power that would be delivered during a melting event, but this power may not be sufficient to melt any snow. Figures 6.8 and 6.9 plot the minimum top surface heat flux,  $q_{min}$ , required to maintain a wet surface (with no snow cover and a minimal frozen precipitation rate) at  $1^\circ\text{C}$ . Figure 6.8 is for clear sky conditions while Figure 6.9 is for heavy overcast. The value of  $\alpha_{sw} q_{solar}$  requires knowledge of the incoming solar radiation ( $q_{solar}$ ) and the top surface solar absorbtivity ( $\alpha_{sw}$ ). A typical value of  $\alpha_{sw}$  for bridge surfaces is 0.6. If  $q_{min}$  is

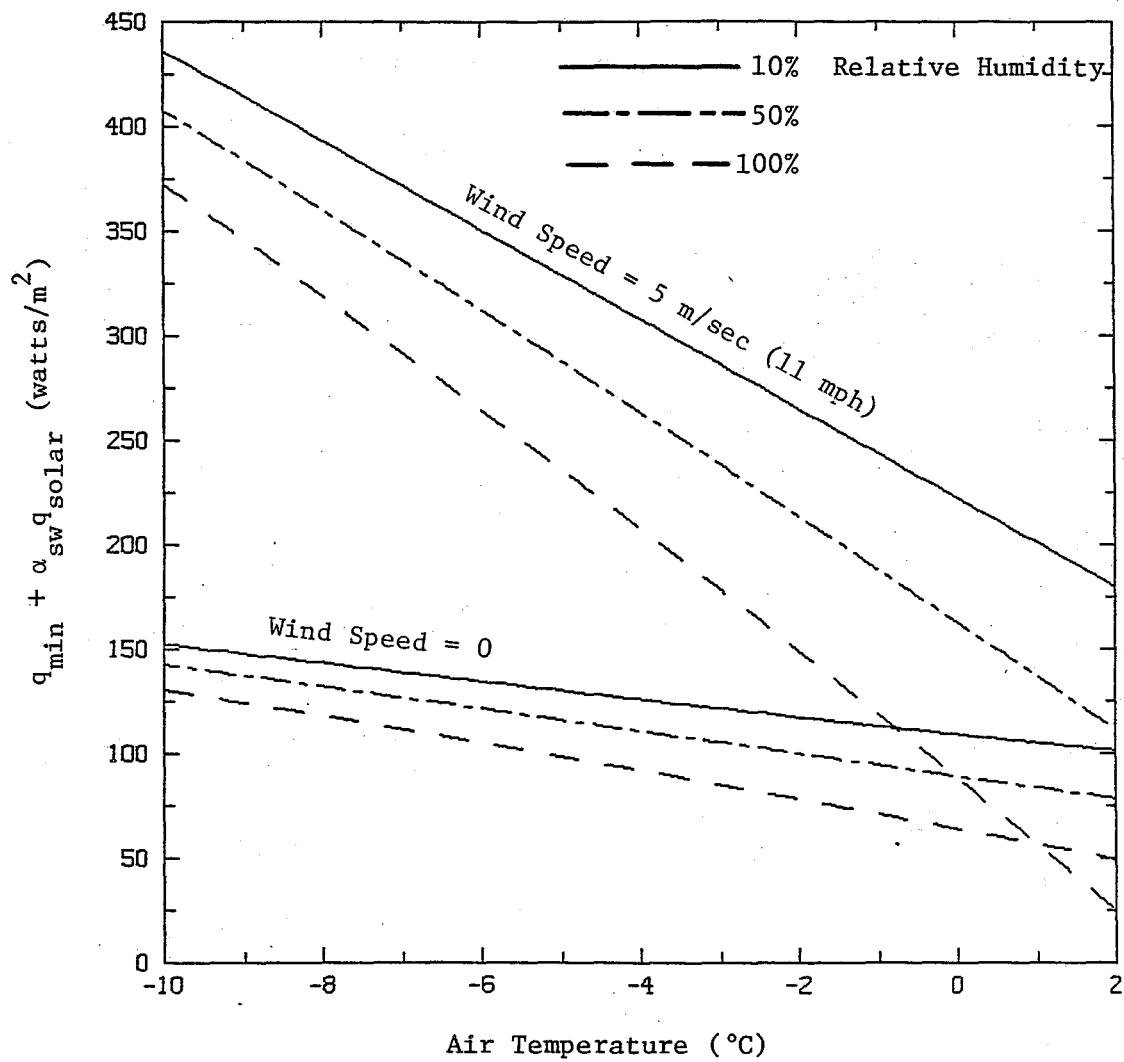


Figure 6.8. Minimum Power Required to Maintain a Wet Surface at 1°C with a Clear Sky.

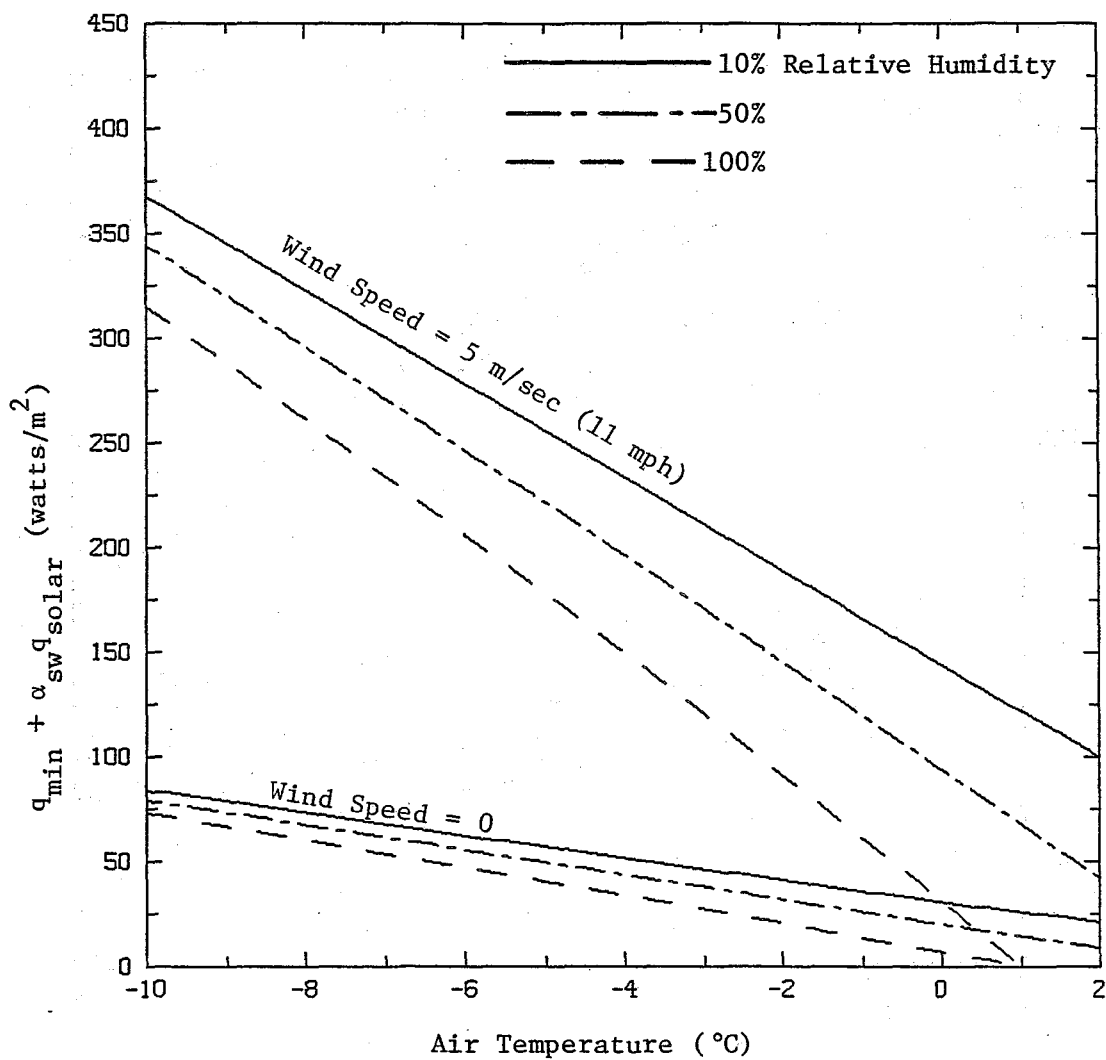


Figure 6.9. Minimum Power Required to Maintain a Wet Surface at  $1^{\circ}\text{C}$  with a Heavy Overcast.

greater than  $q_{\text{melt}}$ , the surface may become snow covered, which introduces an insulating effect that assists the snow melting process at the snow-concrete interface.

Figure 6.10 plots the percent of snowing events that a heating system with a given rating ( $q_{\text{melt}}$ ) will melt snow as rapidly as it falls. The environments which are characterized by Figure 6.10 are eastern states between latitudes  $38^\circ$  and  $42^\circ$  (36). While this figure indicates that the low power produced by a ground heat pipe system ( $50 < q_{\text{melt}} < 100 \text{ W/m}^2$ ) can only melt a small fraction of the snow as rapidly as it falls, the experimental observations show that a significant reduction in the snow cover duration is produced (see Table 3.3 and 4.3 and references 8, 16 and 22). Since there is no simple method of predicting the effect that a proposed system will have on the snow cover duration, one is forced to rely on past experience to make this projection.

### C. Worked Example

The characteristics of the Spring Creek system will be used to illustrate the design procedure described in the previous two sections. The geometric and thermal properties of this system were presented in Figure 1.2, Chapter 2 and Table 5.3. These parameters are again summarized in the following two tables (6.1A and 6.2A) which conform to the format outlined in Tables 6.1 and 6.2. The condenser spacing is not uniform in this case (see Figure 1.2). All the calculations will be made in terms of an equivalent condenser that has a uniform 6" (15.2 cm)

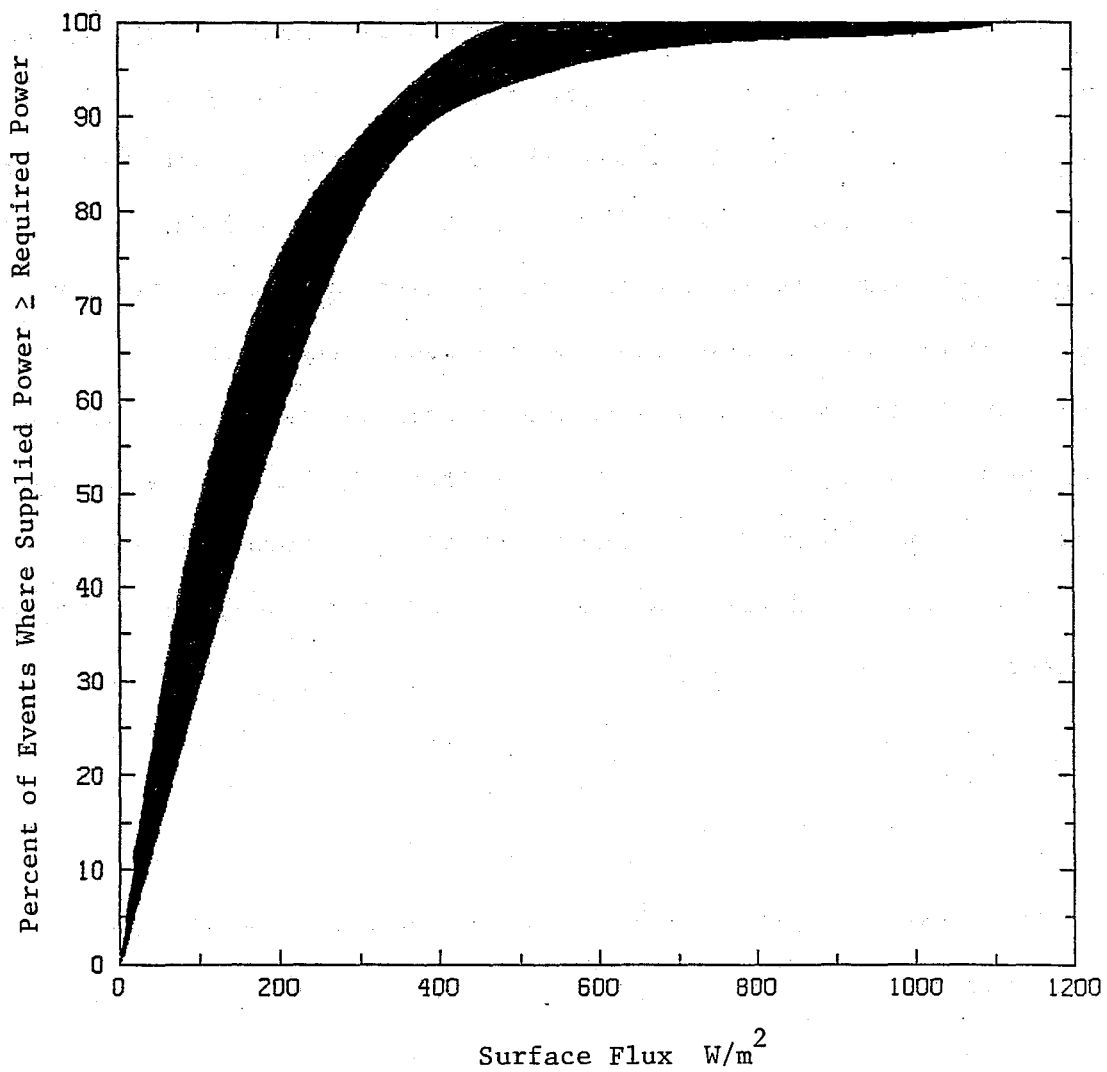


Figure 6.10. Power Required to Typically Melt Snow as Rapidly as It Falls in Eastern States Between Latitudes  $38^\circ$  and  $42^\circ$ .

TABLE 6.1A. REQUIRED GEOMETRIC DESIGN PARAMETERS FOR SPRING CREEK  
(See Figure 6.1)

<u>Symbol</u>	<u>Description</u>	<u>Value</u>
$b_1$	Minimum spacing between condenser pipes (see Figure 1.2)	0.152 m
$b_2$	Maximum spacing between condenser pipes	0.304 m
$h$	Distance from top surface to center of condenser pipes	0.055 m
$H$	Thickness of bridge deck	0.210 m
$d_{co}$	Outside diameter of condenser pipe	0.033 m
$d_{ci}$	Inside diameter of condenser pipe	0.027 m
$\ell_{c1}$	Length of short condenser pipes (see Figure 1.2)	6.4 m
$\ell_{c2}$	Length of long condenser pipes	12.5 m
$\ell_c$	Total equivalent condenser pipe length*	40.5 m
$d_h$	Diameter of the backfilled evaporator hole	0.203 m
$d_{eo}$	Outside diameter of evaporator pipe	0.060 m
$d_{ei}$	Inside diameter of evaporator pipe	0.049 m
$\ell_p$	Length of evaporator pipe	30.48 m
$R_s$	Separation distance between evaporator pipes	3.048 m
$N_e$	Number of evaporator pipes in each heat pipe field	15
$A_{deck}$	Deck surface area associated with each evaporator pipe: $A_{deck} = \ell_c \cdot b_1$	$6.17 \text{ m}^2$

\*The total condenser length of a system with a uniform 15 cm (6") condenser spacing that would product the equivalent steady state conductance (see Eq. 5.30)

$$\ell_c = 4\ell_{c1} + 2(\ell_{c2} - \ell_{c1})S_2/S_1 = \{4(6.4) + 2(12.5 - 6.4)(3.0/2.4)\}m = 40.5m$$

See Table 6.2A for  $S_1$  and  $S_2$

TABLE 6.2A. REQUIRED THERMAL DESIGN PARAMETERS FOR SPRING CREEK

<u>Symbol</u>	<u>Description</u>	<u>Value</u>
$h_c$	Condensing film coefficient	$\sim 8 \times 10^3 \text{ W/m}^2 \cdot ^\circ\text{C}$
$h_e$	Evaporative film coefficient	$\sim 2 \times 10^3 \text{ W/m}^2 \cdot ^\circ\text{C}$
$K_b$	Thermal conductivity of the evaporator hole backfill grout	$2.0 \text{ W/m}^\circ\text{C}$
$K_c = K_e$	Thermal conductivity of the pipe walls	$\sim 45 \text{ W/m}^\circ\text{C}$
$K_{\text{conc}}$	Thermal conductivity of the deck concrete	$2.1 \text{ W/m}^\circ\text{C}$
$K_g$	Thermal conductivity of the ground	$2.1 \text{ W/m}^\circ\text{C}$
$(\rho c)_g$	Heat capacitance of the ground	$2.1 \times 10^6 \text{ J/m}^3 \cdot ^\circ\text{C}$
$S_1$	Deck shape factor, Figure 6.7 using $b_1$ , $h$ and $H$	2.4
$S_2$	Deck shape factor, Figure 6.7 using $b_2$ , $h$ and $H$	3.0
$T_g$	Average far-field ground temperature along evaporator length	$8^\circ\text{C}$
$\tau$	The Fourier modulus of the ground evaporator pipe based on 1 year	
$\tau =$	$\frac{(3.15 \times 10^7 \text{ s}) K_g}{(\rho c)_g l_p^2}$	
	$= \frac{(3.15 \times 10^7 \text{ s}) (2.1 \frac{\text{J}}{\text{sm}^\circ\text{C}})}{(2.1 \times 10^6 \frac{\text{J}}{\text{m}^3 \cdot ^\circ\text{C}}) (30.48 \text{ m})^2} = 0.0339$	
$\sqrt{\tau} =$		0.18

condenser spacing and the same steady-state deck conductance as the actual condenser.

The steady-state thermal resistance of the individual Spring Creek system components are calculated in Table 6.4A. This table indicates that many of component resistances are relatively small and could have been neglected in this example. These calculations also show that the resistance due to the evaporator pipe interactions ( $R_I$ ) is the dominant resistance in the Spring Creek system. For comparison purposes, the resistance due to evaporator thermal interactions for an isolated evaporator ( $N_e = 1$ ) and a twelve pipe field ( $N_e=12$ ) are also included.

Table 6.5A tabulates the steady-state and dynamic conductances for the Spring Creek system. The steady-state specific conductance for an isolated Spring Creek evaporator is  $7.2 \text{ W/m}^2\text{°C}$ . The thermal interaction between the fifteen evaporators in each corner causes this steady-state conductance to drop to only  $1.5 \text{ W/m}^2$  which represents the minimum conductance that would occur if energy were continuously extracted from the ground at a constant rate and no energy was transmitted through the surface of the ground. A correction of this conductance for transient effects results in a dynamic conductance of  $7.1 \text{ W/m}^2\text{°C}$  which, by coincidence, turns out to be very close to the steady-state isolated evaporator conductance. This dynamic conductance,  $\bar{u}$ , represents a conservative estimate of the minimum system conductance during significant heating events.

The experimental data at the site was obtained from a twelve evaporator field since three of the pipes were disabled in the instrumented corner. The dynamic conductance of this twelve evaporator

TABLE 6.4A. STEADY-STATE COMPONENT THERMAL RESISTANCES FOR SPRING CREEK

(See Figure 6.2)

<u>Description and Equation</u>	<u>Value (°C/W)</u>
<u>Deck resistance</u>	
$R_{\text{conc}} = [SK_{\text{conc}} \ell_c]^{-1} = [(2.4) (2.1 \frac{\text{W}}{\text{m}^{\circ}\text{C}}) (40.5 \text{ m})]^{-1} =$	$4.9 \times 10^{-3}$
<u>Resistance of the condenser pipe</u>	
$R_{\text{cp}} = \frac{\ln(d_{\text{co}}/d_{\text{ci}})}{2\pi K_c \ell_c} = \frac{\ln(0.033\text{m}/0.027\text{m})}{2\pi (45 \frac{\text{W}}{\text{m}^{\circ}\text{C}}) (40.5\text{m})} =$	$1.8 \times 10^{-5}$
<u>Condensing resistance</u>	
$R_c = (\pi d_{\text{ci}} \ell_c h_c)^{-1} = [\pi (0.027 \text{ m}) (40.5 \text{ m}) (8 \times 10^3 \frac{\text{W}}{\text{m}^2 \text{ }^{\circ}\text{C}})]^{-1} =$	$3.6 \times 10^{-5}$
<u>Evaporative resistance</u>	
$R_{\text{evap}} = (\pi d_{\text{ei}} \ell_p h_e)^{-1} = [\pi (0.049 \text{ m}) (30.48 \text{ m}) (2 \times 10^3 \frac{\text{W}}{\text{m}^2 \text{ }^{\circ}\text{C}})]^{-1} =$	$1.1 \times 10^{-4}$
<u>Resistance of the evaporator pipe</u>	
$R_{\text{ep}} = \frac{\ln(d_{\text{eo}}/d_{\text{ei}})}{2\pi K_e \ell_p} = \frac{\ln(0.060\text{m}/0.049\text{m})}{2\pi (45 \frac{\text{W}}{\text{m}^{\circ}\text{C}}) (30.48 \text{ m})} =$	$2.4 \times 10^{-5}$
<u>Isolated evaporator resistance</u>	
$R_{\text{eg}} = \frac{\ln(\frac{3.67\ell_p}{d_{\text{eo}}}) + (\frac{K_b}{K_g} - 1) \ln(\frac{3.67\ell_p}{d_h})}{2.162\pi K_b \ell_p}$	

TABLE 6.4A (CONTINUED)

$$= \frac{\ln\left[\frac{(3.67)(30.48 \text{ m})}{0.060 \text{ m}}\right] + \left[\frac{2.0 \text{ W/m}^\circ\text{C}}{2.1 \text{ W/m}^\circ\text{C}} - 1\right] \ln\left[\frac{(3.67)(30.48 \text{ m})}{0.203 \text{ m}}\right]}{2.162\pi(2.0 \text{ W/m}^\circ\text{C})(30.48 \text{ m})} = 1.75 \times 10^{-2}$$

Resistance due to evaporator interations (See Figure 6.3)

$$R_s / \ell_p = 3.048 \text{ m} / 30.48 \text{ m} = 0.1$$

$$N_e = 1 \text{ (Isolated Pipe), } R_I = 0$$

$$N_e = 12, R_I = \frac{R_I K \ell_p}{K \ell_p} = \frac{4.4}{(2.1 \frac{\text{W}}{\text{m}^\circ\text{C}})(30.48 \text{ m})} = 6.87 \times 10^{-2}$$

$$N_e = 15, R_I = \frac{5.3}{(2.1)(30.48)} = 8.28 \times 10^{-2}$$

TABLE 6.5A. STEADY-STATE SUBSYSTEM RESISTANCES, AND STEADY-STATE AND DYNAMIC SYSTEM CONDUCTANCES FOR SPRING CREEK.

<u>Description and Equation</u>	<u>Value</u>
Resistance between the evaporator and the bridge top surface	
$R_{es} = R_{conc} + R_{cp} + R_c + R_{evap} + R_{ep}$ $= (4.9 \times 10^{-3} + 1.8 \times 10^{-5} + 3.6 \times 10^{-5} + 1.1 \times 10^{-4} + 2.4 \times 10^{-5})^\circ\text{C/W} =$	$5.09 \times 10^{-3}^\circ\text{C/W}$
Resistance between the far-field ground and the evaporator	
a) Isolated evaporator ( $N_e = 1$ )	
$R_{field} = R_{eg} =$	$1.75 \times 10^{-2}^\circ\text{C/W}$
b) $N_e = 12$	
$R_{field} = R_{eg} + R_I$ $= (1.75 \times 10^{-2} + 6.87 \times 10^{-2})^\circ\text{C/W} =$	$8.62 \times 10^{-2}^\circ\text{C/W}$
c) $N_e = 15$	
$R_{field} = R_{eg} + R_I$ $= (1.75 \times 10^{-2} + 8.28 \times 10^{-2})^\circ\text{C/W} =$	$0.10^\circ\text{C/W}$
Steady-state total and specific conductance between the ground and the deck top surface	
a) Isolated evaporator	
$U_{ss} = [R_{es} + R_{field}]^{-1}$ $= [(5.09 \times 10^{-3} + 1.75 \times 10^{-2})^\circ\text{C/W}]^{-1} =$	$44.3 \text{ W/}^\circ\text{C}$
$u_{ss} = U_{ss} / A_{deck} = (44.3 \text{ W/}^\circ\text{C}) / (6.17 \text{ m}^2) =$	$7.2 \text{ W/m}^2\text{ }^\circ\text{C}$

TABLE 6.5A (CONTINUED).

b)  $N_e = 12$

$$U_{ss} = [5.09 \times 10^{-3} + 8.62 \times 10^{-2}]^{-1} =$$

11.0 W/°C

$$u_{ss} = 11.0/6.17 =$$

1.8 W/m<sup>2</sup>°C

c)  $N_e = 15$

$$U_{ss} = [5.09 \times 10^{-3} + 0.10]^{-1} =$$

9.5 W/°C

$$u_{ss} = 9.5/6.17$$

1.5 W/m<sup>2</sup>°C

Dynamic specific conductance

a) Isolated Evaporator

$$R_{\text{field}}/R_{\text{es}} = 1.75 \times 10^{-2}/5.09 \times 10^{-3} = 3.4$$

$$\text{and } \sqrt{\tau} = 0.18 \text{ (Table 6.2A)} \Rightarrow \bar{u}/u_{ss} \sim 1.8$$

from Figure 6.4

$$\bar{u} = (1.8)(7.2 \text{ W/m}^2\text{°C}) =$$

13.0 W/m<sup>2</sup>°C

b)  $N_e = 12, R_{\text{field}}/R_{\text{es}}$

$$= 8.62 \times 10^{-2}/5.09 \times 10^{-3} = 16.9$$

$$\bar{u} = (\bar{u}/u_{ss})u_{ss} = (4.4)(1.8 \text{ W/m}^2\text{°C}) =$$

7.9 W/m<sup>2</sup>°C

c)  $N_e = 15, R_{\text{field}}/R_{\text{es}} = 0.10/5.09 \times 10^{-3} = 19.7$

$$\bar{u} = (\bar{u}/u_{ss})u_{ss} = (4.7)(1.5 \text{ W/m}^2\text{°C})$$

7.1 W/m<sup>2</sup>°C

field is predicted to be  $7.9 \text{ W/m}^2\text{°C}$  from the empirical correlations presented in this design chapter as compared to the original simulation value of  $7.8 \text{ W/m}^2\text{°C}$  (see Figure 5.17).

The predicted minimum heat flux of this system during a melting event is

$$q_{\text{melt}} = \bar{u}(T_g - 1^\circ\text{C}) \quad (6.2)$$

$$= 7.1 \frac{\text{W}}{\text{m}^2\text{°C}} (8^\circ\text{C} - 1^\circ\text{C}) = 50 \text{ W/m}^2$$

Figure 6.9 implies that a heat flux of this magnitude will maintain the temperature of a wet surface above  $1^\circ\text{C}$  for air temperatures above  $-5^\circ\text{C}$  under calm, overcast, night conditions and 50% relative humidity. The air temperature must be at or above  $2^\circ\text{C}$  if the calm condition is replaced with a 5 m/s wind. Figure 6.10 indicates that  $50 \text{ W/m}^2$  would typically melt snow as rapidly as it falls in only 15 to 27% of the snow events that occur in the eastern states between  $38^\circ$  and  $42^\circ$  latitude (36). The corresponding experimental percentage was not determined but computations that were made for the Cheyenne environment show  $50 \text{ W/m}^2$  would handle 15% of the snow events on the average. The experimental observations did show a 50% reduction in the duration of the snow and ice cover above the 6" (15.2 cm) spaced condensers relative to the unheated deck. Although this system was not capable of a significant amount of snow melting, it easily prevented any preferential freezing of the heated bridge relative to the road.

If the Spring Creek facility were exposed to a  $14^\circ\text{C}$  far-field

temperature and the implied milder climate, the minimum predicted average power delivered during a melting event would increase to  $92 \text{ W/m}^2$ . Under these conditions which are characteristic of many of the eastern states, the system should keep pace with between 27 and 45% of the snow events. An isolated evaporator would provide over  $170 \text{ W/m}^2$  in this environment during a melting event.

#### D. Mechanical Design

The overall mechanical design of the Spring Creek heat pipe system as described in Chapter II and Appendix A was well conceived and is appropriate for large heat pipe systems. The design was based on the desire to factory assemble components which could be easily handled in the field and at the same time require a minimum amount of field assembly. These goals are at odds with the results of a thermal optimization which indicates that very long evaporators are desirable. On the Spring Creek project this led to a compromise wherein the materials for the evaporators were precut, cleaned and grooved in the heat pipe plant and shipped to the site for field assembly as described in Chapter II.

The condenser manifolds, on the other hand, were completely fabricated as a component in the heat pipe plant. The interconnecting pipes were also cleaned and prebent at the plant.

There are four specific design modifications which should be incorporated in the design of future systems. First, the diameter of the evaporator pipes can be decreased without significantly decreasing the thermal performance of the system. It should be noted that  $1 \frac{1}{2}$ " (3.8

cm)  $\emptyset$  pipe was used for the evaporators on the Cheyenne I 180 ramps and it appears that this can be further reduced to 1" (2.5 cm)  $\emptyset$  pipe.

Socket welded tee's were used to fabricate the condenser manifolds which utilized 1" (2.5 cm)  $\emptyset$  pipe in both the header and condenser fingers. Reducing the condenser fingers to 3/4" (1.9 cm)  $\emptyset$  allows the header to be manufactured by simply drilling the header, composed of 1" (2.5 cm)  $\emptyset$  pipe, and welding the condenser fingers directly to the header. This decreases the number of welds on the manifold by approximately 50% and simplifies the fixturing required for manufacture. A condenser finger diameter of 3/4" (1.9 cm) is believed optimum since it provides the minimum strength needed for construction although the diameter could be reduced and not degrade the thermal performance.

For ease of handling, the interconnecting pipes should be precleaned and shipped to the site in straight lengths. It is essential that adequate fall for drainage of the condensate be provided during installation of this pipe. Compaction problems leading to post construction settling can cause sags that result in liquid locks. It is recommended that the slope be at least 5% in any area where problems might be anticipated.

Insulation of all piping located underground within 1.5 meters (5') of finish grade is suggested in order to minimize heat loss during the winter. Urethane foam has been found to work well for this application when it is provided with a moisture barrier such as butyl or polyurethane paint. A five cm (2") layer is adequate. It should be emphasized that, wherever possible, interconnecting pipes should be bundled together to minimize the overall heat loss.

In addition, the lower surface of the bridge deck must be insulated. A sealing coat such as butyl paint should first be sprayed on the surface to provide both a moisture barrier and a bond for the urethane foam which is recommended. Again, five cm (2") of foam is adequate; however the foam should be coated with butyl or polyurethane paint to prevent ultraviolet degradation.

Weep lines should be provided on the lower deck surface so that excess moisture can drain from the deck. This was done at the Spring Creek facility by tacking boards on edge to the lower deck surface prior to insulating.

The principle cause of failure of the heat pipe system is expected to be corrosive penetration of the steel leading to loss of ammonia. Assuming that a heat pipe system design similar to that described is utilized, the external surfaces of the heat pipe should be coated with either epoxy or urethane foam or, in the case of the evaporator, encased in concrete grout. It is possible that part of the evaporator or inter-connecting pipe may be in direct contact with the earth. This contact is the most likely area for corrosive failure to occur and the life of the system will depend on the nature of the soil. Cathodic protection may be warranted in some situations. Alternative materials to the steel pipe have been investigated in an attempt to eliminate the corrosion problem and reduce cost, but an alternate cannot be recommended at this time.

In view of the difficulties associated with field assembly of large heat pipe systems including: the cleanliness requirements, inert gas welding, vacuum operations and charging of the pipes with working fluid, it is essential that the installer have some previous background in the

area. It is virtually impossible to repair a nonfunctional pipe after the project is complete, especially if it involves a leak at an unknown location.

Appendix B contains an example set of Special Provisions appropriate for use when a heat pipe system is included in the new construction of a bridge or section of highway.

Special provisions should also be included for the heating of gutters and drains to prevent their blockage by snow and ice. One side of each of the Spring Creek drains was attached to a condenser finger but this did not prevent their occasional blockage by ice. The gutters were almost continuously filled with snow that had been pushed into the gutters by the snow plows. The lack of drainage because of the above blockages caused the snow melt to refreeze at times.

## VII. CONCLUSIONS AND RECOMMENDATIONS

The Spring Creek project successfully met most of its objectives. The first earth heated bridge deck was designed, fabricated and its performance monitored over a two year period. The installation of the heat pipe system had a minimal impact upon normal construction activities; the only unique equipment requirement was a crane with a boom that could be extended to 100' (30 m). A chronological listing of the major construction milestones is presented in Appendix C.

The only serious design flaw that has become evident to date was the interconnecting pipe grades in the ground were insufficient to compensate for the settling that occurred in the earth adjacent to the bridge structure. Liquid locks were produced in many of the interconnecting pipes which disabled the heat pipes. To prevent this problem from occurring at future installations, it is recommended that the minimum grade on the interconnecting pipes in the ground be increased from the 2% that was specified at Spring Creek to at least 5%, and that the compaction specification for the earth around these pipes be strengthened to minimize subsidence. This settling problem underscores the meticulous adherence to details that is required in the construction and installation of ground heat pipes. Cleaning, welding or grade flaws are generally not correctable after installation.

The operating heat pipes performed as anticipated in totally preventing preferential freezing of the heated deck relative to the roadway. The heated surface temperature was increased by as much as 15°C

(27°F), while weekly averaged temperature increases of up to 10°C (18°F) were achieved. Similar temperature increases can be expected from a comparable system at a different location, but the reduction that the heating produces in the seasonal duration of icy surfaces depends upon the severity of the local climate which is reflected in the region's far-field ground temperature. Despite a ground temperature of only 8°C (47°F), the Spring Creek system decreased the frozen time of the outer two, nontraffic lanes by 40% and their snow cover time by 47%. Past experiences with ground heating systems for slabs indicate that ground temperatures of the order of 13°C (55°F) can handle most of the nondrifting snow storms that occur in milder climates (6,8,16 and 22). There is, of course, some thermal advantage in heating a slab instead of an elevated deck, but most of the observed increases in snow melting capacity resulted from the significantly higher temperature difference between the frozen surface and the far-field ground.

An easily implemented heat pipe thermal design procedure was formulated which accounts for the system's complex transient nature--including evaporator thermal degradation and interactions. This design procedure predicts the minimum dynamics conductance of power from the ground to the deck surface that can be expected during a significant heating event. The empirical correlations which the method utilizes were developed from a parametric study of the variation of system performance with the principal geometric and thermal properties of the ground, heat pipes, deck and environment. Experimental data from the Spring Creek site indicate that the heat transfer model that was utilized in the parametric studies predicts a minimum conductance that is low, yet appropriate for conservative design.

The Spring Creek system's cost itemization is presented in Appendix C. These data indicate that the heat pipe related items contributed 62% of the project's \$597,414 cost. Discounting the costs of the instrumentation vault, the four service vaults and the two header vaults, which could have been eliminated by embedding the manifolds in the concrete deck, would have reduced the cost to around \$558,000. The heat pipe system accounts for 59% of this total or \$67.43 per square foot ( $\$725.81/m^2$ ) of bridge surface. Thus, despite its conceptual and mechanical simplicity, the primary impediment to the extensive utilization of this thermal system is its capital expense.

Some minor cost reductions were obtained in the Cheyenne system by replacing the welded condenser pipe fittings with simple saddle welds, by reducing the 2" (5 cm) schedule 80 evaporator pipe to 1 1/2" (3.8 cm) pipe, and by not epoxy coating the evaporator pipes. The heat transfer model indicates that the reduction in evaporator pipe diameter should cause only a small degradation in performance. Any effort to produce a significant cost reduction in this system would have to be directed toward the evaporator since it accounted for approximately 70% of the Spring Creek heat pipe cost. Unfortunately, there appears to be no viable inexpensive alternates to drilling, steel pipe, and concrete grouting.

The utilization of this heat pipe technology on a much smaller scale may prove to be economically viable. For instance, the heating of gutters and drains to prevent their blockage by snow and ice, or limiting the heating to the tire tracks would require only a few heat pipes. The thermal performance of a ground heat pipe system also improves as the number of interacting evaporators decreases. Table 6.5A indicates

that an isolated Spring Creek heat pipe should produce a minimum dynamic conductance that is approximately 80% larger than the conductance produced by the pipes in a fifteen evaporator field.

One alternate technique currently under study for extracting energy from the earth utilizes conventional water wells. Water is pumped through an above ground, manifolded evaporator and then reinjected into the ground. A multiplicity of condensers are attached to each manifold to distribute the energy in the deck. This permits the heat pipe system to be manufactured as a complete module in the factory. Modules capable of heating up to  $28 \text{ m}^2$  ( $300 \text{ ft}^2$ ) appear practical. The utilization of heat pipes to distribute the thermal energy to the deck instead of directly circulating the water avoids any pipe fouling, corrosion, water leakage and freeze-up within the deck which could disable the system and possibly cause catastrophic damage to the deck. The heat pipe's very efficient thermal pumping also replaces the energy intensive mechanical pumping that would be required to circulate a warm liquid through the small tubing embedded in the deck. The temperature and pressure drops that occur in the circulation of water in small tubes also require many separate loops to be utilized which leads to balancing problems. The principle advantage of water based systems is economic. It appears that installed costs will be less than \$7.00 per square foot ( $\$75.00/\text{m}^2$ ) of heated surface, excluding the water system's cost.

The disadvantages of a water based system relative to the ground base system include its usage being severely restricted by the availability of a reliable and sufficient water source. Water based systems also require external pumping and control, and maintenance.

In summary, it has been shown that ground based heat pipe systems

are effective for controlling preferential icing and provides some snow control; however the high capital cost will limit their use to sites where the cost can be justified or to the heating of small bridge segments. Water based heat pipe systems appear to provide many of the advantages of the ground systems at a substantially reduced cost. It is recommended that future effort be directed toward further development of water powered heat pipe systems.

#### REFERENCES

1. Murray, D. M. and Ernst, U. F. W., "An Economic Analysis of the Environmental Impact of Highway Deicing," Report No. EPA-600/2-76-105, 1976.
2. Azevedo, W. V.; Deen, R. C. and Havens, J. C., "The Operations of an Electrical Heating System for Bridge Decks," Research Report 564, Department of Transportation, Kentucky, 1980.
3. Sekioka, M.; Xihara, K. and Sato, M., "Thermal Considerations on Snow Melting System with Natural Thermal Water at Jozankei Spa, Sapporo Japan," Journal of Japan Geothermal Energy Association, Vol. 16, No. 2, p. 43, 1979.
4. Nydahl, J. E.; Pell, K. M.; Senser, D.; Twitchell, G. and Ownbey, S., "Data Collection and Analysis for Geothermal Research," Report No. CDH-UW-R-81-11, Colorado Department of Highways, 1981.
5. Nydahl, J.; Pell, K. M.; Donnelly, D.; Swanson, H. and Griffin, R., "Geothermal Heating of Highway Structures," Transportation Research Board 860, p. 1, 1982.
6. Winters, F. and Sasor, S. R., "Pavement Heating-Executive Summary," Report No. 77-003a-7722, New Jersey Department of Transportation, 1977.
7. Tippmann, J. R., "Heat Transfer Method to Preclude Ice Formation on Paving," Patent Number 3,195,619, July 20, 1965.
8. Bienert, W. B.; Pravda, M. F.; Suelau, H. J. and Wolf, D. A., "Snow and Ice Removal from Pavements Using Stored Earth Energy," Report No. FHWA-RD-75-139, 1975.
9. Pravda, M. F.; Trimmer, D. S. and Wolf, D. A., "Heating Systems for Airport Pavement Snow, Slush and Ice Control," Report No. FAA-RD-75-139, 1975.
10. Brinkman, C. P., "Space-Age Technology for Deicing Hazardous Highway Locations," Public Roads, Vol. 39, No. 3, p. 39, 1975.
11. Ferrara, A. and Yenetchi, G., "Prevention of Preferential Bridge Icing Using Heat Pipes," Report No. FHWA-RD-76-168, 1976.

12. Pravda, M. F.; Bienert, W. B.; Wolf, D. A.; Nydahl, J. E.; Pell, K. M. and Ownbey, S. R., "Augmentation of Earth Heating for Purposes of Roadway Deicing," Report No. FHWA-RD-79-81, 1978.
13. Cundy, V. A.; Nydahl, J. E. and Pell, K. M., "Geothermal Heating of Bridge Decks," Snow Removal and Ice Control Research, Special Report 185, Transportation Research Board, p. 169, 1978.
14. Wilson, C. H.; Pope, D. H.; Cundy, V. A.; Nydahl, J. E. and Pell, K. M., "A Demonstration Project for Deicing of Bridge Decks," Transportation Research Record 664, p. 189, 1978.
15. Cundy, V. A., Transmission of Earth Energy by Heat Pipes for Thermal Control of Bridge Decks, Ph.D. Dissertation, University of Wyoming, Laramie, Wyoming, 1979.
16. Long, D. C. and Baldwin, J. S., "Snow and Ice Removal from Pavement Using Stored Earth Energy," FHWA-TS-80-227, 1980.
17. Tanaka, O.; Yamakage, H.; Ogushi, T. and Marakami, M.; "Snow Melting Using Heat Pipes," IV International Heat Pipe Conference, London, p. 11, 1981.
18. Nydahl, J.; Pell, K. and Ownbey, S., "Thermal Design of the Earth Heat Pipe System for the U.P. Railroad Overpass," SETA Corporation Report, Laramie, Wyoming, 1981.
19. Senser, D., "Performance Evaluation of a Runway Heating System Utilizing a Low Grade Energy Source and Heat Pipes," Thesis, University of Wyoming, Laramie, Wyoming, 1982.
20. Sackos, J. T., "Bridge Deck Heating Using Earth Coupled Heat Pipes," Thesis, University of Wyoming, Laramie, Wyoming, 1983.
21. Lee, R. C., "Heat Transfer Analysis of Geothermally Heated Road Structures," Thesis, University of Wyoming, Laramie, Wyoming, 1983.
22. Tanaka, O., "Snow Melting and Deicing System Using Heat Pipes," Heat Pipe Research and Development in Japan; Koichi Oshima, Ed.' The Institute of Space and Astronautical Science, Tokyo, p. 132, April, 1983.
23. Lee, R.; Sackos, J.; Nydahl, J. and Pell, K., "Bridge Heating Using Ground-Source Heat Pipes," Transportation Research Record 962, p. 51, 1984.
24. Chang, Jen-Hu, Ground Temperature, Vols. I and II, Bluehill Meteorological Observatory, Harvard University, 1958.
25. Wyoming Weather Facts, Natural Resources Research Institute, College of Engineering, University of Wyoming, Laramie, Wyoming, 1966.

26. Kusuda, T., "Algorithms for Calculating the Transient Heat Conduction by Thermal Response Factors for Multi-Layer Structures of Various Heat Conduction Systems," NBS Report No. 10-108, U.S. Department of Commerce, National Bureau of Standards, August 1969.
27. DOE-2 Computer Program, IBL-8689, Building Energy Analysis Group, Energy and Environment Division, Lawrence Berkeley Laboratory, Berkeley, California, 1980.
28. DeSalvo, G. J. and J. A. Swanson, ANSYS Engineering Analysis System User's Manual, Swanson Analysis Systems, Inc., February 1982.
29. Ball, D. A.; Fischer, R. D. and Hodgett, D. L., "Design Methods for Ground-Source Heat Pumps," ASHRAE Transactions, Vol. 89, 1983.
30. Ingersoll, L. R. and Plass, H. J., "Theory of the Ground Pipe Heat Source for the Heat Pump," ASHVE Transactions, Vol. 54, p. 339, 1948.
31. Idso, S. B., "On the Apparent Incompatibility of Different Atmospheric Radiation Data Sets," Quarterly J. R. of the Meteorological Society, Vol. 106, 1980.
32. Vehrencamp, J. E., "Experimental Investigations of Heat Transfer at an Air-Earth Interface," Transactions, American Geophysical Union, Vol. 34, No. 1, 1953.
33. Lee, R., "Report on Convective Correlations," unpublished report, University of Wyoming, 1982.
34. Carslaw, H. S. and J. C. Jaeger, Conduction of Heat in Solids, second edition, Oxford University Press, 1980.
35. Kersten, M. S., "Thermal Properties of Soils," Bulletin No. 28, Vol. 52, University of Minnesota Institute of Technology, Engineering Experimental Station, June 1949.
36. "Snow Melting", Chapter 35; ASHRAE Handbook, 1984 Systems; ASHRAE, Inc., Atlanta, Ga.
37. Ollendorf, F., Erdströme, 2. Aufl. Birkhäuser, Basel, 1969.

APPENDIX A

Construction Plans for  
Spring Creek Bridge, Laramie, Wyoming

Wyo. Project BRM-4211(6)

1980



**DESIGN DATA**

**SPECIFICATIONS:** AASHTO, dated 1977, with revisions, and supplemented by Bridge Design Practice Manual.

**LOADING:** MS70-66. Future wearing surface: 18 psf

**STRUCTURAL STEEL:** Service load design - ASTM A588  $F_y = 21000$  psi  
ASTM A588  $F_u = 20000$  psi

**REFERENCES**

Special Provisions:		Dated
S-100 A	Incorporation of 1974 SPECIFICATIONS	5-8-74
S-100 B	Specific Equal Employment Opportunity Responsibilities	5-8-74
S-100 M	Weekly Construction Wage Reports	5-8-74
S-100 N	Liquidated Damages	5-8-74
S-100 GA	Alteration of Plans or Location of Work	9-10-74
S-100 GB	Notice to Proceed	7-11-73
S-100 LE	Maintenance of the Work During Construction	11-4-73
S-100 ME	Contractor's Responsibility for Work	11-26-73
S-100 BF	Definition and Terms	3-18-74
S-100 CF	Determination and Extension of the Contract Completion Date	7-19-74
S-100 TM	Control of Work	1-18-77
S-100 UN	Prosecution and Progress	1-18-77
S-100 FJ	Participation by Minority Contractors	3-31-77
S-100 FQ	Affirmative Action to Ensure Equal Employment Opportunity (Executive Order 11246)	4-1-78
S-100 BH	Allowance for Adverse Weather Delay	10-10-76
S-100 QT	Suspension of Work	6-4-79
S-100 VT	Contractor's Responsibility for Utility Procedures and Services	6-20-76
S-100 EU	Metric Equivalents	5-24-79
S-100 MV	Contract Bond	12-3-79
S-100	Notch Toughness for Structural Steel	1-31-83
S-100 B	Welding	7-22-76
S-100 AF	Welder Qualification	12-9-84

**GENERAL NOTE**

**SPECIFICATIONS:** Wyoming Highway Department's 1976 Specifications for Road and Bridge Construction shall govern unless otherwise noted on Plans or in Contract Special Provisions.

**STRUCTURAL STEEL:** All structural steel, excepting bevel plates, shall conform to ASTM A588. Bevel plates shall conform to ASTM A16. The exterior faces of the exterior girders shall be blast cleaned in accordance with Subsection 501.43 of the Specifications. Bolts, nuts and washers shall conform to ASTM A325, Type 1. ASTM A588 steel shall not be painted.

**DIMENSIONS:** All longitudinal dimensions are measured horizontally and include no correction for grade.

**BEARING PADS:** Elastomeric bearing pads shall be of 30 durometer hardness.

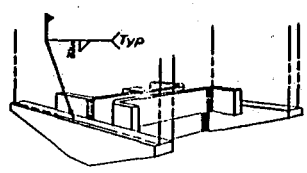
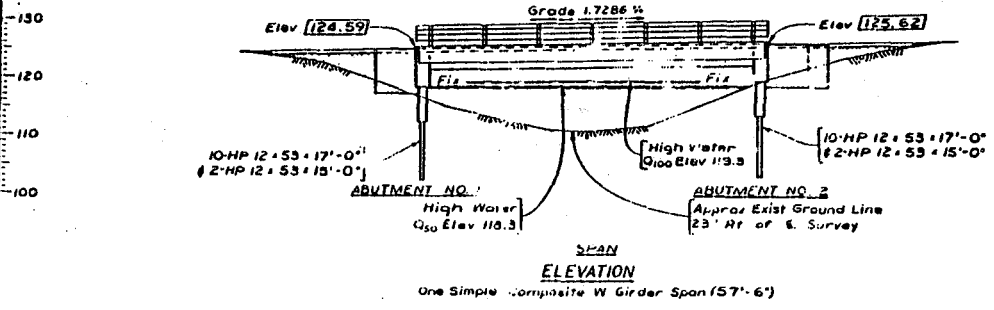
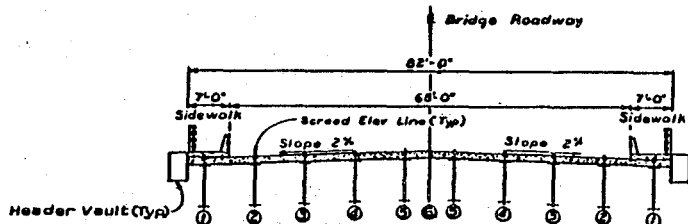
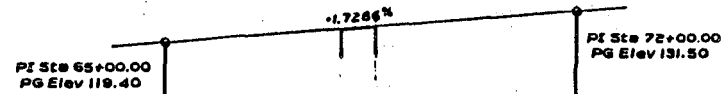
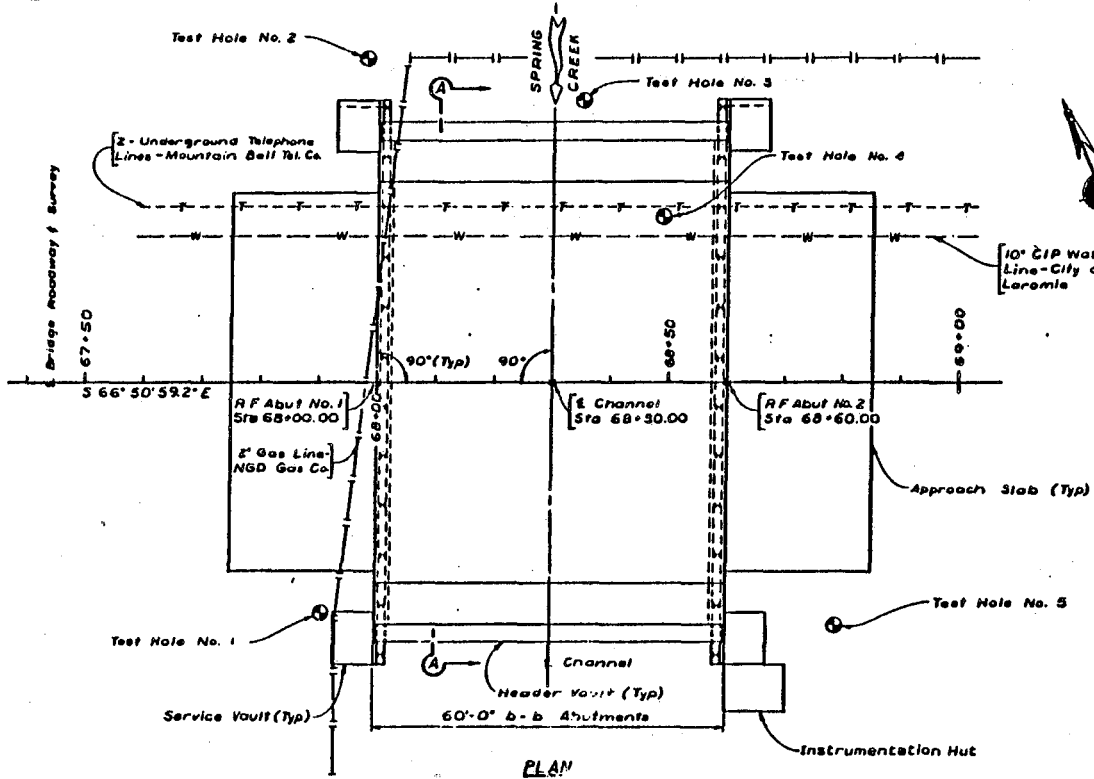
**STEEL PILING:** HP 10-33 piling shall conform to ASTM A588. The furnishing of the single piece pile reinforcing points shall be considered subsidiary to the Contract Bid Item Steel Piling HP 10-33.

**CONTRACT CONTENT:** This contract shall include supplying, fabricating, handling and shipping of the structural steel as shown on the Contract Plans, and supplying, handling and shipping of the steel piling and the 24 single piece pile reinforcing points as shown on the Contract Plans. This work shall conform to the applicable sections of Specifications and to the Contract Special Provisions. The Engineer shall be notified prior to the shipment of this material. The material shall be shipped to the Wyoming Highway Department yards in Laramie, Wyoming, unloaded and stockpiled as directed by the Engineer. The unloading and stockpiling shall be considered part of this contract.

TOTAL ESTIMATED QUANTITIES - Code 7003				
Item No.	Item	Unit	Total Quantity	Estimate
S103.03	Contract Bond	LS	Lump Sum	
S501.11	Structural Steel	LS	Lump Sum	107300 lbs
S504.123	Steel Piling HP 10-33	LF	400	

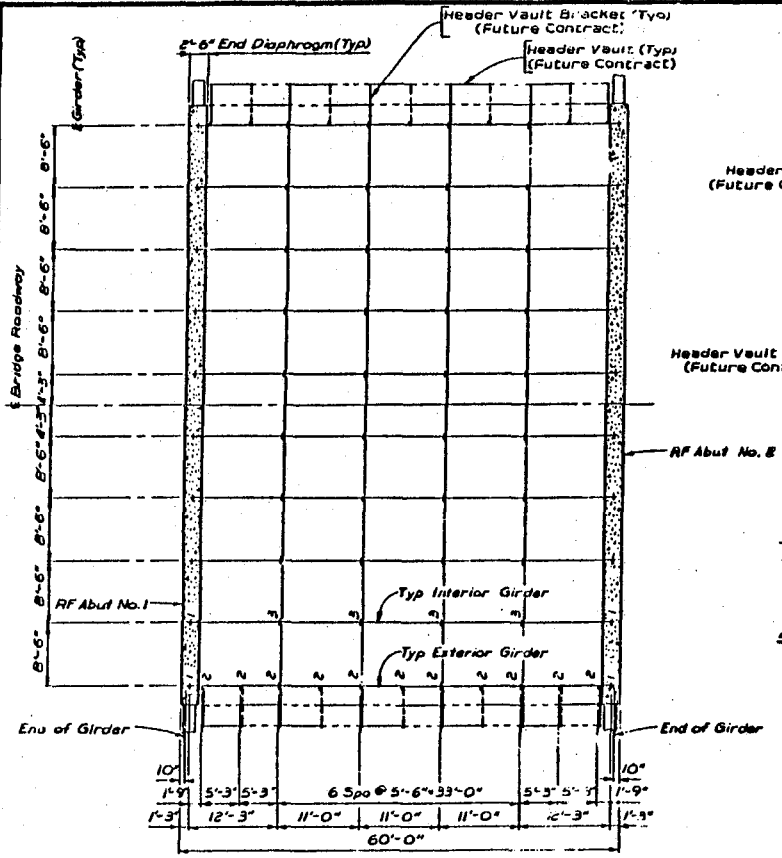
**STRUCTURAL STEEL AND STEEL PILING CONTRACT**

WYOMING HIGHWAY DEPARTMENT BRIDGE DIVISION			
REVISIONS	GENERAL NOTES		
	BRIDGE OVER SPRING CREEK STA 68 + 30 Laramie - Interstate 80 (Grand Ave Exit) BRM-4211(4) AI		
APPROVED	DESIGN DETAIL MHC/BFC DS	Design Section B P Collins Draw No 5042	Sheet 2 of 4

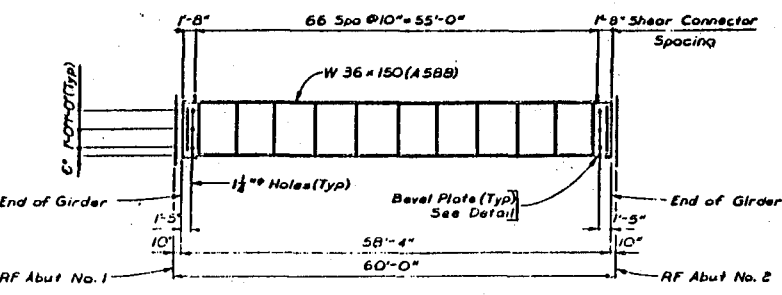


**Notes:**  
 1) Elevations shown thus [124.59] indicate Finished Grade at Rear Face Abutment on & Bridge Roadway.  
 2) R/W Marker, Sta 54+17 Lt. - Elev 7233.66 (State Plane Datum) = Elev 100.00.

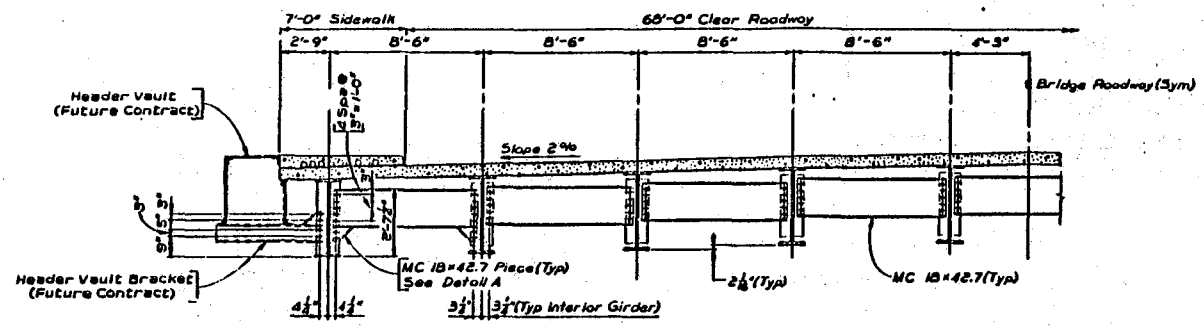
WYOMING HIGHWAY DEPARTMENT BRIDGE DIVISION	
REVISIONS	GENERAL PLAN & ELEVATION BRIDGE OVER SPRING CREEK STA 68+30 Laramie - Interstate 80 (Grand Ave Exit) BRM-4211(4) AI
APPROVED	DESIGN: JHY / MTC DETAIL: JHY / MTC Design Section B P Collins Dirg No. 5042 Sheet 3 of 4



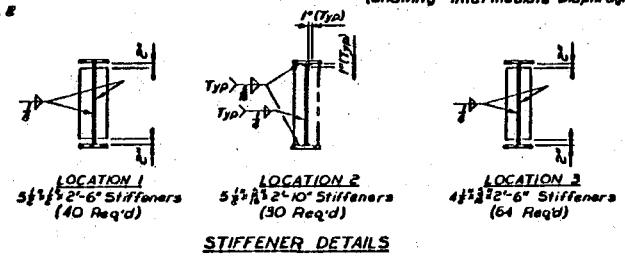
**FRAMING PLAN**



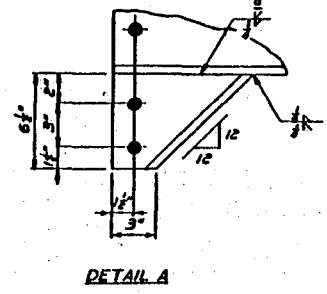
**GIRDER ELEVATION**  
 (Exterior Girder shown - Interior Girder similar)



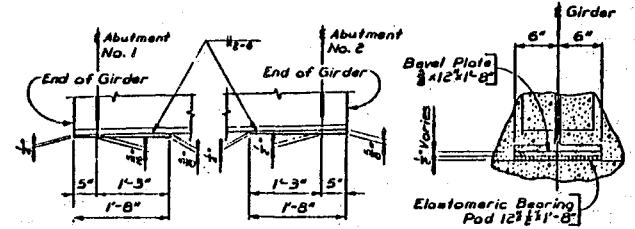
**HALF ROADWAY SECTION**  
 (Showing Intermediate Diaphragms)



**STIFFENER DETAILS**

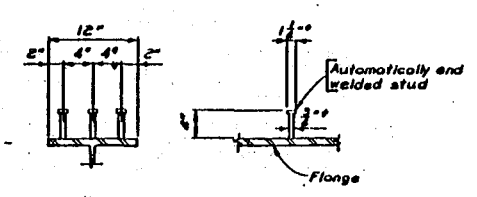


**DETAIL A**



**BEVEL PLATE DETAILS**

**BEARING AT ABUTMENTS**  
 (20 Required)



**TYPICAL SHEAR CONNECTOR DETAILS**  
 (2010 Required)

**TABLE OF SCREED ELEVATIONS**  
 Add base elevation 100.00 to all elevations listed in table. Elevations include grade, slope and correction for dead load deflection. All elevations for line Nos. 1-5 are of  $\frac{1}{2}$  Girder. Elevations for line No. 6 are of  $\frac{1}{2}$  Bridge Roadway. See General Plan and Elevation Sheet No. 2, ft. line locations.

Line No.	E. Abut. No. 1	TENTH POINTS										E. Abut. No. 2
		1.1	1.2	1.3	1.4	1.5	1.6	1.7	1.8	1.9		
1	23.24	23.97	24.70	25.42	26.13	26.83	27.52	28.20	28.87	29.53	30.18	24.64
2	24.01	24.74	25.47	26.19	26.90	27.60	28.29	28.97	29.64	30.30	30.95	25.01
3	24.81	25.54	26.27	27.00	27.71	28.41	29.10	29.78	30.45	31.11	31.76	25.18
4	24.55	25.28	26.01	26.73	27.44	28.14	28.83	29.51	30.18	30.84	31.49	25.35
5	24.51	25.24	25.97	26.69	27.40	28.10	28.79	29.47	30.14	30.80	31.45	25.32
6	24.61	25.34	26.07	26.79	27.50	28.20	28.89	29.57	30.24	30.90	31.55	25.60

Note: 1) No camber required in girders.  
 2) Place natural camber in girders up.

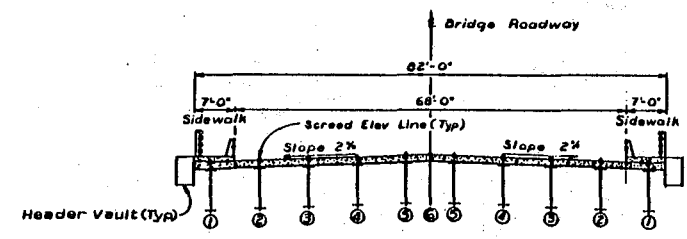
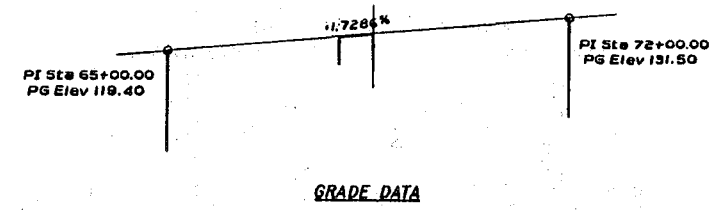
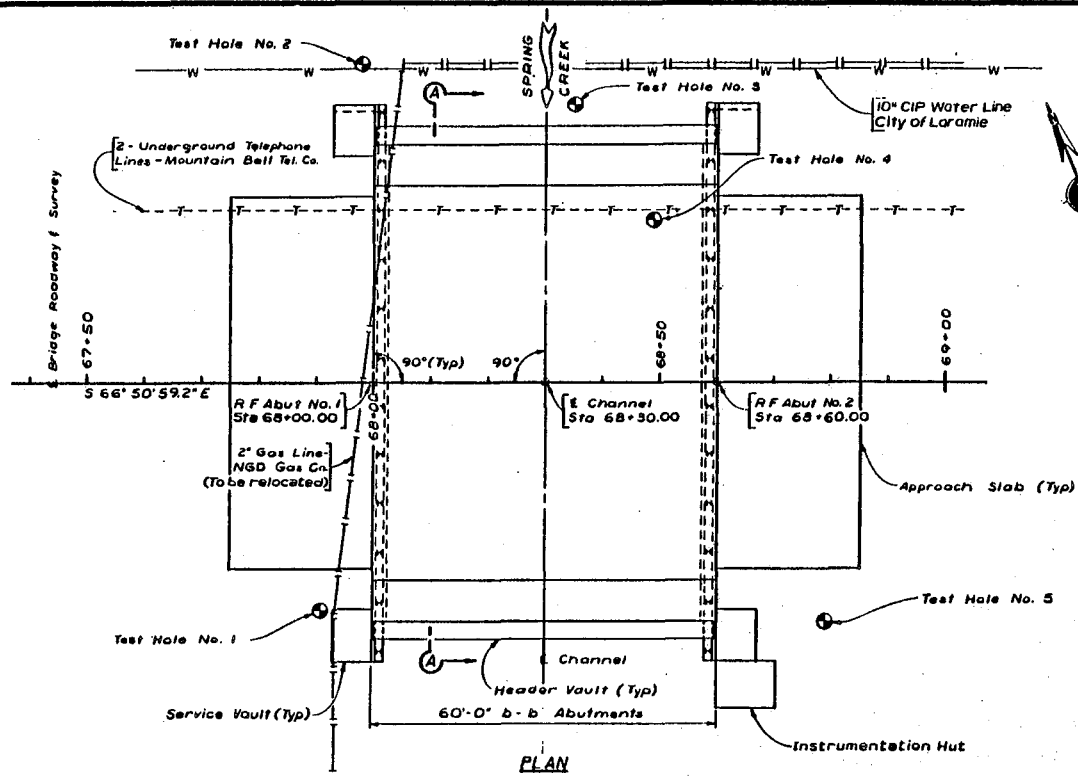
WYOMING HIGHWAY DEPARTMENT  
 BRIDGE DIVISION

**REVISIONS**

**SUPERSTRUCTURE DETAILS**  
**BRIDGE OVER SPRING CREEK**  
 STA 68+30  
 Laramie - Interstate 80  
 (Grand Ave Exit)  
 BRM-4211(4) AI

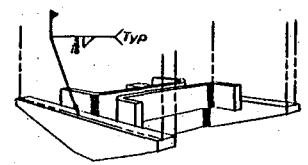
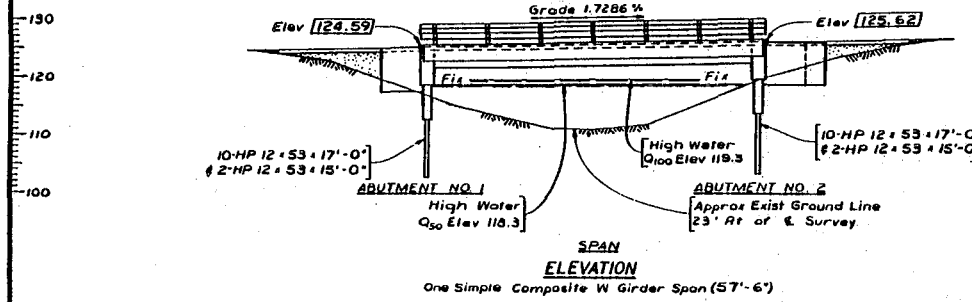
APPROVED: DESIGN: D.P., J.H.C. DETAIL: M.L.O., J.W.C. D.S., M.H.C., L.V.K. Design Section: B.P. Collins  
 Draw No: 5042 Sheet: 4 of 4



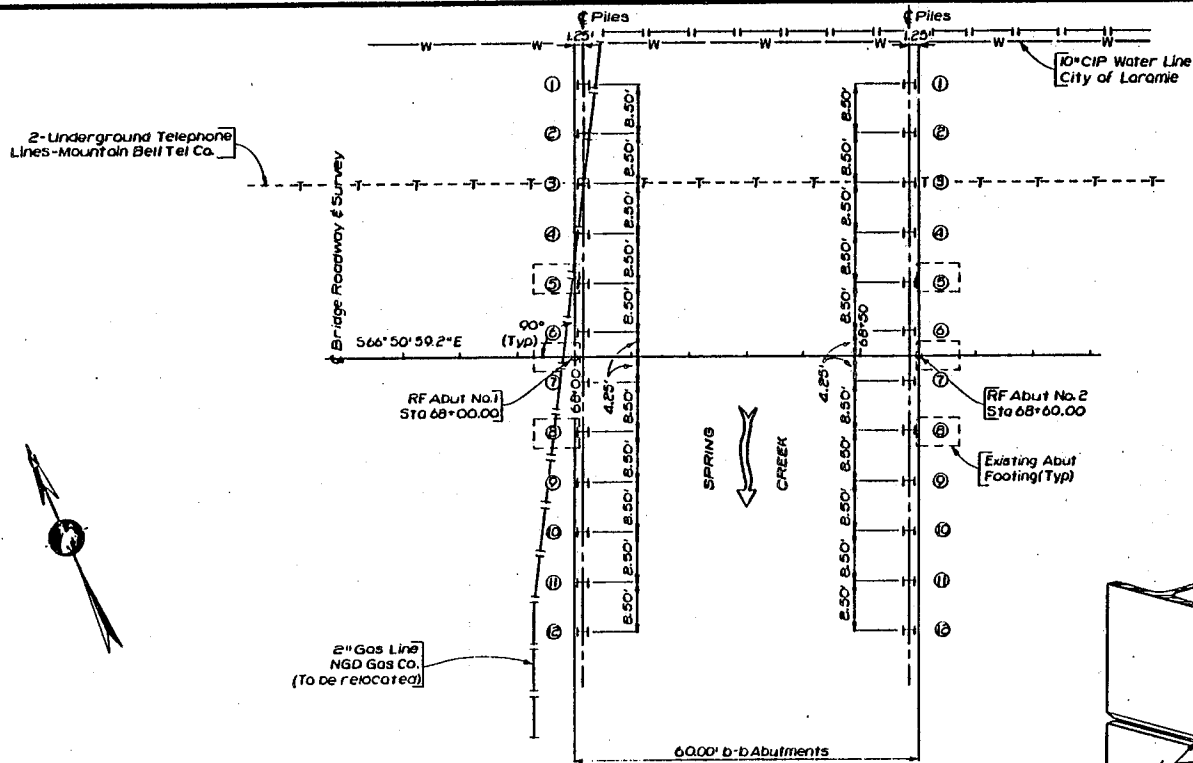


Note: 1) Elevations shown thus 124.59 indicate Finished Grade at Rear Face Abutment on Bridge Roadway.

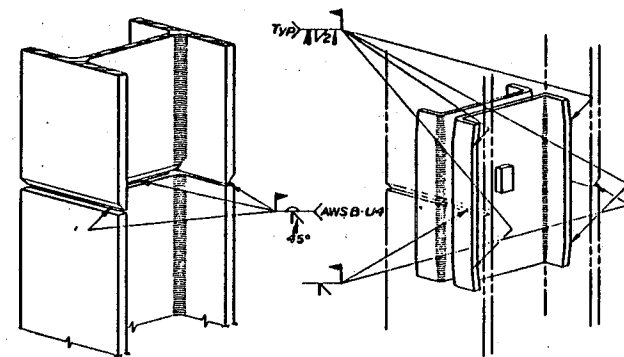
2) R/W Marker, Sta 54+17 Lt. - Elev 7233.56 (State Plane Datum) = Elev 100.00.



WYOMING HIGHWAY DEPARTMENT BRIDGE DIVISION	
REVISIONS	GENERAL PLAN & ELEVATION BRIDGE OVER SPRING CREEK STA 68+30 Laramie - Interstate 80 (Grand Ave Exit) BRM-4211(6) AI
DESIGNED DATE 5/1/60	DESIGN DETAIL BY JHV, BPC DRG. NO. 5111 Sheet 82 of 81



STEEL PILING DATA		
Location	Pile No.	Pile Cutoff Elevation
Abut No.1	1#12	115.36
	2#11	118.41
	3#10	118.58
	4#9	119.75
	5#8	119.92
Abut No.2	6#7	119.09
	1#12	116.33
	2#11	119.39
	3#10	119.56
	4#9	119.73
	5#8	119.90
	6#7	120.07



PILING LAYOUT

WELDED SPLICE

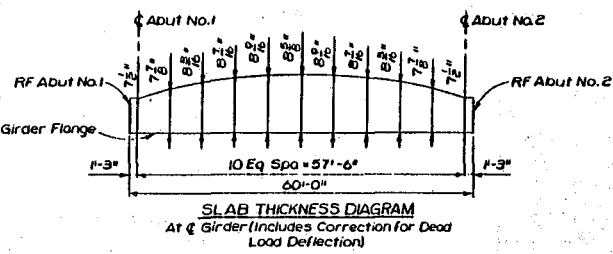
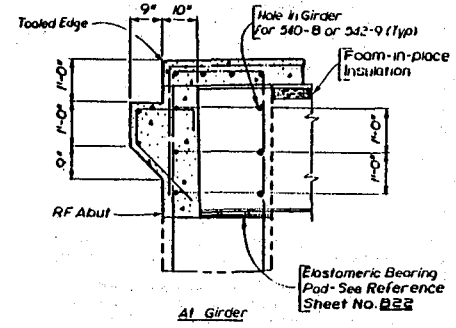
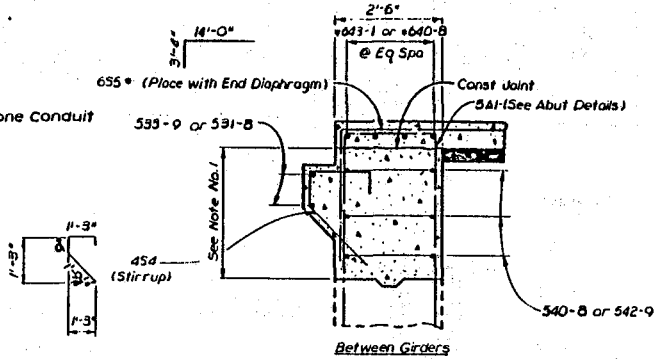
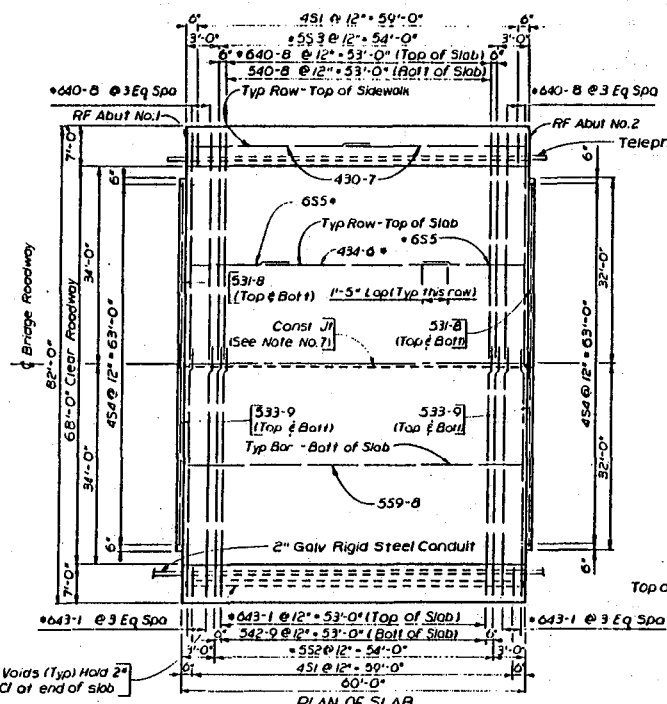
PILE SPlicer

Note: 1) All piles are HP 12 x 59.  
 2) See Sheet No. 2 for driving point detail.

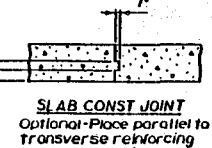
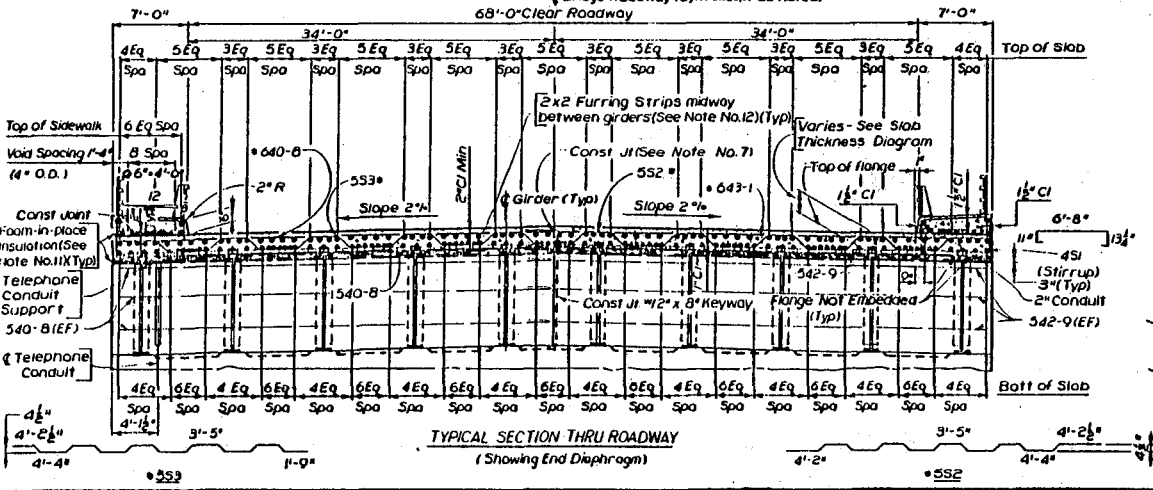
WYOMING HIGHWAY DEPARTMENT BRIDGE DIVISION			
REVISIONS	SUBSTRUCTURE LAYOUT		
	BRIDGE OVER SPRING CREEK		
	STA 68+30		
	Laramie - Interstate 90		
	(Grant Ave Exit)		
	BRM-4211(6)		AI
APPROVED [Signature] 5/11/50	DESIGN [Signature] GJ	DETAIL [Signature] MHC	Design Section BPCollins Drawg No. 5111 Sheet 3 of 21







- NOTE: 1) Indicated portion of end diaphragm shall attain 80% of ultimate design strength by cylinder tests prior to placement of concrete slab.  
2) Concrete in the deck shall be placed in one continuous operation at the minimum rate of 20LF per hour.  
3) For bridge railing and pedestrian railing anchor bolt and drainpipe locations see Sheet No. 12, thru 18.  
4) For screed elevations see Reference Sheet No. B22.  
5) For details pertaining to heat pipe system and header vaults see Sheet No. 2, thru 14.  
6) Bar marks followed by an asterisk (\*) indicate reinforcing steel to be epoxy coated. Refer to Epoxy Coated Reinforcing Steel special provision.  
7) This construction joint shall have the same dimensions as the optional slab construction joint.  
8) The reinforcing steel fabricator shall prefix all superstructure bar marks with numeral 3.  
9) The estimated quantity of Class AAA Concrete is 244CY and the estimated quantity of Class B Concrete is 66.6CY.  
10) For telephone conduit support and 2" rigid steel conduit details see Sheet No. B2.  
11) Run insulation continuous from FF to FF Abutments. Hold sidewalk insulation 2" clear from exposed concrete surfaces.  
12) Attach strips to bottom of deck continuous from FF to FF Abutments, prior to insulating.  
13) The section of deck to be left unheated (Pipe Nos 8, 10 and 12 - Corner No. 3) and another section 12'-0" wide (Pipe Nos 7, 11, 14, 3, 8 and 12 - Corner No. 1) shall be left not insulated for half the width of the bridge deck.



WYOMING HIGHWAY DEPARTMENT BRIDGE DIVISION			
<b>SUPERSTRUCTURE DETAILS</b>			
<b>BRIDGE OVER SPRING CREEK</b>			
<b>STA 68+30</b>			
<b>Laramie - Interstate 80</b>			
<b>(Grand Ave Exit)</b>			
BRM-4211(6) AI			
APPROVED DATE: 5/13/82	DESIGN DIV. / DRK DETAIL: MHC / NMC BY: MHC / NMC	Design Section DRG. No. 5111	BPC/ Collins Sheet 6 of 21

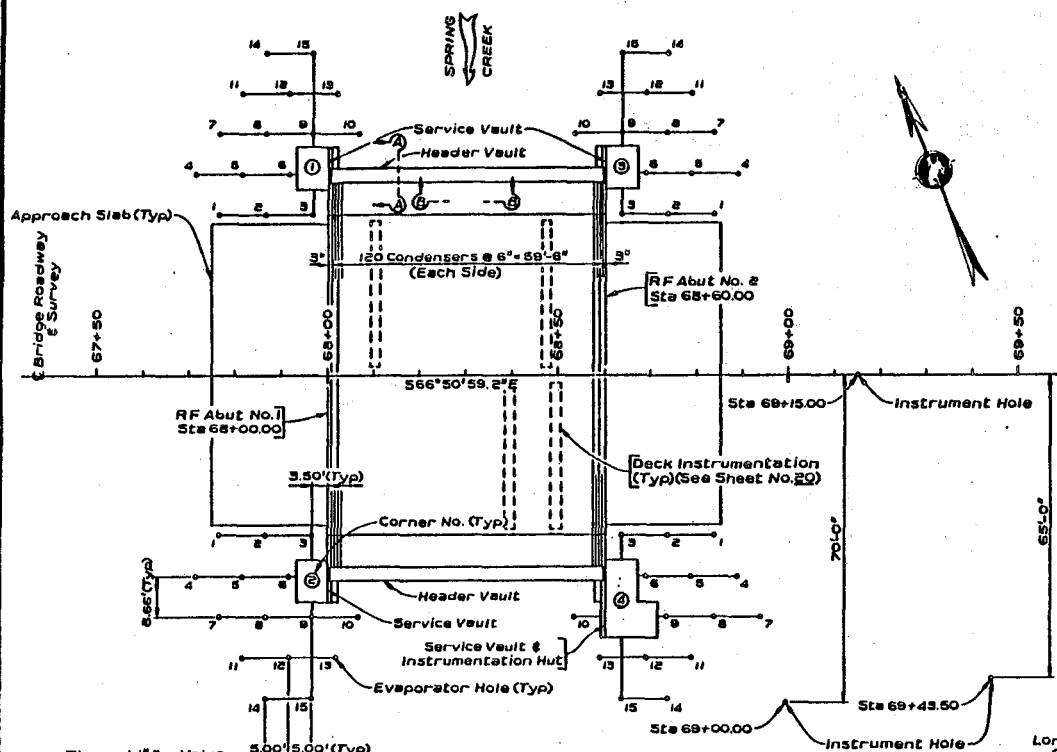
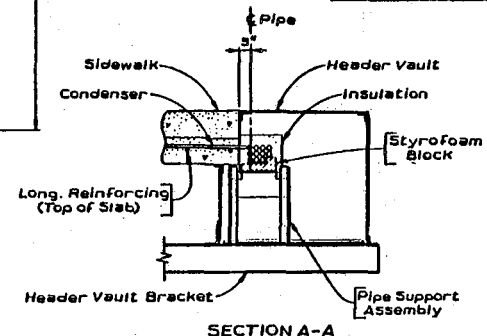
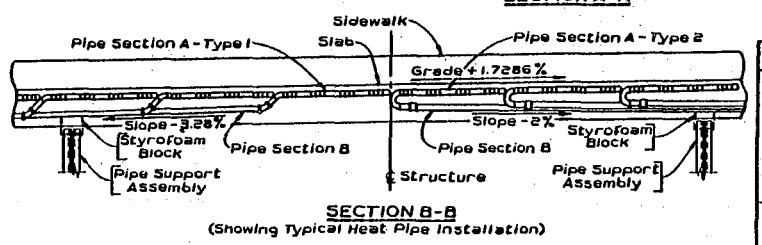
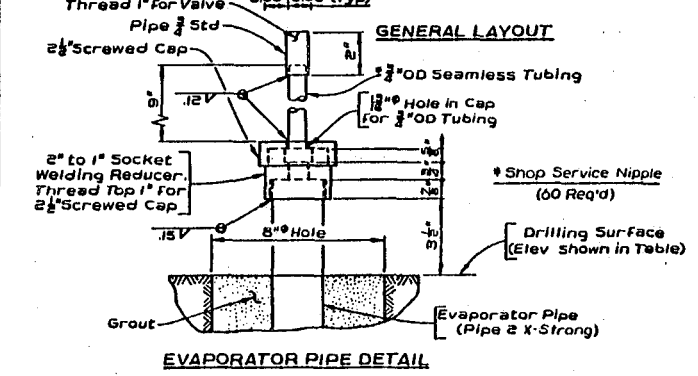


TABLE OF HOLE LOCATIONS & ELEVATIONS

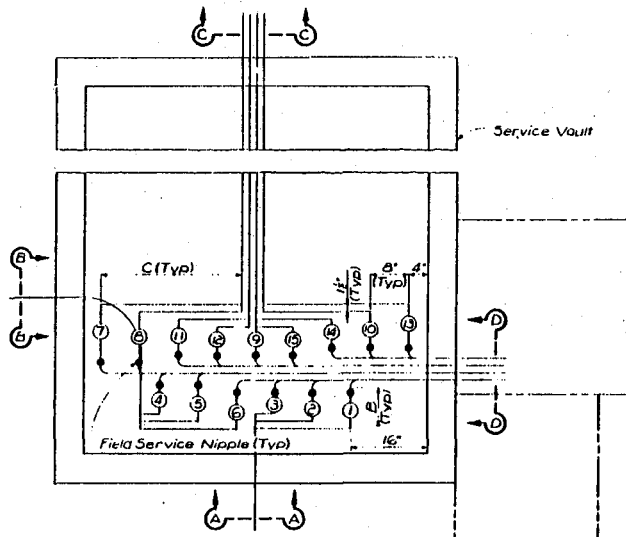
Location	Corner No. 1			Corner No. 2		
	Hole No.	Station	Offset	Elevation	Station	Offset
1	67+76.50	34.00'	117.00	67+76.50	34.00'	117.00
2	67+86.50	34.00'	117.00	67+86.50	34.00'	117.00
3	67+96.50	34.00'	117.00	67+96.50	34.00'	117.00
4	67+71.50	42.66'	117.00	67+71.50	42.66'	117.00
5	67+81.50	42.66'	117.00	67+81.50	42.66'	117.00
6	67+91.50	42.66'	117.00	67+91.50	42.66'	117.00
7	67+76.50	51.32'	115.50	67+76.50	51.32'	116.00
8	67+86.50	51.32'	115.50	67+86.50	51.32'	116.00
9	67+96.50	51.32'	115.50	67+96.50	51.32'	116.00
10	68+06.50	51.32'	108.00	68+06.50	51.32'	112.50
11	67+81.50	59.98'	111.00	67+81.50	59.98'	116.00
12	67+91.50	59.98'	111.00	67+91.50	59.98'	116.00
13	68+01.50	59.98'	108.50	68+01.50	59.98'	116.00
14	67+86.50	68.64'	109.00	67+86.50	68.64'	116.00
15	67+96.50	68.64'	109.00	67+96.50	68.64'	116.00
Location	Corner No. 3			Corner No. 4		
	Hole No.	Station	Offset	Elevation	Station	Offset
1	68+89.50	34.00'	118.50	68+89.50	34.00'	118.50
2	68+79.50	34.00'	118.50	68+79.50	34.00'	118.50
3	68+69.50	34.00'	118.50	68+69.50	34.00'	118.50
4	68+89.50	42.66'	118.50	68+89.50	42.66'	118.50
5	68+79.50	42.66'	118.50	68+79.50	42.66'	118.50
6	68+69.50	42.66'	118.50	68+69.50	42.66'	118.50
7	68+89.50	51.32'	110.00	68+89.50	51.32'	114.50
8	68+79.50	51.32'	110.00	68+79.50	51.32'	114.50
9	68+69.50	51.32'	106.50	68+69.50	51.32'	110.00
10	68+59.50	59.98'	110.00	68+59.50	59.98'	114.50
11	68+79.50	59.98'	110.00	68+79.50	59.98'	114.50
12	68+69.50	59.98'	107.50	68+69.50	59.98'	114.50
13	68+59.50	68.64'	107.50	68+59.50	68.64'	114.50
14	68+79.50	68.64'	107.50	68+79.50	68.64'	114.50
15	68+69.50	68.64'	107.50	68+69.50	68.64'	114.50



Note: 1) The heat pipe system fabricator shall label all heat pipes with the pipe number, section and corner.  
2) Offsets are measured left of center line survey for Corners No. 1 and 3 and right of center line survey for Corners No. 2 and 4.  
3) Evaporator holes 11-15, Corner Nos. 1 and 3, fall beneath the detour fill.

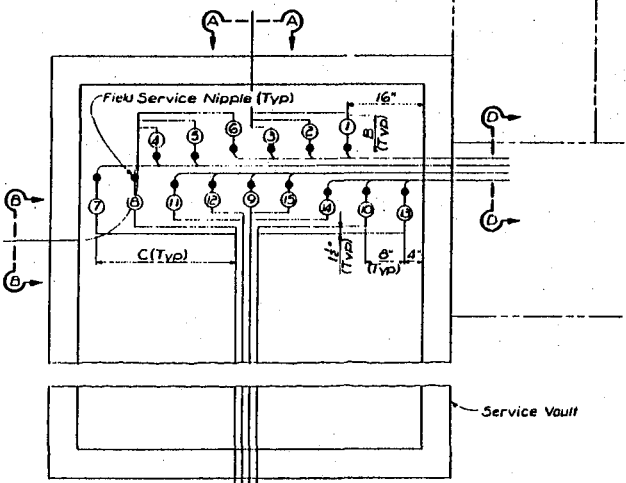


REVISIONS		WYOMING HIGHWAY DEPARTMENT BRIDGE DIVISION	
		HEAT PIPE SYSTEM DETAILS	
		BRIDGE OVER SPRING CREEK	
		STA 68+30	
		Laramie - Interstate 80	
		(Grana Ave Exit)	
		BRM-421(6) AI	
APPROVED DATE 5/1/80	DESIGN DIV. / RLE DETAIL MHS / DIV CS	Design Section Divng No. 5111	BPCollins Sheet 7 of 21

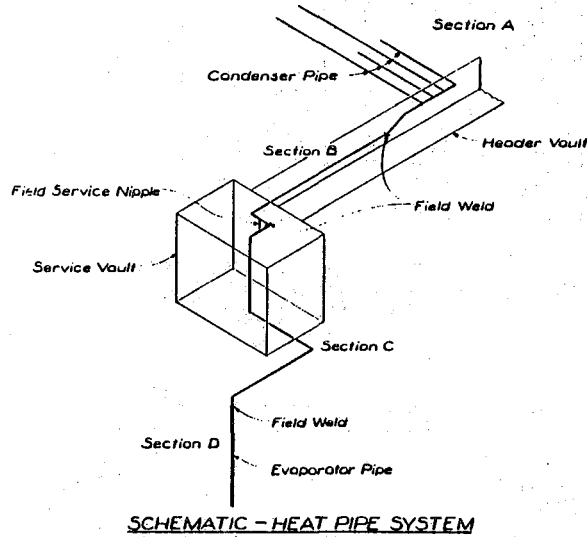


PLAN OF CORNER NO. 1 & 4  
(Showing Pipe Layout)

RF Abut

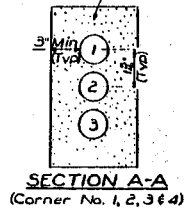


PLAN OF CORNER NO. 2 & 3  
(Showing Pipe Layout)

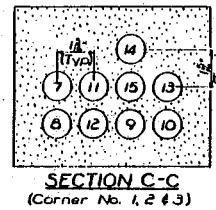


SCHEMATIC - HEAT PIPE SYSTEM

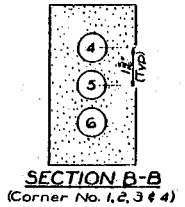
Foam in Place  
(Insulation (Typ))



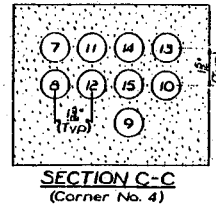
SECTION A-A  
(Corner No. 1, 2, 3 & 4)



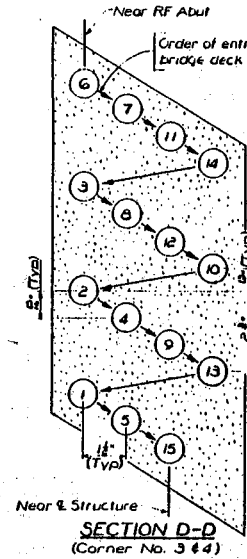
SECTION C-C  
(Corner No. 1, 2 & 3)



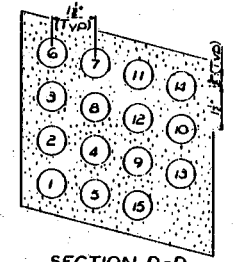
SECTION B-B  
(Corner No. 1, 2, 3 & 4)



SECTION C-C  
(Corner No. 4)



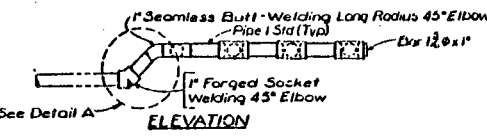
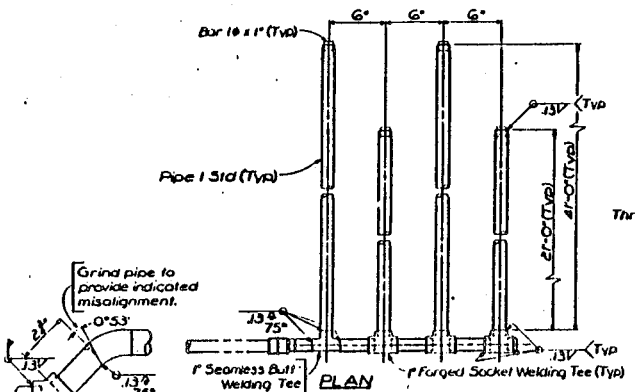
SECTION D-D  
(Corner No. 3 & 4)



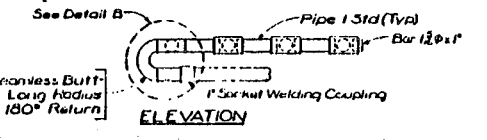
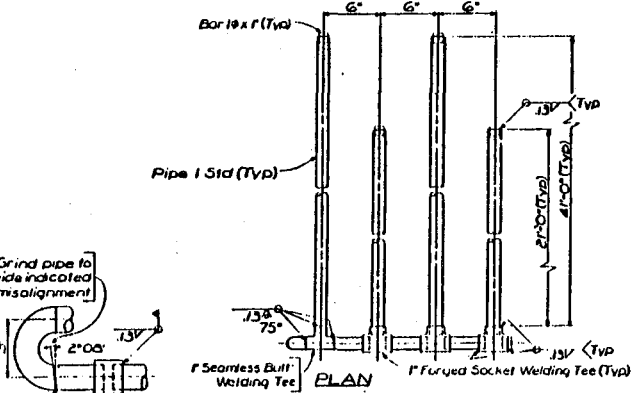
SECTION D-D  
(Corner No. 1 & 2)

- Notes:
- 1) Pipe numbers correspond to Hole numbers shown on Sheet No. 2.
  - 2) See Sheet No. 15 for Corner locations.
  - 3) See Sheet No. 9 for Field Service Nipple details.
  - 4) The connection between Sections B and C on Pipe No. 14 Corner Nos 1 and 2, Pipe Nos 8, 10 and 12 Corner No. 3 and Pipe No. 8 Corner No. 4 shall not be welded by the contractor.
  - 5) Sections B and C, the portion of Section A outside of the deck and the portion of Section D above the drilling surface shall be surrounded by 3 inches (min) of foam in place insulation after heat pipes are assembled.
  - 6) Section C shall be supported by 3 inch styrofoam blocks at intervals not to exceed 10 feet.
  - 7) See Sheet No. 9 for Dim B and Sheet Nos 10 and 11 for Dim C.

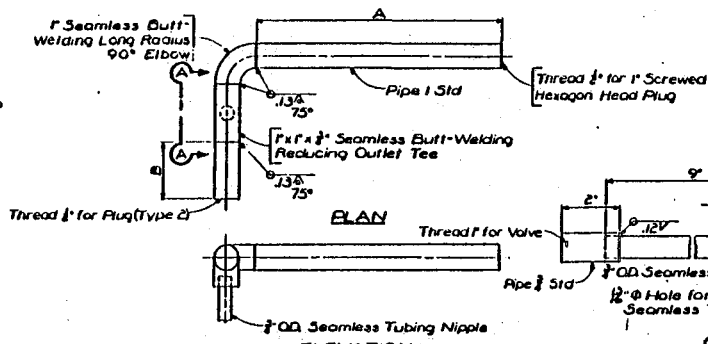
WYOMING HIGHWAY DEPARTMENT BRIDGE DIVISION			
<b>HEAT PIPE SYSTEM DETAILS</b>			
<b>BRIDGE OVER SPRING CREEK</b>			
STA 68+30			
Laramie - Interstate 80			
(Grand Ave Exit)			
BRM-4211(c) AI			
APPROVED	DESIGN DIV, RLP	Design Section	B P Collins
DATE	04/14/03	DETAIL DIV, DEW	
	5/17/03	Drawn By	03
		Draw No.	5111
			Sheet B of 21



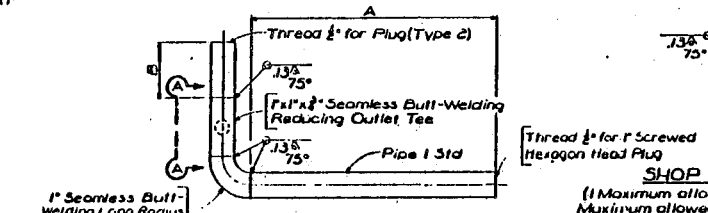
**PIPE SECTION A DETAILS - TYPE 1**  
(15 Req'd - Right Hand Side)  
(15 Req'd - Left Hand Side)



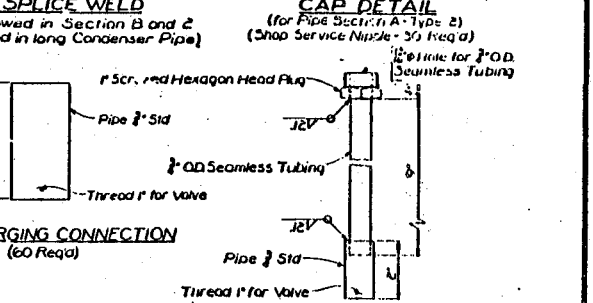
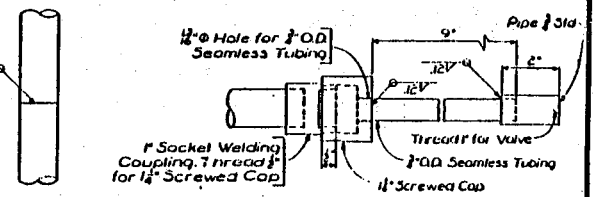
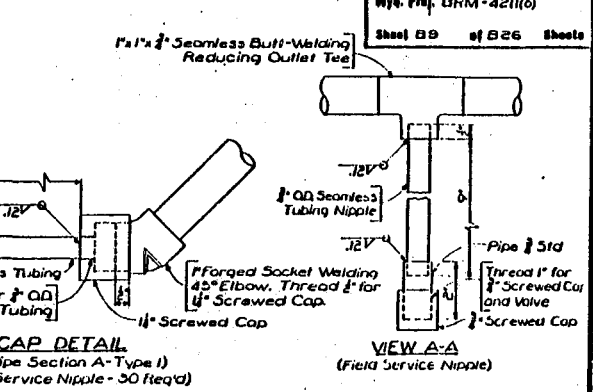
**PIPE SECTION A DETAILS - TYPE 2**  
(15 Req'd - Right Hand Side)  
(15 Req'd - Left Hand Side)



**PIPE SECTION B DETAILS**  
PIPE NO. 1 THRU 6 - CORNER NO. 1 & 4  
PIPE NO. 7 THRU 15 - CORNER NO. 2 & 3



**PIPE SECTION B DETAILS**  
PIPE NO. 1 THRU 6 - CORNER NO. 2 & 3  
PIPE NO. 7 THRU 15 - CORNER NO. 1 & 4



Pipe No.	Corner No. 1 & 2		Corner No. 3 & 4	
	A	B	A	B
1	25'-5 1/2"	41'	27'-4 1/2"	42'
2	26'-0 1/2"	3'	20'-0 1/2"	3'
3	10'-0 1/2"	11'	12'-6 1/2"	11'
4	26'-0 1/2"	31'	24'-5 1/2"	31'
5	30'-1 1/2"	5'	33'-0 1/2"	5'
6	3'-3 1/2"	5'	5'-4 1/2"	5'
7	7'-1 1/2"	9'	9'-4 1/2"	9'
8	17'-1 1/2"	71'	17'-1 1/2"	71'-7 1/2"
9	2'-1 1/2"	18'	2'-1 1/2"	18'
10	11'-1 1/2"	41'	17'-1 1/2"	41'
11	11'-1 1/2"	41'	17'-1 1/2"	41'
12	11'-1 1/2"	41'	17'-1 1/2"	41'
13	5'-1 1/2"	6'	5'-1 1/2"	6'
14	11'-1 1/2"	41'	17'-1 1/2"	41'
15	11'-1 1/2"	41'	17'-1 1/2"	41'

REVISIONS		HEAT PIPE SYSTEM DETAILS	
1	Added 1'-6" to dimensions A, Corner No. 3 & 4.	BRIDGE OVER SPRING CREEK	
2	7-17-00 HSM	STA 65+30	
		Laramie-Interstate 40	
		(Grand Ave Exit)	
WYOMING HIGHWAY DEPARTMENT BRIDGE DIVISION		HEAT PIPE SYSTEM DETAILS	
APPROVED		DESIGNER: J. L. F. / 11/11/00	
DRAWN: J. L. F. / 11/11/00		DESIGN SECTION: J. L. F. / 11/11/00	
DATE: 11/11/00		DRAWING NO.: 111	
		SHEET 89 OF 826	

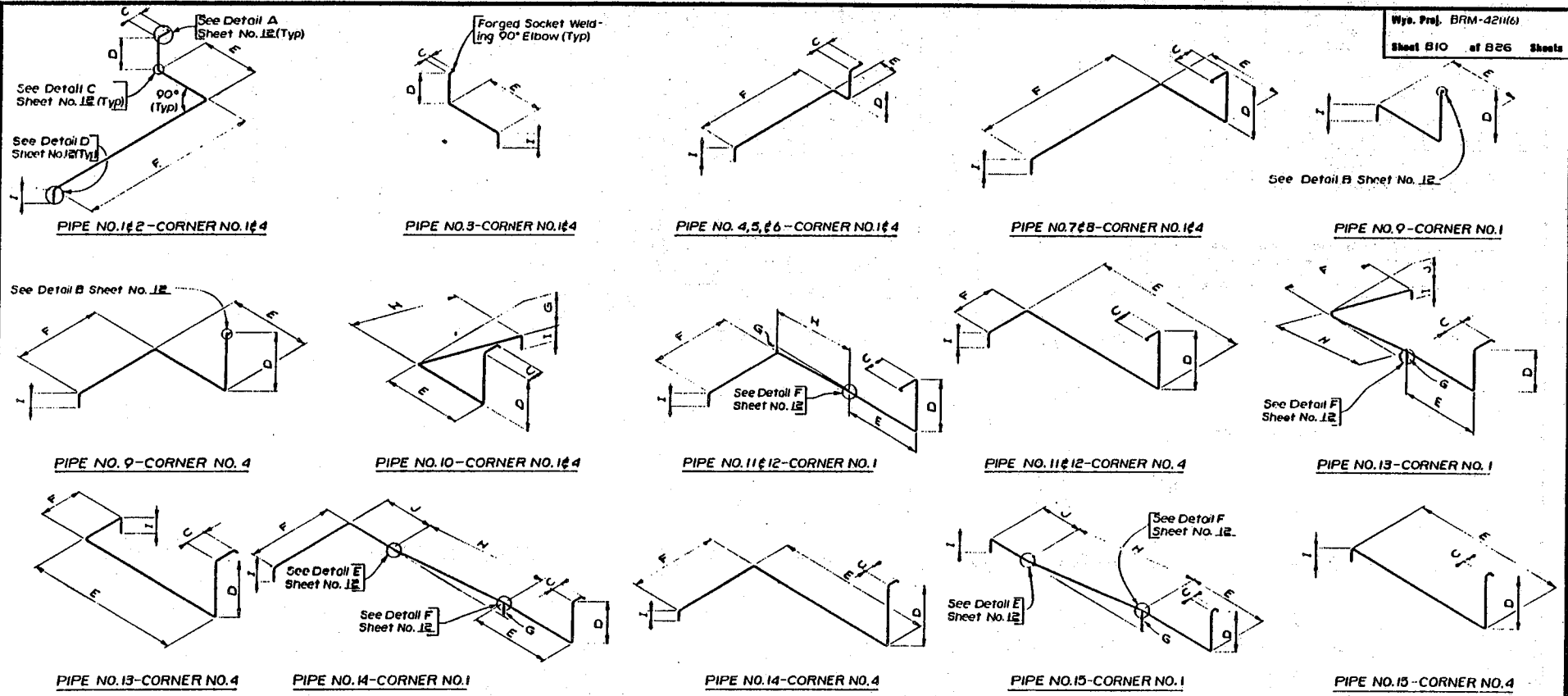


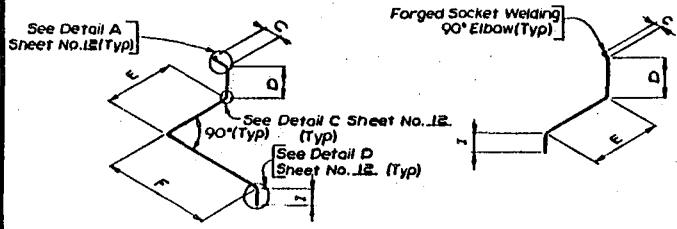
**TABLE OF DIMENSIONS**

Location Pipe	Corner No. 1							Corner No. 4							
	C	D	E	F	G	H	I	J	C	D	E	F	G	H	I
1	1'-5 1/2"	3'-3 3/8"	6'-5 3/8"	20'-0 1/2"			1'-6"		1'-5 1/2"	2'-3 3/8"	6'-5 3/8"	20'-0 1/2"			1'-6"
2	0'-8 1/2"	3'-6"	6'-6 3/8"	10'-0"			1'-7 1/2"		0'-8 1/2"	2'-8 1/2"	6'-6 3/8"	10'-0"			1'-7 1/2"
3	1'-8 1/2"	3'-8 3/8"	6'-8 3/8"				1'-8 3/8"		1'-8 1/2"	3'-1 1/8"	6'-8 3/8"				1'-8 3/8"
4	2"	3'-5 3/8"	2'-0"	23'-0"			1'-6"		2"	2'-6 3/8"	2'-0"	23'-0"			1'-6"
5	10"	3'-3 1/8"	2'-1 1/8"	13'-0"			1'-7 1/2"		10"	2'-3 1/8"	2'-1 1/8"	13'-0"			1'-7 1/2"
6	1'-6"	3'-0 3/8"	2'-3"	2'-11 3/8"			1'-8 3/8"		1'-6"	3'-4 3/8"	2'-3"	2'-11 3/8"			1'-8 3/8"
7	2'-3 3/8"	4'-0 3/8"	8'-9 3/8"	10'-9 3/8"			1'-7 1/2"		2'-3 3/8"	6'-9 3/8"	8'-9 3/8"	29'-9 3/8"			1'-6"
8	1'-7 3/8"	4'-10 3/8"	8'-10 3/8"	0'-9 3/8"			1'-8 3/8"		1'-7 3/8"	6'-7 3/8"	8'-10 3/8"	10'-9 3/8"			1'-7 3/8"
9		4'-10 3/8"	9'-5 3/8"				1'-10 3/8"			6'-5 3/8"	9'-3 3/8"	10'-0"			1'-8 3/8"
10	1'-5 3/8"	4'-10 3/8"	8'-10 3/8"		7'-10 1/2"	12'-7 1/2"	1'-6"		1'-8 3/8"	6'-6 3/8"	8'-10 3/8"		4'-11 3/8"	11'-0 3/8"	1'-6"
11	1'-0 3/8"	4'-10 3/8"	9'-0 3/8"	14'-10 3/8"	4'-8 3/8"	9'-10 3/8"	1'-6"		1'-0 3/8"	6'-6 3/8"	17'-8 3/8"	14'-10 3/8"			1'-7 1/2"
12	4 3/8"	4'-10 3/8"	9'-1 1/8"	4'-10 3/8"	4'-8 3/8"	9'-10 3/8"	1'-6"		4 3/8"	6'-6 3/8"	17'-9 3/8"	4'-10 3/8"			1'-8 3/8"
13	2'-4 3/8"	4'-8 3/8"	8'-9 3/8"	8'-11 3/8"	4'-8 3/8"	9'-10 3/8"	1'-6"	2'-9 3/8"	2'-4 3/8"	6'-11 3/8"	17'-5 3/8"	4'-10 3/8"			1'-9 3/8"
14	1'-1 1/8"	4'-0 3/8"	9'-0 3/8"	10'-0"	6'-9 3/8"	14'-3 3/8"	1'-6"	4'-0 3/8"	1'-1 1/8"	6'-8 3/8"	26'-4 3/8"	10'-0"			1'-6 3/8"
15	6 3/8"	4'-6 3/8"	9'-1 1/8"		6'-9 3/8"	14'-3 3/8"	1'-7 3/8"	4'-0 3/8"	5 3/8"	6'-0 3/8"	26'-5 3/8"				1'-7 3/8"

Note: 1) See Sheet No. 12. For Corner locations.  
 2) All Pipes are sloped at 2% towards dimension I unless otherwise shown.  
 3) Dimensions D, G, I and dimension J Pipe No. 13 Corner No. 1 are measured vertically. All other dimensions are measured along center line of pipe.

**SECTION C DETAILS CORNERS NO. 1 AND 4**

WYOMING HIGHWAY DEPARTMENT BRIDGE DIVISION	
<b>HEAT PIPE SYSTEM DETAILS</b>	
<b>BRIDGE OVER SPRING CREEK</b>	
STA 68+30	
Laramie - Interstate 80 (Grand Ave Exit)	
BRM-421(6) AI	
APPROVED [Signature]	DESIGN BY RLP DETAIL BY RLP MRS. [Signature]
DATE 5/17/60	Design Section BPC Collins Proj. No. 5111 Sheet 10 of 21



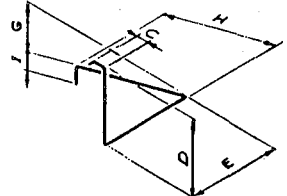
PIPE NO. 1 & 2 - CORNER NO. 2 & 3

PIPE NO. 3 - CORNER 2 & 3

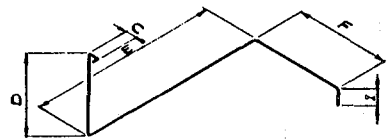
PIPE NO. 4, 5, & 6 - CORNER NO. 2 & 3

PIPE NO. 7 & 8 - CORNER NO. 2 & 3

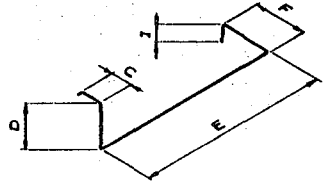
PIPE NO. 9 - CORNER NO. 2 & 3



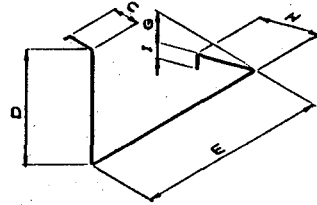
PIPE NO. 10 - CORNER NO. 2 & 3



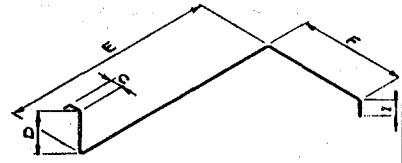
PIPE NO. 11 & 12 - CORNER NO. 2 & 3



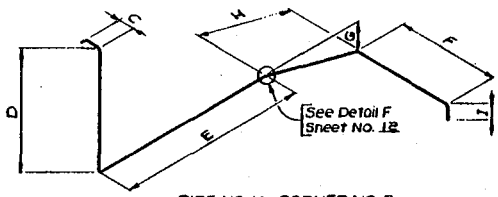
PIPE NO. 13 - CORNER NO. 2



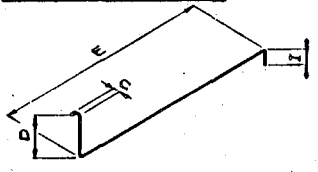
PIPE NO. 15 - CORNER NO. 3



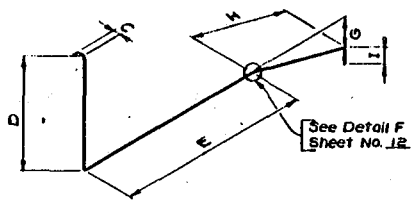
PIPE NO. 14 - CORNER NO. 2



PIPE NO. 14 - CORNER NO. 3



PIPE NO. 15 - CORNER NO. 2

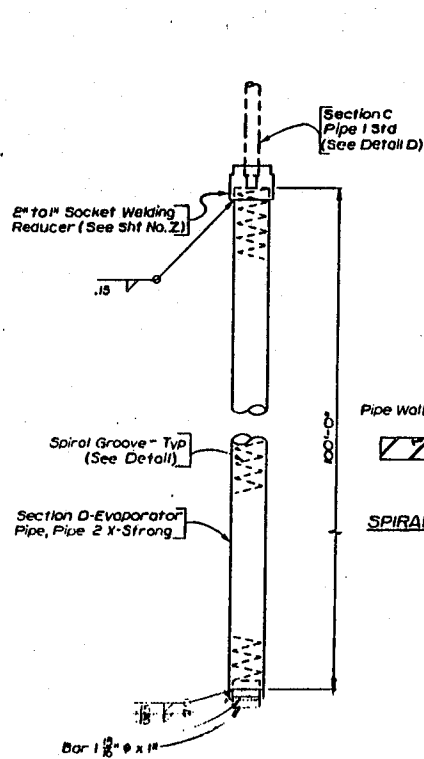


PIPE NO. 15 - CORNER NO. 3

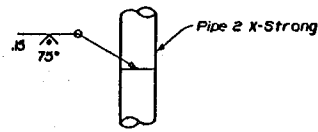
Location Pipe No.	Corner No. 2							Corner No. 3						
	C	D	E	F	G	H	I	C	D	E	F	G	H	I
1	1'-5 3/8"	3'-3 3/8"	6'-5 3/8"	20'-0 1/8"			1'-6"	1'-5 3/8"	2'-3 3/8"	6'-5 3/8"	20'-0 1/8"			1'-6"
2	9 1/8"	3'-6"	6'-6 3/8"	10'-0"			1'-7 1/8"	9 1/8"	2'-8 1/8"	6'-6 3/8"	10'-0"			1'-7 1/8"
3	1 1/8"	3'-8 3/8"	6'-8 3/8"				1'-8 3/8"	1 1/8"	3'-1 1/8"	6'-8 3/8"				1'-8 3/8"
4	2"	3'-3 1/2"	2'-0"	23'-0"				2"	2'-6 1/2"	2'-0"	23'-0"			1'-6"
5	10"	3'-5 3/8"	2'-1 1/2"	13'-0"			1'-7 1/8"	10"	2'-3 3/8"	2'-1 1/2"	13'-0"			1'-7 1/8"
6	1'-6"	3'-9 1/8"	2'-3"	2'-11 3/8"			1'-8 3/8"	1'-6"	3'-4 3/8"	2'-3"	2'-11 3/8"			1'-8 3/8"
7	2'-3 3/8"	4'-3 3/8"	8'-0"	19'-9 3/8"			1'-7 1/8"	2'-3 3/8"	11'-5 3/8"	8'-0"	19'-9 3/8"			1'-5 7/8"
8	1'-7 3/8"	4'-4 3/8"	8'-10 3/8"	0'-9 3/8"			1'-8 3/8"	1'-7 3/8"	11'-3 3/8"	8'-10 3/8"	0'-9 3/8"			1'-6 3/8"
9		4'-4 3/8"	9'-3 3/8"				1'-10 1/2"		11'-1 3/8"	9'-3 3/8"				1'-9 1/2"
10	1'-8 3/8"	4'-4 3/8"	8'-10 3/8"		3'-10 1/2"	10'-7 1/8"	1'-6"	1'-8 3/8"	11'-2 3/8"	8'-10 3/8"		3'-10 1/2"	10'-7 1/8"	1'-6"
11	1'-0 3/8"	4'-4 3/8"	17'-8 3/8"	14'-10 3/8"			1'-6 3/8"	1'-0 3/8"	11'-5 3/8"	17'-8 3/8"	14'-10 3/8"			1'-4 3/8"
12	4 3/8"	4'-4 3/8"	17'-9 3/8"	4'-10 3/8"			1'-7 1/8"	4 3/8"	11'-3 1/8"	17'-9 3/8"	4'-10 3/8"			1'-6"
13	2'-4 3/8"	4'-2 3/8"	17'-5 3/8"	4'-10 3/8"			1'-8 3/8"	2'-4 3/8"	10'-10"	17'-5 3/8"	4'-10 3/8"			1'-6"
14	1'-1 3/8"	4'-3 3/8"	26'-4 3/8"	10'-0"			1'-6 3/8"	1'-1 3/8"	11'-3 3/8"	17'-8 3/8"	10'-0"			1'-6"
15	5 1/8"	4'-0 3/8"	20'-5 1/8"				1'-7 3/8"	5 1/8"	10'-7 3/8"	17'-9 3/8"				1'-7 1/8"

NOTE: 1) See Sheet No. 15 For Corner location.  
2) All pipes are sloped at 2% toward dimension I unless otherwise shown.  
3) Dimensions D, G, and I are measured vertically. All other dimensions are measured along center line of pipe.

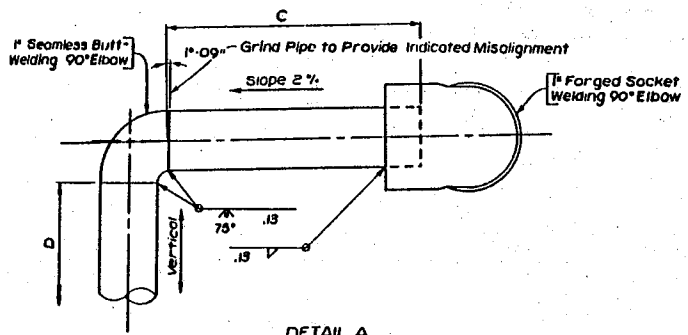
SECTION C DETAILS CORNERS NO. 2 AND 3			
WYOMING HIGHWAY DEPARTMENT BRIDGE DIVISION			
HEAT PIPE SYSTEM DETAILS			
BRIDGE OVER SPRING CREEK			
STA 68+30			
Laramie - Interstate 80			
(Grand Ave Exit)			
BRM-421(A) AI			
APPROVED	DESIGN	BY / RLD	Design Section BPCollins
5/1/76	5/1/76	MHS / UIC	Draw. No. 5111
			Sheet 11 of 21



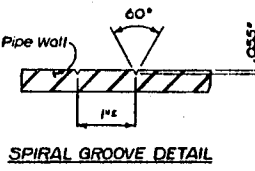
**SECTION D-EVAPORATOR PIPE DETAIL**  
 (60 Required)



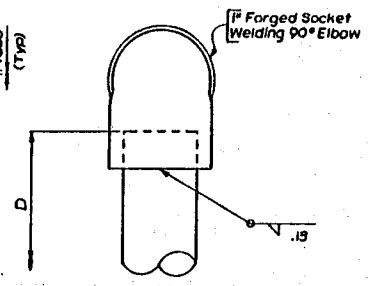
**SHOP SPLICE WELD**  
 (5 Maximum allowed per Evaporator Pipe)



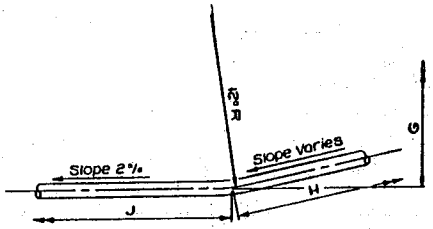
**DETAIL A**



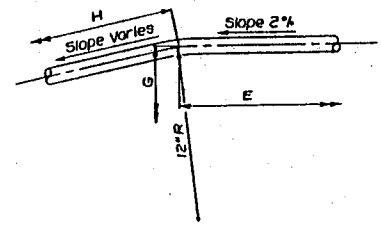
**SPIRAL GROOVE DETAIL**



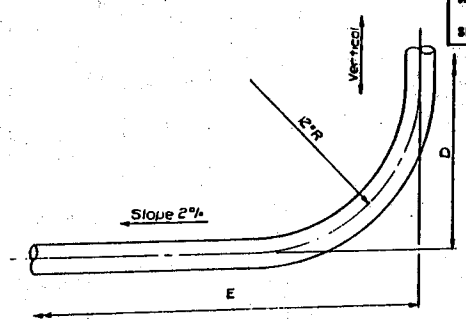
**DETAIL B**



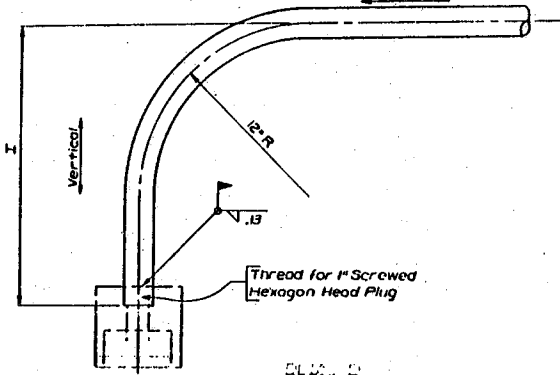
**DETAIL E**



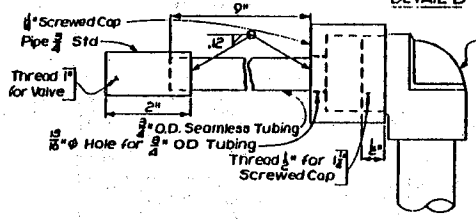
**DETAIL F**



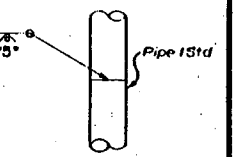
**DETAIL C**



**DETAIL D**



**CAP DETAIL**



**SHOP SPLICE WELD**  
 (May be located in Section C at least 1' apart not in areas to be bent.)

Note: 1) See Sheet No. 10 and 11 for location of Details A, B, C, D, E and F.  
 \* 2) Shop Service Nipple for Section C - 60 Req'd.

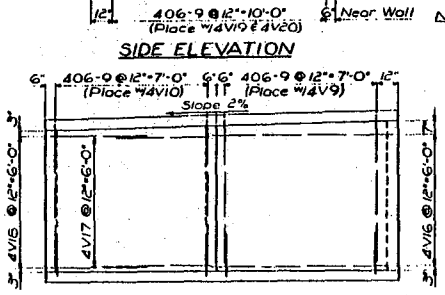
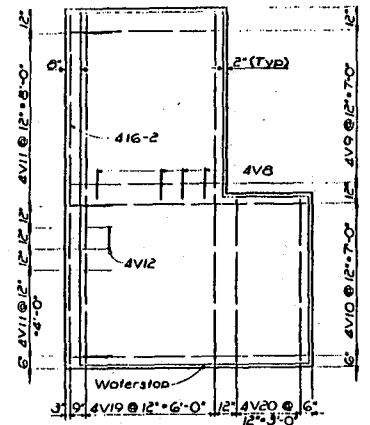
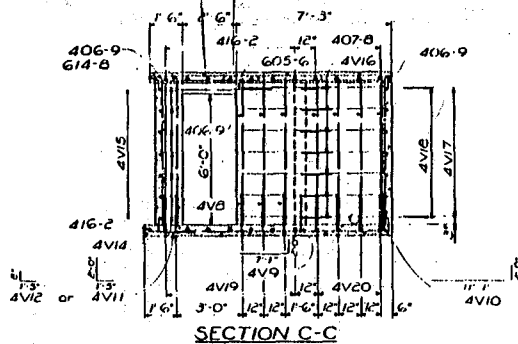
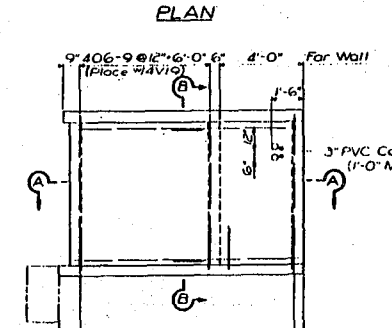
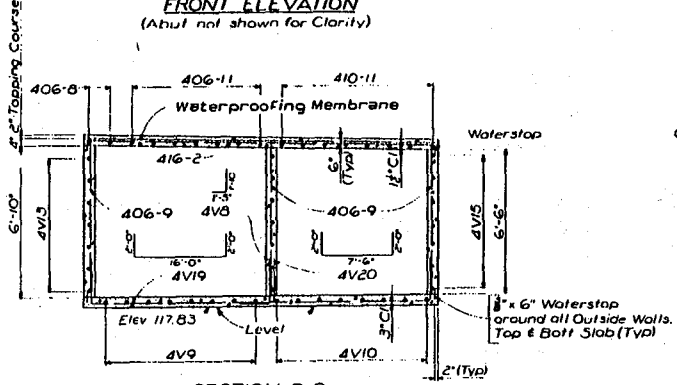
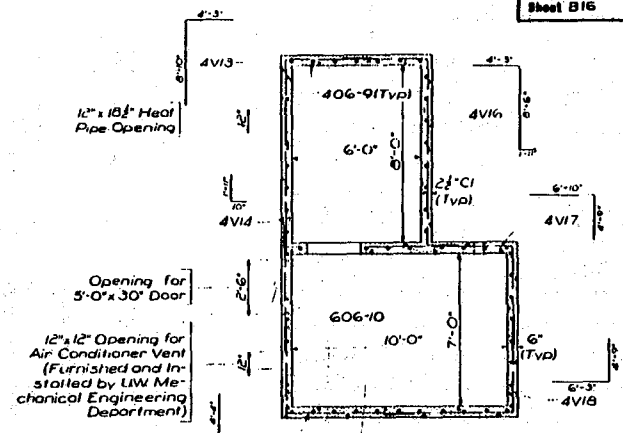
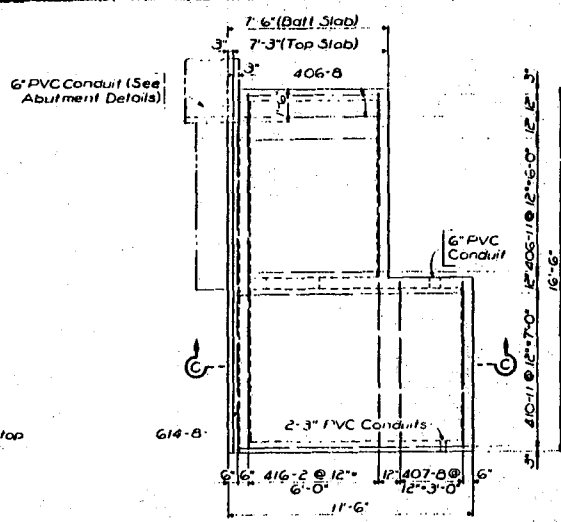
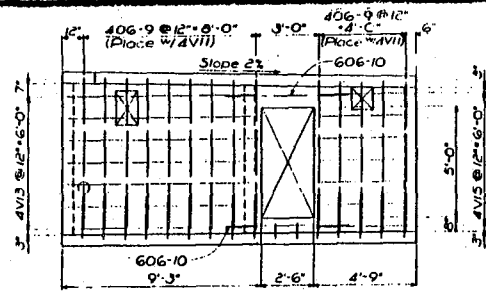
**SECTION C AND D DETAILS**

REVISIONS		WYOMING HIGHWAY DEPARTMENT BRIDGE DIVISION	
		<b>HEAT PIPE SYSTEM DETAILS</b>	
		<b>BRIDGE OVER SPRING CREEK</b>	
		STA 68+30	
		Laramie-Interstate 80 (Grand Ave Exit)	
		BRM-4211(b)	AI
APPROVED	DESIGN	DETAIL	DATE
	DJW, RLP	MLB, DJS	2/17/80
	Design Section B Collins	Drawn by GIB	Sheet 12 of 21







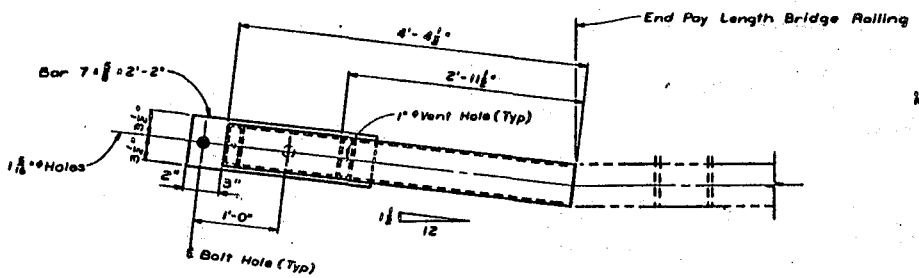


- Notes:**
- 1) Door frame assembly shall be in place prior to placing concrete in walls.
  - 2) Lap 4V15 bars with 4V19 and 606-10 bars, 4V13 bars with 4V14 and 4V16 bars, 4V17 bars with 4V16 and 4V18 bars, 4V18 bars with 4V15 bars, and 605-6 bars with 4V17 bars 1'-11". Lap 406-9 bars with 4V9, 4V10, 4V11, 4V12, 4V19, 4V20 and 4V8 bars, 4V11 bars with 4V9 and 4V10 bars, 4V12 bars with 4V10 bars, and 4V8 bars with 4V19 bars 1'-5".
  - 3) The reinforcing steel fabricator shall prefix all bar marks for Service Vault and Instrumentation Hut with the numeral 7.
  - 4) Reinforcing steel may be cut as directed by the Engineer to allow placing conduits and blocking out Heat Pipe Opening and Air Conditioner Vent Opening.
  - 5) The estimated quantity of Class B Concrete for the Service Vault and Instrumentation Hut is 12.4 CY.
  - 6) Use styrofoam block-outs around heat pipes.

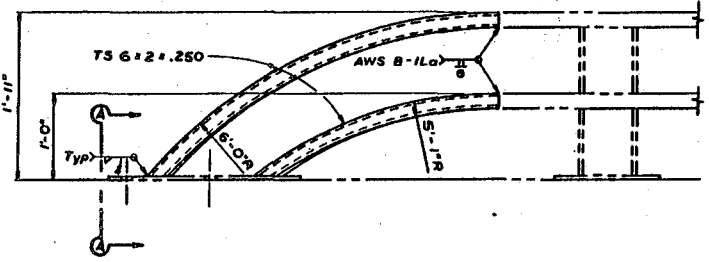
WYOMING HIGHWAY DEPARTMENT BRIDGE DIVISION			
REVISIONS	SERVICE VAULT & INSTRUMENTATION HUT BRIDGE OVER SPRING CREEK STA 68+30 Laramie Inter State 80 (Grand Ave Exit)		
	BRM-421(6)		AI
APPROVED DATE 2/17/80	DESIGN BY JRM DETAIL BY MAM, BLM GS, KHB, HMC	Design Section BPCollins Draw No. 5111	Sheet 16 of 21



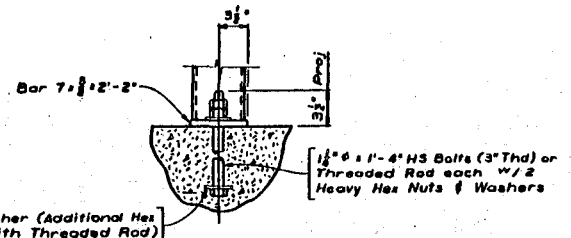




PLAN

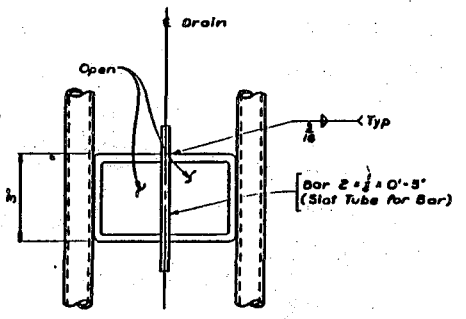


ELEVATION

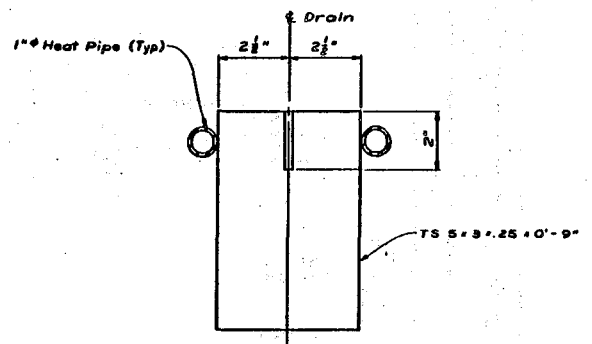


SECTION A-A

END ANCHORAGE DETAILS

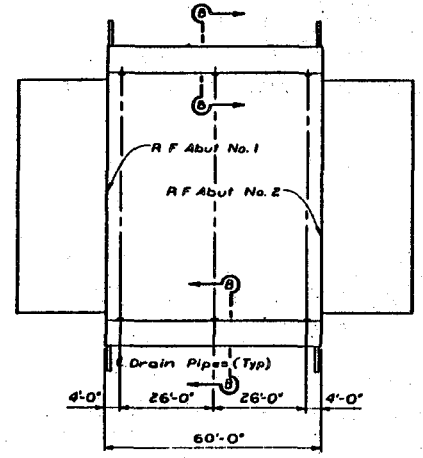


PLAN

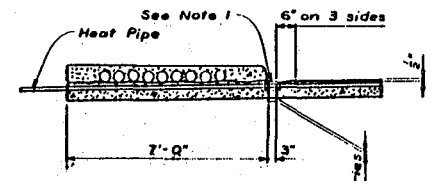


ELEVATION

DRAIN PIPE DETAILS  
(6 Required)



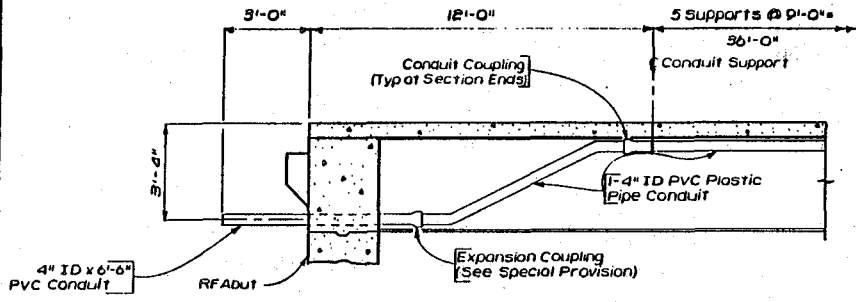
PLAN



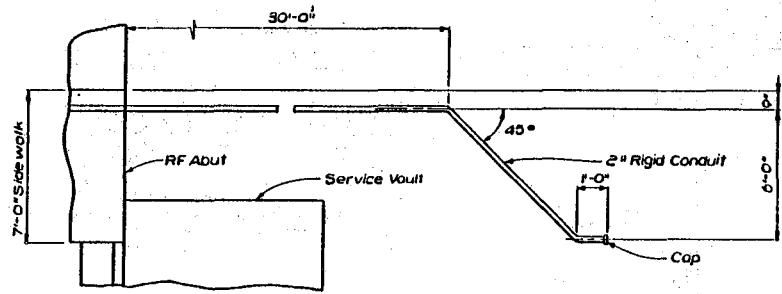
SECTION B-B

- Notes:**
- 1) Drain pipe shall be placed between adjacent heat pipes and shall be fastened securely to the heat pipes using tie wire.
  - 2) All rough edges on rails shall be ground smooth.
  - 3) Drain pipes shall be galvanized in accordance with Subsection 501.43 of the Specifications.
  - 4) Approach railing, including end anchorages shall be considered subsidiary to the Contract Bid Item Bridge Railing.
  - 5) Deck reinforcing shall be cut to clear drain pipes.

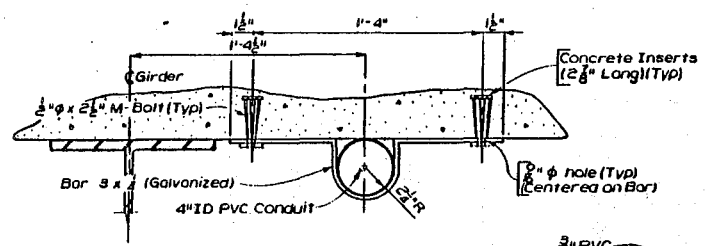
WYOMING HIGHWAY DEPARTMENT BRIDGE DIVISION			
<b>RAILING &amp; DRAIN PIPE DETAILS</b>			
<b>BRIDGE OVER SPRING CREEK</b>			
<b>STA 68 + 30</b>			
<b>Laramie - Interstate Bp</b>			
<b>(Grand Ave Exit)</b>			
BRM-4211 (6)			A1
DESIGNED BY JWW, MTC	DESIGN CHECKED BY JWW, MTC	Design Section B P. Collins	
Sheet B19 of 626		Draw No. 5111	Sheet 19 of 21



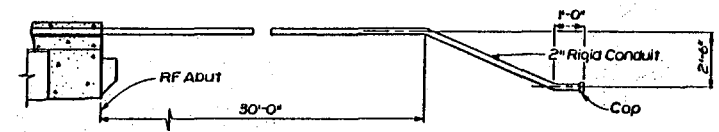
CONDUIT PLACEMENT DETAIL



PLAN

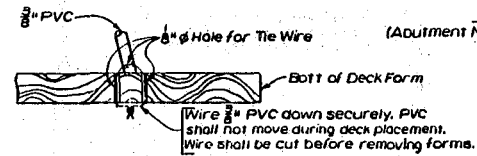


CONDUIT SUPPORT DETAIL  
 TELEPHONE CONDUIT DETAILS

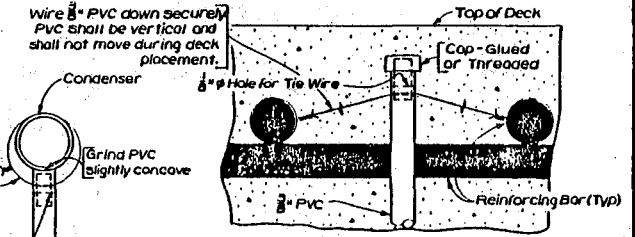


ELEVATION

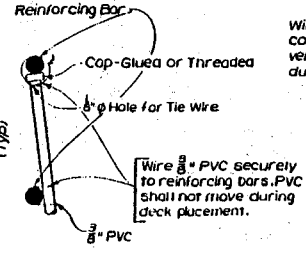
RIGID CONDUIT DETAILS  
 (Abutment No. 2 Shown - Abutment No. 1 Similar)



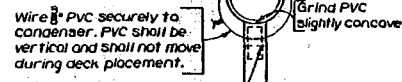
DETAIL A



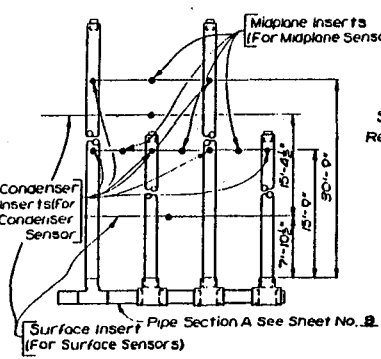
DETAIL D



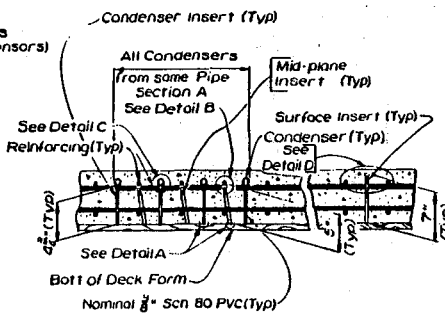
DETAIL B



DETAIL C



PLAN

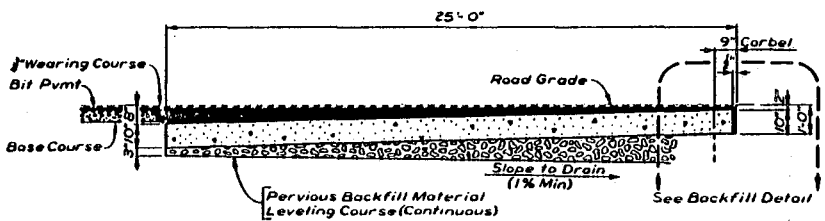
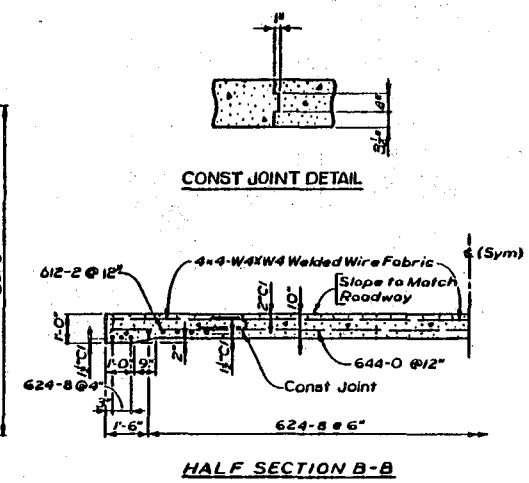
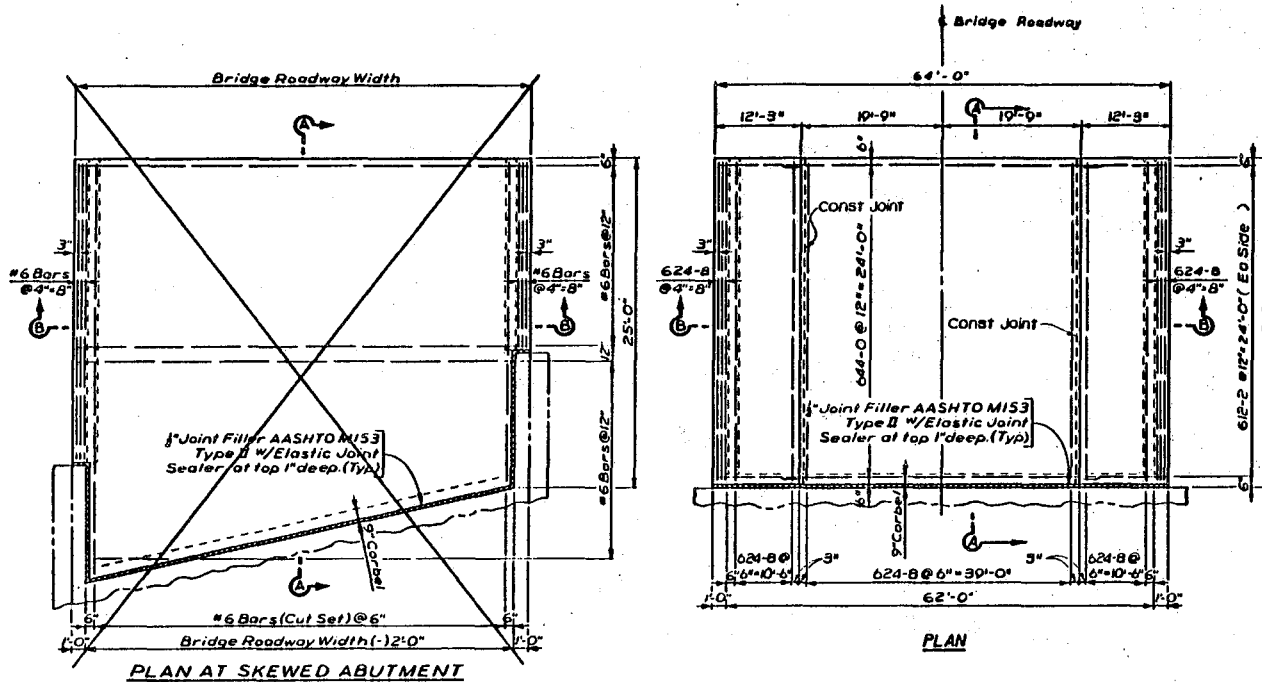


SECTION THRU SLAB

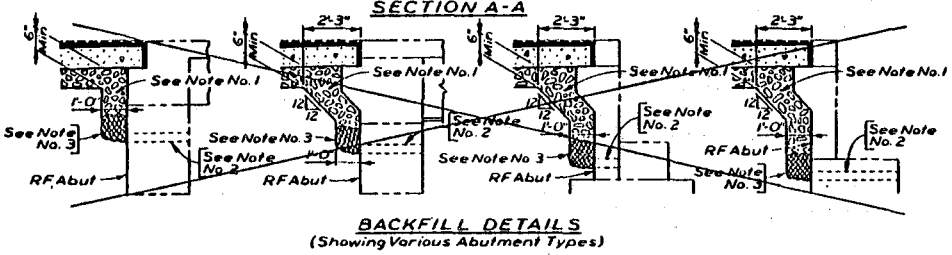
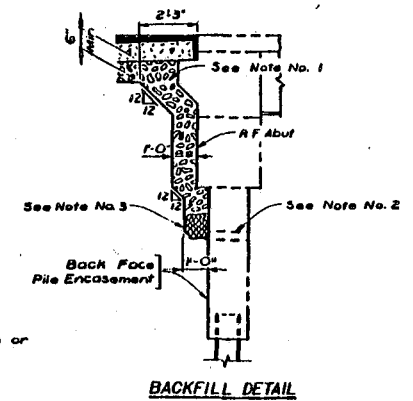
DECK INSTRUMENTATION DETAILS

Note: 1) Inserts shall be placed as shown along the condensers for Pipe No. 14 Corner No. 1, Pipe No. 12 Corner No. 3 and Pipe Nos 8 and 9 Corner No. 4.  
 2) Sensors will be supplied and installed by UW Mechanical Engineering Department.

WYOMING HIGHWAY DEPARTMENT BRIDGE DIVISION			
CONDUIT & DECK INSERT DETAILS			
BRIDGE OVER SPRING CREEK			
STA 68+30			
Oronie-Interstate 80			
(Grand Ave Exit)			
BRM-4211(6)		AI	
APPROVED	DESIGN	Design Section	B Collins
1/14/80	RHB / GJW	Draw No. 5111	Sheet 200 of 21
2/17/80	q's RHB / MHC		



- Note:**
- 1) Pervious backfill material shall be placed behind abutment, continuous underneath approach slab and sidewalks.
  - 2) For location of weep holes see Abutment Details.
  - 3) The weep hole assembly shall consist of Pipe 4 5/8 thru pile encasement, 6" x aluminum or galvanized steel wire 4 mesh hardware cloth (min wire diameter 0.03") anchored firmly to back face and one cu ft of coarse aggregate in a burlap sack, securely tied.
  - 4) No. 4 bars at 12" each way may be substituted for welded wire fabric, LQP 11-5".
  - 5) Approach slabs are required behind each abutment.
  - 6) Lap 612-2 bars with 644-0 bars 2'-2".
  - 7) The reinforcing steel fabricator shall prefix all approach slab bar marks with numerals as follows: B (at Abut No. 1), O (at Abut No. 2).
  - 8) The construction joints shall be used only if so directed by the Engineer.



REVISIONS		APPROACH SLAB DETAILS	
		<b>BRIDGE OVER SPRING CREEK</b>	
		STA 68 + 30	
		Laramie - Interstate 80	
		(Grand Ave Exit)	
		BRM - 4211(6) AI	
APPROVED	DESIGN	Design Section B P Calline	
DATE	BY	DATE	BY
5/17/88	JHL, MHS	03	MHS, JHJ
		Draw No. 5111	Sheet 21 of 21

**APPENDIX B**

**EXAMPLE SPECIAL PROVISIONS**

## 1. SPECIAL PROVISION FOR EXCAVATION FOR PAVEMENT HEATING SYSTEM

### DESCRIPTION

This work shall consist of all work necessary to excavate and backfill earth in the process of installing heat pipes for a pavement heating system.

### EXCAVATION AND BACKFILL

Some excavation may be necessary preparatory to boring holes for the heat pipes. Excavation shall also be necessary to construct the heat pipes at the locations shown on the plans. The Contractor shall establish a plan for excavating and backfilling, and shall obtain the agreement of the Engineer before proceeding.

It is anticipated that some dozer type of earth displacement will be necessary to level-up the hole locations for drilling operations. The excavation for construction of the heat pipes will be mainly backhoe type of excavation, with some handwork.

Backfilling operations shall not commence until the heat pipes have been constructed and accepted. The backfilling shall be to existing ground lines, to the extent practicable, outside the roadway embankment and to specified embankment slopes elsewhere. Compaction within the roadway embankment shall match that specified for the roadway embankment. Compaction outside the roadway embankment shall match the surrounding material.

Backfilling around the completed and insulated heat pipes shall be done with great care, so as not to displace the pipes or to damage the insulation. It is intended that all heat pipes up to the slab be buried

a minimum of 5' (1.5 m).

Where it is not possible to backfill around and beneath heat pipes, previous backfill material shall be used to bring the excavation up to grade, or as directed by the Engineer.

## 2. SPECIAL PROVISION FOR EVAPORATOR HOLES

### DESCRIPTION

This item shall consist of constructing evaporator holes as part of a pavement heating system.

### MATERIALS

The grout for the holes shall be a pumpable grout conforming to the following approximate proportions for a one yard batch:

658 lbs (296 kg) cement (7 sacks)

329 lbs (148 kg) water

1078 lbs (485 kg) aggregate

1924 lbs (866 kg) sand

This mix may be altered with approval from the Engineer.

Coarse aggregate shall be graded so that it is uniform in size at around 3/8 inches (10 mm) and shall otherwise conform to any COARSE AGGREGATE FOR CONCRETE Specification. Sand shall conform to the mortar requirements of any FINE AGGREGATE FOR CONCRETE Specification. The casing used to case the holes shall be a schedule 40 PVC conforming to ASTM D1785.

### CONSTRUCTION

The evaporator holes shall be bored to the depth indicated on the project plans.

The evaporator holes shall be 8" (205 mm) diameter holes. The holes shall be cased to the top of bedrock or as required, to prevent caving. The casing shall be 8" (205 mm) nominal diameter PVC casing. Therefore,

the holes shall be bored down to the top of bedrock with a sufficient diameter to get the casing down. These casings shall remain in place until the holes are grouted. The casings shall extend 1'± (.3 m%) above the ground. After the evaporator sections have been placed in the holes, the grout shall be placed.

The grout shall be mixed to a uniform consistency. The grout shall be placed by extending a grout tube, between the evaporator section and the side of the hole, to the bottom of the hole, forcing the grout into the hole in a continuous manner until grout comes out the top of the hole. The grout tube shall then be removed, and then the casing shall be removed. The evaporator hole shall then be topped off with grout. The evaporator section shall be braced so the top is in the middle of the hole. An alternate grout placement method may be utilized upon approval of the Engineer.

### 3. SPECIAL PROVISION FOR EPOXY COATING HEAT PIPES

#### DESCRIPTION

This item shall consist of furnishing the materials for, and placing an epoxy coating on steel pipes to be used in a pavement heating system.

#### MATERIALS

The epoxy coating material used to coat the steel pipes shall be one of the following products:

Scotchkote 202 or 213

CORVEL ECA - 1440

DK23-0679

An alternate product may be used, but only after the product has been approved by the State Bridge Engineer.

Once a product has been selected for use on a project, every effort shall be made to use only the said product on the project. If this cannot be accomplished feasibly, approval shall be obtained from the State Bridge Engineer prior to switching to another product, whether it be one of the products listed above or an alternate.

In addition to the coating material itself, patching or repair material shall be made available by the epoxy coating manufacturer. This material shall be compatible with the coating material and shall be inert in concrete. Additionally, the patching or repair material shall be suitable for use in the field by the Contractor installing the epoxy coated steel pipes.

### CONSTRUCTION

Only the heat pipe elements in the pavement slab shall be epoxy coated. Prior to coating, the surface of the steel pipes shall be blast cleaned in accordance with the Steel Structures Painting Council's Surface Preparation Specification SP 10-63T. The anchor pattern shall have a profile of 1.5-2.5 mils (0.04-0.06 mm). Any remaining raised slivers, scabs, laminations or bristles of steel shall be removed without burnishing or destroying the anchor pattern. In no instance shall the steel pipes be cleaned more than eight hours prior to coating.

The coating shall be applied as an electrostatically charged dry powder onto the grounded steel pipes, using electrostatic spray guns. The temperature of the pipes during coating and cure, as well as the duration of the cure and the method of quenching, shall be as specified by the coating manufacturer.

Great care shall be taken in handling, shipping, storing and placing the coated pipes to prevent damaging the coating. Handling and bundling systems shall be padded, or otherwise designed, to prevent damage to the coating. All bundles shall be lifted with a strong back, multiple supports, or a platform bridge to prevent sagging of the bundles and subsequent pipe-to-pipe abrasion. Pipes or bundles shall not be dropped or dragged and shall be stored above ground on wooden or padded supports.

Areas damaged during fabrication shall be patched or repaired as soon as practicable, using patching material as previously specified, and always prior to shipping. However, any pipe with a total damage area of two percent or more of the pipe surface area shall be deemed not

suitable for patching. The pipe may be cleaned and recoated.

Areas damaged during shipping shall be patched or repaired using material as previously specified. However, areas smaller than 1/4" x 1/4" (6 mm x 6 mm) need not be patched. If the sum of all damaged areas on any one pipe equals or exceeds two percent of the total surface area of the pipe, as determined by the Engineer, the pipe shall be rejected and replaced at the expense of the Contractor.

It shall be the ultimate responsibility of the Contractor to repair all damaged areas, regardless of the source of the damage. The Contractor, at his option, may use coated tie wire and support chairs to reduce installation damage. The coating used first shall be approved by the Engineer and shall be inert in concrete.

In all cases of damage repair, the damaged area(s) shall be thoroughly cleaned of all rust, oxidation, and other foreign material prior to patching or repairing.

#### SAMPLING, TESTING, AND CERTIFICATION

The Engineer shall be furnished with two 3'-6" (1065 mm) long samples of each pipe size coated. The samples shall be accompanied by certification stating the samples were taken directly from the coating run(s) for the steel pipes for the project. In addition, the Engineer shall be furnished with a certification for the coating material which properly identifies the batch and/or lot number(s), material, quantity of each batch, date of manufacture, name and address of the manufacturer, and a statement to the fact that the production pipes were coated with the material identified in the certification and that the

coating material is of the same composition and quality as that submitted by the manufacturer to the National Board of Standards or Valley Forge Laboratories for evaluation and testing.

The coated steel pipes shall be subjected to tests for thickness of coating, continuity of coating, and flexibility of coating. For purposes of testing the thickness and continuity of the epoxy coating, at least one sample shall be taken from each production run of twenty-five coated pipes. These tests shall be performed by the designated Engineer's Inspector at the place of coating application. The Engineer's Inspector shall have access to those areas of the coating plant dealing with surface preparation and coating at all times while work on the project is being performed. In addition, the coating applicator shall afford the Engineer's Inspector all reasonable facilities to satisfy that the coating is being furnished in accordance with these specifications.

Non-destructive coating thickness measurements shall be made in accordance with procedures defined in ASTM G12-72T with the following exceptions: 1) The thickness device shall be calibrated on a cleaned, but uncoated, steel pipe which is from the same lot and of the same size as the steel pipes being production coated. The cleaning process for the pipes used for calibrating shall be identical to that used for production pipes. A minimum of two calibration shims ranging in thickness from about three to fifteen mils (0.08 to 0.38 mm) shall be used to define the instrument calibration curve. 2) A single recorded thickness measurement shall be defined as the average of four individual tests taken evenly spaced along a one foot (0.3 m) length on both sides of the pipe under test. A minimum of five recorded measurements defined

above shall be obtained at equally spaced points along each test pipe. For acceptance purposes, thickness measurements shall not be permitted on patched areas of pipes, and all recorded coating film thickness measurements shall be five to nine mils (0.13 to 0.23 mm) after cure.

The coating shall be inspected visually after cure for continuity of coating and shall be free from holes, voids, contamination, cracks, and damaged areas. In addition, there shall be no more than an average of two holidays per linear foot (six per metre) on each test pipe when tested as herein specified. Patching may be utilized to comply with the holiday requirement, except that, in no case, shall the total pipe surface area covered by patching material exceed five percent. A holiday detector shall be used in accordance with the manufacturer's instructions to check the coating for holidays. The detector shall be 67-1/2 volts D.C. and may be either hand held or on line.

Flexibility of coating shall be evaluated by a bending test on at least one pipe of each size coated per eight-hour shift, but with a minimum of two tests per eight-hour shift. The coated pipe shall be bent 90 degrees (after rebound) over a mandrel. The bend shall be made at a uniform rate and may take up to one minute to complete. The diameter of the test mandrel shall be twelve times the nominal diameter of the pipe.

If there is evidence of cracking or disbonding of coatings to the naked eye, two additional test samples from different pipes shall be secured and tested, from the pipes previously coated on the day's shift. Evidence of cracking or disbonding on either of these two additional samples will be considered cause for rejection of the coated pipes represented by these samples.

Coated pipes that have been rejected may be repaired, or stripped and recoated, and again submitted for test and inspection. They shall conform to the requirements of these specifications; otherwise, the entire lot shall be rejected.

Visual inspection of coated pipes ready for shipment shall be made by the Engineer's Inspector to indicate conformity with the general requirements of these specifications. When inspection provides evidence to warrant rejection of a lot, the applicator may rearrange the lot and submit it once again for inspection.

#### 4. SPECIAL PROVISION FOR FABRICATION AND INSTALLATION OF HEAT PIPES

##### DESCRIPTION

This item shall consist of all the work necessary to fabricate and install the heat pipes for a pavement heating system.

##### MATERIALS

Except for the field and shop service nipples, the piping as shown on the project plans shall conform to ASTM A53, Type E, Grade B, or better, shall be used in the straight portions. Grade A shall be used in the bent portions. The pipe shall be black pipe with plain ends. The 1" (25 mm) and 3/4" (19 mm) pipe shall be schedule 40, and the 1 1/2" (38 mm) pipe shall be schedule 80. The pipe may be furnished in random lengths, but shall be epoxy coated in lengths of approximately 40' (12.2 m). The 3/4" (19mm) OD seamless tubing in the field and shop service nipples shall be ASTM A179, or better, crimpable tubing. The tubing shall have a 16 gage (U.S. Standard) wall thickness.

The associated pipe fittings shall be American Standard, or equivalent, schedule 40 fittings, compatible with the pipe supplied. The bar stock used for pipe plugs and service nipples shall conform to ASTM A36 or to an approved alternate.

The valves used in the testing, backfilling, and charging shall be stainless steel vacuum type valves. The valves shall remain the property of the fabricator and/or installer.

##### SHOP DRAWINGS

Shop drawings shall be required.

CONSTRUCTION

SHOP FABRICATION: It is suggested that the heat pipe fabrication to be done in-shop should proceed according to the following general sequence:

1. Coat pipes with epoxy coating. (See Special Provision for Epoxy Coating Heat Pipes.)
2. Make joint preparations for indicated welds and splice welds as required.
3. Fabricate service nipples and bore for spiral groove.
4. Clean the pipe lengths.
5. Weld the pipe into heat pipe sections.
6. Cap and/or plug the sections as indicated.
7. Evacuate individual sections and test the welds and the caps and/or plugs.
8. Backfill the individual sections with dry nitrogen and crimp for shipment.

It is suggested that the pipe be ordered in approximately 40' (12.2 m) lengths. It shall be permissible to order the pipe in random lengths and splice the lengths into approximately 40' (12.2 m) lengths prior to epoxy coating. The splices shall be left uncoated for subsequent testing. It will not be necessary to coat the material to be used in the shop and field service nipples.

The weld joint preparation shall be as shown on the project plans. As part of the weld joint preparation, care shall be taken that welds are not made over epoxy coating. Pipe ends where welds are to be made shall be thoroughly cleaned for a length of 1 1/2" (38 mm) of all epoxy coating and other weld contaminants prior to welding and/or shipping to the job site.

As shown on the project plans, the evaporator sections shall be bored to provide a spiral groove. The groove shall be bored in individual pipe lengths prior to connecting the lengths into a completed evaporator section. The groove shall be continuous within each pipe length, but need not be continuous from one length to the next.

Before fabricating the prepared lengths of pipe and the prepared hardware into a heat pipe section, all surfaces of the aforementioned components that will comprise the inner surface of a heat pipe section shall receive a thorough cleaning.

Immediately after cleaning, the components shall be fabricated into a complete heat pipe section, which shall then be evacuated, tested, backfilled with dry nitrogen, and sealed for shipping. Any delay in doing so may allow the formation of rust on the interior of the components and necessitate recleaning.

The initial or root pass on the welds shall be a full penetration inert gas weld made without flux. The subsequent passes, when necessary, may be made using any conventional technique. The welds shall be made while flowing an inert gas past the interior of the weld, as a purge.

A method that has worked successfully for evacuating, testing and backfilling heat pipe sections is as follows:

- A. The component was plumbed to a vacuum system as shown in Figure B.1.
- B. The component was evacuated to  $5 \times 10^{-5}$  torr or less. (Heating of the component may promote outgassing.)
- C. With valve #1 closed and valves #2 and #3 open, the outside of each weld was flooded with acetone and the vacuum gauge monitored for indication of leaking.

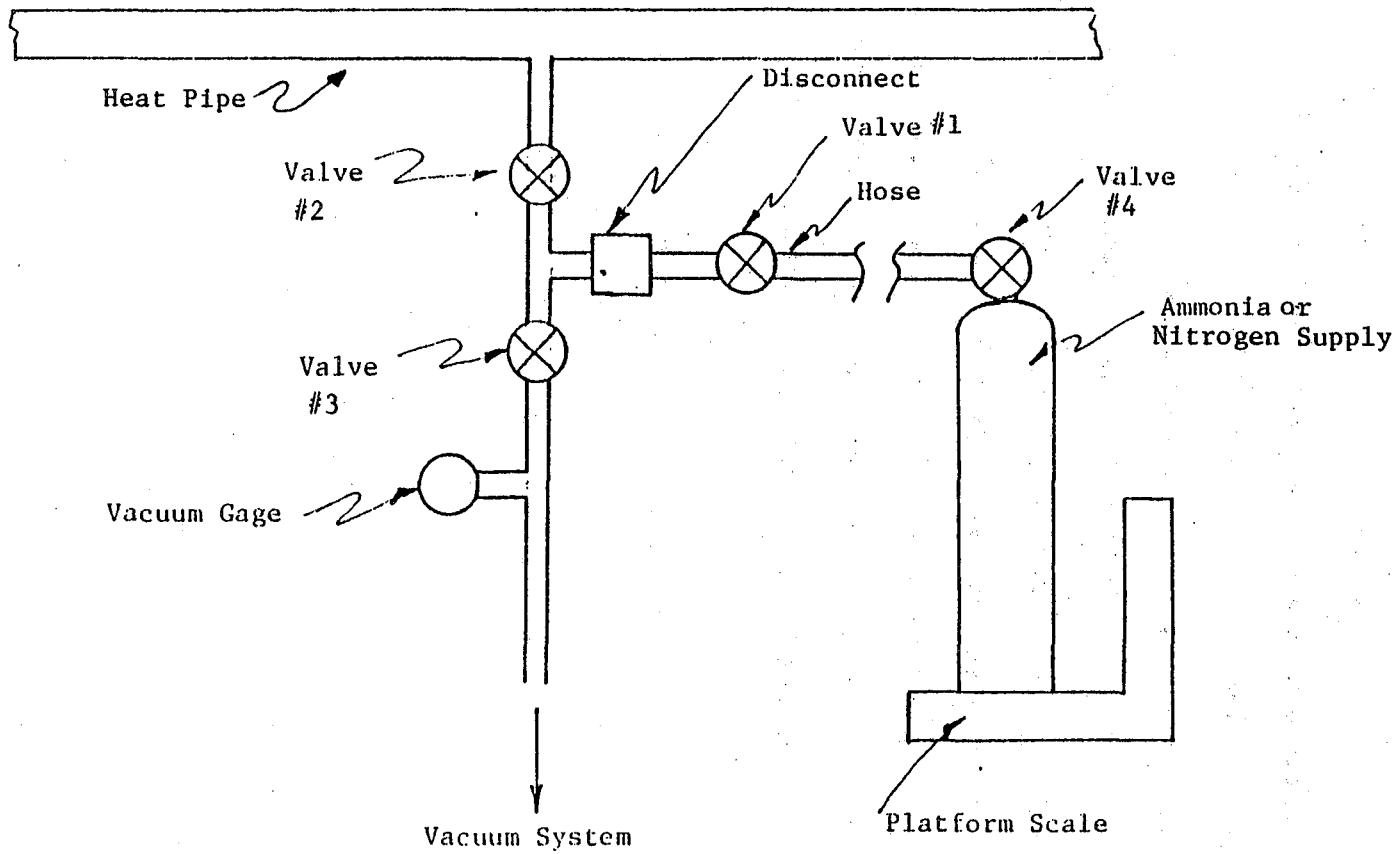


Figure B.1. System for Evacuation and Charging of Heat Pipes.

- D. If no indication of leaking was found and if the pressure did not increase over a period of 3 hours, the component was considered leak free.
- E. Valves #1 and #2 were opened, and the component was pressurized to 1.5 atm absolute with dry nitrogen.
- F. Valves #2 and #3 were closed and the component, with valve #2 attached, was removed for crimping.

It shall be the responsibility of the fabricator to devise a method for crimp-sealing the components. The crimp shall be placed in the service nipples between the heat pipe section and valve #2 and shall be 1"± (25 mm±) long. After opening valve #2, a commercial leak test solution shall be used to insure that the crimp has held. Once the crimp is leak tight, the end of the nipple is flattened and this end of the nipple welded across.

The heat pipe sections shall be bent as shown on the project plans. For ease of shipping, the major bends may be made in the field. If the Contractor elects to make bends in the field, he shall submit to the Engineer for approval a plan for making the bends.

Following the shop bending and prior to shipment, the shop welded areas that are not subject to field welding shall be thoroughly cleaned of all weld slag and other foreign material, preparatory to the areas being coated with epoxy coating. The coating to be used shall be "SCOTCHKOTE" 213PC or an approved alternate. The cleaning, coating and curing shall be done in strict accordance with the manufacturer's recommendations.

Following coating and curing, the pipe sections shall be shipped to

the job site. The handling and shipping shall be done as specified in the Special Provision for Epoxy Coating Heat Pipes.

FIELD INSTALLATION: The piping shall be erected as shown on the project plans and in sequence with the rest of the project work. Care shall be taken that each heat pipe has a continuous downward slope from the extreme tips of the heat pipes in the pavement to the top of the evaporator section. Additionally, that portion of each heat pipe in the pavement slab shall be securely fastened down to prevent it from floating up during concrete placement operations.

Each heat pipe will require field welding to complete assembly. Care shall be taken to insure that, following the unplugging of sections and prior to making field welds, no foreign material is in either section. The field welds shall be made in the same manner as specified for shop welds, except that an inert gas purge need not be used. The welds shall be tested as specified for the shop welds.

It is suggested that, once all heat pipes at each module are completed, the field welds be tested as specified for shop welds, using the field service nipples. Then, as the last operation after weld acceptance, the heat pipe being tested can be backfilled with ammonia by utilizing the vacuum in the pipe. Each heat pipe shall be backfilled with a minimum of 6.5 pounds (2.9 kg) of anhydrous ammonia. A procedure that has been used successfully for testing the welds and backfilling with ammonia is as follows:

#### Field Evacuation

Field evacuation and leak test will involve plumbing between the fill nipple and vacuum system as shown in Figure B.1 and proceeding as

described previously for shop evacuation and testing.

#### Charging the System

Charging the system was effected by introducing a fixed amount of ammonia into the heat pipe system. This was accomplished by weighing a liquid ammonia supply bottle.

- A. After the filling reservoir was removed from the supply bottle, it was weighed to insure that, in fact, the appropriate amount of ammonia was loaded.
- B. The supply bottle was plumbed to the fill nipple as shown in Figure B.1.
- C. The piping between valves #2, #3 and #4 was evacuated by leaving valves #2 and #4 closed and opening valves #1 and #3.
- D. Once the piping was evacuated, valve #3 was closed, and then valves #2 and #4 were opened.
- E. Heating of the fill reservoir expedited transfer of the ammonia from the reservoir to the heat pipe system.
- F. After charging was complete, valves #2 and #4 were closed, and the piping was bled and removed from valve #2.

After charging is complete, the nipples shall be crimped leak tight between valve #2 and the heat pipe. The crimp shall be welded across, as described for shop crimping.

After charging and sealing are complete, the field weld areas shall be thoroughly cleaned of all weld slag and other foreign material, preparatory to the areas being coated with field applied epoxy coating.

This shall be done as previously specified for in-shop coating of weld areas.

#### WELDING

Prior to initiating any fabrication, the fabricator and/or installer shall submit to the designated Engineer's Inspector sufficient documentation to indicate each different weld, position, and procedure, complete with type of welding machine and welding consumables, to be used during fabrication, for the Inspector's approval. The Inspector shall then observe each production welder making a butt splice weld connecting two 18" (460 mm) long pieces of 1" (25 mm) nominal diameter production pipe. The weld shall be made with the pipe in a horizontal position and not rotated. The pipe sample thus produced will be tested by the Inspector by bending 90° over a 12" (305 mm) diameter mandrel. When the Inspector is satisfied that the weld is of good visual quality and has passed the bend test, the welder may proceed with production welding.

The fabricator and/or installer may request a letter of certification from the State Bridge Engineer for any of his production welders. Any welder so certified shall be approved to do production heat pipe welding on any project for a period of 3 years without recertification. The fabricator and/or installer need only provide the designated Engineer's Inspector with this documentation prior to initiating any fabrication.

#### INSPECTION AND CERTIFICATION

The designated Engineer's Inspector shall be notified in advance of

the anticipated commencement of shop fabrication. The Inspector shall be allowed access to all portions of the fabricator's facilities in which the project work is being conducted, in order that the Inspector can observe, as he sees fit, any or all of the fabrication process. The Inspector shall be notified in advance of the anticipated commencement of field installation and shall have free access to all facilities and operations. The Inspector shall have the authority to temporarily terminate any operation that, in his judgment, does not meet the intent of these specifications. The subject operation shall be commenced only at which time the Inspector is satisfied that the intent is being met.

The Inspector shall be furnished with written certification from the fabricator and/or installer that all welds have been tested and are leak free, as herein specified. This certification shall be two part. The first part shall cover the welds made in the shop and shall be received by the Inspector prior to shipment to the job site of the subject sections. The second part shall cover the field welds and shall be received prior to insulating any of the heat pipes.

#### BACKGROUND

The fabricator and/or installer shall have a proven background, both technical and practical, in the fabricating and/or installing of the system implied in this Special Provision, or similar systems. The fabricator and/or installer shall be prepared to produce, upon request, evidence of said background to the Engineer for the Department's use.

## 5. SPECIAL PROVISION FOR INSULATION FOR PAVEMENT HEATING SYSTEM

### DESCRIPTION

This item shall consist of all work necessary to insulate portions of a pavement heating system.

### INSULATION

Following the charging of the heat pipes with ammonia and the sealing of the heat pipes, they shall be insulated. In general, the heat pipes shall be insulated all around, as shown on the project plans, all the way from the top of the evaporator sections to the edge of the pavement slab. The insulation at each heat pipe shall begin at the top of grout in the evaporator holes. Whenever possible, the pipes shall be insulated as a bundle. Styrofoam blocks shall be used to block the pipes off the ground. The insulation used shall be a foam-in-place type Polyurethane or an approved alternate. The material shall be installed in strict accordance with the manufacturer's recommendations and as directed by the Engineer.

The insulation will be provided with a coating to act as a moisture barrier. The insulation and coating will conform to the following specifications:

#### Primary Insulation

Type: Polyurethane

Density: 1.5 to 3 lb/in<sup>3</sup>

Percent closed cell: 90% or greater

Aged K factor: .16 or lower per inch

Compressive strength: 18 psi or greater

Method of application: spray or molded pour with internal mixing

Insulation Coating

Type: 2 component urethane

Elongation: 450% or greater

Tensile strength: 1000 psi or greater

Permeability: less than 1

Application rate: 18-20 mils

Method of application: air or airless spray, brush or roller

**APPENDIX C**

**CONSTRUCTION RECORD AND COSTS**

The bridge over Spring Creek is located in S. 1 T. 16 R. 73 on Wyoming Urban Route M-4211 at M.P. 330.64. This route serves as a connector for the town of Laramie to Interstate 80. The construction of the bridge was a result of an on-going state-wide bridge replacement program.

The structure replaced was built in 1934 and consisted of a 39'0" (11.9 m) steel I beam center span with 16'-0" (4.9 m) concrete slab approach spans for a total length of 71'-0" (21.6 m). Reinforced concrete abutments and bents were founded on spread footings. From bridge inspections it was found that this structure was in poor condition. The condition of the structure combined with a narrow roadway, 30'-0" clear (9.1 m), dictated the need for the structure to be replaced.

Based on the encouraging results of the Sybille experimental heat pipe project, it was felt that the heating of a small concrete bridge deck was not only feasible but would be a worthwhile demonstration project. The Spring Creek location was determined to be ideal due to its proximity to the University of Wyoming and the size of structure required for the crossing.

Engineering studies were made not only to determine the most economical structure type, but also how to integrate an earth-heat pipe system into the bridge deck. Complete hydraulic and geologic investigations were made to obtain data for determining the required structure length and foundation type. A structure 60'0" (18.3 m) in length was found to be adequate to convey the predicted floods. Using past cost histories, it was determined that a simple span, steel I beam superstructure utilizing composite action with the concrete deck was the most economical solution. The steel beams rest on concrete abutment caps

founded on steel piling driven to refusal in very hard siltstone. Predrilled holes in the bedrock were specified to insure proper penetration of the steel piling.

The impact of installing the heat pipe with regard to normal construction activities was minimal. The only equipment required, which normally would not have been used for constructing a bridge of this type, was a crane with boom long enough to install the 100-foot (30.5 m) evaporator pipes in the ground. The type of construction and equipment used for building the structure were quite common and no major problems occurred. Specialized equipment was not required for installation of the condenser pipes in the deck. They were placed along with reinforcing steel in the deck without difficulty and caused no problems with placing the concrete and no cracking has occurred in the deck. Structural steel header vaults were constructed on each edge of the bridge deck to protect the heat pipes emerging from the deck. Also, no major problems occurred with integrating these vaults into the bridge construction.

Some problems did occur with the grouting of the evaporator holes but these difficulties were associated with the evaporator thermal instrumentation and not the heat pipe itself. This is discussed in section II.C of this report.

Settlement of the fill behind and adjacent to the abutments has occurred, causing cracking of the approach sidewalks and rough approaches to the structure. Also, it appears that the settlement of the fill has deflected some of the heat pipes downward, causing them to become inoperable. This problem is discussed in Chapter 3 of this report.

The deck surface is sanded in the winter months. However, the

amount of salt included was found to be quite small. Cores of the deck, obtained after the bridge had been in service for two years, contained insignificant amounts of sodium chloride.

In order to decrease construction time, it was decided to break the project into two contracts:

1. Supply, fabrication, handling, shipping, unloading and stockpiling of structural steel, steel piling, and piling points.
2. Construction of the bridge and heat pipe system. Since the supply contract was let first, the structural steel and piling were at the contractor's disposal when the second contract for actual construction of the bridge was awarded. This eliminated the normal waiting period for these items (which is usually four to six months) that is incurred when a complete contract is let, and the contractor is responsible for ordering the material after award of contract. The two contract approach was desirable, since the time required for preparation of plans dictated a July 17, 1980 letting date, and it was felt that having steel items pre-delivered would allow completion of the bridge in early summer of 1981. This would then allow four to five months for the University of Wyoming to install instrumentation and data acquisition equipment in order to take data on the heat pipe system performance during the winter of 1981-1982.

Bids were opened for the steel supply contract on March 5, 1980. The award of the contract was made by the Wyoming Highway Department Commission on March 13, 1980 to the successful low bidder, Tri-State Steel Co., Cheyenne, Wyoming.

Bids were opened for the structure on July 9, 1980. The award of the contract was made by the Wyoming Highway Department Commission on

July 17, 1980 to the successful bidder, Structures Incorporated, of Riverton, Wyoming.

The actual itemized bid prices, along with the Engineer's estimate, are shown in Table C.1, and the chronological listing of major construction activities during the life of the project is delineated in Table C.2. A complete set of contract plans are included in Appendix A.

TABLE C.1. COST SUMMARY OF SPRING CREEK BRIDGE (PROJECT BRM-4211(6))

A. Supply, Fabrication, Handling, Shipping, Unloading and Stockpiling of Structural Steel and Steel Piling and Piling Points

Item	Unit	Quantity	ENGINEER'S ESTIMATE		CONTRACT	
			Unit Cost	Total Cost	Unit Cost	Total Cost
Structural Steel	LS	107500 Lbs	\$ 0.60*	\$64,500.00	\$ 0.428	\$45,973.00
Steel Piling HP 12x53	LF	400	20.00**	8,000.00	19.39	7,756.00
Contract Bond	LS		1.2% of total	900.00		128.95
TOTAL COST				\$73,400.00		\$53,857.95

\* 80% of \$ .75

\*\* 50% of \$40.00

B. Bridge Deck Heating System

Item	Unit	Quantity	ENGINEER'S ESTIMATE		CONTRACT	
			Unit Cost	Total Cost	Unit Cost	Total Cost
Heat Pipes	LS			\$89,000.00		\$184,000.00
Excavation	CY	2000	\$ 15.00	30,000.00	\$ 9.00	18,000.00
Structural Steel	LS	12400 Lbs	1.00	12,400.00	2.50	31,000.00
Evaporator Holes	LS			80,000.00		91,700.00
Insulation	LS			15,000.00		19,000.00
Class B Concrete	LS	31.5 CY	275.00	8,662.50	815.87	25,700.00
Reinforcing Steel	LS	2760 Lbs	0.75	2,070.00	0.43	1,200.00
TOTAL COST				\$237,132.50		\$370,600.00

TABLE C.1 (CONTINUED)  
C. Cost Summary for Bridges

Item	Unit	Quantity	ENGINEER'S ESTIMATE		CONTRACT	
			Unit Cost	Total Cost	Unit Cost	Total Cost
<b>SUPERSTRUCTURE</b>						
Class AAA Concrete	LS	124.4 CY	\$ 275.00	\$34,210.00	\$ 285.37	\$ 35,500.00
Class B Concrete	LS	66.6 CY	250.00	16,650.00	249.43	16,612.33
Reinforcing Steel	LS	13610 Lbs	0.50	6,805.00	0.50	6,795.73
Bridge Railing	LF	100	45.00	4,500.00	38.00	3,800.00
Erection of Structural Steel	LS	107500 Lbs	0.20	21,500.00	0.11	12,000.00
Reinforcing Steel (Epoxy Coated)	LS	18580 Lbs	1.00	18,580.00	0.70	13,000.00
Pedestrian Railing	LF	121	45.00	5,445.00	65.00	7,865.00
Subtotal, Superstructure Cost				\$107,690.00		\$ 95,573.06
<b>SUBSTRUCTURE</b>						
Class B Concrete	LS	110.2 CY	\$ 250.00	\$27,550.00	\$ 249.43	\$ 27,487.67
Reinforcing Steel	LS	8420 Lbs	0.50	4,210.00	0.50	4,204.27
Dry Excavation	CY	140	15.00	2,100.00	20.00	2,800.00
Predrilled Holes	LF	236	12.00	2,832.00	1.00	236.00
Pile Driving	LF	400	20.00	8,000.00	22.00	8,800.00
Steel Pile Splices	Ea	5	100.00	500.00	100.00	500.00
Subtotal, Substructure Cost				\$ 45,192.00		\$ 44,027.94
<b>MISCELLANEOUS</b>						
Reinf Conc Approach Slabs	Sq Yd	355	\$ 45.00	\$ 15,975.00	\$ 51.00	\$ 18,105.00
Pervious Backfill Material	CY	150	20.00	3,000.00	19.00	2,850.00
Removal of Bridges	Ea	1	15,000.00	15,000.00	10,400.00	10,400.00
Bridge Telephone Conduit System	LS	66 LF	15±	1,000.00	15.15	1,000.00
2" Rigid Steel Conduit System (for Bridges)	LS	140 LF	7±	1,000.00	7.14	1,000.00
Bridge Deck Heating System Items (See attached breakdown)				237,132.50		370,600.00
Subtotal, Miscellaneous Cost				\$273,107.50		\$403,955.00
<b>TOTAL COST</b>				\$425,989.50		\$543,556.00
UNIT	Superstructure	Sq Ft		\$21.89		\$ 19.43
	Substructure	Sq Ft		9.19		8.95
COSTS	Miscellaneous	Sq Ft		55.51		82.10
	Total	Sq Ft		86.59		110.48

TABLE C.2

## Chronological Listing of Major Construction Activities

## 1. Supply, Fabrication, Handling, Shipping, Unloading and Stockpiling of Structural Steel, Steel Piling, and Piling Points.

1. Let to contract . . . . .	3- 5-80
2. Contractor started fabrication. . . . .	3-27-80
3. Material delivered to site. . . . .	.10- 1-80
4. Contract completed and accepted by Engineer . . . . .	.10-22-80

## 2. Construction of Bridge and Heat Pipe System

1. Let to contract . . . . .	7- 9-80
2. Contractor started work . . . . .	8-15-80
3. Steel piling driven at abutments. . . . .	9-22-80
4. Abutment concrete placement complete. . . . .	.10-28-80
5. Structural steel erected. . . . .	.11-13-80
6. Heat pipes placed in deck (complete). . . . .	.12-17-80
7. Bridge deck placed. . . . .	.12-16-80
8. Insulation placed under deck. . . . .	1-22-81
9. Concrete placed for instrumentation hut and service vaults (complete) . . . . .	4-24-81
10. Steel headers on side of deck complete. . . . .	5- 7-81
11. Evaporator holes complete . . . . .	5-14-81
12. Heat pipe system completed . . . . .	6-15-81